SH
11
A2 F53
FISH

U.S. Department
of Commerce

Volume 117
Numbers 1–2
January–April 2019

Fishery Bulletin

SHOUT
SHARE
IT

U.S. Department of Commerce

Wilbur L. Ross Jr.
Secretary

National Oceanic and Atmospheric Administration

Neil A. Jacobs
Acting Administrator

National Marine Fisheries Service

Chris Oliver
Assistant Administrator
for Fisheries

The *Fishery Bulletin* (ISSN 0090-0656) is published quarterly by the Scientific Publications Office, National Marine Fisheries Service, NOAA, 7600 Sand Point Way NE, Seattle, WA 98115-0070.

Although the contents of this publication have not been copyrighted and may be reprinted entirely, reference to source is appreciated.

The Secretary of Commerce has determined that the publication of this periodical is necessary according to law for the transaction of public business of this Department. Use of funds for printing of this periodical has been approved by the Director of the Office of Management and Budget.

For Sale by the Superintendent of Documents, U.S. Government Printing Office, Washington, DC 20402. Subscription price per year: $32.00 domestic and $44.80 foreign. Cost per single issue: $19.00 domestic and $26.60 foreign. **See back for order form.**

Fishery Bulletin

Scientific Editor
José I. Castro
National Marine Fisheries Service, NOAA
263 13th Avenue South
Saint Petersburg, Florida 33701

Managing Editor
Kathryn Dennis
National Marine Fisheries Service, NOAA
Scientific Publications Office
1845 Wasp Blvd., Bldg. 176
Honolulu, Hawaii 96818

Sharyn Matriotti (retired*)
National Marine Fisheries Service, NOAA
Scientific Publications Office
7600 Sand Point Way NE
Seattle, Washington 98115-0070

Associate Editor
Cara Mayo
National Marine Fisheries Service, NOAA
Scientific Publications Office
7600 Sand Point Way NE
Seattle, Washington 98115-0070

Editorial Board

Henry L. Bart Jr.	Tulane University, New Orleans, Louisiana
Shannon L. Cass-Calay	National Marine Fisheries Service, Miami, Florida
William B. Driggers III	National Marine Fisheries Service, Pascagoula, Mississippi
Gretchen L. Grammer	South Australian Research and Development Institute, Adelaide, Australia
Richard Langton	National Marine Fisheries Service, Walpole, Maine (retired)
Richard S. McBride	National Marine Fisheries Service, Woods Hole, Massachusetts
Richard L. Merrick	National Marine Fisheries Service, Falmouth, Massachusetts (retired)
Richard D. Methot	National Marine Fisheries Service, Seattle, Washington
Lisa J. Natanson	National Marine Fisheries Service, Narragansett, Rhode Island
Joseph M. Quattro	University of South Carolina, Columbia, South Carolina
Mark S. Peterson	University of Southern Mississippi, Ocean Springs, Mississippi
John F. Walter III	National Marine Fisheries Service, Miami, Florida
Bruce Wright	Aleutian Pribilof Island Association, Anchorage, Alaska

*Sharyn Matriotti, a superb and dedicated editor, retired in December 2018 after 29 years of service as managing editor of *Fishery Bulletin*.

***Fishery Bulletin* website: https://spo.nmfs.noaa.gov/fb.htm**

The *Fishery Bulletin* carries original research reports on investigations in fishery science, engineering, and economics. It began as the Bulletin of the United States Fish Commission in 1881; it became the Bulletin of the Bureau of Fisheries in 1904 and the *Fishery Bulletin* of the Fish and Wildlife Service in 1941. Separates were issued as documents through volume 46; the last document was no. 1103. Beginning with volume 47 in 1931 and continuing through volume 62 in 1963, each separate appeared as a numbered bulletin. A new system began in 1963 with volume 63 in which papers are bound together in a single issue. Beginning with volume 70, number 1, January 1972, *Fishery Bulletin* became a periodical, issued quarterly. In this form, it is available by subscription from the Superintendent of Documents, U.S. Government Printing Office, Washington, DC 20402. It is also available free in limited numbers to libraries, research institutions, state and federal agencies, and in exchange for other scientific publications.

U.S. Department of Commerce
Seattle, Washington

Volume 117
Numbers 1–2
January–April 2019

Fishery Bulletin

Contents

Short contributions

1–7 Sean P. Powers and Kevin Anson

Compression and relaxation of fishing effort in response to changes in length of fishing season for red snapper *(Lutjanus campechanus)* in the northern Gulf of Mexico

8–14 Duane E. Stevenson, Gerald R. Hoff, James W. Orr, Ingrid Spies, and Christopher N. Rooper

Interactions between fisheries and early life stages of skates in nursery areas of the eastern Bering Sea

Articles

15–23 Eric S. Orbesen, Craig A. Brown, Derke Snodgrass, Joseph E. Serafy, and John F. Walter III

At-vessel and postrelease mortality rates of bluefin tuna (*Thunnus thynnus*) associated with pelagic longline gear in the northern Gulf of Mexico

24–36 Ryo Misawa, Yoji Narimatsu, Hiromitsu Endo, and Yoshiaki Kai

Population structure of the ocellate spot skate (*Okamejei kenojei*) inferred from variations in mitochondrial DNA (mtDNA) sequences and from morphological characters of regional populations

37–49 Nancy J. Brown-Peterson, Christopher R. Peterson, and Gary R. Fitzhugh

Multidecadal meta-analysis of reproductive parameters of female red snapper (*Lutjanus campechanus*) in the northern Gulf of Mexico

The National Marine Fisheries Service (NMFS) does not approve, recommend, or endorse any proprietary product or proprietary material mentioned in this publication. No reference shall be made to NMFS, or to this publication furnished by NMFS, in any advertising or sales promotion which would indicate or imply that NMFS approves, recommends, or endorses any proprietary product or proprietary material mentioned herein, or which has as its purpose an intent to cause directly or indirectly the advertised product to be used or purchased because of this NMFS publication.

The NMFS Scientific Publications Office is not responsible for the contents of the articles.

SMITHSONIAN
JUL 16 2019
LIBRARIES

Short contribution

50–58 Lisa J. Natanson and Bethany M. Deacy

Using oxytetracycline validation for confirmation of changes in vertebral band-pair deposition rates with ontogeny in sandbar sharks (*Carcharhinus plumbeus*) in the western North Atlantic Ocean

Article

59–69 C. J. Carroll Schlick and Kim de Mutsert

Growth of adult river herring that spawn in tributaries of the Potomac River in northern Virginia

Short contributions

70–77 Lisa J. Natanson, Bethany M. Deacy, Warren Joyce, and James Sulikowski

Presence of a resting population of female porbeagles (*Lamna nasus*), indicating a biennial reproductive cycle, in the western North Atlantic Ocean

78–86 Rui Matsumoto, Yosuke Matsumoto, Keiichi Ueda, Miwa Suzuki, Kiyoshi Asahina, and Keiichi Sato

Sexual maturation in a male whale shark (*Rhincodon typus*) based on observations made over 20 years of captivity

Articles

87–96 Roldan C. Muñoz and Michael L. Burton

Comparison of video and diver observations of sharks from a fishery-independent trap-video survey off east-central Florida, including utility of an alternative method of video analysis

97–106 Donald M. Van Doornik, David R. Kuligowski, Cheryl A. Morgan, Brian J. Burke, and Todd R. Seamons

Insights, from genetic analyses, into stock-specific distribution of juvenile steelhead (*Oncorhynchus mykiss*) from the Columbia River during early marine migration

107–120 Yuki Fujinami, Yasuko Semba, and Sho Tanaka

Age determination and growth of the blue shark (*Prionace glauca*) in the western North Pacific Ocean

121–124 Guidelines for authors

National Marine Fisheries Service
NOAA

Fishery Bulletin
established in 1881

Spencer F. Baird
First U.S. Commissioner of Fisheries and founder of *Fishery Bulletin*

Compression and relaxation of fishing effort in response to changes in length of fishing season for red snapper (*Lutjanus campechanus*) in the northern Gulf of Mexico

Sean P. Powers (contact author)[1]
Kevin Anson[2]

Email address for contact author: spowers@disl.org

[1] Department of Marine Sciences
University of South Alabama and
Dauphin Island Sea Lab
101 Bienville Boulevard
Dauphin Island, Alabama 36528

[2] Marine Resources Division
Alabama Department of Conservation and Natural Resources
P.O. Drawer 458
Gulf Shores, Alabama 36547

Abstract—A standard method used by fisheries managers to decrease catch and effort is to shorten the length of a fishery; however, data on recreational angler response to this simple approach are surprisingly lacking. We assessed the effect of variable season length on daily fishing effort, measured by using numbers of boat launches per day, anglers per boat, and anglers per day from video observations, in the recreational sector of the federal fishery for red snapper (*Lutjanus campechanus*) in coastal Alabama. From 2012 through 2017, season length fluctuated from 3 to 40 d. Daily effort, measured by using mean number of boat launches per day (coefficient of multiple determination [R^2]=0.58) and mean number of anglers per day (R^2=0.67), increased linearly with season shortening, indicating effort compression. In 2017, 2 seasons were allowed: an early season (3 d) and an unanticipated late season (39 d). Daily effort decreased during the late season, indicating that effort can also be relaxed if anglers anticipate longer seasons. Model fit for mean number of anglers per day improved with the addition of a daily wind factor (R^2=0.94). The results of this study indicate that responses of anglers to changing fishing seasons are dynamic.

Manuscript submitted 5 May 2018.
Manuscript accepted 24 October 2018.
Fish. Bull. 117:1–7 (2019).
Online publication date: 16 November 2018.
doi: 10.7755/FB.117.1.1

The views and opinions expressed or implied in this article are those of the author (or authors) and do not necessarily reflect the position of the National Marine Fisheries Service, NOAA.

Fisheries managers have several options to reduce effort and decrease catch in a fishery. Among the most popular of these options is limitation of the length of the fishing season. Shortening the length of a fishing season is assumed to reduce catch because effort is reduced; however, the response of anglers may not be proportional to the reduction in season length (Powers and Anson, 2016). The advent of derby-style fisheries (in which anglers race to take their catch and fish at an ever increasing rate; Chu, 2009) resulted in part from the reduction in season length in several commercial fisheries. Such a race to fish compromises angler safety. The adoption of individual fishing quotas has eliminated many derby-style fisheries in the commercial sector and has resulted in increased economic yields and greater angler safety (Costello et al., 2008; Chu, 2009). In a marine recreational fishery, Powers and Anson (2016) documented effort compression (i.e., increases in per unit effort in response to decreasing season length); however, that study did not address whether effort compression was reversible. In the study described in this paper, we used the unique conditions of the federal seasons of the recreational fishery for red snapper (*Lutjanus campechanus*) in 2017, including both the short season (3 d) and the long season (39 d), to not only further examine effort compression in response to shortened seasons but also to determine if relaxation in effort can be measured in response to extended season lengths.

The management of the fishery for red snapper in the northern Gulf of Mexico is highly controversial (Strelcheck and Hood, 2007; Cowan et al., 2011). After decades of overfishing, the stock in the Gulf of Mexico is currently classified as not experiencing overfishing and recently was declared no longer overfished (SEDAR, 2013, 2018). This stock is expected to be fully rebuilt at a spawning potential ratio of 26% in 2032. The fishery is composed of both commercial and recreational sectors, which share the overall quota on a 51% to 49% split.

Since 2007, the commercial sector of the fishery for red snapper has been managed under an individual fishing quota system with no overage on the sector quota. In 2015, the recreational sector was divided into a charter and for-hire sector and a private recreational sector with each sector sharing a percentage of the recreational annual catch limit (ACL). The for-hire sector is a closed fishery with a defined number of permits, and the length of the season is set each year on the basis of the sector's share of the recreational quota and recent catch history. The private recreational sector is an open fishery, and the length of the season is based on the same inputs as the for-hire sector. Because of several factors, such as additional fishing days for the state season and large estimates of daily catches, the federal season for the private recreational sector has been reduced to a derby-style fishery.

Increasingly restrictive regulations designed to limit catch of red snapper in the private recreational fishery, which has routinely exceeded its share of the ACL, have been enacted over the last decade, progressively shortening the season from 194 d in 2007 to 11 d in 2016. Growing frustration by recreational anglers, who see clear signs of recovery of the stock as it rebuilds (higher catch per unit of effort and larger sized red snapper) yet face shorter federal seasons, has led to public questioning of the stock assessment and management process. Public frustration rose to its highest level in 2017, when the National Marine Fisheries Service initially set the recreational season for red snapper in federal waters at 3 d. Logical reasons existed for the shortened federal season in earlier federal regulations, including the existence of separate recreational fisheries in state regulated waters, which increased in 2015 from 4.8 to 14.5 km, or from 3 to 9 mi, from the shoreline. However, demands of anglers and policy makers to extend the season grew. An appeal by state management agencies from all 5 Gulf states to the secretary of the U.S. Department of Commerce resulted in the National Marine Fisheries Service setting a second season of 39 d for 2017 (Fridays, Saturdays, Sundays, and federal holidays from 16 June through 4 September). In exchange for the extended federal season, most of the Gulf states agreed to close state waters outside of the federal season for the remainder of 2017. Of relevance to this study is that anglers had little prior notice (2–3 d) of the second season and had no reasonable expectation a second season would be adopted for 2017 at the time of the initial 3-d season. Hence, the 2 seasons in 2017 provided a unique opportunity to assess angler effort during 2 seasons of different lengths.

Materials and methods

Study site

We counted boat launches and anglers viewed in videos recorded in 2012–2017 by cameras installed at 6 public launch sites throughout coastal Alabama. We used these counts to quantify total daily effort of anglers in the private recreational sector of the fishery for red snapper who used those monitored public boat launches. The 6 boat ramps are located at Bayou La Batre, Billy Goat Hole, Little Billy Goat Hole, Fort Morgan, Boggy Point, and Cotton Bayou. The private recreational community is made up of anglers who tow and launch boats at public boat launches and those who have private marina or dock access. In 2015, approximately 60% of anglers were estimated to have used public boat launches (K. Anson, unpubl. data). Recreational anglers have a limited number of public boat launches that are used to launch vessels to fish for red snapper in offshore waters, and video cameras were installed at the majority of these public launches. Boaters leave these offshore boat launches to fish for reef-associated fishes, including red snapper, in the Alabama Artificial Reef Zone—a 2670 km^2 area encompassing a network of thousands of artificial reefs and scattered natural reefs beginning 25 km south of the Alabama coast (Minton and Heath, 1998; Patterson et al., 2001). Because of their affinity for structured habitats, red snapper are relatively easy to target on artificial and natural reef habitats (Gallaway et al., 2009; Powers et al., 2018).

Angler and boat counts

Since 2012, each of the 6 public boat launches has been monitored by MIC412[1] video cameras (Bosch Security Systems, Inc., Fairport, NY) that aid law enforcement activities. During the federal recreational fishery for red snapper, the video recordings are archived and available for analysis of angler effort. Powers and Anson (2016) demonstrated the efficacy of the analysis of these archived videos in estimating angler effort. We used the data available in Powers and Anson (2016) for the federal fishery for red snapper in 2012–2015 and collected additional data by using identical methods for the federal fishery seasons for red snapper in 2016 and 2017. Season lengths varied each year: 40 d in 2012, 28 d in 2013, 9 d in 2014, 10 d in 2015, 11 d in 2016, 3 d in the short season of 2017, and 39 d in the long season of 2017.

Analysis of video footage followed 1 of 2 protocols depending on season length: short (≤11 d) and long (>11 d) seasons. For both protocols, analysts counted boat launches and anglers per boat while viewing the archived videos for randomly chosen 5-min periods in each hour of footage recorded from 0500 to 2059 at each public boat ramp. For the short seasons (2014, 2015, 2016, and the short season of 2017), counting was done every day of the federal season. For the long seasons (2012, 2013, and the long season of 2017), 20% of the days were selected at random for counting. Choosing days randomly does have the potential to bias our data

[1] Mention of trade names or commercial companies is for identification purposes only and does not imply endorsement by the National Marine Fisheries Service, NOAA.

because effort probably is not similar between weekend days and holidays and weekdays. This issue applies only to the 2012 and 2013 seasons because in 2017 the season was opened only on Friday–Sunday (considered weekend days) and major holidays (e.g., the Fourth of July). For the seasons in 2012 and 2013, we used the modeled estimates directly from Powers and Anson (2016) that included a weekend and holiday factor (for further details, see Powers and Anson, 2016). For the other seasons in the time series (2014, 2015, 2016, and the short season of 2017), fishing days were consecutive from 0000 on 1 June to 1159 on the last day. Finally, for the seasons in 2014–2017, the frequency of 5-min intervals analyzed for each hour from 0500 to 1000 was increased from 1 interval to 5 intervals to better capture the increased boat traffic during these hours.

When watching the videos, analysts recorded the number of boats launched and the number of anglers on each boat. For a boat launch to have been counted, the analyst had to have observed the boat coming off the trailer during the 5-min interval. To count the total number of potential anglers, the analyst was allowed to observe the boat outside of the 5-min interval to account for the time anglers might have taken to return from parking the towing vehicle. Analysts classified boats into 1 of 4 categories: offshore fishing, inshore fishing, non-fishing, and unknown. Categorization was based on the size and design of fishing vessel as well as on the presence and type of fishing gear. All analysts were trained on videos recorded prior to the study period by an experienced staff member before they began analyzing video recordings from the study period. All videos were viewed by a second analyst, and the 2 sets of observations were averaged to estimate the number of boat launches per 5-min interval per ramp and the number of potential anglers per 5-min interval. The averaged observations were then transformed to hourly estimates depending on the number of 5-min intervals observed within the designated hour. Daily estimates were made by summing the hourly estimates for each day. Finally, the daily estimates for each of the 6 boat launches were summed across all days to calculate the potential numbers of anglers and offshore boats during the short seasons. For the long seasons, a daily average of potential numbers of anglers and offshore boats was calculated by multiplying the average of each metric from observed days at each boat ramp by the total number of days in the season and then summing estimates for all boat launches to provide an estimate for the season (see Powers and Anson, 2016).

Because weather may affect angler effort (Fraidenburg and Bargmann, 1982; Powers and Anson, 2016), observations of weather conditions were gathered by the analyst watching the videos as well as from nearby monitoring stations. Analysts recorded precipitation events and cloud cover as binary responses (1 for rain, 0 for no rain; 1 for dark clouds present, 0 for dark clouds not present). Maximum nearshore hourly wind speed and daily precipitation were obtained from the weather station located near the public boat ramp at Billy Goat Hole on Dauphin Island (Mobile Bay Estuary Program, website). Offshore hourly maximum wind speed and sea height were obtained from the sea buoy located 22 km offshore from Orange Beach, Alabama (station 42012; National Data Buoy Center, website).

Analyses

We used linear and nonlinear regression analyses of the estimates for mean number of anglers per day and of boat launches per day during each season to examine the relationship between angler effort and season duration. Mean daily numbers of boat launches and anglers were normally distributed; hence, no transformation was applied (Shapiro–Wilk test for both dependent variables: $P>0.90$). Next, multiple linear regressions were used to determine if the model prediction could be improved by the addition of weather variables. Because of the limited number of years in our study, interactions of main effects could not be included in the models. The corrected Akaike's information criterion (AICc) was used to compare model fits and determine the most parsimonious model. Because nearshore and offshore winds were expected to be strongly correlated and nearshore winds may influence anglers' decisions to fish for reef fishes more than offshore wind speeds, only wind data from the nearshore weather station at Dauphin Island were used in calculating the daily average wind speed. Previous work has indicated that the nearshore wind measurements were the better predictor of daily effort (Powers and Anson, 2016). Both wind speeds and offshore sea heights from Dauphin Island were explored in the models because the 2 conditions were not found to be significantly correlated.

To estimate total harvest of red snapper in the segment of the recreational sector that used public boat launches, seasonal estimates of the number of anglers were multiplied by the observed average number of red snapper harvested per angler and average weight of red snapper. Estimates of average number of red snapper caught per angler and average weight were derived from dockside intercepts of anglers interviewed at the 6 boat ramps included in this study. In 2012 and 2013, data necessary to produce these averages for each year were collected as part of the Marine Recreational Information Program of the National Marine Fisheries Service. For 2014–2017, data collected as part of dockside surveys conducted by the Marine Resources Division of the Alabama Department of Conservation and Natural Resources to complement a new mandatory reporting program were used to calculate the average number of red snapper harvested per angler and the average weight of red snapper for each year. Once these seasonal estimates of harvest in number and weight were calculated, the relationship between these estimates and season duration were examined by linear regression. The seasonal estimates of number and weight of red snapper were normally distributed (Shapiro–Wilk test for both dependent variables: $P>0.70$), and no trans-

Discussion

The intensity of derby-style fisheries has increased as fishing seasons shorten. In accordance with this notion, recreational anglers in coastal Alabama have responded to the shortening of the fishery for red snapper by increasing daily effort. We observed the highest daily effort during the shortest season on record (3 d). The late season in 2017 offered a test of whether daily effort would relax, given that this additional (long) season was unanticipated. Daily effort decreased in this long season in number of boat launches and anglers per day. The estimate for number of anglers per day was 60% higher during the short season in 2017. The 3-d season, which represented 7.7% of the long season in 2017, resulted in a harvest, estimated by using landings by weight, that was 16.6% of the harvest of the long season. This nonproportional response in harvest to the difference in length of fishing season must be considered when examining the potential of changes in recreational season length to reduce catch. More broadly, the results of our analysis provide another example of dynamic responses of anglers to changes in fishing regulations (Johnson and Carpenter, 1994). Such outcomes are likely difficult to predict at the onset of a regulatory change; therefore, intensive monitoring of angler response following such a regulatory change is needed.

In addition to season length, one weather condition was a significant factor in explaining fishing effort. Higher wind speeds decreased daily effort. Although this pattern is not surprising for an offshore-based fishery, it does provide some insight into the applicability of these findings to study of fishing effort in future years. Both the short and long seasons of 2017 were characterized by modest winds throughout the season (mean of 2.9 m/s, or 6.5 mph, per day for both seasons); hence, this weather condition did not confound our predictions for 2017. In earlier years of the study period, higher winds (4.5–5.4 m/s or 10–12 mph) were recorded and dampened daily effort. Currently, there are not sufficient data to determine the effects of high winds on angler effort during an extremely short season; however, the negative relationship between wind speed and effort in our study period indicates that most anglers would not go fishing under conditions with high wind speeds.

The red snapper is an immensely popular target species in the Gulf of Mexico. For recreational anglers with boats capable of going out to offshore waters, catching red snapper is almost viewed as a fundamental right. The controversy over the management of this fishery will likely persist as the stock rebuilds because anglers will continue to observe first-hand signs of recovery while they remain under the restrictive regulations of a stock rebuilding plan. As more fisheries experience stock rebuilding, similar issues involving a perceived disconnect between angler experiences and rebuilding regulations are likely to arise. Our analysis indicates that achieving rebuilding targets is even more challenging when fishing effort is compressed—when anglers take more trips over a short period of time as they anticipate shortened seasons. Effort compression and the fact that this compression varies with wind speed contributes to management uncertainty and must be considered in formulations of management strategies designed to maintain landings of red snapper below ACLs. The results of this study indicate that, as ACLs increase and longer seasons are warranted, effort compression may be relaxed and afford even longer seasons.

Acknowledgments

We thank C. Hightower for coordinating the many analysts who examined hundreds of hours of video footage for this project. Funding was provided by grants from the National Fish and Wildlife Foundation's Gulf Environmental Benefit Fund through subawards from the Alabama Department of Conservation and Natural Resources, Marine Resources Division.

Literature cited

Chu, C.
2009. Thirty years later: the global growth of ITQs and their influence on stock status in marine fisheries. Fish Fish. 10:217–230.

Costello, C., S. D. Gaines, and J. Lynham.
2008. Can catch shares prevent fisheries collapse? Science 321:1678–1681.

Cowan, J. H., C. B. Grimes, W. F. Patterson III, C. J. Walters, A. C. Jones, W. J. Lindberg, D. J. Sheehy, W. E. Pine III, J. E. Powers, M. D. Campbell et al.
2011. Red snapper management in the Gulf of Mexico: science- or faith-based? Rev. Fish Biol. Fish. 21:187–204.

Fraidenburg, M. E., and G. G. Bargmann.
1982. Estimating boat-based fishing effort in a marine recreational fishery. North Am. J. Fish. Manage. 2:351–358.

Gallaway, B. J., S. T. Szedlmayer, and W. J. Gazey.
2009. A life history review for red snapper in the Gulf of Mexico with an evaluation of the importance of offshore petroleum platforms and other artificial reefs. Rev. Fish. Sci. 17:48–67.

Johnson, B. M., and S. R. Carpenter.
1994. Functional and numerical responses: a framework for fish-angler interactions. Ecol. Appl. 4:808–821.

Minton, R. V., and S. R. Heath.
1998. Alabama's artificial reef program: building oases in the desert. Gulf Mex. Sci. 16:105–106.

Patterson, W. F., III, J. H. Cowan Jr., C.A. Wilson, and R. L. Shipp.
2001. Age and growth of red snapper, *Lutjanus campechanus*, from an artificial reef area off Alabama in the northern Gulf of Mexico. Fish. Bull. 99:617–627.

Powers, S. P., and K. Anson.
2016. Estimating recreational effort in the Gulf of Mexico Red Snapper fishery using boat ramp cameras: reduction in federal season length does not proportionally

reduce catch. North Am. J. Fish. Manage. 36:1156–1166.

Powers, S. P., J. M. Drymon, C. L. Hightower, T. Spearman, G. S. Bosarge, and A. Jefferson.
2018. Distribution and age composition of Red Snapper across the inner continental shelf of the north-central Gulf of Mexico. Trans. Am. Fish. Soc. 147:791–805.

SEDAR (Southeast Data Assessment and Review).
2013. SEDAR 31—Gulf of Mexico red snapper stock assessment report, 1103 p. SEDAR, North Charleston, SC. [Available from website.]
2018. SEDAR 52—Gulf of Mexico red snapper stock assessment report, 277 p. SEDAR, North Charleston, SC. [Available from website.]

Strelcheck, A. J., and P. B. Hood.
2007. Rebuilding red snapper: recent management activities and future management challenges. Am. Fish. Soc. Symp. 60:385–396.

National Marine Fisheries Service
NOAA

Fishery Bulletin
established in 1881

Spencer F. Baird
First U.S. Commissioner of Fisheries and founder of *Fishery Bulletin*

Interactions between fisheries and early life stages of skates in nursery areas of the eastern Bering Sea

Duane E. Stevenson
Gerald R. Hoff
James W. Orr
Ingrid Spies
Christopher N. Rooper

Email address for contact author: duane.stevenson@noaa.gov

Alaska Fisheries Science Center
National Marine Fisheries Service, NOAA
7600 Sand Point Way NE
Seattle, Washington 98115-6349

Abstract—From late 2014 through 2017, fishery observers in the North Pacific Observer Program, National Marine Fisheries Service, were trained in the identification and sampling of skate egg cases to investigate the interactions between fisheries and skate nursery areas in the eastern Bering Sea. Trained observers identified and assessed 2887 egg cases in a wide range of fisheries across all gear types, with the majority of egg cases being encountered on vessels targeting deepwater species, such as the arrowtooth flounder (*Atheresthes stomias*), Greenland halibut (*Reinhardtius hippoglossoides*), Pacific cod (*Gadus macrocephalus*), and sablefish (*Anoplopoma fimbria*). A large proportion of the egg cases identified were reported on boats using bottom trawling gear, but an even greater proportion were reported on longliners. Egg cases identified represent 10 skate taxa. Over half (67%) of them were identified as Alaska skate (*Bathyraja parmifera*), and 19% were identified as either Aleutian skate (*B. aleutica*) or Bering skate (*B. interrupta*). More than 42% of all the egg cases assessed were viable (contained a living skate); over 50% of egg cases of Alaska skate and of egg cases encountered on longliners were viable. The highest concentrations of egg cases generally were reported near known skate nursery areas, particularly in the Bering, Pribilof, and Pervenets Canyons.

Manuscript submitted 28 June 2018.
Manuscript accepted 29 October 2018.
Fish. Bull. 117:8–14 (2019).
Online publication date: 21 November 2018.
doi: 10.7755/FB.117.1.2

The views and opinions expressed or implied in this article are those of the author (or authors) and do not necessarily reflect the position of the National Marine Fisheries Service, NOAA.

Skates (Rajiformes) form an important and diverse component of the ichthyofauna in the eastern Bering Sea (EBS). At least 12 species of skates are currently known to occur in the EBS (Stevenson et al., 2007), and the overall biomass of skates in this region is currently estimated at about 600,000 metric tons (Ormseth, 2017). On the EBS shelf, the skate fauna is dominated by the Alaska skate (*Bathyraja parmifera*), which accounts for over 90% of the skate biomass at depths <200 m (Stevenson et al., 2008). In the deeper waters of the EBS outer shelf and upper continental slope, skate diversity increases as other species, such as the Aleutian skate (*B. aleutica*), Bering skate[1] (*B. interrupta*), mud skate (*B. taranetzi*), Commander skate (*B. lindbergi*), and whiteblotched skate (*B. maculata*), are encountered more frequently (Hoff, 2016). The continental slope of the EBS is an area of particularly high skate diversity, and as many as 7 species have been encountered in a single haul (Stevenson et al., 2008).

Skates are oviparous, depositing their eggs in egg cases on the seafloor. In the Bering Sea, several species of skates congregate in small, localized nursery areas along the outer continental shelf and upper slope to deposit their eggs (Hoff, 2008, 2010). These sites may reach densities of 800,000 eggs/km^2, are occupied by skates continuously throughout the year, and have been persistently used by skates for decades (Hoff, 2010). For at least some species of skates, the incubation time from egg deposition to hatching may be 3–4 years (Hoff, 2008), and hatchlings are relatively large (14–25 cm in total length) and fully developed (Hoff, 2009). These early life history characteristics, combined with the adult characteristics of large size, slow growth, late maturation, and low fecundity, make skates particularly vulnerable to both natural and anthropogenic disturbances (Dulvy et al., 2000; Frisk et al., 2005; Matta and Gunderson, 2007).

Alaska's marine ecosystems are highly productive, supporting numerous fisheries for benthic and

[1] We recognize *Bathyraja kincaidii* on the west coast of North America as a species distinct from *B. interrupta* in Alaska waters; therefore, we retain the common name Bering skate, rather than sandpaper skate, for this species (see Ebert, 2003; Stevenson et al., 2007).

benthopelagic species, such as walleye pollock (*Gadus chalcogrammus*), Pacific cod (*Gadus macrocephalus*), sablefish (*Anoplopoma fimbria*), and several species of rockfishes (Scorpaenidae) and flatfish (Pleuronectidae). Although they are not targeted, significant numbers of skates are encountered as bycatch in a number of the fisheries of Alaska, particularly the longline fishery for Pacific cod (Stevenson and Lewis, 2010). These fisheries regularly encounter skate egg cases, in addition to adult and juvenile skates (senior author, personal observ.; North Pacific Observer Program[2]). Egg cases are brought to the surface when they are captured in trawl nets or entangled in longline gear. Egg cases captured during fishing operations are generally returned to the sea. Unknown are the proportion of captured egg cases that contain viable embryos and the mortality associated with viable eggs that are subjected to capture and subsequent release by fisheries.

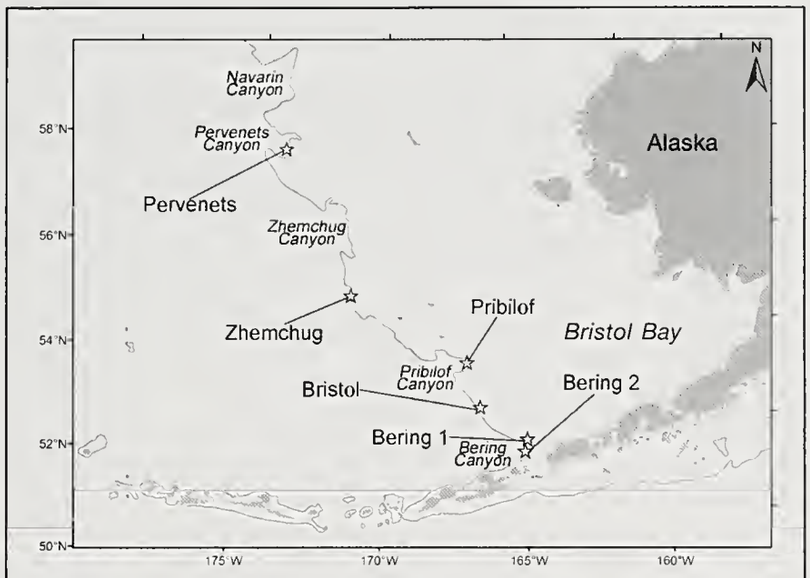

Figure 1

Map of the eastern Bering Sea, showing locations (open stars) of skate nursery areas designated as habitat areas of particular concern and the 200-m isobath.

At least 26 nursery areas for 6 species of skates have been identified in the EBS (Rooper et al., in press). These sites are located along the outer continental shelf and upper slope, at depths ranging from ~150 m to 1069 m. In 2015, the North Pacific Fishery Management Council designated 6 of the known skate nursery areas in the EBS (Fig. 1) as habitat areas of particular concern (HAPC), suggesting that these areas "are rare and provide an important ecological function" (Federal Register, 2015). Although this designation did not provide any protection for these 6 HAPC, it included a recommendation that the National Marine Fisheries Service monitor these sites for potential effects of fishing. The overall goal of this study was to provide additional information on fishery interactions with skate egg cases and skate nursery areas in the EBS, by using data collected by fishery observers in the North Pacific Observer Program. Specifically, the objectives of this study were 1) to identify the species of skates for which fisheries encounter eggs, 2) to determine the proportion of skate eggs encountered by fisheries that are viable, and 3) to identify potentially unknown nursery areas by determining the location of viable skate eggs encountered by fisheries relative to documented skate nursery areas.

Materials and methods

All data used in this study were collected by fishery observers in the North Pacific Observer Program, which monitors commercial fishing activity in the federal waters of the U.S. exclusive economic zone of the North Pacific Ocean, Gulf of Alaska, Aleutian Islands, and EBS. All vessels over 12 m (40 ft) in length that participate in federally managed commercial groundfish fisheries are required to carry a fishery observer for at least a portion of their fishing activity. Observers record data on fishing effort and catch composition, using a variety of subsampling methods depending on gear type and logistical constraints, as detailed in the sampling manual produced annually by the program (AFSC[3]). To the extent possible, observers identify sampled individuals of all federally managed groups (e.g., rockfish, flatfish, skate) to the species level and other species to the family level. Skate egg cases appearing in observer samples are counted and recorded simply as *skate egg case unidentified*, regardless of species or condition.

Data collection for this study was restricted to the EBS and occurred from 15 November 2014 through 15 November 2017. During this period, over 500 experienced observers were trained in the species-level identification of skate egg cases. Trainees were issued several tools for the identification of skate egg cases, including a dichotomous key, a picture guide, and a length-width chart. They were also given data forms, on which they were instructed to record observer name, gear type, cruise number, permit number, haul, date, species, total number non-viable, total number viable, and comments. An egg case was considered viable if it contained a yolk mass or a skate embryo in any

[2] North Pacific Observer Program. 2018. Unpubl. data. North Pac. Obs. Program, 7600 Sand Point Way NE, Seattle, WA 98115.

[3] AFSC (Alaska Fisheries Science Center). 2016. 2017 observer sampling manual, 585 p. Fish. Monit. Anal. Div., North Pac. Groundfish Obs. Program, Alaska Fish. Sci. Cent., Seattle, WA. [Available from website.]

Table 1

Number of egg cases of skates identified by observers aboard commercial fishing vessels in the eastern Bering Sea from November 2014 through November 2017, by gear type and presumed target species.

	Predominant (target) species								
Gear type	Pacific cod	Deepwater flatfish species	Sablefish	Walleye pollock	Pacific halibut	Other flatfish species	Rockfish species	Other	Total
Longline	1514		308	1	17	1		27	1868
Bottom trawl	3	612		39	91	71	59	1	876
Pelagic trawl		5		133		2	1		141
Pot	1		1						2
Total	1518	617	309	173	108	74	60	28	2887

stage of development; an egg case was determined to be non-viable if it was empty or full of sediment. Observers trained for this project recorded species identifications and viability assessments of skate egg cases on data forms, and they turned in their forms during post-cruise debriefing. Ultimately, these data forms were returned to the main office of the North Pacific Observer Program in Seattle.

Only species-level data recorded by project participants were used to create distribution maps for individual species. The position of each haul was determined by the deployment latitude and longitude recorded by the observer in the field. Because observers did not record the target species of commercial fishing operations, the predominant species was used to infer target species for each haul. Nonparametric Mann–Whitney *U* tests were conducted to determine the significance of differences among proportions of egg cases that were viable.

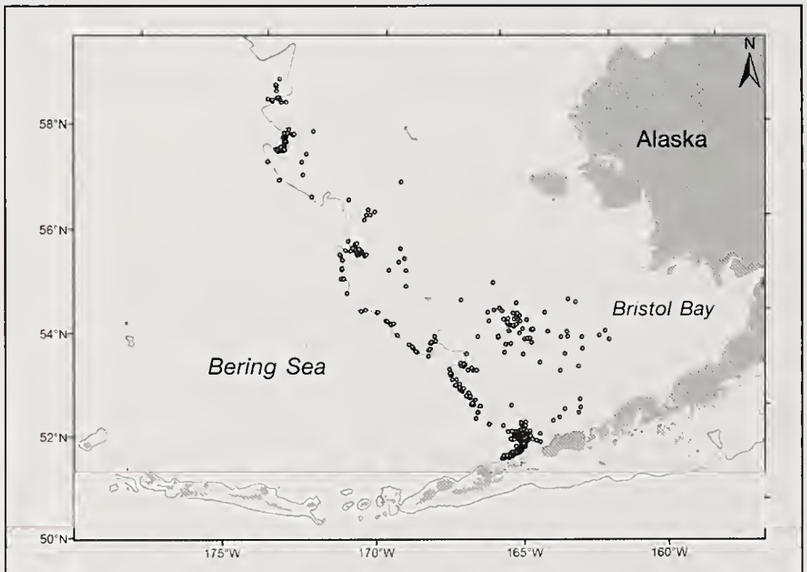

Figure 2

Map of the locations (gray dots) of all hauls from which egg cases of skates were identified and assessed by fishery observers aboard commercial fishing vessels in the eastern Bering Sea from November 2014 through November 2017. The gray line indicates the 200 m isobath.

Results

Fishery observers in the EBS identified and assessed the viability of 2887 skate egg cases from 408 hauls of commercial fishing vessels for this project (Fig. 2). Sampled hauls were distributed broadly across the continental shelf and upper slope, ranging in depth from 45 to 684 m, but they were concentrated near the break between the shelf and slope. The number of egg cases in a single sampled haul ranged from 1 to 204 (mean: 5.4 egg cases), and as many as 3 species of skates were identified from egg cases sampled in a single haul.

Observers identified egg cases from a wide variety of fisheries and gear types, but over half of all egg cases identified for this study were encountered on longline vessels targeting Pacific cod (Table 1). Smaller numbers of egg cases were encountered on vessels using bottom trawling gear, particularly those targeting deepwater flatfish species (arrowtooth flounder, *Atheresthes stomias*, and Greenland halibut, *Reinhardtius hippoglossoides*), and on vessels using pelagic trawls and even pots.

Egg cases identified by observers represent 10 putative taxa (Table 2). Over 67% of egg cases were identified as *Bathyraja parmifera*, and the next most common taxa were *B. aleutica* (12%) and *B. interrupta* (7%). The other 7 taxa combined for the remaining 14% of the identified egg cases. The egg cases of Commander skate and whiteblotched skate are very similar and are extremely difficult to distinguish without magnification. Therefore, for the purposes of this study, the 2 species were combined into a single taxon.

Table 2

Viability of egg cases of skates identified by observers aboard commercial fishing vessels in the eastern Bering Sea from November 2014 through November 2017. Viable egg cases contained a yolk mass or an embryo in some stage of development. Mean percentages of viable egg cases are presented with standard errors (SEs) in parentheses.

Species	Empty	Viable	Viable (%)	Total
Bathyraja parmifera	976	979	50.1 (2.4)	1955
Bathyraja aleutica	259	88	25.4 (3.8)	347
Bathyraja interrupta	157	46	22.7 (4.8)	203
Bathyraja lindbergi/maculata	153	61	28.5 (6.7)	214
Bathyraja minispinosa	92	36	28.1 (6.9)	128
Bathyraja abyssicola	16	7	30.4 (7.9)	23
Bathyraja taranetzi	6	3	33.3 (16.7)	9
Raja rhina	4	0	0	4
Bathyraja trachura	2	1	33.3 (33.3)	3
Amblyraja hyperborea	1	0	0	1
Total	1666	1221	42.3 (1.8)	2887

Approximately 42% of egg cases assessed by observers were classified as viable, although viability proportions were not uniform across species or gear type. For most species, viability proportions ranged from about 20% to 30% (Table 2), but the proportion for egg cases of Alaska skate was significantly higher ($P<0.0001$). Among gear types, over half (53.9%) of egg cases assessed on longline vessels were classified as viable (Table 3), but the percentages of egg cases that were viable for the 2 types of trawling gear were significantly lower ($P<0.0001$). The sample sizes for several species and from boats using pot gear were too low to provide credible estimates of viability.

Most of the egg cases identified by observers as *B. parmifera*, *B. aleutica*, or *B. interrupta* were concentrated near the 6 nursery areas designated as HAPC. Egg cases of Alaska skate were the most broadly distributed, with high concentrations caught near the Bering 1, Pribilof, and Pervenets sites (Fig. 3A). Additional high concentrations were reported in the northern part of Pribilof Canyon and the southern part of Zhemchug Canyon. Egg cases of Aleutian skate were concentrated near the Bering 2 and Pervenets sites, with very few reported in other areas (Fig. 3B). Egg cases of Bering skate were encountered primarily near the Pervenets site, although some were also reported near the Bristol site and farther south in Bering Canyon (Fig. 3C). Observers identified large numbers (20 or more) of egg cases of Alaska skate in 18 separate hauls, but egg cases of Aleutian skate and Bering skate were recorded in large numbers much less frequently (1 and 2 hauls, respectively). The other 2 taxa that were identified in moderate numbers (*B. minispinosa* and the taxon for individuals that could be *B. lindbergi* or *B. maculata*) were reported primarily from the southern rim of Bering Canyon, near the eastern Aleutian Islands.

Table 3

Viability by gear type for egg cases of skates identified and assessed by observers aboard commercial fishing vessels in the eastern Bering Sea from November 2014 through November 2017. Viable egg cases contained a yolk mass or an embryo in some stage of development. Mean percentages of viable egg cases are presented with standard errors (SEs) in parentheses.

Gear type	Empty	Viable	Viable (%)	Total
Longline	861	1008	53.9 (2.7)	1868
Bottom trawl	697	178	20.3 (2.2)	876
Pelagic trawl	106	35	24.8 (4.5)	141
Pot	2	0	0	2
Total	1666	1221	42.3 (1.8)	2887

Discussion

The results of this study indicate that the egg cases of a variety of skate species are regularly encountered in the commercial fisheries of Alaska. These encounters are most common in the canyon areas of the EBS, near the shelf break, at depths favored by skates for egg deposition (Hoff, 2008, 2010). Therefore, fisheries for relatively deepwater species, such as the arrowtooth flounder, Greenland halibut, Pacific cod, and sablefish, are more likely to encounter egg cases of skates than fisheries for relatively shallow-water species, such as walleye pollock and small flatfish species.

A somewhat surprising result of this study was the relatively high number of egg cases of skates reported on vessels fishing with longline gear. It is clear that a trawl sweeping the seafloor would collect the egg cases

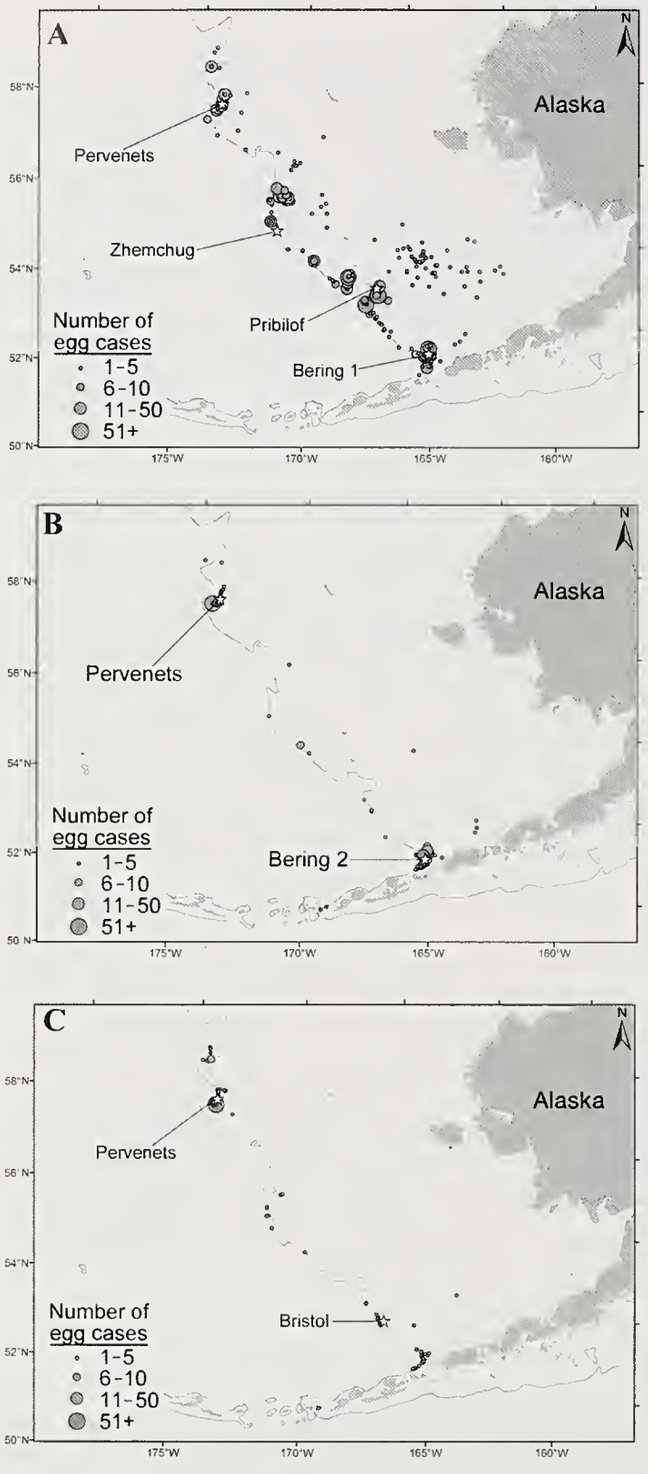

Figure 3

Maps of the geographic distribution of skate egg cases (gray circles) identified as (**A**) Alaska skate (*Bathyraja parmifera*), (**B**) Aleutian skate (*B. aleutica*), and (**C**) Bering skate (*B. interrupta*) by fishery observers aboard commercial fishing vessels in the eastern Bering Sea from November 2014 through November 2017. Open stars represent skate nursery areas designated as habitat areas of particular concern. The gray lines indicate the 200-m isobath.

that it sweeps over; however, longline gear catches fish by attracting them to bite baited hooks, an action skate egg cases obviously cannot take. Still, although longline gear does not sweep the seafloor in the same way that trawling gear does, the groundline of a longline gear can move considerable distances across the bottom, under the influence of currents or large hooked fish and during gear retrieval (High[4]). As a result, sessile benthic organisms, such as corals and sponges, are commonly caught with longline gear (Durán Muñoz et al., 2011; Sampaio et al., 2012), and clearly skate egg cases fall into this category as well. In fact, the structure of egg cases—with long, curled horns on the ends and sticky byssal threads attached along the margins (Stevenson et al., 2007), adaptations that presumably keep them from being swept into less favorable areas by bottom currents—makes them ideally suited to cling to passing lines and hooks as well as to other egg cases. These results indicate that the effects of longline fishing on skate nursery areas may be similar to the effects of bottom trawling.

The relative abundance of skate egg cases identified to the species level by observers in this study is consistent with abundance patterns reported for adult skates in the EBS. The Alaska skate is by far the most abundant skate on the EBS shelf, accounting for 95% of the overall skate abundance at depths <200 m (Stevenson et al., 2008; Stevenson and Lewis, 2010), and it is also by far the most common species of egg case identified by observers in this study. In the deeper waters of the continental shelf and upper continental slope, other species of skates, such as the Aleutian, Bering, Commander , and whiteblotched skates, become more abundant (Stevenson et al., 2008), and egg cases of these species were identified with regularity by observers in this project.

Both for the taxon that combined the Commander and whiteblotched skates and for *B. minispinosa*, over 80% of all the egg cases identified for this study were reported by a single observer on a single cruise, indicating the possibility that the abundance of these taxa may be inflated by misidentification. Likewise, a small number of egg cases were identified by observers as deepsea skate (*B. abyssicola*), and one egg case was identified as an Arctic skate (*Amblyraja hyperborea*, previously known as *A. badia* in the North Pacific). Both of those species are extremely rare in the Bering Sea and are found only in very deep water (Stevenson et al., 2007). Because none of these specimens were photographed or collected for species verification, the possibility remains that they could have been misidentified.

Less than half of the egg cases examined by observers in this study were classified as viable; therefore, most of the fishery interactions documented here involved empty egg cases. However, for one spe-

[4] High, W. L. 1998. Observations of a scientist/diver on fishing technology and fisheries biology. AFSC Proc. Rep. 98-01, 48 p. Alaska Fish. Sci. Cent., Natl. Mar. Fish. Serv., Seattle, WA. [Available from website.]

cies (Alaska skate) and one gear type (longline), over half of the egg cases were assessed as viable. For all other species and gear types, the proportion of egg cases that were viable was no more than 30%. This discrepancy may indicate that more fishing activity is occurring near the central portion of nursery areas used by Alaska skate than near those used by other species and that longline vessels are fishing closer to these areas than trawlers.

Hoff (2010) found that skate nursery areas generally consist of small areas with a high percentage of viable eggs surrounded by larger areas of predominantly (>70%) empty egg cases; therefore, fishing activity near these high-density areas of nursery sites lead to interactions with higher proportions of viable eggs. However, this difference in viability proportion among gear types may be at least partially due to sampling artifacts. Egg cases captured in trawls may be subjected to very different forces than egg cases pulled up on a longline. Skate embryos can be expelled from their egg cases during capture and gear retrieval, and it can be difficult to determine whether a particular egg case was empty when encountered by the fishing gear or it had an embryo that was squeezed out at some point between capture and assessment. Therefore, without additional information on the relative expulsion rate of skate embryos from egg cases captured in different gear types, it is difficult to interpret the differences in viability rates presented here for egg cases captured with different gear types.

For viable egg cases, the mortality rate of skate embryos brought to the surface by fishing gear is unknown. In fact, discard mortality even for adult skates is not well known, although recent studies have begun to examine at least the short-term mortality of skate bycatch (see review by Ellis et al., 2017). Skate embryos of viable egg cases caught in fishing gear may suffer increased mortality for a number of reasons, including hook puncture, thermal stress, barotrauma, and crushing and concussive stress. Even if they are not injured directly, discarded egg cases may be displaced several kilometers or more from the nursery area, leaving them more vulnerable to predation and possibly exposing them to environmental conditions that are developmentally suboptimal or even lethal.

The majority of egg cases identified for this study were encountered near documented skate nursery areas, particularly the nursery areas designated as HAPC. Egg case densities at these sites can be as high as 800,000 eggs/km^2 (Hoff, 2008, 2010), and nursery areas cover several square kilometers of seafloor. Therefore, fishing operations conducted near these sites are expected to encounter high concentrations of egg cases. Concentrations of egg cases for Alaska skate were reported in 2 additional areas well away from all nursery areas designated as HAPC. One of these areas of concentration, in the southern part of Zhemchug Canyon, is near a known nursery area for Alaska skate that has not been designated as an HPAC (Rooper et al., in press), likely explaining the abundance of egg cases in that area. The other area of concentration, in the northwestern part of Pribilof Canyon, is not near any known nursery area for Alaska skate, although 2 nursery areas for other species (*B. minispinosa* and the deepsea skate) are known in this area (Rooper et al., in press). This area of concentration of egg cases may indicate the presence of an additional nursery area for Alaska skate that has not yet been documented.

The overall number of egg cases reported by observers, and the locations of those encounters, indicate that fishing gear is being deployed in and around skate nursery areas, including those designated as HAPC. Clearly, skate embryos of viable egg cases caught in fishing gear are exposed to increased mortality rates. However, fishing activities have a variety of both short- and long-term effects on benthic marine communities (Auster et al., 1996; Auster and Langton, 1999), including the disturbance and redistribution of sediments and benthic organisms as well as the outright physical impacts on organisms contacted, but not captured by, fishing gear. In addition, although some types of benthic habitat are more vulnerable than others and some types of fishing gear are more damaging than others (Grabowski et al., 2014; Hiddink et al., 2017), the effects of any fishing gear on skate nursery areas have not been assessed. Therefore, fishing activity may be causing additional mortality to embryos not recorded in catch statistics, and the overall effects of fishery interactions with skate egg cases and nursery areas are still largely unknown.

Skate populations in the EBS appear to be healthy, and their overall biomass has been stable over the past 30 years (Hoff, 2006; Ormseth, 2017). However, significant community shifts in skate assemblages are not necessarily accompanied by declines in overall biomass (Dulvy et al., 2000; Stevens et al., 2000), and the slow growth and low reproductive potential exhibited by most skates (Ebert, 2005; Ebert et al., 2008) make them particularly vulnerable to environmental disturbance. Therefore, a cautious approach to the management and conservation of skate species is warranted. Previous work has documented the prevalence of adult skates commonly caught as bycatch in commercial fisheries (Stevenson and Lewis, 2010), and this study documents the interactions of fisheries with the early life history stages of skates and their nursery habitats. The mortality associated with fishing activities and the long-term effects of fishing pressure on the skate populations of the EBS are difficult to quantify. However, the potential for fishing activities to have significant detrimental effects on skate species exists, and this study emphasizes the need to continue monitoring these interactions, both with adults and with skates in early life history stages.

Acknowledgments

This research was supported by grant no. 1404 from the North Pacific Research Board. We thank the ob-

servers, trainers, and staff of the North Pacific Observer Program for their cooperation and facilitation of this project. J. Ferdinand, R. Lauth, and B. Mason reviewed earlier drafts of this manuscript.

Literature cited

Auster, P. J., R. J. Malatesta, R. W. Langton, L. Watting, P. C. Valentine, C. L. S. Donaldson, E. W. Langton, A. N. Shepard, and W. G. Babb.
1996. The impacts of mobile fishing gear on seafloor habitats in the Gulf of Maine (Northwest Atlantic): implications for conservation of fish populations. Rev. Fish. Sci. 4:185–202.

Auster, P. J., and R. W. Langton.
1999. The effects of fishing on habitat. Am. Fish. Soc. Symp. 22:150–187.

Dulvy, N. K., J. D. Metcalfe, J. Glanville, M. G. Pawson, and J. D. Reynolds.
2000. Fishery stability, local extinctions, and shifts in community structure in skates. Conserv. Biol. 14:283–293.

Durán Muñoz, P., F. J. Murillo, M. Sayago-Gil, A. Serrano, M. Laporta, I. Otero, and C. Gómez.
2011. Effects of deep-sea bottom longlining on the Hatton Bank fish communities and benthic ecosystem, northeast Atlantic. J. Mar. Biol. Ass. U.K. 91:939–952.

Ebert, D. A.
2003. Sharks, rays, and chimaeras of California, 297 p. Univ. Calif. Press, Berkeley, CA.
2005. Reproductive biology of skates, *Bathyraja* (Ishiyama), along the eastern Bering Sea continental slope. J. Fish Biol. 66:618–649.

Ebert, D. A., W. D. Smith, and G. M. Cailliet.
2008. Reproductive biology of two commercially exploited skates, *Raja binoculata* and *R. rhina*, in the western Gulf of Alaska. Fish. Res. 94:48–57.

Ellis, J. R., S. R. McCully Phillips, and F. Poisson.
2017. A review of capture and post-release mortality of elasmobranchs. J. Fish Biol. 90:653–722.

Federal Register.
2015. Fisheries of the exclusive economic zone off Alaska; skates management in the Bering Sea and Aleutian Islands Management Area; habitat areas of particular concern. 80:1378–1379. [Available from website.]

Frisk, M. G., T. J. Miller, and N. K. Dulvy.
2005. Life histories and vulnerability to exploitation of elasmobranchs: inferences from elasticity, perturbation and phylogenetic analyses. J. Northwest Atl. Fish. Sci. 35:27–45.

Grabowski, J. H., M. Bachman, C. Demarest, S. Eayrs, B. P. Harris, V. Malkoski, D. Packer, and D. Stevenson.
2014. Assessing the vulnerability of marine benthos to fishing gear impacts. Rev. Fish. Sci. Aquacult. 22:142–155.

Hiddink, J. G., S. Jennings, M. Sciberras, C. L. Szostek, K. M. Hughes, N. Ellis, A. D. Rijnsdorp, R. A. McConnaughey, T. Mazor, R. Hilborn, et al.
2017. Global analysis of depletion and recovery of seabed biota after bottom trawling disturbance. Proc. Natl. Acad. Sci. U.S.A. 114:8301–8306.

Hoff, G. R.
2006. Biodiversity as an index of regime shift in the eastern Bering Sea. Fish. Bull. 104:226–237.
2008. A nursery site of the Alaska skate (*Bathyraja parmifera*) in the eastern Bering Sea. Fish. Bull. 106:233–244.
2009. Skate *Bathyraja* spp. egg predation in the eastern Bering Sea. J. Fish Biol. 74:250–269.
2010. Identification of skate nursery habitat in the eastern Bering Sea. Mar. Ecol. Prog. Ser. 403:243–254.
2016. Results of the 2016 eastern Bering Sea upper continental slope survey of groundfish and invertebrate resources. NOAA Tech. Memo. NMFS-AFSC-339, 242 p.

Matta, M. E., and D. R. Gunderson.
2007. Age, growth, maturity, and mortality of the Alaska skate, *Bathyraja parmifera*, in the eastern Bering Sea. Environ. Biol. Fish. 80:309–323.

Ormseth, O. A.
2017. Partial assessment of the skate stock complex in the Bering Sea and Aleutian Islands *In* Stock assessment and fishery evaluation report for the groundfish resources of the Bering Sea/Aleutian Islands regions, p. 1045–1054. North Pacific Fishery Management Council, Anchorage, AK. [Available from website.]

Rooper, C. N., G. R. Hoff, D. E. Stevenson, J. W. Orr, and I. B. Spies.
In press. A predictive model for skate nursery habitat in the eastern Bering Sea. Mar. Ecol. Prog. Ser.

Sampaio, I., A. Braga-Henriques, C. Pham, O. Ocaña, V. de Matos, T. Morato, and F. M. Porteiro.
2012. Cold-water corals landed by bottom longline fisheries in the Azores (north-eastern Atlantic). J. Mar. Biol. Ass. U.K. 92:1547–1555.

Stevens, J. D., R. Bonfil, N. K. Dulvy, and P. A. Walker.
2000. The effects of fishing on sharks, rays, and chimaeras (chondrichthyans), and the implications for marine ecosystems. ICES J. Mar. Sci. 57:476–494.

Stevenson, D. E., and K. A. Lewis.
2010. Observer-reported skate bycatch in the commercial groundfish fisheries of Alaska. Fish. Bull. 108:208–217.

Stevenson, D. E., J. W. Orr, G. R. Hoff, and J. D. McEachran.
2007. Field guide to sharks, skates, and ratfish of Alaska, 85 p. Alaska Sea Grant Coll. Prog., Univ. Alaska Fairbanks, Fairbanks, AK.
2008. Emerging patterns of species richness, diversity, population density, and distribution in the skates (Rajidae) of Alaska. Fish. Bull. 106:24–39.

National Marine Fisheries Service
NOAA

Fishery Bulletin
established in 1881

Spencer F. Baird
First U.S. Commissioner of Fisheries and founder of *Fishery Bulletin*

At-vessel and postrelease mortality rates of bluefin tuna (*Thunnus thynnus*) associated with pelagic longline gear in the northern Gulf of Mexico

Eric S. Orbesen (contact author)
Craig A. Brown
Derke Snodgrass
Joseph E. Serafy
John F. Walter III

Email address for contact author: eric.orbesen@noaa.gov

Southeast Fisheries Science Center
National Marine Fisheries Service, NOAA
75 Virginia Beach Drive
Miami, Florida 33149-1003

Abstract—Bluefin tuna (*Thunnus thynnus*) of the western Atlantic Ocean are often incidentally caught in the pelagic longline fishery that targets swordfish (*Xiphias gladius*) and yellowfin tuna (*Thunnus albacares*) in the Gulf of Mexico. Data on at-vessel and postrelease mortality are lacking. Using the database of the NOAA Southeast Fisheries Science Center's Pelagic Observer Program, we estimated the mortality rate occurring at-vessel to be 54% (95% confidence interval [CI]: 46–62%) when the currently mandated weak circle hook (with a reduced diameter ≤3.65 mm) was used. To estimate rates of postrelease mortality, we deployed 41 pop-up satellite archival tags (PSATs) on bluefin tuna captured in the pelagic longline fishery operating in the northern Gulf of Mexico from May 2010 through April 2015. Data from the PSATs indicate that 29 fish survived for at least 30 d and that 4 fish died within 12 d of tagging. Six PSATs detached prior to the programed release date, and 2 PSATs did not report. We estimate a postrelease mortality rate between 12% and 29%. Combining the postrelease mortality estimate with the at-vessel mortality rate, we estimate a total mortality rate of 59% (95% CI: 47–71%) associated with capture and subsequent release of bluefin tuna in this fishery according to its current fishing practices.

Manuscript submitted 8 May 2018.
Manuscript accepted 14 November 2018.
Fish. Bull. 117:15–23 (2019).
Online publication date: 12 December 2018.
doi: 10.7755/FB.117.1.3

The views and opinions expressed or implied in this article are those of the author (or authors) and do not necessarily reflect the position of the National Marine Fisheries Service, NOAA.

The bluefin tuna (*Thunnus thynnus*) is the largest member of the family Scombridae and has a specialized cardiovascular physiology that allows it to exploit subarctic to subtropical pelagic waters (Carey and Lawson, 1973; Block et al., 2005). Bluefin tuna of the western Atlantic Ocean forage in the North Atlantic Ocean, and many of them migrate to the Gulf of Mexico (GOM) (Mather et al., 1995; Block et al., 2005; Knapp et al., 2014) to spawn, although spawning is not exclusive to the GOM (Mather et al., 1995; Richardson et al., 2016). Bluefin tuna can be found in the GOM from December through July, but the timing can vary with oceanographic conditions (Block et al., 2005; Teo et al., 2007; Galuardi et al.; 2010). During these months, bluefin tuna are incidentally caught by the U.S. pelagic longline (PLL) fleet, which targets swordfish (*Xiphias gladius*) and yellowfin tuna (*Thunnus albacares*) in the northern GOM (Springer, 1957).

Currently, the bluefin tuna in the GOM is managed as an incidental bycatch species, and no active targeting of it is allowed. As a result, various management actions have either required or resulted in substantial numbers of fish released alive or discarded dead. Beginning in 1981, the National Marine Fisheries Service (NMFS) prohibited directed fisheries for bluefin tuna on the GOM spawning grounds and established quotas for the fishery (Federal Register, 1981). To further reduce the incentive to target bluefin tuna, the NMFS enacted target species catch requirements for bluefin tuna retention (Federal Register, 1992). In 2011, the NMFS mandated that all U.S. PLL vessels fishing in the GOM use a *weak hook* with a reduced wire diameter (i.e., ≤3.65 mm) (Federal Register, 2011). A weak hook is a circle hook designed to allow a bluefin tuna and other similarly large animals to straighten the hook, thereby reducing their catch by more than 50% while not significantly reducing the catch of target species (Foster and Bergmann[1]). Additional measures were taken in 2006 with the

[1] Foster, D., and C. Bergmann. 2010. 2010 interim report: update on Gulf of Mexico pelagic longline bluefin tuna mitigation research, 11 p. [Available from Harvesting Eng. Branch, Southeast Fish. Sci. Cent., Natl. Mar. Fish. Serv., 3209 Frederic St., Pascagoula, MS 39567.]

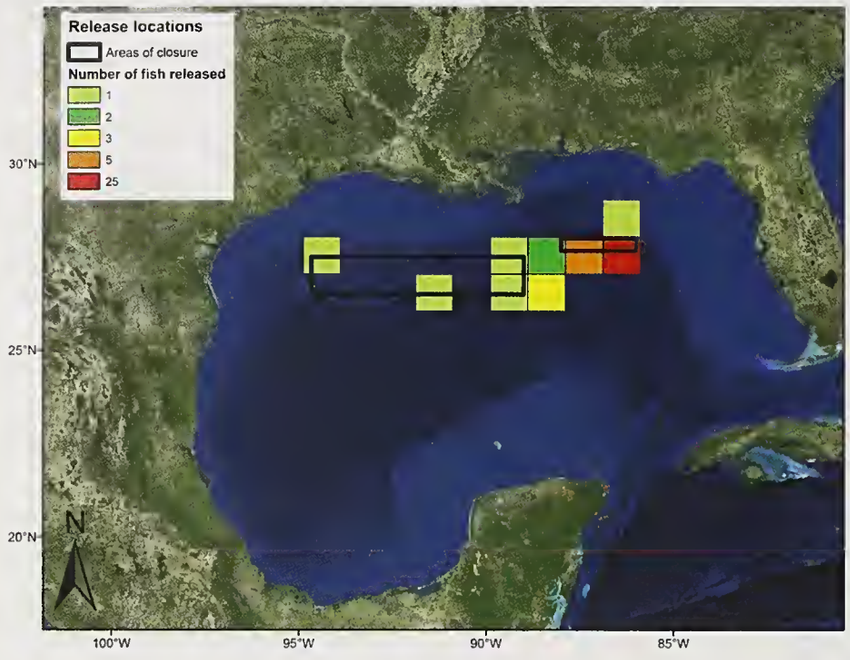

Figure 1

Spatial distribution of release locations for bluefin tuna (*Thunnus thynnus*) tagged with pop-up satellite archival tags in the pelagic longline fishery of the Gulf of Mexico from 2010 through 2015. Data for the number of fish released are presented in 1° grids of density. The 2 open rectangles indicate the areas closed to the use of pelagic longline gear during April and May. Sources for satellite image: Esri, DigitalGlobe, GeoEye, Earthstar Geographics, CNES/Airbus DS, USDA, USGS, AeroGRID, IGN, and the GIS user community.

implementation of Amendment 7 to the Consolidated Atlantic Highly Migratory Species Fishery Management Plan (Federal Register, 2014), which created a system to assign individual quotas for bluefin tuna to vessels and closed 2 areas that cover the majority of the spawning habitat of bluefin tuna in the northern GOM to the use of PLL gear during the peak spawning months of April and May (Fig. 1). The closure of these areas, in conjunction with the requirement to use weak hooks, has greatly reduced total discards of dead bluefin tuna.

The effectiveness of management measures that require or promote release of fish hinges on 2 components of mortality associated with interactions with fishing operations. The first component of mortality is the fraction of fish dead at-vessel upon retrieval of the gear, and the second component is the fraction of fish that die after being released. At-vessel mortality and survival have been documented from commercial longline fishing operations for several species of billfishes, tunas, and sharks (Serafy et al., 2012a; Walter et al., 2012; Musyl et al., 2015) but have yet to be quantified for bluefin tuna in the GOM PLL fishery. Similarly, the second component, postrelease mortality from fishing operations, has been quantified for bluefin tuna from recreational fisheries (Marcek and Graves, 2014; Goldsmith et al., 2017) and for other species on PLL operations (Kerstetter et al., 2003; Musyl et al., 2011a) but has not been evaluated for bluefin tuna from the U.S. GOM PLL fishery operating under normal fishing conditions.

Both components of mortality are necessary to determine the total mortality associated with fishing interactions and to evaluate the efficacy of management regulations (Coggins et al., 2007) designed to promote release of live fish. Mortality from fishing operations can have a substantial effect on populations; therefore, it is critical to consider such mortality in population assessments (Musyl et al., 2015).

For this study, we quantified both components of mortality associated with interactions of bluefin tuna with the U.S. GOM PLL fishery. We first examined the database of the NOAA Southeast Fisheries Science Center's Pelagic Observer Program (POP) to determine an at-vessel mortality rate as a function of several covariates. Next we electronically tagged bluefin tuna caught incidentally by the U.S. PLL fishery in the GOM to obtain estimates of postrelease mortality that apply to the fishery operating under normal commercial fishing practices. Fish were tagged from commercial fishing vessels, and all live fish captured, regardless of apparent condition, were tagged. Finally, we combined the results of our tagging study with the proportion of bluefin tuna reported dead at-vessel from the POP database to determine an overall mortality estimate for interactions of bluefin tuna with PLL gear in the GOM.

Materials and methods

Examination of Pelagic Observer Program database

The POP deploys NMFS-trained observers on a portion of PLL vessel trips to collect details on gear configuration, catch composition, and environmental conditions (for further details about observer protocols, see the training manual available from the Southeast Fisheries Science Center at website). To perform analyses similar to those used by Serafy et al. (2012a), we used a logistic regression to examine data for the influence of several key variables on the probability of mortality of 1498 bluefin tuna captured in the GOM PLL fishery during 1993–2017. For the logistic regression, we used the PROC GENMOD procedure in SAS/STAT[2] software

[2] Mention of trade names or commercial companies is for identification purposes only and does not imply endorsement by the National Marine Fisheries Service, NOAA.

(vers. 9.4; SAS Institute, Inc. Cary, NC). The following model was applied:

$$Mortality = H_i + D_j + T_k + C_l + S_m + L_n, \quad (1)$$

where mortality = the probability of a fish being dead at-vessel;
H = the i^{th} type of hook used (circle hook, J-hook, weak hook);
D = the j^{th} maximum hook depth (in the water column, meters);
T = the k^{th} target species (swordfish, tuna, mixed);
C = the l^{th} sea-surface temperature (SST, in degrees Celcius, measured by the vessel during gear deployment);
S = the m^{th} soak duration (time from last hook deployed to first hook retrieved); and
L = the n^{th} fish length (straight fork length, in centimeters).

All factors were modeled as continuous variables with the exception of hook type and target species. To test for an effect of hook type on mortality, least square means were generated as estimates of mortality for each hook type.

Tagging

From 2010 through 2015, we deployed 41 PAT-Mk10 pop-up satellite archival tags (PSATs; Wildlife Computers, Inc., Redmond, WA) on bluefin tuna captured on PLL vessels fishing in the GOM (Fig. 1). These PSATs were programmed to archive pressure (depth), ambient temperature (in degrees Celsius), and light intensity every 10 s. Each PSAT was equipped with a corrodible *burn pin* that detaches the tag on a preprogrammed date (90–365 d) or when the PSAT has been at a constant depth (±5 m) for a 24-h period, indicating that either the tag is no longer attached to the animal or the animal has died. Upon detachment of a tag, profiles of depth and temperature and proportions of time spent in 14 user-defined depth (time at depth) and temperature (time at temperature) bins were summarized into 1-h (4 PSATs) or 4-h (37 PSATs) periods and transmitted through the Advanced Research and Global Observation Satellite system. For those cases in which the tag was physically recovered (11 PSATs), the full archival data set was obtained and analyzed.

All PSATs were equipped with a surgical-grade, nylon toggle anchor and an RD-1800 (Wildlife Computers, Inc.), a device designed to sever the PSAT link before hydrostatic pressure damages the tag (typically at a depth of approximately 1800 m). The tether rigging had 3 variations over the course of this study. The tags deployed in 2010 and 2011 (5 PSATs) were equipped with double-crimped monofilament tethers. In a concurrent study on yellowfin tuna, several tags were recovered with visible teeth marks on the PSAT and float, raising a concern that monofilament might result in an increase in attachment failures (C. Brown, unpubl. data); therefore, in 2012 tethers were constructed from stainless steel cable (22 PSATs). However, during a failed tagging attempt, a PSAT fell overboard. This PSAT, which was still equipped with a stainless steel tether, was observed to be negatively buoyant. Subsequent buoyancy testing indicated that rigged PSATs were very sensitive to small changes in weight, and the previous design with a double-crimped tether also resulted in tags being negatively buoyant. All subsequently deployed tags (14 PSATs) were rigged with a single-crimped monofilament tether, to allow the PSAT to float with the tether attached, and each of these PSATs was checked for positive buoyancy prior to deployment.

All PSATs were deployed by NMFS-trained observers aboard commercial fishing vessels that targeted yellowfin tuna with PLL gear in the GOM between the months of February and May of each year (2010–2015). Observers were given strict guidance to tag any live bluefin tuna, regardless of condition. When a fish was released by using methods similar to those of a normally operating PLL vessel, care was taken so that the fish remained in the water for tagging, and the hook, for the most part, was not removed.

Operational changes

A study of PLL gear that employed a design with alternating hook types found that a new 16/0 weak hook could reduce catches of bluefin tuna in the GOM PLL fishery by an estimated 56.5% (Foster and Bergmann[1]) from levels observed when a typical circle hook was used. In that study, hook timers, devices that measure the total time a fish spends hooked on a line, were attached to a portion of the gangion. The results of that study led the NMFS to mandate the use of these weak hooks in the GOM PLL fishery, and this regulation went into effect in 2011 (Federal Register, 2011). Prior to this rule being enacted, fish tagged in 2010 (4 fish) were captured by using regular-strength 16/0 circle hooks. In 2012, tags were deployed in conjunction with a continuation of the weak hook study (30 fish). For fish captured on a leader with an accompanying hook timer, total time on the line was obtained. All remaining fish were deployed on PLL sets by using the 16/0 weak hook (7 fish).

Determination of mortality

Postrelease mortality mostly has been estimated to occur shortly after release because of acute injury (Muoneke and Childress, 1994; Stokesbury et al., 2004; Wilson et al., 2005). However, delayed mortality due to loss of ability to feed or infection can occur several days to weeks postrelease (Burns and Froeschke, 2012). Although increasing the duration of monitoring beyond several days allows the incorporation of delayed mortalities, there is a risk of confounding results with mortality unassociated with the initial cap-

ture event (e.g., with mortality caused by predation). Consequently, some researchers have restricted their analysis to the first 5–10 d after tagging (Graves et al., 2002; Kerstetter et al., 2003; Horodysky and Graves, 2005; Marcek and Graves, 2014); however, given the relatively low natural mortality rate of adult bluefin tuna relative to other species (Fromentin and Powers, 2005), we extended the time frame from 5–10 d to 30 d, following Stokesbury et al. (2011). The penalty for use of a longer time frame is that natural (and fishing) mortality begins to bias estimates of release mortality, but it would be highly unlikely (0.8% chance) for a bluefin tuna to not survive 30 d because of natural mortality, given the currently assumed natural mortality rate for bluefin tuna (0.1/year; ICCAT, 2017).

Any fish that appeared to live past this 30-d threshold was determined to have successfully survived the capture event. Wilson score intervals and 95% confidence intervals (CIs) were calculated for the binomial proportions (Wilson, 1927). The standard method for determining mortality by using PSATs involves inferring mortality from behavior of the fish as recorded by the tag. Below, we outline this method; however, in this study, we had to address an added complication. To distinguish between a mortality event and a premature tag release, we considered whether a tag floated after it was shed by a fish or it remained on a dead fish until it reached either the release depth of the RD-1800 device or the programmed tag release time. Given the ability of bluefin tuna to swim at high rates of speed (Wardle et al., 1989) and because fish remained in the water for tagging that occurred at night often on poorly lit vessels and varying states of sea conditions, some premature tag shedding was likely to have occurred in our study, and it is commonly observed in most PSAT tagging studies (Musyl et al., 2011b). The negative buoyancy associated with some of the deployed tags complicates the interpretation of the recorded depth data because a tag attachment failure would result in the tag sinking in a similar fashion to a dead fish. In all, 27 of the 41 deployed PSATs were negatively buoyant.

Despite the negative buoyancy of those tags, we were able to distinguish between likely premature release of a tag and a fish mortality by calculating the sinking rates for each of the 10 prematurely released tags and comparing these rates to the rate (0.251 m/s) for the tag that was dropped overboard (the reference tag). In addition, there was an apparent mortality of a bluefin tuna that was tagged with a positively buoyant PSAT and tether; the sinking rate calculated for this tag was 0.408 m/s, a rate that is over 60% faster than the rate of the reference tag. Assuming that all dead fish would sink at a faster rate than the reference tag, we classified each tag according to whether it likely sunk because of a premature release (sinking rate<rate of reference tag) or because of a fish mortality (sinking rate>rate of reference tag). Fish were then assigned to 1 of 4 categories on the basis of the observed behavior of the fish as recorded by the tag: 1) survived (consistent vertical movement for ≥30 d), 2) mortality (fish was at large for <30 d, tag detachment occurred at a depth ≥1200 m, and the sinking rate was >0.251 m/s), 3) tag attachment failure (fish was at large for <30 d, and the tag was positively buoyant and detached at a depth <1200 m, or the tag was negatively buoyant and detachment occurred at a depth ≥1200 m, but the sinking rate was <0.251 m/s), and 4) non-reporting tag (tag failed to transmit any data).

To account for the uncertainty of the eventual fate of fish that were equipped with tags that either failed to report or failed to remain attached for ≥30 d, we calculated the mortality rate by using 2 methods. One method used this expression that includes the number of fish assigned to 3 of the 4 categories, yielding the highest possible mortality estimate: (mortality+tag attachment failure+non-reporting tag)/total number of tags deployed. The other method used the following expression: mortality/(survived+mortality). The first method assumes that all fish in the tag attachment failure and non-reporting tag categories were dead fish, but the second effectively considers that tag data for fish in the non-reporting tag or tag attachment failure categories are uninformative and discards those fish from the sample.

Estimation of overall mortality

Overall mortality (M) was calculated as the probability of a mortality occurring during the entire capture and release process. It is calculated as the probability of being dead at-vessel ($P(C)$) times the probability of dying after being released ($P(R)$):

$$M = P(C) \times P(R). \quad (1)$$

The variance of estimates from this equation was derived as the variance of the product of 2 assumed uncorrelated random variables (Goodman, 1960).

Results

Pelagic Observer Program database

The results of the logistic regression found that only one variable of the independent model, hook type, significantly (P<0.05) affected the probability of at-vessel mortality for bluefin tuna (Table 1). Therefore, we report the least square means as estimates of at-vessel mortality rate for the 3 hook types, standard (strong) circle hook (65%, 95% CI: 57–72%), J-hook (68%, 95% CI: 56–78%), and the currently mandated weak hook (54%, 95% CI: 46–62%).

Tagging

From 2010 to 2015, 41 adult bluefin tuna from PLL vessels were tagged with Wildlife Computers PSATs in the GOM (Table 2). The size range of the 41 bluefin tuna was 190–270 cm straight fork length (Table 2),

Table 1

Results of logistic regression examining the influence of hook type, target species, sea-surface temperature (SST), soak duration, straight fork length (SFL), and maximum hook depth on the probability of at-vessel mortality of 1498 bluefin tuna (*Thunnus thynnus*) captured in the pelagic longline fishery of the Gulf of Mexico during 1993–2017.

Variable	Estimate	Standard error	*P*-value
Standard circle hook	−0.464	0.129	<0.001
J-hook	−0.602	0.224	0.007
Weak circle hook	0.000	0.000	–
Mixed target	0.090	0.131	0.493
Swordfish	−0.354	0.473	0.454
Yellowfin tuna	0.000	0.000	–
SST	−0.021	0.015	0.149
Soak duration	−0.035	0.040	0.382
SFL	−0.001	0.002	0.374
Maximum hook depth	0.0046	0.010	0.711

and they were tagged in the months of February–June at SSTs ranging from 21.8°C to 29.7°C. Representing fish that successfully survived the fishery interaction, 29 PSATs remained attached for at least 30 d. Ten PSATs failed to reach the 30 d threshold, and 2 additional PSATs failed to transmit any data.

Tagged fish at large for fewer than 30 days

Ten PSATs began transmitting data less than 30 d after tagging (1–18 d). Six of these tags were equipped with tethers that we identified as negatively buoyant. Four tags sunk at a rate greater than the rate of the reference tag (0.251 m/s); therefore, the fish tracked with those tags were put in the mortality category (Table 3). Three tags had sinking rates that were slower than the rate of the reference tag, indicating likely tag attachment failures and not observed mortalities. The remaining 3 tags were equipped with positively buoyant tethers, detached from the fish at a depth <1000 m, and floated to the surface, indicating tag attachment failures.

Postrelease mortality

An upper bound estimate of postrelease mortality was obtained by treating all fish with tags that either did not report (2 PSATs) or failed to attach (6 PSATs) as potential dead fish (12 of 41 fish tagged with PSATs), giving a maximum postrelease mortality estimate of 29% (95% CI: 18–44%). Assuming that these non-reporting tags and tags that failed to remain attached were not associated with fish mortalities, and, therefore, that the fish tagged with them were removed from the sample, we determined that the most likely estimate of postrelease mortality is 12% (95% CI: 5–27%) (i.e., 4 of 33 PSATs associated with mortalities).

Hook timers

Twelve tagged fish were captured on leaders that included a hook timer, which measures the length of time a fish is on the line prior to crew engagement (Table 2). Tag data indicates an apparent mortality for only 1 fish captured on a line with a hook timer (8.3 h attached to a longline). Three additional tagged fish were associated with either attachment failures (2 PSATs) or their tag failed to report (1 PSAT). The remaining 8 PSATs were deployed on surviving fish with an average time on the line of 7.4 h (2.2–14.4 h).

Overall mortality

We estimated the probability of a mortality of a bluefin tuna occurring as a result of an interaction with, and release from, PLL gear in the GOM, using Equation 1 with the most likely estimate of postrelease mortality (12%, 95% CI: 5–27%) as $P(R)$ and $P(C)$ obtained from the logistic regression model predicted for fishing with weak hooks (54%, 95% CI: 46–62%). The resulting overall estimate of the probability of capture-induced mortality of bluefin tuna in the GOM PLL fishery, operating as it currently does with weak hooks, is 59% (95% CI: 47–71%).

Discussion

On the basis of the data presented in this study, we estimated postrelease mortality of bluefin tuna from PLL fishery operations in the GOM at a range of 12–29%, depending on the treatment of the non-reporting or premature release of tags. The highest estimates of mortality were obtained when all non-reporting tags were assumed to be associated to a mortality event. However, we considered that there is a sound basis for eliminating fish with non-reporting tags from the sample. Our non-reporting rate for this study is relatively low (5%) in comparison to the rates of other studies (Musyl et al., 2011b). Furthermore, with an RD-1800 device attached to its tether, a PSAT would detach from a sinking, dead fish before it reached the tag crush depth, making it unlikely that non-reporting was a result of such a mortality. Non-reporting, therefore, was the result of either equipment failure or damage (perhaps, due to predation) (Musyl et al., 2011b), with neither cause being informative on mortality due to a capture event. Given that we can separate attachment failures from mortalities by examining sinking rates, we removed fish associated with both non-reporting tags and attachment failures from the sample to provide what we believe is a more accurate postrelease mortality estimate of 12%. Under either assumption regarding the fate of malfunctioning tags, the postrelease mortality estimates are relatively low (12–29%), indicating that,

Table 2

Summary information for electronically tagged bluefin tuna (*Thunnus thynnus*) and the corresponding data for the pelagic longline set during which each fish was captured in the Gulf of Mexico from 2010 through 2015. An en dash indicates unknown or unrecorded data. SFL=straight fork length.

Tag number	Estimated SFL (cm)	Estimated weight (kg)	Tagging date	No. of monitoring days	Tagging depth (cm)	Time on line (h)	Hook location	Hook removed	Length of remaining leader (m)	Weak circle hook	No. of hooks per set	Hook depth (m)	Soak duration (h)
10A0919	240	227	4/15/2012	–	23	1.3	Upper jaw	No	1.2	No	425	97	5.9
11A0898	240	–	5/20/2013	–	23	–	Hinge	No	<0.3	Yes	420	97	9.4
10A0921	220	227	5/10/2011	2	25	–	Hinge	No	2.1	Yes	500	91	8.6
11A0914	270	295	3/20/2012	3	28	8.3	–	No	3	No	430	95	6.3
10A0917	240	227	4/26/2012	3	23	1.1	Hinge	No	0.9	Yes	445	97	6.4
10A1041	210	–	3/23/2012	7	23	–	Hinge	No	1.2	Yes	355	82	6.3
10A0915	270	272	3/28/2012	7	25	–	–	No	2.4	Yes	438	95	7.2
10A0896	210	–	5/10/2012	10	25	–	Hinge	No	0.9	Yes	590	82	5.8
10A1042	270	340	5/25/2012	10	23	–	Hinge	No	1.5	No	410	97	8.9
11A0981	150	181	4/21/2015	12	23	–	–	No	–	Yes	472	97	7.2
10A1030	195	–	5/11/2012	15	25	–	Hinge	No	0.6	No	520	82	7.1
10A0931	240	–	4/10/2012	18	23	4.6	–	No	0.6	No	610	82	5.5
10A0930	240	227	4/26/2012	32	23	–	Hinge	No	1.2	No	445	97	6.4
10A0938	210	–	3/28/2012	40	23	–	Hinge	No	0.6	No	520	82	4.9
10A1035	210	170	5/23/2012	42	23	2.8	Hinge	No	1.2	Yes	410	97	10.0
10A1047	210	–	4/12/2013	42	23	–	Hinge	No	<0.3	Yes	702	73	8.5
11A0978	210	–	5/18/2012	43	25	–	Hinge	No	0.9	No	530	82	7.7
10A0942	240	204	5/13/2012	48	23	–	Hinge	No	0.9	No	445	97	7.8
10A0939	240	227	4/25/2012	50	23	–	Hinge	No	0.6	No	445	97	8.0
10A0946	240	204	5/16/2012	53	23	–	Hinge	No	0.9	No	445	97	8.1
10A0898	240	227	3/1/2012	54	25	–	–	No	4.6	Yes	590	95	7.5
11A0963	195	–	4/9/2012	55	23	7.3	Hinge	Yes	–	Yes	630	82	6.5
10A0945	240	227	5/14/2012	57	23	–	Hinge	No	1.2	No	445	97	8.3
10A0916	270	295	3/22/2012	61	28	11.7	Hinge	No	2.1	No	425	95	5.7
10A0775	210	181	4/26/2012	63	23	–	Upper jaw	No	0.9	No	445	97	8.0
10A0918	240	227	4/25/2012	64	23	1.8	Hinge	No	0.9	Yes	445	97	8.0
10A0928	225	–	3/28/2013	70	28	–	Hinge	Yes	–	Yes	876	66	8.6
10A1045	240	204	4/9/2012	70	23	12.9	Hinge	No	0.3	–	460	97	6.5
11A0969	225	–	5/20/2012	81	25	6.5	Hinge	No	1.8	Yes	505	82	6.1
11A0949	240	227	5/24/2012	82	23	–	Hinge	No	0.9	No	410	97	8.1
11A0950	240	204	5/24/2012	84	23	–	Upper jaw	No	0.9	Yes	410	97	8.1
10A1032	190	159	5/12/2013	89	23	–	Hinge	No	0.6	Yes	504	82	5.8
08A0152	240	204	5/12/2010	90	15	–	Hinge	No	1.5	No	702	84	7.3
08A0153	260	363	5/22/2010	90	20	–	Hinge	No	–	No	590	82	8.0
08A0155	250	340	5/22/2010	90	20	–	–	No	–	No	590	82	8.0
08A0156	260	363	5/22/2010	90	18	–	Hinge	No	–	No	624	82	7.5
10A0929	240	181	4/24/2012	90	23	2.2	Hinge	No	0.6	No	445	97	6.5
10A0933	210	–	3/19/2012	93	23	14.4	Hinge	No	0.6	No	384	82	8.5
10A1034	210	204	5/14/2013	100	23	–	Hinge	No	3	Yes	588	82	8.4
10A0949	240	227	5/28/2012	116	23	–	Hinge	No	1.2	No	400	97	10.2
10A0943	210	181	5/26/2012	119	23	–	Upper jaw	No	1.5	No	410	97	8.3

if a fish is alive at-vessel, its likelihood of surviving after its release is remarkably good.

It is worth noting the negative buoyancy aspect of the tag harness rigging design. Musyl et al. (2015) emphasized the importance of testing for tag buoyancy with the tether and anchor mechanism attached; however, they found that most researchers failed to indicate whether these tests were conducted prior to tag deployment. Clearly, our study had this issue, and future researchers should take note. It may also be necessary to consider whether some presumed mortalities in prior PSAT studies could actually have been instances when tags equipped with negatively buoyant harnesses were shed.

No other estimates of release survival for bluefin tuna captured in PLL fisheries operating under nor-

Table 3

Summary information for pop-up satellite archival tags that were deployed on bluefin tuna (*Thunnus thynnus*) during 2010–2015 in the Gulf of Mexico and failed to reach the 30-d threshold at which fish were deemed to have survived capture. The rate of descent (sinking rate) was calculated for all negatively buoyant tags that transmitted data. The sinking rates then were compared to the rate of a reference tag (this tag was dropped overboard, and its descent rate indicates the sinking speed of a negatively buoyant tag absent of a fish). Each tagged fish that did not survive was classified in the following categories: non-reporting tag, tag attachment failure (sinking rate<reference tag), or mortality (sinking rate>reference tag).

Tag number	Tether design	Tag buoyancy	Sinking rate (m/s)	Monitoring days	Release depth (m)	Data type	Category
10A0919	Cable tether	Negative	N/A	–	–	N/A	Non-reporting
11A0898	Mono single crimped	Positive	N/A	–	–	N/A	Non-reporting
10A0896	Mono single crimped	Positive	N/A	10	22	Recovered	Attachment failure
10A1042	Mono single crimped	Positive	N/A	10	288	Transmitted	Attachment failure
10A1030	Mono single crimped	Positive	N/A	15	712	Transmitted	Attachment failure
10A0921	Mono double crimped	Negative	0.122	2	1320	Transmitted	Attachment failure
10A0931	Cable tether	Negative	0.224	18	1200	Transmitted	Attachment failure
10A0917	Cable tether	Negative	0.227	3	1546	Recovered	Attachment failure
Reference tag	Cable tether	Negative	0.251	1	1808	Recovered	N/A
10A0915	Cable tether	Negative	0.316	7	1840	Transmitted	Mortality
10A1041	Cable tether	Negative	0.319	7	1850	Recovered	Mortality
11A0914	Cable tether	Negative	0.346	3	1808	Transmitted	Mortality
11A0981	Mono single crimped	Positive	0.408	12	1768	Transmitted	Mortality

mal commercial practices exist. However, a study by Block et al. (2005) that used short experimental sets designed to capture bluefin tuna alive reported an at-vessel mortality rate of 30%, a rate that is nearly 25% lower than the overall nominal rate derived from the POP observer database (54%). Block et al. (2005) postulated that mortality rates of bluefin tuna in the GOM PLL fishery could be a result of asphyxiation due to inability to ram ventilate, thermal stress from confinement in warm surface waters, or other capture related trauma that could be exacerbated by longer time on the line.

Block et al. (2005) used relatively short sets designed to mitigate mortality. In contrast, our study operated under standard commercial fishing operations with an average soak duration of 7.5 h. Hook timer data indicate that fish in our study were on the lines for an average of 6.2 h, a period that is longer than the entire duration of the experimental sets in Block et al (2005). An additional factor related to observed mortality differences could be gear configuration. Although we did not detect significant effects of hook depth or SST on mortality in our analysis of POP data, the experimental design of their study (with a maximum hook depth of 200 m, compared with 97 m in our study; Table 2) could have allowed fish to access deeper, cooler waters and a fish's ability to access such water could have been a mitigating factor for some of the thermal stress that a fish may have experienced. Furthermore, one static SST measurement might not accurately reflect the range of temperatures at the locations where fish encountered the gear throughout sets, and the use of this single measurement could be the reason that we did not detect a significance for SST. Musyl et al. (2009) highlighted the importance of using fishery-specific features when attempting to estimate postrelease survival, and our results support this notion.

Postrelease mortality has been quantified to be relatively low in recreational fisheries (from 0% [95% CI: 0–7%] to 32% [95% CI: 14–55%]) (Goldsmith et al., 2017) and in commercial hand-line and rod-and-reel fisheries in Canada (from 3% [95% CI: 1–13%] to 6% [95% CI: 2–6%]) (Stokesbury et al., 2011). Both sets of authors calculated mortality in 2 ways; hence, separate 95% CIs are given for each estimate. Although these fisheries and the ocean conditions where they occur are very different from those of the GOM, the low rate of postrelease mortality in those studies and in our study indicates that bluefin tuna, if they survive the initial capture process, appear to have a high probability of survival regardless of the gear type used or the geographic region of release.

Nonetheless, the high at-vessel mortality rate that we estimated (54%) for weak hooks in the GOM PLL fishery would diminish the effectiveness of a no-retention policy in reducing fishing mortality and achieving stock status benchmarks (Coggins et al., 2007), in isolation of other measures. The relatively low postrelease mortality from our study, however, does provide support for encouraging live release of bluefin tuna. Currently, live bluefin tuna can either be retained or released with control over the total retention rate through an individual quota system for bluefin tuna, in which vessels are required to have quota of bluefin

tuna available to retain live fish or to account for any dead captures. This management measure is accompanied by a closure of 2 areas in the spring to minimize encounters with bluefin tuna and by the use of weak hooks that facilitate escape.

Mitigation of bycatch of bluefin tuna in PLL fisheries has been a high priority for the NMFS. The results of this study generally indicate that management measures taken by that agency to minimize bycatch of bluefin tuna are effective, measures that reduce the probability of capture of bluefin tuna on a longline and, then, once captured, provide opportunities to vessels to retain dead fish or to release live fish. The currently mandated weak hooks do appear to have some conservation benefits. In our analysis, we observed that at-vessel mortality was 11% lower for weak hooks than for traditionally used circle hooks, and Foster and Bergmann[1] estimated that weak hooks also could reduce the bycatch of bluefin tuna by 56.5%. Gallagher et al. (2017) found a strong correlation of plasma lactate with maximum acceleration of hooked sharks, a correlation indicating that the behavioral response of the fish could influence the probability of mortality. Despite the high probability that we would observe an at-vessel mortality, our hook timer data revealed that it is possible for bluefin tuna to survive after ≥14 h on the line and that the behavioral response of an individual fish might contribute to the probability of its mortality. These findings might explain why we see a reduction in at-vessel mortality associated with the weak hook, with the more vigorous fighters that would likely die on the line able to straighten a weak hook and escape capture. Nevertheless, it is important to note that the at-vessel catch estimate is based on *observed* reduction in bycatch of bluefin tuna and that the actual fate of escapees from weak hooks remains unknown (Serafy et al., 2012b).

Because the degree of injury sustained by fish that straighten their hooks and elude observation has yet to be quantified, the total mortality estimate in our study may be considered conservative. On the other hand, it is possible that survival was enhanced for fish that would have otherwise died on the standard circle hooks because they were spared the prolonged stress and injury of being firmly hooked until gear retrieval. Further research is warranted on this topic; however, determining precisely how to track the survival of fish that have effectively escaped capture by straightening weak hooks is a serious, perhaps insurmountable, research challenge. In any case, on the basis of observed interactions in the POP database, the results of our study indicate that weak hooks provide the additional benefit of increasing at-vessel survival in comparison with standard circle hooks. Further mitigation efforts could be directed to evaluation of factors that might promote an even greater at-vessel survival rate; however, changes in factors, such as gear configuration, set duration, set location, or bait, may negatively affect catches of yellowfin tuna and swordfish, the target species of PLL fisheries in the GOM.

Acknowledgments

We would like to thank J. Sheldon, J. Rollo, and R. Jones for all their hard work and dedication as observers and for deploying many of the tags used in this project. We would also like to thank the captains and crews of the vessels from which we were allowed to tag fish. We thank C. Porch, E. Prince, and J. Hoolihan for their assistance in the design of this study. Lastly, we would like to thank S. Cushner, K. Keene, L. Beerkircher, and D. Foster for assisting in vessel coordination.

Literature cited

Block, B. A., S. L. H. Teo, A. Walli, A. Boustany, M. J. W. Stokesbury, C. J. Farwell, K. C. Weng, H. Dewar, and T. D. Williams.
2005. Electronic tagging and population structure of Atlantic bluefin tuna. Nature 434:1121–1127.

Burns, K. M., and J. T. Froeschke.
2012. Survival of red grouper (*Epinephalus morio*) and red snapper (*Lutjanus campechanus*) caught on J-hooks and circle hooks in the Florida recreational and recreational-for-hire-fisheries. Bull. Mar. Sci. 88:633–646.

Carey, F. G., and K. D. Lawson.
1973. Temperature regulation in free-swimming bluefin tuna Comp. Biochem. Physiol. A. 44:375–392.

Coggins, L. G., Jr., M. J. Catalano, M. S. Allen, W. E. Pine III, and C. J. Walters.
2007. Effects of cryptic mortality and the hidden costs of using length limits in fishery management. Fish Fish. 8:196–210.

Federal Register.
1981. Atlantic bluefin tuna. Fed. Reg. 46:8012–8015.
1992. Atlantic bluefin tuna fishery. Fed. Reg. 57:365–380.
2011. Atlantic highly migratory species; bluefin tuna bycatch reduction in the Gulf of Mexico pelagic longline fishery. Fed Reg. 76:18653–18661.
2014. Atlantic highly migratory species; 2006 consolidated Atlantic highly migratory species (HMS) fishery management plan; amendment 7; final rule. Fed. Reg. 79:71510–71608.

Fromentin, J.-M., and J. E. Powers.
2005. Atlantic bluefin tuna: population dynamics, ecology, fisheries and management. Fish Fish. 6:281–306.

Gallagher, A. J., E. R. Staaterman, S. J. Cooke, and N. Hammerschlag.
2017. Behavioural responses to fisheries capture among sharks caught using experimental fishery gear. Can. J. Fish. Aquat. Sci. 74:1–7.

Galuardi, B., F. Royer, W. Golet, J. Logan, J. Neilson, and M. Lutcavage.
2010. Complex migration routes of Atlantic bluefin tuna (*Thunnus thynnus*) question current population structure paradigm. Can. J. Fish. Aquat. Sci. 67:966–976.

Graves, J. E., B. E. Luckhurst, and E. D. Prince.
2002. An evaluation of pop-up satellite tags for estimating postrelease survival of blue marlin (*Makaira nigricans*) from a recreational fishery. Fish. Bull. 100:134–142.

Goldsmith, W. M., A. M. Scheld, and J. E. Graves.
2017. Performance of a low-cost, solar-powered pop-up

satellite archival tag for assessing post-release mortality of Atlantic bluefin tuna (*Thunnus thynnus*) caught in the US east coast light-tackle recreational fishery. Anim. Biotelem. 5:29.

Goodman, L. A.
1960. On the exact variance of products. J. Am. Stat. Assoc. 55:708–713.

Horodysky, A. Z., and J. E. Graves.
2005. Application of pop-up satellite archival tag technology to estimate postrelease survival of white marlin (*Tetrapturus albidus*) caught on circle and straight-shank ("J") hooks in the western North Atlantic recreational fishery Fish. Bull. 103:84–96.

ICCAT (International Commission for the Conservation of Atlantic Tunas).
2017. Report of the 2017 ICCAT bluefin stock assessment meeting, 91 p. [Available from website.]

Kerstetter, D. W., B. E. Luckhurst, E. D. Prince, and J. E. Graves.
2003. Use of pop-up satellite archival tags to demonstrate survival of blue marlin (*Makaira nigricans*) released from pelagic longline gear. Fish. Bull. 101:939–948.

Knapp, J. M, G. Aranda, A. Medina, and M. Lutcavage.
2014. Comparative assessment of reproductive status of female Atlantic bluefin tuna from the Gulf of Mexico and the Mediterranean Sea. PLoS ONE 9(6):e98233.

Marcek, B. J., and J. E. Graves.
2014. An estimate of postrelease mortality of school-size bluefin tuna in the U.S. recreational troll fishery. North Am. J. Fish. Manage. 34:602–608.

Mather, F. J., III, J. M. Mason Jr., and A. C. Jones.
1995. Historical document: life history and fisheries of Atlantic bluefin tuna. NOAA Tech. Memo. NMFS-SEFSC-370, 165 p.

Muoneke, M. I., and W. M. Childress.
1994. Hooking mortality: a review for recreational fisheries. Rev. Fish. Sci. 2:123–156.

Musyl, M. K., C. D. Moyes, R. W. Brill, and N. M. Fragoso.
2009. Factors influencing mortality estimates in postrelease survival studies. Mar. Ecol. Prog. Ser. 396:157–159.

Musyl, M. K., R. W. Brill, D. S. Curran, N. M. Fragoso, L. M. McNaughton, A. Nielsen, B. S. Kikkawa, and C. D. Moyes.
2011a. Postrelease survival, vertical and horizontal movements, and thermal habitats of five species of pelagic sharks in the central Pacific Ocean. Fish. Bull. 109:341–368.

Musyl, M. K., M. L. Domeier, N. Nasby-Lucas, R. W. Brill, L. M. McNaughton, J. Y. Swimmer, M. S. Lutcavage, S. G. Wilson, B. Galuardi, and J. B. Liddle.
2011b. Performance of pop-up satellite archival tags. Mar. Ecol. Prog. Ser. 433:1–28.

Musyl, M. K., C. D. Moyes, R. W. Brill, B. L. Mourato, A. West, L. M. McNaughton, W.-C. Chiang, and C.-L. Sun.
2015. Postrelease mortality in istiophorid billfish. Can. J. Fish. Aquat. Sci. 72:538–556.

Richardson, D. E, K. E. Marancik, J. R. Guyon, M. E. Lutcavage, B. Galuardi, C. H. Lam, H. J. Walsh, S. Wildes, D. A. Yates, and J. A. Hare.
2016. Discovery of a spawning ground reveals diverse migration strategies in Atlantic bluefin tuna (*Thunnus thynnus*). Proc. Natl. Acad. Sci. U.S.A.. 113:3299–3304.

Serafy, J. E., E. S. Orbesen, D. J. G. Snodgrass, L. R. Beerkircher, and J. F. Walter.
2012a. Hooking survival of fishes captured by the United States Atlantic pelagic longline fishery: impact of the 2004 circle hook rule Bull. Mar. Sci. 88:605–621.

Serafy, J. E., S. J. Cooke, G. A. Diaz, J. E. Graves, M. Hall, M. Shivji, and Y. Swimmer.
2012b. Circle hooks in commercial, recreational, and artisanal fisheries: research status and needs for improved conservation and management. Bull. Mar. Sci. 88:371–391.

Springer, S.
1957. Tuna resources of the tropical and sub-tropical western Atlantic. Trans. Am. Fish. Soc. 85:13–17.

Stokesbury, M. J., S. L. H. Teo, A. Seitz, R. K. O'Dor, and B. A. Block.
2004. Movement of Atlantic bluefin tuna (*Thunnus thynnus*) as determined by satellite tagging experiments initiated off New England. Can. J. Fish. Aquat. Sci. 61:1976–1987.

Stokesbury, M. J. W., J. D. Neilson, E. Susko, and S. J. Cooke.
2011. Estimating mortality of Atlantic bluefin tuna (*Thunnus thynnus*) in an experimental recreational catch-and-release fishery. Biol. Conserv. 144:2684–2691.

Teo, S. L. H., A. Boustany, H. Dewar, M. J. W. Stokesbury, K. C. Weng, S. Beemer, A. C. Seitz, C. J. Farwell, E. D. Prince, and B. A. Block.
2007 Annual migrations, diving behavior, and thermal biology of Atlantic bluefin tuna, *Thunnus thynnus*, on their Gulf of Mexico breeding grounds. Mar. Biol. 151:1–18.

Walter, J. F., E. S. Orbesen, C. Liese, and J. E. Serafy.
2012. Can circle hooks improve Western Atlantic sailfish, *Istiophorus platypterus*, populations? Bull. Mar. Sci. 88:755–770.

Wardle, C. S., J. J. Videler, T. Arimoto, J. M. Franco, and P. He.
1989. The muscle twitch and the maximum swimming speed of giant bluefin tuna, *Thunnus thynnus* L. J. Fish Biol. 35:129–137.

Wilson, E. B.
1927. Probable inference, the law of succession, and statistical inference. J. Am. Stat. Assoc. 22:209–212.

Wilson, S. G., M. E. Lutcavage, R. W. Brill, M. P. Genovese, A. B. Cooper, and A. W. Everly.
2005. Movements of bluefin tuna (*Thunnus thynnus*) in the northwestern Atlantic Ocean recorded by pop-up satellite archival tags Mar. Biol. 146:409–423.

National Marine Fisheries Service
NOAA

Fishery Bulletin
established in 1881

Spencer F. Baird
First U.S. Commissioner of Fisheries and founder of *Fishery Bulletin*

Population structure of the ocellate spot skate (*Okamejei kenojei*) inferred from variations in mitochondrial DNA (mtDNA) sequences and from morphological characters of regional populations

Ryo Misawa (contact author)[1]
Yoji Narimatsu[2]
Hiromitsu Endo[3]
Yoshiaki Kai[1]

Email address for contact author: batoideafish@gmail.com

[1] Maizuru Fisheries Research Station
Field Science Education and Research Center
Kyoto University, Nagahama, Maizuru,
Kyoto 625-0086, Japan

[2] Tohoku National Fisheries Research Institute
Fisheries Research and Education Agency
25-259 Same-machi, Hachinohe,
Aomori 031-0841, Japan

[3] Laboratory of Marine Biology
Faculty of Science and Technology
Kochi University,
2-5-1 Akebono-cho,
Kochi 780-8520, Japan

Abstract—The population structure of the ocellate spot skate (*Okamejei kenojei*), distributed in the western North Pacific, was assessed on the basis of genetic variations in the mitochondrial DNA control region (mtCR) and differences in morphological characters and features. Significant genetic differentiation in mtCR was observed among 6 regional populations along the Japanese Archipelago and Korean Peninsula. Unique haplotypes found in Osaka Bay and off the east coast of Kyushu Island suggested an absence of gene flow from the other 5 regions. In addition, comparisons of morphological characters and features, including measurements, nuchal thorn counts, differences in maturity size, and coloration, indicated that populations of ocellate spot skate from Osaka Bay and from off the Pacific coast of northern Japan were clearly distinguishable from 4 other regional populations. Together with molecular differentiation among the regional populations, they suggest that the straits, ocean currents, and limited migrations are significant barriers to gene flow between populations. Future fisheries management of the species is discussed on the basis of the present findings.

Manuscript submitted 6 July 2018.
Manuscript accepted 26 November 2018.
Fish. Bull. 117:24–36 (2019).
Online publication date: 4 December 2018.
doi: 10.7755/FB.117.1.4

The views and opinions expressed or implied in this article are those of the author (or authors) and do not necessarily reflect the position of the National Marine Fisheries Service, NOAA.

Many elasmobranch fishes (sharks, rays, and skates) are particularly vulnerable to overfishing because of their large size, slow growth, late maturity, and low fecundity (Brander, 1981; Dulvy et al., 2000; Griffiths et al., 2010; Griffiths et al., 2011). These life-history traits translate into low rates of reproduction and low potential rates of population increase (Walker and Hislop, 1998). Elasmobranch fishes are also targeted by fisheries because their meat, fins, and liver oil are commercially valuable (Dulvy et al., 2014; Davidson et al., 2016). In addition, elasmobranch fishes are often caught as bycatch of fisheries that focus on more commercially valuable teleost fish species, such as tunas and demersal fishes (Dulvy et al., 2014). The fishing pressure on elasmobranchs is increasing and therefore their extinction risk and conservation interest are being discussed on a global scale (e.g., Dulvy et al., 2014; Davidson et al., 2016). Shallow-water elasmobranchs particularly have a higher risk of extinction or decrease in population because of their constant exposure to coastal fisheries (Dulvy et al., 2014). The ocellate spot (or spiny) skate *Okamejei kenojei* (family Rajidae) is widely distributed 1) in shallow coastal waters of 20–230 m depth (mainly 30–100 m) in the western North Pacific: 2) from the coastal waters off southern Hokkaido, Japan, southward to waters off northern Taiwan, including 3) along the Pacific coast of Japan; 4) within the Sea of Japan; 5) the East China Sea; and 6) the Yellow Sea (Ishihara, 1987; Hatooka et al., 2013; Last et al., 2016). The age at maturity of the species has been estimated to be about 3 years, and females produce at least 300 egg capsules during

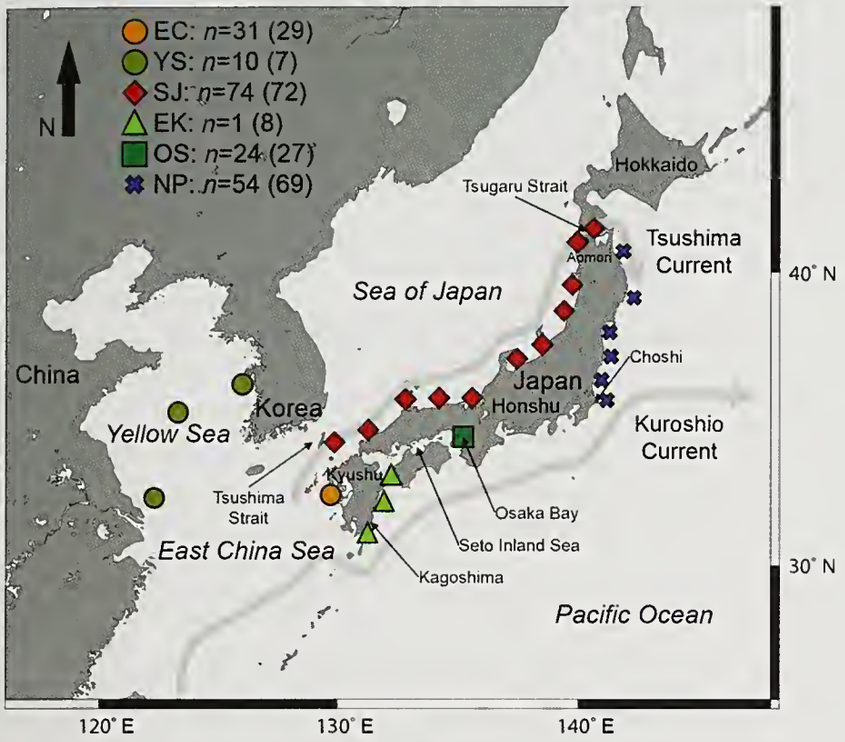

Figure 1

Sampling area and number of examined specimens of *Okamejei kenojei*. Each symbol represents a sampling site. *n*=number of specimens used in mtCR analysis and numbers in parentheses=number of specimens used in morphological comparisons. EC=East China Sea; YS=Yellow Sea; SJ=Sea of Japan; EK=East coast of Kyushu Is.; OS=Osaka Bay; NP=Pacific coast of northern Japan.

their lifetime, although some may produce up to 600 over 4 years (Ishihara et al., 2009). The egg capsules (43–59 mm length) have tendrils on each corner, which anchor the capsules to the seafloor (Ishiyama, 1958).

Skates generally have a low dispersal ability (Vargas-Caro et al., 2017). In fact, previous tagging studies have suggested that some skates have relatively small home ranges (e.g., Walker et al., 1997), and population genetics have also revealed evidence of a local population structure of skates (e.g., Chevolot et al., 2006). Similarly, *O. kenojei* was formerly recognized as two allopatric species, *Raja porosa*, known from the East China Sea, Yellow Sea, Sea of Japan, and the Pacific coast of southern Japan, and *R. fusca*, known from the Pacific coast of northern Japan (Ishiyama, 1967). According to Ishiyama (1967), the nominal forms could be distinguished by differences in external characters, such as snout length, interorbital width, and cranium shape. Later, Boeseman (1979) suggested that *R. porosa* was a junior synonym of *R. kenojei* (=*Okamejei kenojei*), and was followed by Ishihara (1987), who considered both *R. porosa* and *R. fusca* to be junior synonyms of *O. kenojei* owing to similarities in the distributional pattern of ventral sensory pores and similarities in clasper structure. Nevertheless, Ishihara (1987) recognized several morphological variants among local populations, in particular in reference to individuals from the Pacific coast of northern Japan, which were previously recognized as *R. fusca*, i.e., as the "northern form." Ishihara (1987) suggested that the "northern form" differed from forms in other areas in having a bluntly angled and extremely translucent snout, numerous nuchal thorns, and black spots or reticulated patterns scattered over the entire dorsal surface of the disc. Such morphological divergence among local populations has suggested the existence of a complex population structure within the species.

Okamejei kenojei has considerable economic value in Korea and Japan (Ishihara, 1990; Ishihara et al., 2009; Baeck et al., 2011). Domingues et al (2018) suggested that management and conservation policies for shark and ray fisheries should include information on genetic diversity. However, despite the potential population structuring and high economic value of *O. kenojei*, there have been no studies of genetic structure at the population level for this species—information that is crucial for fisheries management and conservation practices. In some skate species, molecular genetic studies have revealed both population structure and demographic history, as well as the existence of cryptic species based on mitochondrial DNA (mtDNA) sequences (e.g., Valsecchi et al., 2005; Chevolot et al., 2006; Griffiths et al., 2010; Griffiths et al., 2011; Spies et al., 2011; Dudgeon et al., 2012; Frodella et al., 2016; Im et al., 2017; Vargas-Caro et al., 2017). The mtDNA control region (mtCR) has been frequently used to infer population structures within species because of the high levels of nucleotide polymorphism evident in several skate species (Valsecchi et al., 2005). In this context, we examined the population structure of *O. kenojei* by analyzing mtCR sequences and morphological variations and present an outline of population boundaries and their connectivity for fisheries management.

Materials and methods

Samples

For the mtCR analysis and morphological comparisons, a total of 293 individuals of *Okamejei kenojei* were collected from six regions along the Japanese Archipelago (regional populations abbreviated as EC (East China Sea); SJ (Sea of Japan); EK (East coast of Kyushu Is.); OS (Osaka Bay); NP (Pacific coast of northern Japan); and YS (Yellow Sea) (Fig. 1; Suppl. Table) (online only). Of these, 194 individuals (EC=31; YS=10; SJ=74; EK=1; OS=24; NP=54) were used for mtCR sequence analysis, 212 individuals (EC=29; YS=7; SJ =72; EK=8; OS=27; NP=69) for morphological comparisons, and 113 indi-

viduals (EC=22; YS=0; SJ=44; EK=1; OS=20; NP=26) for both mtCR analysis and morphological comparisons. The individuals for both mtCR analysis and morphological comparisons only partly overlapped because some of the individuals were in poor condition and could not be used for either of the mtCR analysis or morphological comparisons.

mtCR analysis

Total DNA was extracted from muscle tissue preserved in 99.5% ethanol by using the DNeasy Tissue Kit (Qiagen, Japan) or Wizard Genomic DNA Purification Kit (Promega Corp., Madison, WI[1]), according to the manufacturer's protocols. Polymerase chain reaction (PCR) was performed with the primers ElDloopF (5′-TCC CAA AGC CAA GAT TCT GC-3′) and RajinaeP7r (5′-AAA CTG GGA GGG CTG GAA ATC TTG A-3′) (Valsecchi et al., 2005), which amplified 597 base pairs (bp) of mtCR. The fragment was amplified by using the Veriti Thermal Cycler (Applied Biosystems, Foster City, CA) with 15.1 µL PCR reaction mix, including 8.3 µL of distilled water, 1.5 µL of 10× PCR buffer, 1.2 µL of 2.5 mM dNTPs, 1.5 µL of 5 mM each primer, 0.1 µL of EX-Taq polymerase (TaKaRa Bio Inc., Shiga, Japan) and 1 µL of DNA template or 10.2 µL PCR reaction mix, including 2.2 µL of distilled water, 5 µL of KAPA2G Robust HotStart Ready Mix PCR Kit (KAPA Biosystems, Wilmington, MA), 1 µL of 5 mM of each primer and 1 µL of DNA template. The cycling conditions consisted of an initial denaturation cycle at 94°C for 5 min, followed by 30 cycles at 94°C for 15 s (denaturation), 56°C for 15 s (annealing) and 72°C for 30 s (extension), and a single final extension cycle at 72°C for 7 min. Successful amplification was confirmed by electrophoresis of the PCR products on 1% agarose gel, stained with RedSafe (iNtRON Biotechnology, Seoul, South Korea). The PCR products were purified with ExoSAP-IT (Affymetrix Inc., Santa Clara, CA). DNA sequencing was performed with BigDye Terminator Cycle Sequencing Kit,vers. 1.1, and an ABI Prism 310 Genetic Analyzer (Applied Biosystems). The sequences determined here were deposited in INSDC (International Nucleotide Sequence Database Collaboration) under accession numbers LC386653–LC386846 (Suppl. Table) (online only).

The mtCR sequences were edited with BioEdit, vers. 7.2.5 (Hall, 1999), and aligned with ClustalW interface, available in MEGA 6 (Tamura et al., 2013). A haplotype network was inferred by using the median-joining network method with Network, vers. 5.0.0.1 (Fluxus Technology Ltd, Sudbury, Suffolk, UK). Haplotype diversity (h) and nucleotide diversity (ϖ) were calculated by using Arlequin, vers. 3.5.1.3 (Excoffier and Lischer, 2010). The pairwise F_{ST} values that included information on haplotype frequencies were used for indices of genetic differentiation. The null hypothesis of genetic homogeneity was assessed by 10,000 replications with Arlequin and sequential Bonferroni corrections (Rice, 1989).

Morphological comparisons

Morphological characters were examined after fixation in 10% formalin and preservation in 70% ethanol or 50% isopropanol. For comparisons of coloration among regional populations, photographs of the fresh color of most specimens (before fixation) were taken by digital photography, except for specimens from YS and EK. For morphological comparisons, 13 measurements, those of Last et al. (2008) and Ishiyama (1958), were taken: 1) total length (TL); 2) disc length; 3) disc width; 4) tail length; 5) head length; 6) dorsal snout length; 7) eye diameter; 8) distance between orbits; 9) ventral head length; 10) ventral snout length; 11) prenasal snout length; 12) distance between nostrils; and 13) distance between 1st gill openings. The numbers of nuchal thorns were also counted. Differences in measurements among regional populations were assessed for respective males and females by analysis of covariance (ANCOVA) by using TL as a covariate. A covariance matrix of arcsine-transformed morphometric ratios (with TL as denominator) was prepared for ANCOVA. If significant differences among the regional populations were observed in ANCOVA (P<0.05), post-hoc pairwise comparisons with Holm's adjustment were used to establish differences between individual regional populations. All statistical analyses for morphological comparisons were conducted with R language, vers. 3.1.2 (R Core Team, 2014).

Differences in maturity size or developmental stage among regional populations were estimated from clasper length in males; claspers elongate with growth and are indicative of maturity size and developmental stage (Stehmann, 2002). Following Stehmann (2002), we considered males to be mature if they had both alar and malar thorns and a hard clasper skeleton. The number of rows of tail thorns in females was also compared, the number increasing with growth to a maximum of 5 in the genus *Okamejei* (Ishiyama, 1967; Ishihara, 1987). The number of rows of tail thorns was therefore considered to be indicative of developmental stage. The estimated maturity size in males and females was also assessed by post-hoc pairwise comparisons with Holm's adjustment.

Results

mtCR analyses

The mtCR sequences of 597 base pairs revealed 11 variable nucleotide sites with 10 transitions and 1 transversion, without any deletions and insertions, and a total of 14 haplotypes (haplotype codes were defined as Ok1–14) in 194 individuals. Among the 5 regional

[1] Mention of trade names or commercial companies is for identification purposes only and does not imply endorsement by the National Marine Fisheries Service, NOAA.

Table 1

Genetic diversity indices calculated from mtCR 597 base pairs from 6 regional populations within *Okamejei kenojei*. n=number of individuals sampled; H=number of haplotypes; h=haplotype diversity; π=nucleotide diversity. Range is followed by mean ±standard deviation.

Population	Area	n	H	h	π
EC	East China Sea	31	5	0.6989 ±0.0498	0.0016 ±0.0013
YS	Yellow Sea	10	3	0.5111 ±0.1643	0.0011 ±0.0011
SJ	Sea of Japan	74	7	0.5050 ±0.0654	0.0011 ±0.0010
EK	East coast of Kyushu Is.	1	1	0	0
OS	Osaka Bay	24	2	0.0833 ±0.0749	0.0001 ±0.0003
NP	Pacific coast of northern Japan	54	2	0.2013 ±0.0667	0.0003 ±0.0005
Total		194	14	0.8191 ±0.0137	0.0036 ±0.0022

Table 2

Pairwise F_{ST} (below diagonal) and associated significance (above diagonal) of mtCR 597 base pairs from 5 regional populations (except EK) of *Okamejei kenojei*. +=significant at $P<0.001$ level (after Bonferroni correction). Population abbreviations are given in Table 1.

	EC	YS	SJ	OS	NP
EC		+	+	+	+
YS	0.372		+	+	+
SJ	0.416	0.493		+	+
OS	0.584	0.778	0.634		+
NP	0.592	0.727	0.631	0.838	

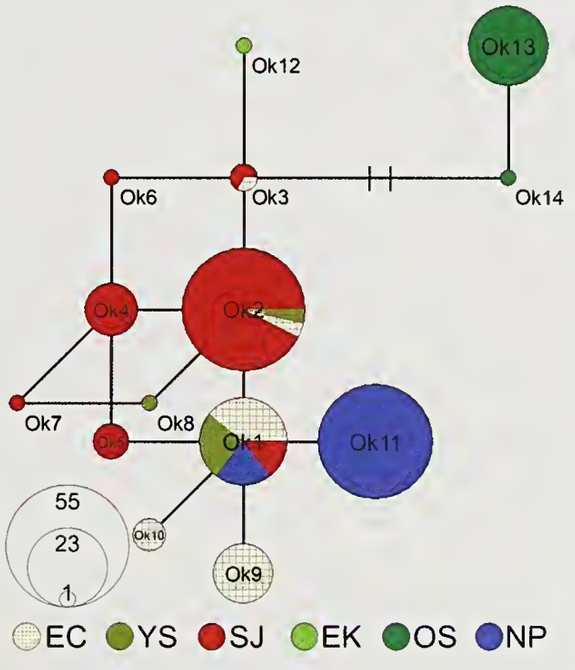

Figure 2

Haplotype network constructed from the mtCR (597 bp) variations of *Okamejei kenojei* from 6 regional populations. Each circle represents a single haplotype. Circle size represents number of individuals. Each bar represents one substitution. Numerals indicate haplotype codes. EC=East China Sea; YS=Yellow Sea; SJ=Sea of Japan; EK=East coast of Kyushu Is.; OS=Osaka Bay; NP=Pacific coast of northern Japan.

populations, except for EK, the number of haplotypes ranged from 2 to 7, and haplotype (h) and nucleotide (π) diversity ranged from 0.0833 to 0.6989 and from 0.0001 to 0.0016, respectively (Table 1). Genetic diversity indices were highest in the EC population, and lowest in the OS population.

Among a total of 14 haplotypes, 11 haplotypes were unique to a regional population (i.e., were private haplotypes), and 5 singletons seen in only one individual (having an unshared haplotype) (Fig. 2). Three haplotypes (Ok1–3) were shared among different regional populations and placed in central positions in the network; one among EC, YS, SJ and NP populations (Ok1), another among EC, YS and SJ (Ok2), and the others between EC and SJ (Ok3). Although most of the haplotypes differed from each other by single substitutions, two unique haplotypes found in the OS population (Ok13 and 14) were characterized by 2 and 3 substitutions, respectively. The frequency of private haplotypes was high, which accounted for 45% (88/194) of all observations (EC=55%, 17/31; YS=10%, 1/10; SJ: 23%, 17/74; EK=100%, 1/1; OS=100%, 24/24; NP=52%, 28/54).

The pairwise F_{ST} values among the five regional populations (except that of EK) ranged from 0.372 to 0.838, and were statistically significant after Bonferroni corrections in all cases ($P<0.001$) (Table 2). The F_{ST} values between OS or NP and the other populations were especially high (OS: 0.584–0.838; NP: 0.592–0.838).

Table 3

Proportional measurements of males (in % of total length) from 6 regional populations of *Okamejei kenojei* and their morphological differentiation significance among populations. Ranges are followed by mean (±standard deviation in parentheses). Numbers under "significance" indicate *P* values in ANCOVA. Populations separated by < are significantly different. NS=not significant. Population abbreviations are given in Table 1.

	EC n=13	YS n=3	SJ n=36	EK n=3	OS n=10	NP n=30	Significance
Total length (mm)	97–408 (258 ±99)	428–455 (441 ±11)	104–453 (334 ±97)	185–390 (271 ±87)	323–435 (409 ±31)	98–566 (376 ±154)	
Disc length	54.0–58.4 (56.7 ±1.2)	54.2–59.0 (56.2 ±2.1)	54.0–61.4 (57.3 ±1.7)	56.6–61.7 (59.1 ±2.1)	55.1–61.1 (57.6 ±1.8)	54.5–60.2 (58.5 ±1.6)	NS
Disc width	63.5–69.9 (67.9 ±2.1)	64.4–70.7 (67.1 ±2.7)	64.2–73.4 (68.1 ±2.7)	65.6–73.5 (69.6 ±3.2)	61.5–72.7 (67.0 ± 3.0)	66.9–74.3 (70.6 ±2.0)	NS
Tail length	48.5–54.4 (50.1 ±1.5)	46.9–50.2 (49.0 ±1.5)	46.2–51.4 (48.5 ±1.2)	45.6–50.8 (47.4 ±2.4)	45.6–49.1 (47.3 ±0.8)	45.7–54.1 (48.1 ±2.5)	NS
Dorsal head length	19.4–23.3 (21.5 ±1.3)	19.0–20.5 (19.8 ± 0.6)	18.9–24.5 (21.1 ±1.5)	21.6–24.5 (22.7 ±1.3)	20.4–23.4 (21.3 ±0.8)	18.0–22.6 (20.6 ±1.0)	NS
Dorsal snout length	12.9–16.8 (15.1 ±1.3)	13.0–13.7x (15.1 ±1.3)	12.5–17.9 (14.4 ±1.3)	14.3–18.1 (15.8 ±1.7)	13.8–16.4 (14.5 ±0.7)	11.9–16.1 (14.2 ±0.9)	NS
Eye diameter	3.0–5.0 (3.7 ±0.6)	2.6–3.4 (2.9 ±0.4)	3.1–4.3 (3.6 ±0.3)	3.4–3.6 (3.6 ±0.1)	2.8–3.5 (3.2 ±0.2)	2.6–4.4 (3.3 ±0.4)	NS
Distance between orbits	4.1–5.2 (4.6 ±0.4)	4.7–5.0 (4.9 ±0.1)	4.3–5.2 (4.8 ±0.2)	3.7–5.1 (4.6 ±0.6)	4.8–5.6 (5.1 ±0.3)	4.9–5.8 (5.3 ±0.2)	< 0.001 [EC, YS, SJ<NP] [SJ<OS]
Ventral head length	26.4–30.5 (29.3 ±1.1)	27.2–29.2 (28.1 ±0.8)	27.2–31.5 (29.5 ±1.1)	29.0–32.8 (29.5 ±1.1)	28.5–31.0 (29.6 ±0.7)	26.0–30.7 (29.0 ±1.1)	NS
Ventral snout length	14.0–17.8 (15.7 ±1.4)	13.0–14.2 (13.5 ±0.5)	12.5–19.1 (14.9 ±1.5)	14.4–18.5 (16.4 ±1.7)	14.2–16.7 (14.7 ±0.7)	11.9–16.5 (14.4 ±1.2)	NS
Prenasal snout length	10.2–14.2 (12.3 ± 1.4)	10.0–10.9 (10.6 ± 0.4)	9.6–15.6 (11.8 ±1.5)	11.5–15.0 (13.4 ±1.4)	11.1–13.3 (11.6 ±0.6)	9.4–13.5 (11.6 ±1.0)	NS
Distance between nostrils	7.0–8.4 (7.8 ±0.4)	7.2–8.2 (7.6 ±0.4)	6.9–8.8 (7.9 ±0.4)	7.6–8.4 (8.0 ±0.3)	7.2–8.3 (7.8 ±0.3)	7.6–9.4 (8.6 ±0.4)	NS
Distance between 1st gill openings	14.1–16.1 (15.0 ±0.6)	13.9–14.8 (14.2 ±0.4)	13.4–17.0 (15.1 ±1.0)	14.1–15.7 (15.1 ±0.7)	13.1–15.1 (14.2 ±0.7)	14.8–17.5 (16.2 ±0.7)	NS

Morphological comparisons

Measurements and count Excluding TL, measurements of 12 characters (1 in males and 11 in females) differed significantly among some of the regional populations (Tables 3 and 4); for example, distance between orbits in males, NP individuals was characterized by a more widely separated orbits than those of other populations (Table 3; Fig. 3C). NP females were easily distinguished from females of other populations in having a broader disc, smaller eye, shorter head and snout, and more widely separated nostrils and gill openings (Table 4; Fig. 3, B, F, H). Furthermore, OS females were also characterized by a smaller eye, and by a longer head and snout than the corresponding features of females of other populations (Table 4; Fig. 3, B and F). Among 4 regional populations (EC, YS, SJ, and EK), EC females had longer tails than females of SJ, SJ females had a shorter head and snout than females of EK, and YS females had a smaller eye than females of EC and SJ (Table 4; Fig. 3, B and F).

Individuals (>ca. 300 mm TL) from NP usually had more than 4 nuchal thorns (range: 3–12) in both sexes, but similar-size individuals from the other 4 populations (except OS) usually had 2 or 3 (range: 2–4) (Fig. 4, A and B). Individuals of both sexes from OS (>ca. 300 mm TL) usually had 2 nuchal thorns (range: 1–3), which were somewhat lower numbers overall than those of other populations. Among smaller specimens of males and females (< ca. 200 mm TL), NP individuals had 2 nuchal thorns, those of other populations having only 1.

Maturity size Clasper length of males fitted a single sigmoid curve against TL (Fig. 5). Specimens with clasper length >24% TL were considered mature because they possessed both alar and malar thorns and hard claspers. The size of mature NP males ranged from 454 to 566 mm TL (average: 493 ±32 mm TL), but between 343 and 455 mm TL (average: 410 ±25 mm TL) in other populations. The estimated maturity size in males differed significantly between NP and other three populations, excluding EK and YS (P<0.05).

Number of rows of tail thorns in females also fitted a single sigmoid curve against TL (Fig. 6, A and B) and were similar to clasper growth. Individuals from

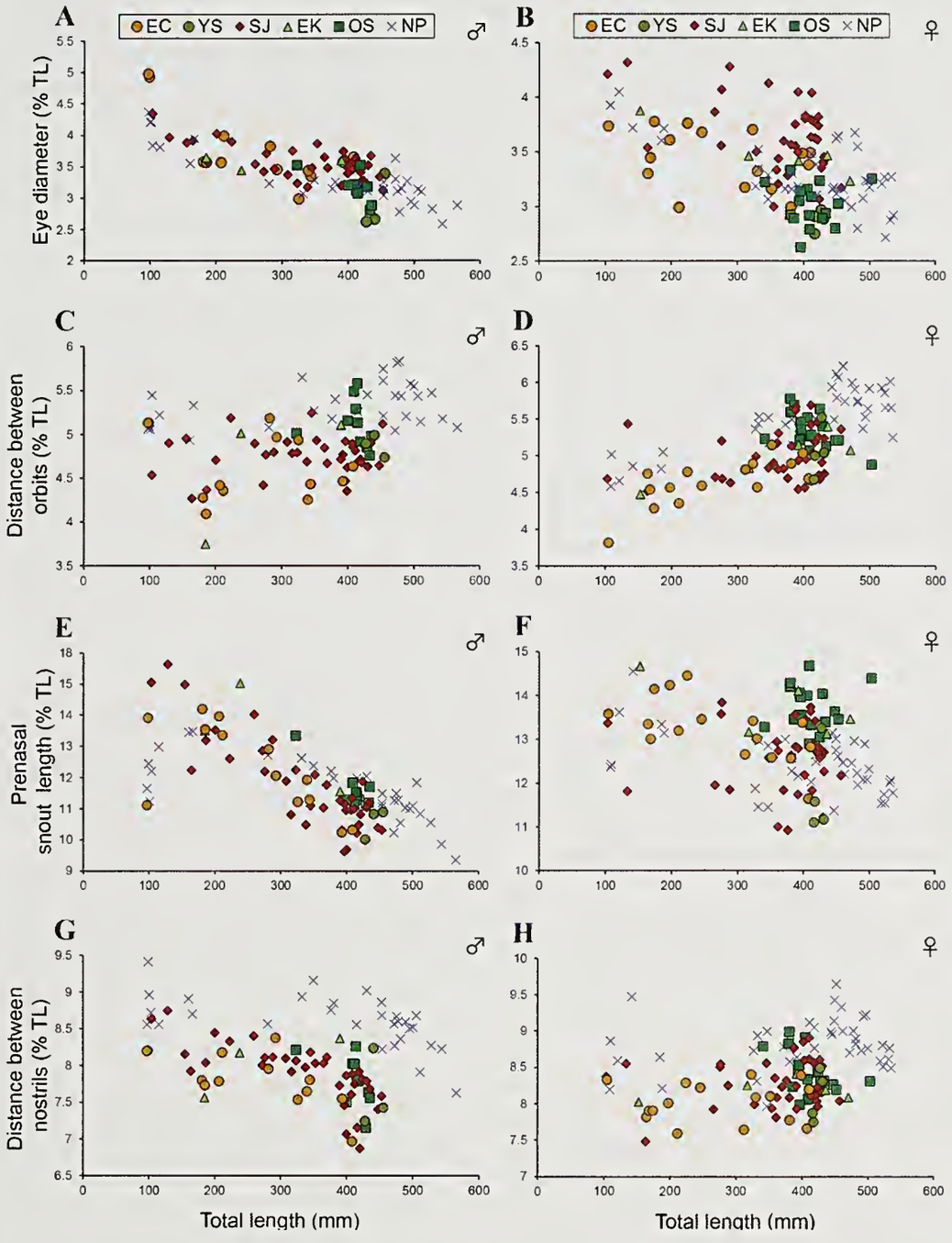

Figure 3

Plots of selected proportional morphometric characters (in % of total length) for 6 regional populations of *Okamejei kenojei*. (**A**, **B**) eye diameter, males and females, (**C**, **D**) distance between orbits, males and females, (**E**, **F**) prenasal snout length, males and females, (**G**, **H**) distance between nostrils, males and females. EC=East China Sea; YS=Yellow Sea; SJ=Sea of Japan; EK=East coast of Kyushu Is.; OS=Osaka Bay; NP=Pacific coast of northern Japan.

NP that had 5 rows of tail thorns ranged between 450 and 536 mm TL (average: 495 ±28 mm TL), but similar individuals from other populations ranged between 288 and 503 mm TL (400 ±37 mm TL), mostly 350–430 mm TL. Given that the specimens with 5 rows of tail thorns were mature, these estimated maturity sizes for females differed significantly between NP and the other 4 populations, excluding EK ($P<0.05$).

Coloration Typical fresh body coloration of 4 regional populations (except YS and EK) observed in the present study was as follows: EC—dorsal surface dark

Table 4

Proportional measurements of females (in % of total length) from 6 regional populations of *Okamejei kenojei* and their morphological differentiation significance among populations. Ranges are followed by mean ±standard deviation in parentheses. Numbers under Significance indicate *P* values in ANCOVA. Populations separated by < are significantly different. NS=nonsignificant. Population abbreviations are given in Table 1.

	EC n=16	YS n=4	SJ n=36	EK n=5	OS n=17	NP n=39	Significance
Total length (mm)	104–410 (275 ±97)	415–430 (422 ±6)	103–457 (362 ±83)	153–471 (354 ±113)	341–503 (411 ±35)	108–536 (398 ±125)	
Disc length	55.3–59.0 (57.4 ±1.1)	55.7–60.8 (57.9 ±2.0)	54.4–61.2 (57.8 ±1.8)	57.1–61.7 (59.6 ±1.4)	56.5–61.1 (59.4 ±1.2)	54.3–64.5 (59.2 ±1.8)	0.001 [EC, SJ<OS, NP]
Disc width	67.8–72.2 (69.8 ±1.5)	67.5–72.7 (70.5 ±2.1)	64.5–73.7 (69.4 ±2.4)	66.7–74.4 (70.9 ±2.7)	67.2–73.0 (69.6 ±1.7)	65.3–78.1 (71.8 ±2.4)	< 0.001 [EC, SJ, OS<NP]
Tail length	45.4–52.1 (48.7 ±1.7)	42.5–47.4 (45.8 ±1.9)	42.0–51.1 (45.8 ±2.3)	43.2–49.9 (45.4 ±2.4)	41.1–46.4 (44.3 ±1.1)	42.9–52.5 (45.8 ±2.3)	< 0.001 [SJ, OS, NP<EC]
Dorsal head length	20.6–24.1 (22.6 ±0.9)	19.3–22.7 (20.5 ±1.3)	19.8–23.9 (21.9 ±0.9)	22.9–24.0 (23.4 ±0.4)	22.0–24.0 (23.0 ±0.7)	19.8–23.7 (21.4 ±0.9)	< 0.001 [EC, EK, OS<NP] [EK, OS<SJ]
Dorsal snout length	14.3–17.6 (15.9 ±0.8)	14.1–16.2 (14.7 ±0.9)	13.4–16.8 (15.3 ±0.9)	16.1–17.3 (16.6 ±0.4)	16.0–17.7 (16.7 ±0.6)	13.8–16.9 (15.1 ±0.7)	< 0.001 [EC, SJ, NP<OS] [EC, EK<NP] [SJ<EK]
Eye diameter	3.0–3.8 (3.4 ±0.3)	2.8–3.0 (2.9 ±0.1)	3.0–4.3 (3.6 ±0.3)	3.2–3.9 (3.5 ±0.2)	2.6–3.3 (3.0 ±0.2)	2.7–4.1 (3.3 ±0.3)	< 0.001 [EC, SJ, NP<YS, OS] [SJ<NP] [EK<OS]
Distance between orbits	3.8–5.1 (4.7 ±0.3)	4.8–5.5 (5.2 ±0.3)	4.5–5.7 (5.0 ±0.3)	4.5–5.4 (5.0±0.3)	4.9–5.8 (5.4 ±0.2)	4.6–6.2 (5.5 ±0.4)	NS
Ventral head length	27.2–31.4 (29.8 ±1.1)	27.9–32.2 (29.2 ±1.8)	27.3–32.0 (29.8 ±1.0)	30.2–31.4 (30.8 ±0.4)	29.6–32.1 (30.7 ±0.7)	26.7–31.7 (29.5 ±1.1)	0.001 [SJ, NP<OS]
Ventral snout length	14.5–18.2 (16.6 ±0.9)	14.0–16.6 (14.9 ±1.0)	13.6–17.7 (15.9 ±0.9)	16.7–18.8 (17.4 ±0.8)	15.8–17.7 (16.8 ±0.5)	13.9–17.5 (15.4 ±0.8)	0.001 [SJ, NP<OS]
Prenasal snout length	11.7–14.5 (13.2 ±0.7)	11.1–13.3 (11.8 ±0.9)	10.9–13.8 (12.6 ±0.7)	13.1–14.7 (13.7 ±0.6)	12.9–14.7 (13.7 ±0.5)	11.4–14.5 (12.4 ±0.7)	< 0.001 [YS, SJ, NP<OS] [EC, EK<NP] [SJ<EK]
Distance between nostrils	7.6–8.4 (8.0 ±0.3)	7.8–8.5 (8.1 ±0.3)	7.5–8.9 (8.3 ±0.3)	8.0–8.4 (8.2 ±0.1)	8.0–9.0 (8.4 ±0.3)	8.0–9.6 (8.8 ±0.3)	< 0.001 [EC, YS, SJ, EK, OS<NP] [EC<OS]
Distance between 1st gill openings	14.8–16.5 (15.6 ±0.5)	14.7–15.9 (15.5 ±0.4)	14.8–18.0 (16.1 ±0.7)	15.2–16.2 (15.6 ±0.4)	14.9–16.1 (15.5 ±0.3)	15.2–18.5 (16.7 ±0.6)	< 0.001 [EC, YS, SJ, EK, OS<NP] [SJ<OS]

brown or chocolate brown with a pair of pale ocelli and several small paler spots, these markings sometimes indistinct (Fig. 7A); SJ—dorsal surface dark, light, or yellowish brown with 2 pairs of pale or whitish ocelli, and several paler or yellowish spots (Fig. 7B); OS —dorsal surface dark brown or chocolate brown with a pair of pale ocelli and several lighter spots, these markings somewhat indistinct (Fig. 7C); NP—dorsal surface dark brown or grayish brown with 2 pairs of light brown and whitish ocelli, and numerous small black specks and several irregular whitish and yellowish spots, and pairs of whitish spots close together on dorsal tail (Fig. 7D).

Discussion

Population structure of ocellate spot skate

Both nucleotide and haplotype variation seen in mtCR sequences occurred at lower levels in the 5 populations of *O. kenojei* (Table 1), than those seen in other demersal bony fishes (Heyden et al., 2010). Low levels of genetic diversity have been frequently reported in other elasmobranchs (e.g. Hoelzel et al., 2006; Cannas et al., 2010; Daly-Engel at al., 2010; Veríssimo et al., 2010; Vargas-Caro et al., 2017), because they exhibit slower rates of genetic evolution than other vertebrates (Martin et al., 1992; Martin, 1999). In addition, Feutry et al. (2014) suggested that mtCR in elasmobranchs could be under higher evolutionary constraints than those of other mitochondrial regions. In the present study, however, the significant F_{ST} indices among the regional populations revealed a fine-scale population structure within *O. kenojei*, clearly indicating the limits of gene flow (Table 2). In fact, 11 of a total of 14 haplotypes were unique to each regional population (Fig. 2, Ok4–14), and the frequency of private haplotypes was high, which accounted for 45% of all observations. The results of the morphological comparisons, including measurements (Tables 3 and 4; Fig. 3), nuchal thorn counts (Fig. 4), sizes at maturity in males and females (Figs. 5 and 6), and coloration (Fig. 7) also almost corresponded with the results from the mtCR

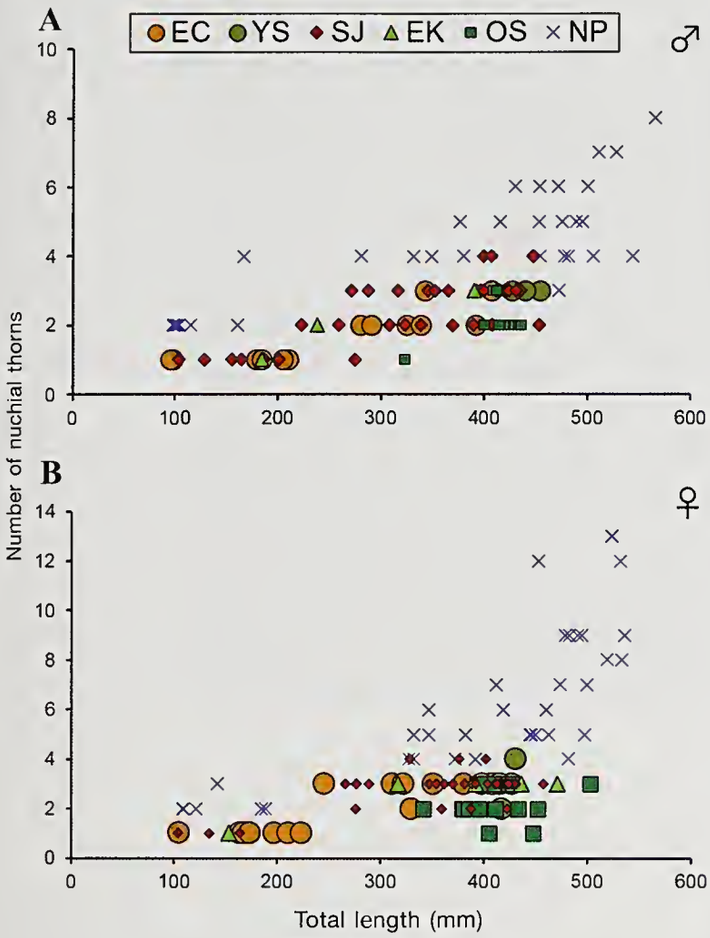

Figure 4

Plots of nuchal thorn numbers from 6 regional populations of *Okamejei kenojei*: (**A**) males, (**B**) females. EC=East China Sea; YS=Yellow Sea; SJ=Sea of Japan; EK=East coast of Kyushu Is.; OS=Osaka Bay; NP=Pacific coast of northern Japan.

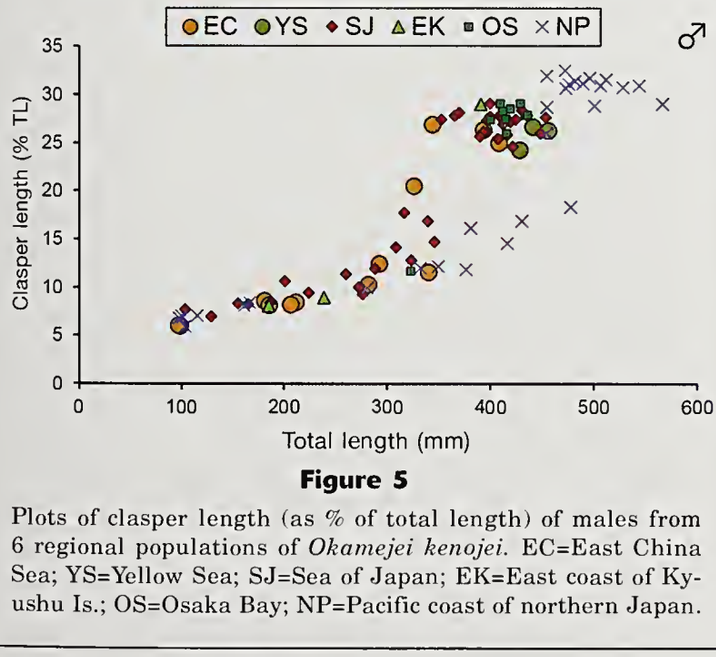

Figure 5

Plots of clasper length (as % of total length) of males from 6 regional populations of *Okamejei kenojei*. EC=East China Sea; YS=Yellow Sea; SJ=Sea of Japan; EK=East coast of Kyushu Is.; OS=Osaka Bay; NP=Pacific coast of northern Japan.

analysis; our results supported the uniqueness of the regional populations and suggested limits to migration. Such fine-scale population structures in other skate species have already been well documented (e.g., Chevolot et al., 2006; Griffiths et al., 2010, 2011; Dudgeon et al., 2012; Im et al., 2017; Vargas-Caro et al., 2017) and are considered to have been derived from the constraints of low dispersal because of large benthic egg capsules and the absence of a pelagic larval stage. Vargas-Caro et al. (2017) suggested that smaller skates inhabiting coastal areas had well-defined population structures than larger skates inhabiting offshore areas because body size and habitat are related to dispersal potential. Maximum size of members of the family Rajidae vary from 33 cm to more than 2 m TL, and most members occur from continental shelves to more than 4000 m depth (Last et al., 2016). Studies on migration and habitat preference of *O. kenojei* are few; however, the species is a typical small skate maturing at ca. 400–500 mm TL and inhabits coastal areas shallower than 150 m depth (Ishihara et al., 2009; Hatooka et al., 2013; Last et al., 2016).

In comparison with the OS population, however, morphological divergence of the NP population was somewhat remarkable against genetic differentiation; both genetic and morphological data sets did not agree completely. Among 12 measurements of characters (excluding TL), as well as nuchal thorn counts, maturity size, and coloration, NP individuals were distinguished by 8 of the 15 characters (disc width, dorsal head length, distance between orbits, distance between nostrils, distance between 1st gill openings, maturity size, nuchal thorn, and coloration), but OS individuals were distinguished by 6 of the 15 characters (dorsal snout length, eye diameter, ventral head length, ventral snout length, prenasal snout length, and nuchal thorn) (see Tables 3–4; Figs. 3–7). It should be noted that we examined a single maternally inherited gene (mtCR) which cannot be considered derived from male-mediated gene flow. This single gene may also explain the partial mismatch between our mtCR analysis and our morphological comparisons. Furthermore, genetic differences may also be random to some extent; Spies et al. (2006) indicated that genetic differences at mtDNA cytochrome c oxidase subunit I (COI) were not observed even among different species. In another case, incongruence between genetic and morphological variation may be due to adaptations to different environments. For example, adaptive evolutionary changes in life history, physiology, and phenotype in the winter skate (*Leucoraja ocellata*) have been associated with epigenetic regulation that causes changes in gene expression for adaptation to different environments without obvious genetic change (Kelly and Hanson, 2013; Lighten et al.,

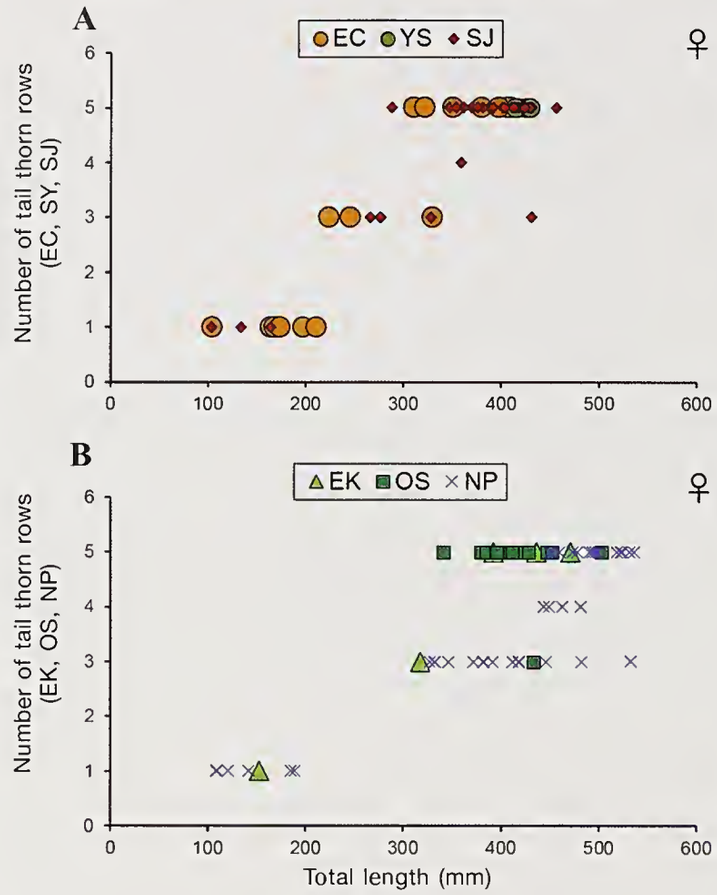

Figure 6

Plots of number of tail thorn rows of females within 6 regional populations of *Okamejei kenojei*. (**A**) EC, YS, and SJ, (**B**) EK, OS, and NP. EC=East China Sea; YS=Yellow Sea; SJ=Sea of Japan; EK=East coast of Kyushu Is.; OS=Osaka Bay; NP=Pacific coast of northern Japan.

2016). Therefore, further study of the species based on nuclear DNA or other mtDNA markers, or both, would reveal more details in population structure and associated morphological variations.

In the haplotype network for ocellate spot skate, the OS haplotypes (Ok13 and Ok14) were distant from others, but these two haplotypes are closely related to each other in the network (Fig. 2). In addition, OS individuals were characterized by a smaller eye, longer head and snout, and fewer nuchal thorns than those in other regional populations (Tables 3 and 4; Figs. 3 and 4), clearly suggesting significant isolation of the OS population from the other populations. In fact, the OS individuals were collected only from Osaka Bay, situated at the innermost part of the Seto Inland Sea (Fig. 1), and *O. kenojei* were not collected from other marginal areas of Osaka Bay. This finding may suggest that this species is inhabiting patchy areas and exhibiting discontinuity in around the Seto Inland Sea, and its distributional area is also isolated from other areas.

Although one of two haplotypes of the ocellate spot skate in NP was shared with other regional populations (Fig. 2, Ok1), NP individuals clearly differed in morphological characters from other populations, by having a broader disc, smaller eye, shorter head and snout, widely separated orbits, nostrils and gill openings, a greater number of nuchal thorns and numerous small black specks present on its dorsal surface (Figs. 3, 4, and 7). The size at maturity of males and females was also greater than that in other regional populations (Figs. 5 and 6). Such morphological divergence of NP from the other regional populations agreed well with the findings of Ishiyama (1967) and Ishihara (1987). Although the former recognized NP individuals as a separate species, the sharing of a haplotype with other regional populations (Ok1) indicates the absence of reproductive isolation between them. Although gene flow between NP and other regional populations has been limited, as suggested by a significant F_{ST}, we treated the NP as the area of a local population within *O. kenojei*, as suggested by Ishihara (1987). Gene flow between it and the other populations seems to be restricted by the Tsugaru Strait between the Sea of Japan and Pacific Ocean (Fig. 1)—further evidence of a phylogeographical break across the Tsugaru Strait (Kai et al., 2014; Kai and Yamanaka[2]).

Size at maturity was clearly larger in NP individuals than in other regional populations (Figs. 5 and 6). Such differences between Sea of Japan, Sea of Okhotsk, and Pacific Ocean populations have been noted for several fish species. For example, Tamate (2012) showed that the body size of the anadromous masu salmon (*Oncorhynchus masou*) returning to the coast from the Sea of Okhotsk was significantly smaller than that of the same species from the Pacific and Sea of Japan coasts. In contrast, Tohkairin et al. (2014) showed that the maximum body size of the marbled snailfish (*Crystallichthys matsushimae*) was much smaller in the Sea of Japan population than in the Pacific and Sea of Okhotsk population. Because the genetic divergence between NP and other populations was at the intraspecific level, some other evolutionary factors may have shaped the geographic size variations in *O. kenojei*.

It should be noted that the NP haplotypes were similar to those of SJ, YC and EC, but distantly related to those of OS, suggesting that NP was colonized from SJ through the Tsugaru Strait, not from OS along the Pacific coast of Japan. Although no obvious geographic barriers are known between OS and NP, the absence of a major population of *O. kenojei* from the Pacific coast of central Japan suggests that the strong Kuroshio Current, originating from tropical waters, may have prevented dispersal of the species. In fact, the main

[2] Kai, Y., and T. Yamanaka. 2017. Tsugaru Straight hybrid zone between two Japanese marine sculpins (genus *Cottiusculus*). [Available at website, accessed May 2018]

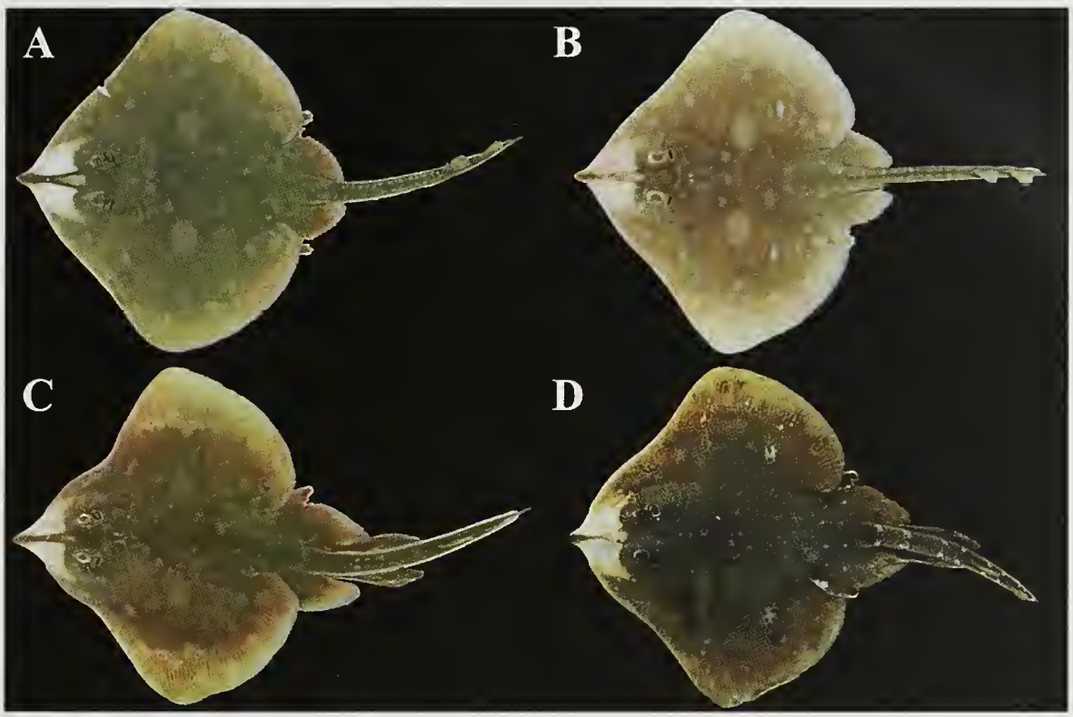

Figure 7

Typical coloration of 4 regional populations of *Okamejei kenojei*. (**A**) FAKU 140518, 384 mm total length (TL), adult female, East China Sea (**B**) BSKU 116603, 289 mm TL, immature male, Sea of Japan, (**C**) FAKU 140521, 430 mm TL, adult male, Osaka Bay, (**D**) BSKU 112173, 462 mm TL, adult male, Pacific coast of northern Japan.

route of the Kuroshio Current has been stable at least since the last glacial period (Kojima et al., 2000), shaping the distributional range of various coastal species along the Japanese Archipelago (Matsuura, 2012).

The genetic and morphological divergence of ocellate spot skate populations between the Sea of Japan and East China Sea, suggested by significant F_{ST} values (Table 2) and measurements (Table 4), is mirrored in several coastal marine species. For example, Liu et al. (2007) disclosed 3 mtDNA lineages in redlip mullet (*Chelon haematocheilus*)—lineages that diverged among the Sea of Japan and the East and South China seas during Pleistocene glaciations. In addition, genetic and morphological divergence was also detected between EC and YS, which are separated by the Tsushima Strait and Tsushima Current (Fig. 1). Similarly, genetic divergence between the Yellow Sea and Japanese coast of the East China Sea has been noted in several marine fishes, including the white croaker (*Pennahia argentata*), spotted halibut (*Verasper variegatus*), and gizzard shad (*Konosirus punctatus*) (see Han et al., 2008; Sekino et al., 2011; Gwak et al., 2015). As noted in the above examples with *C. haematocheilus* and *K. punctatus*, 3 regional populations (EC, YS, and SJ) of *O. kenojei* also diverged on account of Tsushima Strait and the Tsushima Current, which act as geographical barriers.

Implications for fisheries management Small and benthic (or benthopelagic) elasmobranch species tend to exhibit more distinct population structures at smaller spatial scales than those exhibited by large pelagic species (Larson et al., 2017). In fact, movement patterns of some skate species investigated in tagging studies, have shown that most had a small home range (within a 100-km^2 area) (Walker et al., 1997; Hunter et al., 2005; King and McFarlane, 2010; Neat et al., 2015; Farrugia et al., 2016; Vargas-Caro et al., 2017) in spite of their potential ability to migrate hundreds of kilometers (King and McFarlane, 2010). Regarding *O. kenojei*, a lack of tagging studies has meant no insights on migratory range, although the extensive population structure found in this study suggests that the species has a small home range.

Because fish populations have a unique set of dynamics, such as recruitment, growth, and mortality that influence current and future status, it is important, even within the same species (Pope et al., 2010), to define management units (MUs) based on population structure and to execute subsequent assessment and management of stocks according to each MU. Clearly, MUs for *O. kenojei* need to be set according to the population structure of the species because of the genetic and morphological differentiation of populations among the investigated regions. We suggest at least 6 MUs for

O. kenojei: East China Sea (EC), Yellow Sea (YS), Sea of Japan (SJ), east coast of Kyushu Is. (EK), Osaka Bay (OS), and Pacific coast of northern Japan (NP). In particular, careful monitoring of population (stock) abundance of local populations characterized by low genetic diversity and geographical isolation, such as the abundance of OS and NP populations of *O. kenojei,* is necessary. Tagging studies, which may reveal some aspects of migratory behavior, may also help to clarify factors contributing to the population structure of *O. kenojei.*

Acknowledgments

We are very grateful to N. Nakatsuka, S. Ikeguchi, T. Kintaka, T. Mochizuki, T. Imaizumi, T. Mukai, R. Komoto, Y. Uchida, S. Suzuki, D. Noguchi, J.-K. Kim, and K. Sakai for collecting samples. We sincerely thank the captains, officers and crews of the RV *Wakataka-maru* and RV *Taka-maru* (Fisheries Research and Education Agency), and RV *Shimane-maru* (Shimane Prefectural Fisheries Technology Center) for assistance in the field. We also thank G. S. Hardy (Ngunguru, New Zealand) for his critical reading of the manuscript.

Literature cited

Baeck, G. W., C.-I. Park, H. C. Choi, S.-H. Huh, and J. M. Park.
2011. Feeding habitats of ocellate spot skate, *Okamejei kenojei* (Müller & Henle, 1841), in coastal waters of Taean, Korea. J. Appl. Ichthyol. 27:1079–1085.

Boeseman, M.
1979. Some remarks on the identity of the Japanese rays *Raja kenojei* Müller & Henle, 1841, and *Raja meerdervoortii* Bleeker, 1860. Zool. Meded. 53:273–281, pls. 1–8.

Brander, K.
1981. Disappearance of common skate *Raia batis* from Irish Sea. Nature 290:48–49.

Cannas, R., M. C. Follesa, S. Cabiddu, C. Porcu, S. Salvadori, S. P. Iglésias, A. M. Deiana, and A. Cau.
2010. Molecular and morphological evidence of the occurrence of the Norwegian skate *Dipturus nidarosiensis* (Storm, 1881) in the Mediterranean Sea. Mar. Biol. Res. 6:341–350.

Chevolot, M., G. Hoarau, A. D. Rijnsdorp, W. T. Stam, and J. L. Olsen.
2006. Phylogeography and population structure of thornback rays (*Raja clavata* L., Rajidae). Mol. Ecol. 15:3693–3705.

Chevolot, M., P. H. J. Wolfs, J. Pálsson, A. D. Rijnsdorp, W. T. Stam, and J. L. Olsen.
2007. Population structure and historical demography of the thorny skate (*Amblyraja radiata*, Rajidae) in the North Atlantic. Mar. Biol. 151:1275–1286.

Daly-Engel, T. S., R, D. Grubbs, K. A. Feldheim, B. W. Bowen, and R. J. Toonen.
2010. Is multiple mating beneficial or unavoidable? Low multiple paternity and genetic diversity in the short-spine spurdog *Squalus mitsukurii*. Mar. Eco. Prog. Ser. 403:55–267.

Davidson, L. N. K., M. A. Krawchuk, and N. K. Dulvy.
2016. Why have global shark and ray landings declined: improved management or overfishing? Fish and Fish. 17:438–458.

Domingues, R. R., A. W. S. Hilsdorf, and O. B. F. Gadig.
2018. The importance of considering genetic diversity in shark and ray conservation policies. Conserv. Genet. 19:501–525.

Dudgeon, C. L., D. C. Blower, D. Broderick, J. L. Giles, B. J. Holmes, T. Kashiwagi, N. C. Krück, J. A. T. Morgan, B. J. Tillett, and J. R. Ovenden.
2012. A review of the application of molecular genetics for fisheries management and conservation of sharks and rays. J. Fish Biol. 80:1789–1843.

Dulvy, N. K., J. D. Metcalfe, J. Glanville, M. G. Pawson, and J. D. Reynolds.
2000. Fishery stability, local extinctions, and shifts in community structure in skates. Conserv. Biol. 14:283–293.

Dulvy, N. K., S. L. Fowler, J. A. Musick, R. D. Cavanagh, P. M. Kyne, L. R. Harrison, J. K. Carlson, L. N. K. Davidson, S. V. Fordham, M. P. Francis, et al.
2014. Extinction risk and conservation of the world's sharks and rays. eLife 3:e00590.

Excoffier, L., and H. E. L. Lischer.
2010. Arlequin suite ver. 3.5: a new series of programs to perform population genetics analyses under Linux and Windows. Mol. Ecol. Res. 10:564–567.

Farrugia, T. J., K. J. Goldman, C. Tribuzio, and A. A. Seitz.
2016. First use satellite tags to examine movement and habitat use of big skates *Beringraja binoculata* in the Gulf of Alaska. Mar. Ecol. Prog. Ser. 556:209–221.

Feutry, P., P. M. Kyne, R. D. Pillans, X. Chen, G. J. P. Naylor, and P. M. Grewe.
2014. Mitogenomics of the speartooth shark challenges ten years of control region sequencing. BMC Evol. Biol. 14:1–9.

Frodella, N., R. Cannas, A. Velonà, P. Carbonara, E. D. Farrell, F. Fiorentino, M. C. Follesa, G. Garofalo, F. Hemida, C. Mancusi, et al.
2016. Population connectivity and phylogeography of the Mediterranean endemic skate *Raja polystigma* and evidence of its hybridization with the parapatric sibling *R. montagui*. Mar. Ecol. Prog. Ser. 554:99–113.

Griffiths, A. M., D. W. Sims, S. P. Cotterell, A. E. Nagar, J. R. Ellis, A. Lynghammar, M. McHugh, F. C. Neat, N. G. Pade, N. Queiroz, et al.
2010. Molecular markers reveal spatially segregated cryptic species in a critically endangered fish, the common skate (*Dipturus batis*). Proc. R. Soc. B, 277:1497–1503.

Griffiths, A. M., D. W. Sims, A. Johnson, A. Lynghammar, M. McHugh, T. Bakken, and M. J. Genner.
2011. Levels of connectivity between longnose skate (*Dipturus oxyrinchus*) in the Mediterranean Sea and the north-eastern Atlantic Ocean. Conserv. Genet. 12:577–582.

Gwak, W.-S., Y.-D. Lee, and K. Nakayama.
2015. Population structure and sequence divergence in the mitochondrial DNA control region of gizzard shad *Konosirus punctatus* in Korea and Japan. Ichthyol. Res. 62:379–385.

Hall, T. A.
1999. BioEdit: a user-friendly biological sequence alignment editor and analysis program for Windows 95/98/NT. Nucl. Acids Symp. Ser. 41:95–98.
Han, Z.-Q., T.-X. Gao, T. Yanagimoto, and Y. Sakurai.
2008. Deep phylogeographic break among white croaker *Pennahia argentata* (Sciaenidae, Perciformes) populations in North-western Pacific. Fisher. Sci. 74:770–780.
Hatooka, K., U. Yamada, M. Aizawa, A. Yamaguchi, and N. Yagishita.
2013. Rajidae. *In* Fishes of Japan with pictorial keys to the species, 3rd ed. (T. Nakabo, ed.), p. 205–216, 1771–1773. Tokai Univ. Press, Hadano, Japan. [In Japanese.]
Heyden, S. V. D., M. R. Lipinski, and C. A. Matthee.
2010. Remarkable low mtDNA control region diversity in an abundant demersal fish. Mol. Phylogenet. Evol. 55: 1183–1188.
Hoelzel, A. R., M. S. Shivji, J. Magnussen, and M. P. Francis.
2006. Low worldwide genetic diversity in the basking shark (*Cetorhinus maximus*). Biol. Lett. 2:639–642.
Hunter, E., A. A. Buckley, C. Stewart, and J. D. Metcalfe.
2005. Migratory behavior of the thornback ray, *Raja clavate*, in the southern North Sea. J. Mar. Biol. Assoc. U. K. 85:1095–1105.
Im, Y.-J., H.-S. Jo, H.-S. Ji, S.-H. Myoung, and J.-K. Kim.
2017. Geographic variations of the mottled skate, *Beringraja pulchra* (Liu, 1932) (Rajidae) in the Yellow and East seas based on molecular and morphometric data. J. Appl. Ichthyol. 33:950–956.
Ishihara, H.
1987. Revision of the western north pacific species of the genus *Raja*. Jpn. J. Ichthyol., 34: 241–285.
1990. The skates and rays of the western north Pacific: an overview of their fisheries, utilization, and classification. *In* Elasmobranchs as living resources: advance in the biology, ecology, systematics, and the status of the fisheries (H. L. Pratt Jr., S. H. Gruber, T. Taniuchi, eds.), p. 485–497. NOAA Tech. Rep., NMFS 90.
Ishihara, H., Y. Wang, S. Tanaka, and K. Nakaya.
2009. *Okamejei kenojei*. IUCN Red List of Threatened Species 2009. Version 2017-3. [Available at website, accessed February 2018.]
Ishiyama, R.
1958. Studies on the rajid fishes (Rajidae) found in the waters around Japan. J. Shimon. Coll. Fish. 7:193–394, pls. 1–3.
1967. Fauna Japonica. Rajidae (Pisces), vi+82 p., 32 pls. Biogeograph. Soc., Japan, Tokyo, Japan.
Kai, Y, Y. Ueda, K. Fujiwara, M. Itoh, A. Yamasaki, and T. Nakabo.
2014. Population structure and demographic history of *Davidijordania poecilimon* (Perciformes: Zoarcidae). Spec. Diver. 19:15–19.
Kelly, J. T., and J. M. Hanson.
2013. Maturity, size at age and predator-prey relationships of winter skate *Leucoraja ocellata* in the southern Gulf of St Lawrence: potentially an undescribed endemic facing extirpation. J. Fish Biol., 82: 959–978.
King, J. R., and G. A. McFarlane.
2010. Movement patterns and growth estimates of big skate (*Raja binoculata*) based on tag-recapture data. Fish. Res. 101:50–59.
Kojima, S., R. Segawa, R., and I. Hayashi.
2000. Stability of the courses of the warm coastal currents along the Kyushu Island suggested by the population structure of the Japanese turban shell, *Turbo* (*Batillus*) *cornutus*. J. Oceanogr. 56:601–604.
Larson, S. E., T. S. Daly-Engel, and N. M. Phillips.
2017. Review of current conservation genetic analysis of northeastern Pacific sharks. Adv. Mar. Biol. 77: 79–110.
Last, P. R., B. Séret, M. F. W. Stehmann, and S. Weigmann.
2016. Family Rajidae. *In* Rays of the world (P. R. Last, W. T. White, M. R. de Carvalho, B. Séret, M. F. W. Stehmann, and G. J. P. Naylor, eds.), p. 204–363. CSIRO Publishing, Clayton, Victoria, Australia.
Last, P. R., W. T. White, J. J. Pogonoski, and D. C. Gledhill.
2008. New Australian skates (Batoidea: Rajoidei)—background and methodology. *In* Description of new Australian skates (P. R. Last, W. T. White, J. J. Pogonoski, and D. C. Gledhill, eds.), p. 1–8. CSIRO Mar. Atmos. Res. 21.
Lighten, J., D. Incarnate, B. J. Ward, C. V. Oosterhout, I. Bradbury, M. Hanson, and P. Bentzen.
2016. Adaptive phenotypic response to climate enabled by epigenetics in a K-strategy species, the fish *Leucoraja ocellata* (Rajidae). R. Soc. Open Sci. 2016 Oct. 3 (10):160299.
Liu, J.-X., T.-X. Gao, S.-F. Wu, and Y.-P. Zhang.
2007. Pleistocene isolation in the Northwestern Pacific marginal seas and limited dispersal in a marine fish, *Chelon haematocheilus* (Temminck & Schlege, 1845). Mol. Ecol. 16:275–288.
Martin, A. P.
1999. Substitution rates of organelle and nuclear genes in sharks: implicating metabolic rate (again). Mol. Biol. Evol. 16:996–1002.
Martin, A. P., G. J. P. Naylor, and S. R. Palumbi.
1992. Rates of mitochondrial DNA evolution in sharks are slow compared with mammals. Nature 357:153–155.
Matsuura, K. (ed.).
2012. Fishes in the Kuroshio Current, 221 p. Tokai University Press, Hadano, Japan. [In Japanese.]
Neat, F., C. Pinto, I. Burrett, L. Cowie, J. Travis, J. Thorburn, F. Gibb, and P. J. Wright.
2015. Site fidelity, survival and conservation options for the threatened flapper skate (*Dipturus* cf. *intermedia*). Aquatic Conserv.: Mar. Freshw. Ecosyst. 25:6–20.
Pope, K. L., S. E. Lochmann, and M. K. Young.
2010. Methods for assessing fish populations. *In* Inland fisheries management in North America, 3rd edn. (M. C. Quist, and W. A. Hubert, eds.), p. 325–351. Am. Fish. Soc., MD.
R Development Core Team.
2014. R: a language and environment for statistical computing. R Foundation for Statistical Computing, Vienna, Austria. [Available at website, accessed December 2017.]
Rice, W. R.
1989. Analyzing tables of statistical tests. Evolution 43: 223–225.
Sekino, M., K. Saitoh, D. Shimizu, T. Wada, K. Kamiyama, S. Gambe, S. Chen, and M. Aritaki.
2011. Genetic structure in species with shallow evolutionary lineages: a case study of the rare flatfish *Versasper variegatus*. Conserv. Genet. 12:139–159.
Spies, I. B., S. Gaichas, D. E. Stevenson, J. W. Orr, and M. F. Canino.
2006. DNA-based identification of Alaska skates (*Amblyraja*, *Bathyraja* and *Raja*: Rajidae) using cytochrome c

oxidase subunit I (coI) variation. J. Fish Biol. 69:283–292.

Spies, I. B., D. E. Stevenson, J. W. Orr, and G. R. Hoff.
2011. Molecular systematics of the skate subgenus *Arctoraja* (*Bathyraja*: Rajidae) and support for an undescribed species, the leopard skate, with comments on the phylogenetics of *Bathyraja*. Ichthyol. Res. 58:77–83.

Stehmann, M. F. W.
2002. Proposal of a maturity stages scale for oviparous and viviparous cartilaginous fishes (Pisces, Chondrichthyes). Arch. Fish. Mar. Res. 50:23–48.

Tamate, T.
2012. A concise review of geographic variation in adult body size in anadromous masu salmon, *Oncorhynchus masou*. Environ. Biol. Fish. 94:527–532.

Tamura, K., G. Stecher, D. Peterson, A. Filipski, and S. Kumar.
2013. MEGA6: molecular evolutionary genetics analysis version 6.0. Mol. Biol. Evol. 30:2725–2729.

Tohkairin, A., Y. Kai, Y. Ueda, T. Hamatsu, M. Ito, and T. Nakabo.
2014. Morphological divergence between two color morphotypes of *Crystallichthys matsushimae* (Cottoidei: Liparidae). Ichthyol. Res. 62:145–155.

Valsecchi, E., P. Pasolini, M. Bertozzi, F. Garoia, N. Ungaro, M. Vacchi, B. Sabelli, and F. Tinti.
2005. Rapid Miocene-Pliocene dispersal and evolution of Mediterranean rajid fauna as inferred by mitochondrial gene variation. J. Evol. Biol. 18:436–446.

Vargas-Caro, C., C. Bustamante, M. B. Bennett, and J. R. Ovenden.
2017. Towards sustainable fishery management for skates in South America: the genetic population structure of *Zearaja chilensis* and *Dipturus trachyderma* (Chondrichthyes, Rajiformes) in the south-east Pacific Ocean. PLoS ONE 12:e0172255.

Veríssimo, A., J. R. McDowell, and J. E. Graves.
2010. Global population structure of the spiny dogfish *Squalus acanthias*, a temperate shark with an antitropical distribution. Mol. Ecol. 19:1651–1662.

Walker, P. A., and J. R. G. Hislop.
1998. Sensitive skates or resilient rays? Spatial and temporal shifts in ray species composition in the central and north-western North Sea between 1930 and the present day. J. Mar. Sci. 55:392–402.

Walker, P., G. Howlett, and R. Millner.
1997. Distribution, movement and stock structure of three ray species in the North Sea and eastern English Channel. ICES J. Mar. Sci. 54:797–808.

National Marine Fisheries Service
NOAA

Fishery Bulletin
established in 1881

Spencer F. Baird
First U.S. Commissioner of Fisheries and founder of *Fishery Bulletin*

Multidecadal meta-analysis of reproductive parameters of female red snapper (*Lutjanus campechanus*) in the northern Gulf of Mexico

Nancy J. Brown-Peterson (contact author)[1]
Christopher R. Peterson[2]
Gary R. Fitzhugh[3]

Email address for contact author: nancy.brown-peterson@usm.edu

[1] Center for Fisheries Research and Development
School of Ocean Science and Engineering
University of Southern Mississippi
703 East Beach Dr.
Ocean Springs, Mississippi 39564

[2] Department of Integrative Biology
The University of Texas at Austin
2415 Speedway #C0930
Austin, Texas 78712

[3] Southeast Fisheries Science Center
National Marine Fisheries Service
3500 Delwood Beach Rd.
Panama City, Florida 32408

Abstract—Stocks of red snapper (*Lutjanus campechanus*) exhibited a dramatic decline in abundance in the northern Gulf of Mexico (GOM) between 1960 and 1991; management regulations implemented since 1991 have resulted in a modest recovery. To examine potential temporal and regional changes in reproductive parameters of female red snapper during recovery of the stock, we used meta-analytical models to analyze data collected during 1991–2017 throughout the northeastern (Florida, Alabama, Mississippi) and northwestern (Louisiana and Texas) GOM; no data were available for 2003–2008. Peak red snapper spawning occurred from June through August throughout the time period, and a high probability (>75%) of spawning occurred during May from 1995 through 2017. The reproductive season was estimated to average 4.5 months from 1994 through 2017. Increases in spawning interval were estimated across time in the northwestern region (2.3–4.7 days between spawnings from 1992 through 2015) and for regions combined (2.4–2.9 days from 1991 through 2017) but showed no changes in the northeastern region (2.3–2.4 days from 1991 through 2017). Relative batch fecundity generally decreased from 1991 through 2017 for all models; however, this decrease was more notable in the northwestern GOM than in the northeastern GOM after 2013. Our analyses suggest evidence of reproductive compensation, particularly because the estimated changes in reproductive parameters were more pronounced in the northwestern GOM.

Manuscript submitted 19 July 2018.
Manuscript accepted 10 December 2018.
Fish. Bull. 117:37–49 (2019).
Online publication date: 19 December 2018.
doi: 10.7755/FB.117.1.5

The views and opinions expressed or implied in this article are those of the author (or authors) and do not necessarily reflect the position of the National Marine Fisheries Service, NOAA.

Red snapper (*Lutjanus campechanus*) is one of the most popular recreational and commercial species throughout the northern Gulf of Mexico (GOM). This popularity has resulted in high fishing pressure on the species, resulting in dramatic declines in the stocks since the 1960s and reaching a low point in 1990 (SEDAR 52, 2018). The first stock assessment for red snapper, conducted in 1988, concluded that the stock was overfished and continues to be overfished (i.e., is undergoing "overfishing"; Goodyear, 1988). A series of regulations have been implemented since that time, including bag limits, size limits, gear restrictions, limits on the length of the commercial and recreational fishing seasons, and the institution of an individual fishing quota (IFQ) program. In 2005, new, stricter regulations were put into place in an effort to end overfishing of red snapper by 2009 or 2010 (GMFMC, 2007). The most recent stock assessment, completed in April 2018, concluded that red snapper stocks are in recovery and that they are not overfished and are not in the process of being overfished on a gulf-wide basis (SEDAR 52, 2018). The stock is expected to continue to increase and should be within a few percentage points of the target spawning stock biomass (26%) by 2028 (SEDAR 52, 2018).

Knowledge of red snapper reproductive biology is important for understanding both the decline and potential recovery of the species. However, between 1965 and 2000 only 13 publications were devoted to red snapper reproductive biology (0.37 publications/year; Fig. 1), despite the dramatic decline in red snapper stocks in the 1960s through the 1990s. Since 2000, red snapper pub-

lications on reproductive biology have increased to 2.16/year according to a search of the internet with Google Scholar (Fig. 1). It is well documented that red snapper have an extended spawning season in the GOM, generally ranging from May through October, and peak spawning occurs from June through mid-September (SEDAR 31, 2013). Female red snapper are batch spawners with indeterminate fecundity, and the spawning interval, or number of days between consecutive spawnings, decreases with increasing female size or age (Porch et al., 2015). Female red snapper can reach sexual maturity as early as age-2 (SEDAR 31, 2013, Porch et al., 2015).

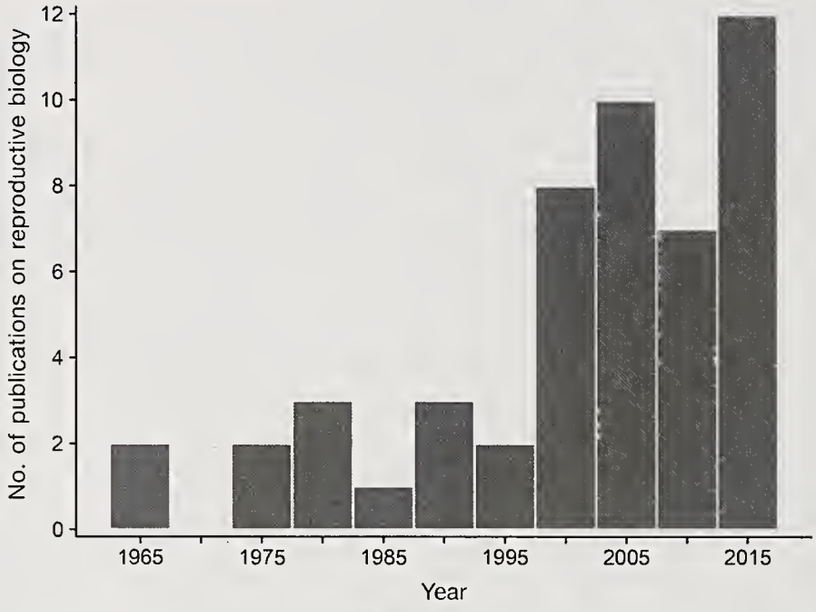

Figure 1

Number of publications related to red snapper (*Lutjanus campechanus*) reproductive biology from 1965 through 2017. Each bar represents a 5-year bin, with the exception of 2015, which represents 3 years. Figure includes all publications from the Gulf of Mexico and the Atlantic Ocean.

The reproductive potential of female red snapper has been shown to vary with region, habitat, and time. Red snapper from the east coast of the United States were more fecund and had a shorter spawning interval than those from off the Dry Tortugas in the Gulf of Mexico, although spawning seasonality appeared similar in both areas (Brown-Peterson et al., 2009). Recent modeling of red snapper biomass and fecundity has indicated that both estimates are higher for the northwestern GOM than for the northeastern GOM (Porch et al., 2015, Karnauskas et al., 2017). These reported differences are likely related to the higher proportion of larger, older individuals in the northwestern GOM than in the northeastern GOM (Porch et al., 2015). Reproductive potential has also been hypothesized to be related to habitat; fish captured on natural reef banks reproduce earlier, at a smaller size, more frequently, and with a higher fecundity than fish captured on artificial reefs in Louisiana (Glenn et al., 2017). However, small sample sizes and differences in depth between the natural reefs and artificial reefs reported in Glenn et al. (2017) may confound the conclusions from this article. For example, no difference was found in spawning behavior or fecundity of female red snapper captured from oil platforms or natural hard bottom in Texas within the same depth zone (Downey et al., 2018). However, female red snapper captured on nearshore artificial reefs in Texas exhibited more active spawning and higher fecundity than those taken from offshore artificial reefs (Alexander, 2015), despite similarities in depth between nearshore and offshore reefs. Finally, female red snapper showed a decrease in fecundity and spawning frequency, as well as a slower progression to sexual maturity between 2000 and 2010, and these results were more pronounced in fish from the northwestern GOM than in the northeastern GOM (Kulaw et al., 2017). However, the conclusions of Kulaw et al. (2017) may have been influenced by small sample sizes during 2009–2010, particularly from the northeastern GOM.

To further examine potential temporal and spatial changes in reproductive parameters of GOM female red snapper, we conducted an expanded meta-analysis of several reproductive parameters from 1991 through 2017. This 27-year period represents a time during which red snapper stocks have increased from historic low levels despite undergoing relatively high levels of fishing pressure. Specifically, we evaluated differences in spawning seasonality, batch fecundity, and spawning interval across time. Additionally, we modeled differences in spawning interval and batch fecundity between eastern and western subgroups of red snapper in the northern GOM.

Materials and methods

Data sources

We searched Google Scholar for "red snapper reproduction" and "*Lutjanus campechanus* reproduction" and selected articles published between 1991 and 2018 containing information on any of the following terms: spawning, spawning seasonality, fecundity, spawning interval/frequency, spawning behavior, and gonadal histology. Additional relevant papers not found in the search were included on the basis of those with expert knowledge. The relatively few articles published on red snapper reproduction before 1991 that contained usable data resulted in large gaps in the time series of

Table 1

Data sources and parameters used for analysis of female red snapper reproduction in the northern Gulf of Mexico (GOM); E=northeastern GOM; W=northwestern GOM; R=raw data; S=summary data.

		Reproductive parameter			
Year	Region	GSI	Spawning interval	Relative batch fecundity	Reference
1991–1992	E	R	R	R	SEDAR 7, 2005
1993–1995	E, W	R	R	R	SEDAR 7, 2005
1998–2002	E, W	R	R	R	SEDAR 7, 2005
1999–2001	E, W	R	R	R	Kulaw et al., 2017
1999	E			R	Szedlmayer and Furman, 2000[a]
2004	E			R	Brown-Peterson et al., 2009
2007–2010				R	SEDAR 31, 2013
2009	E		S		Lowerre-Barbieri et al., 2012
2009–2010	W	S		R	Cowan et al., 2012
2009–2010	E, W	R	R	R	Kulaw et al., 2017
2011	E, W	R	R	R	Fitzhugh et al., 2012a
2012	E, W			R	Lang and Falterman, 2017
2012–2013	W	R	R	R	Glenn et al., 2017
2012–2016	E, W	R	R	R	SEDAR 52, 2018
2013–2014	W	S	S		Alexander, 2015
2013–2015	W	S	S	R	Downey et al., 2018
2016–2017	E	R	R	R	Brown-Peterson, current study

[a] Szedlmayer, S. T., and C. Furman. 2000. Estimation of abundance, mortality, fecundity, age frequency, and growth rates of red snapper *Lutjanus campechanus*, from a fishery-independent stratified random survey. Report to the Gulf and South Atlantic Fisheries Foundation, Inc. National Oceanographic and Atmospheric Administration, Department of Commerce Cooperative agreement NA87FM0221.

data, and therefore no papers published before 1991 were included in the analyses. Although Render (1995) contains information on spawning seasonality and spawning interval, insufficient details were provided to be able to use the data in our analyses.

When possible and necessary, we contacted the authors of articles to receive their original data. In all other cases, the data provided within the articles themselves were used in the meta-analysis. Additionally, data from an ongoing, unpublished study by the first author were included in the analyses. All data sources used for analyses are shown in Table 1 and include peer-reviewed, published manuscripts, graduate theses, and final or interim reports.

Data collection—2016 and 2017 samples

Red snapper were collected monthly in Mississippi waters from April through November 2016 and from April through October 2017 during daylight hours by using vertical longlines baited with Atlantic mackerel (*Scomber scomber*). Sampling gear consisted of 3 electric reels rigged with an 8-m vertical mainline that was outfitted with ten 45.7-cm leaders spaced 0.67-m apart and a 4.5-kg weight at the terminal end. All leaders on each line were rigged with one hook size (8/0, 11/0 or 15/0 circle hooks of 0 offset). Lines were fished just off the bottom for 5 min/set. Habitats sampled included permitted fishing zones around artificial reefs, oil and gas platforms, and rigs-to-reef sites at 3 depth zones (< 20 m, 20–49 m, 50–100 m). Sites at reefs were fished at the 2 shallowest depth zones, whereas rigs-to-reef sites were fished only at the deepest depth zone. Three 5-min sets were made at platforms and at reef zones where fishing was permitted at each depth zone, and two 5-min sets were made at rigs-to-reefs sites. All fish were stored on ice immediately upon capture.

Fish were measured (FL, mm) and weighed (0.01 kg). Gonadal tissue was removed, weighed (0.1 g) and macroscopically assessed to determine reproductive phase (Brown-Peterson et al., 2011). A section of ovary from each fish was preserved in 10% neutral buffered formalin within 15 hours of capture for histological analysis and assignment of reproductive phase (Brown-Peterson et al., 2011). A portion (1–4 g) of the ovary of all females macroscopically identified in the actively spawning subphase was weighed (0.01 g) and preserved for a minimum of 3 months in Gilson's solu-

tion for fecundity analysis. Batch fecundity was determined volumetrically for 6 subsamples per individual for fish histologically verified in the actively spawning subphase (Bagenal and Braum, 1971).

Reproductive parameters

Reproductive parameters were calculated from original data when available. When only summary data were available, the mean, standard error, and number of samples were taken or calculated from tables or graphs provided in the publication. Spawning seasonality was defined on the basis of the Gonadosomatic Index (GSI), with

$$GSI = (gonad\ weight / gonad\text{-}free\ weight) \times 100. \quad (1)$$

Fish were considered reproductively active if their GSI was ≥1.0, and reproductively inactive if their GSI was <1.0. This GSI threshold was based on histological assessments of developing and spawning-capable fish. Spawning interval (estimated days between spawnings) was calculated in 2 ways using 2 separate types of spawning markers. First, the reciprocal of the total number of actively spawning females (i.e., those undergoing oocyte maturation (OM), including those with hydrated oocytes) was divided by the number of spawning capable females. For the second method, we used the reciprocal of the total number of females with postovulatory follicles (POFs) ≤24 h that were observed in the ovary divided by the number of spawning capable females. We assumed that both types of spawning markers are equivalent in both detectability and duration (approximately 24 hours, but see Porch et al., 2015). Because batch fecundity is positively correlated with fish size (Lowerre-Barbieri et al., 2015), relative batch fecundity (RBF, number of eggs/g ovary-free body weight) was used in all models to remove the influence of fish size and was calculated as batch fecundity divided by ovary-free body weight.

Data analysis

Our analyses involved the use of hierarchical Bayesian models, which are well suited to account for statistical uncertainty at multiple levels and from multiple sources (Gelman et al., 2013). An essential component to Bayesian analysis is prior distributions, which can be thought of as formalized assumptions of our uncertainty about the parameters. In particular, we used weakly informative priors that place a low probability on extraordinarily unreasonable parameter values without excluding anything in a broad range of plausibility. A Bayesian analysis combines the prior distributions with the likelihood of the data to create a posterior distribution that describes the uncertainty around the parameter estimates. Posteriors are often described by their median and their credible intervals (usually 50% and 95%), which are the corresponding quantiles of the distribution. The posterior distribution is generally estimated with an algorithm that explores and samples parameter values over a series of iterations. Once the posterior distribution has been estimated, it can be used to perform a posterior predictive check (i.e., simulate new data from the parameters to evaluate the suitability of the model). If these generated data are not similar to the real data, the model may need revision. For further details, an introduction to Bayesian methodology is provided by McElreath (2016).

We examined the potential change in red snapper reproductive variables (spawning seasonality, spawning interval, and fecundity) over a 27-year period. Our data came from multiple studies conducted by different researchers at varying times throughout the northern GOM, and all data sets shown in Table 1 were used in our analyses. Although we have full data sets for many of these studies, a substantial subset provided only means and standard errors. For each reproductive parameter, we combined a Gaussian process time series model, which is a flexible method that estimates temporal trends where there is similarity among nearby years but not a linear increase or decrease in years, with a random effects meta-analysis, which accounts for variation among studies. Unless otherwise noted, all estimates and predictions produced by these analyses are posterior distributions.

To estimate spawning seasonality, we used a Gaussian process time series to estimate the mean GSI for each month and year within the data range; both raw and summarized data were used in this analysis. Separate Gaussian processes estimated monthly, yearly, and monthly-by-yearly interactions. We calculated the probability of spawning activity for each month and year from the proportion of the posterior distribution corresponding to a mean GSI estimate that was ≥1. The sum of monthly spawning probabilities for each year is the expected spawning period for the year.

Because spawning interval is the reciprocal of a proportion (i.e., the proportion of fish spawning at a given time), it can be analyzed with a modified logistic regression. When available, we used the number of fish caught and the number spawning to fit the model. When original data were unavailable, we used published estimates of spawning intervals and calculated standard errors from sample sizes. To examine potential differences between the northeastern and northwestern GOM, we compared models with a single time series with models where the 2 regions were modeled separately. We ran these models for both of the methods to determine spawning interval (for individuals undergoing OM or POF). In addition to the time series and meta-analysis, our model re-estimated spawning interval for each study from the raw data. This approach improves spawning interval estimates from studies with small sample sizes and allows a credible interval calculation.

We used only individual-level data for our analysis of RBF. As with the spawning interval analysis, we compared a model that estimated separate time series for the northeastern and northwestern GOM with a model that pooled the regions.

All models were written with Stan software, vers. 2.17[1] (Carpenter et al., 2017). Pre- and postprocessing data were analyzed in R, vers. 3.4.1 (R Core Team, 2017). Results were checked for nonconvergence as recommended in the Stan user manual (Stan Development Team, 2017), and model fit was checked with posterior predictive checks. To assess the robustness of the models to prior assumptions, we re-ran each model multiple times with different hyperparameters. Prior sensitivity was assessed by comparing the posterior predictive summary statistics. Full details of all analyses and validations are provided in the online Supplementary methods (online only) section.

Results

Model performance

All models converged onto stationary posterior distributions (Suppl. Figs. 1–4) (online only). Posterior predictive checks showed the spawning seasonality model (Suppl. Figs. 5 and 6) (online only), the spawning interval models for OM (Suppl. Figs. 7–10) (online only) and POF (Suppl. Figs. 11–14) (online only) and the batch fecundity models (Suppl. Figs. 15 and 16) (online only) performed well, with summary statistics matching the real data. Although the batch fecundity models had difficulty predicting individual fecundity values because of the large amount of variation among individuals (Suppl. Figs. 17 and 18) (online only), they predicted group-level fecundity well (Suppl. Figs. 19 and 20) (online only). Forest plots showed there was not a consistent temporal trend in study-level effects for spawning seasonality (Suppl. Fig. 21) (online only), and no temporal or regional trend for spawning interval (Suppl. Figs. 22 and 23) (online only) or fecundity (Suppl. Fig. 24) (online only). Finally, the sensitivity analyses showed qualitative agreement and therefore robustness to prior assumptions across the different sensitivity trials for all models (Suppl. Figs. 25–31) (online only). Details about model validity checks are provided in the *Validation Results* section of the Supplementary methods (online only).

Spawning seasonality

Spawning seasonality was modeled by using data combined from the northeastern and northwestern GOM. Owing to the complexity of the GSI model, we did not have enough data to estimate monthly GSI parameters for each region separately. No data were available from 2003 through 2008 and therefore models are not presented for these years. In general, the estimated monthly GSI values were a close match to the observed mean monthly GSI values, with the exception of May 1994 and 1995, April, May, and September 1999 and April and June 2001, when some studies had much higher mean GSI values than the estimates (Fig. 2A). Lower mean GSI values than the estimates were seen in July 1999, May 2000, June and July 2001, April 2013, May 2014 and June 2016 (Fig. 2A).

Our analysis showed that peak spawning occurs during June, July and August for the entire 27-year time period of analysis (Fig. 2A). A high spawning probability is also estimated in May for 1994–2017. During the months of high spawning probability, the 95% credible intervals rarely extended below the threshold GSI value of 1.0. Additionally, the reproductive season extended from April to September for 1995 through 2017, and a 25–50% probability of spawning was estimated for these months (Fig. 2A). The estimated probability of spawning was <10% between November and February and the 95% credible intervals were larger, likely because of limited data during these months. There was a low probability of spawning (<25%) during March and October in some years, although limited data collection lends uncertainty to these estimates, particularly for collections in March.

The estimated spawning season based on GSI values ≥1 remained relatively constant from 1994 through 2017; the average duration was 4.54 months (Fig. 2B). The spawning season was shorter from 1991 through 1993 (average 2.59 months), and longest in 2001 (6.03 months). However, variability within the data and the lack of data during most of the colder months (i.e., November–March) could result in less precise estimates of spawning season duration.

Spawning interval

Mean spawning interval varied among studies and by method. No data were available from 2003 through 2008 and therefore models are not presented for these years. In the northeastern GOM, spawning interval varied from 1.5 days (August 2011) to 4.5 days (April 2011) (overall mean (±SE): 3.18 ±0.26 with the OM method, whereas spawning interval estimated with the POF method varied from 1.0 days (July 2011) to 35 days (2009) (overall mean: 6.57 ±2.45). In the northwestern GOM, spawning interval varied from 1.7 days (September 2011) to 16 days (April 2011) (overall mean: 5.32 ±1.01) for the OM method, whereas the spawning interval estimated with the POF method varied from 1.4 days (July 2011) to 8.1 days (2009) (overall mean: 4.66 ±0.81). Data from some studies suggest red snapper are capable of spawning daily (i.e., spawning interval=1). Histological evidence of actively spawning red snapper with POF < 24 h (Fig. 3) confirms that at least some individuals are capable of daily spawning, although this was not reported for fish collected before 2000.

Minimal increases in spawning interval were estimated between 1991 and 2017 for the northern GOM with both methods when data from the eastern and western regions were combined (Fig. 4, A and D; 2.4–2.9 d with the OM method, 1.9–2.3 d with the POF method), although there was greater uncertainty with the

[1] Mention of trade names or commercial companies is for identification purposes only and does not imply endorsement by the National Marine Fisheries Service, NOAA.

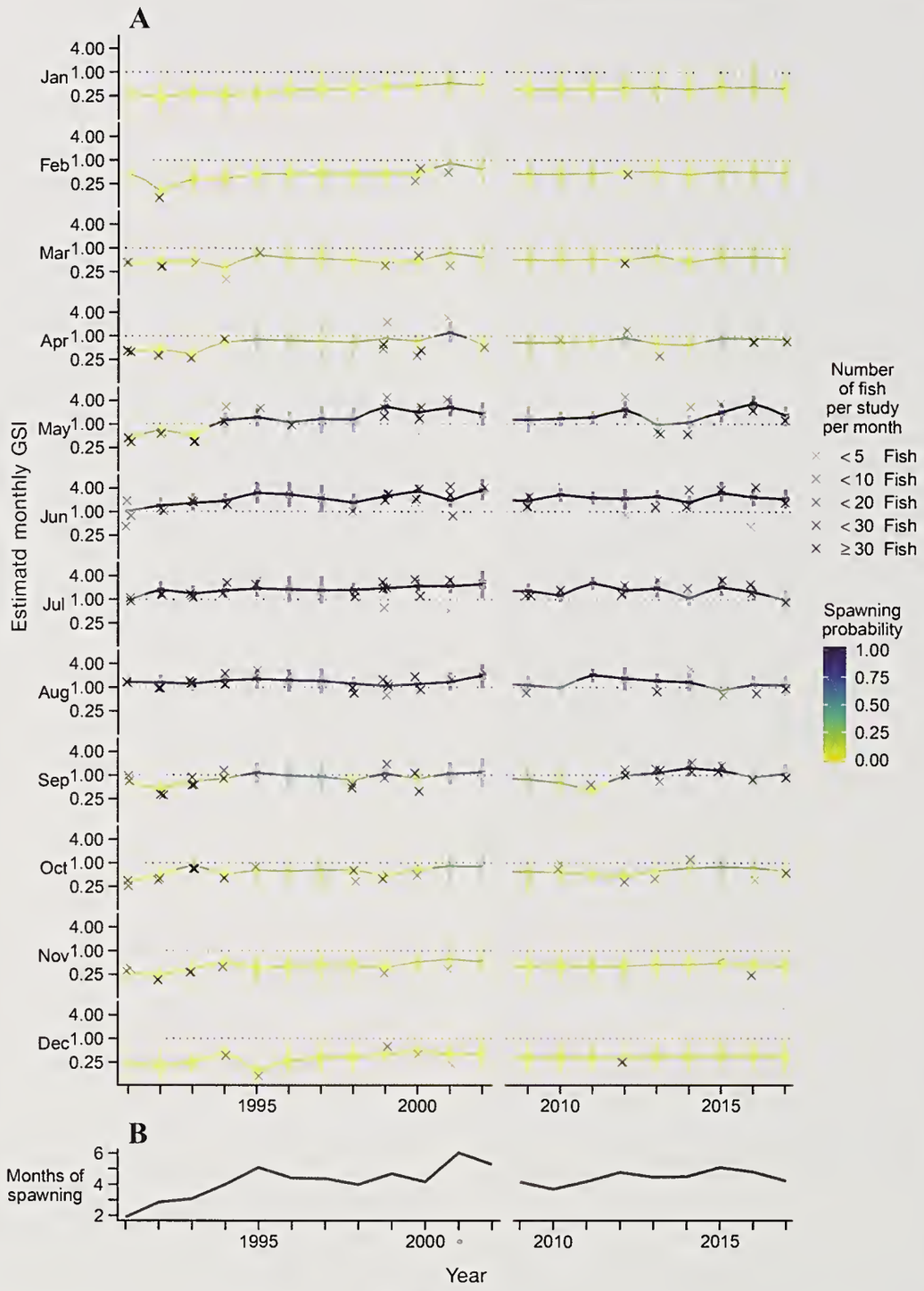

Figure 2

Spawning seasonality of northern Gulf of Mexico female red snapper (*Lutjanus campechanus*), estimated from a monthly Gonadosomatic Index (GSI). (**A**) Colored lines show estimated monthly GSI, including 50% and 95% credible intervals. These time series predictions were estimated from GSI data across multiple studies from 1991 through 2002 and from 2009 through 2017. Each × represents the mean GSI value of a study at a particular month and year. The number of individual GSI measurements used to calculate these means is indicated by the gradation of darkness of the ×'s. Red snapper are considered reproductively active when GSI ≥ 1 (dotted line), and the time series line color indicates the estimated probability of spawning. The y axis is presented as a back-transformed $\log_2$ scale. (**B**) The estimated number of months with reproductively active female red snapper.

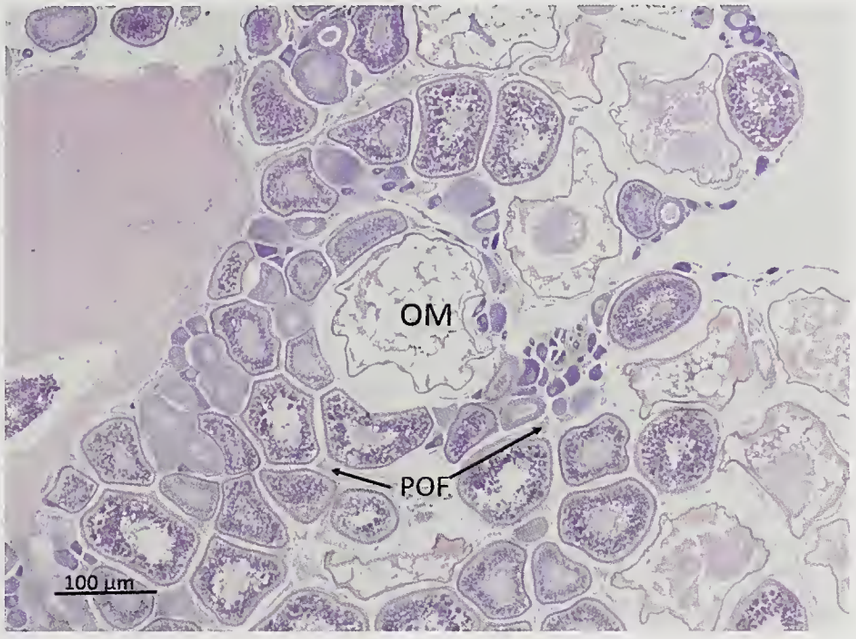

Figure 3

Photomicrograph of ovarian tissue from a female red snapper (*Lutjanus campechanus*) in the actively spawning reproductive subphase with 24-h postovulatory follicles (POFs) that show evidence of daily spawning. OM=oocytes undergoing oocyte maturation.

POF method. In contrast, spawning interval differed with the OM method when regions were considered separately. Although spawning interval remained stable in the northeastern GOM with a median estimated value of 2.30 days in 1991 to 2.37 days in 2017, the median estimate for the northwestern GOM increased from 2.3 days in 1992 to 4.7 days in 2015 (Fig. 4, B and C). Additionally, estimations of spawning interval for the northwestern region showed more uncertainty because the upper 95% credible intervals were larger than those for the northeastern region, particularly from 2009 through 2015 (excluding missing data from 2003 through 2008). In contrast, spawning interval remained relatively stable across time in both regions with the POF method (Fig. 4, E and F), but the northeast region had slightly higher estimated values for spawning interval (median estimated spawning interval: northeastern=2.2–2.4 days, 1991–2017; northwestern=2.0–1.9 days, 1992–2015). Both regions showed higher uncertainty from 1999 through 2010 (excluding missing data from 2003 through 2008), but the upper 95% credible intervals were larger in the northeastern region. However, it should be noted that mean spawning interval estimates (Fig. 4, horizontal lines) are less precise when individual study-level spawning interval values are large. Large spawning interval values are inherently more uncertain because they correspond with a very low proportion of individuals spawning at any given time, which can occur in studies with small sample sizes or with sample collections focused either early or late in the spawning season. Thus, even a small amount of variation is greatly magnified when spawning interval is calculated (e.g., 2009 POF data and 2010 OM data).

Batch fecundity

Individual RBF values varied greatly within all studies. Values ranged from 0.179 eggs/g ovary-free body weight in 1994 to 394.0 eggs/g ovary-free body weight in 2013 in the northeastern GOM and 0.048 eggs/g ovary-free body weight in 1998 to 557.39 eggs/g ovary-free body weight in 2001 in the northwestern GOM. Some of this variation was likely due to including RBF values collected from all months of the spawning season, including the beginning (April) and ending (September) of the spawning season. Despite the wide variation in individual RBF values the model is moderately robust to outliers, which can be seen in the relatively narrow credible intervals (Fig. 5). There were no RBF data available from the northeastern GOM during 2005–2006 (2003–2008 for the northwestern GOM), and therefore those years are not included in the model.

Relative batch fecundity showed a trend of decreasing values over time, particularly after 2012 (Fig. 5). Estimated mean (50% confidence interval [lower–upper as 25% and 75% CI]) RBF values for regions combined were initially 58.0 (45.8–71.4) eggs/g ovary-free body weight in 1991, increased to 83.8 (74.4–93.5) eggs/g ovary-free body weight in 2001, then decreased to

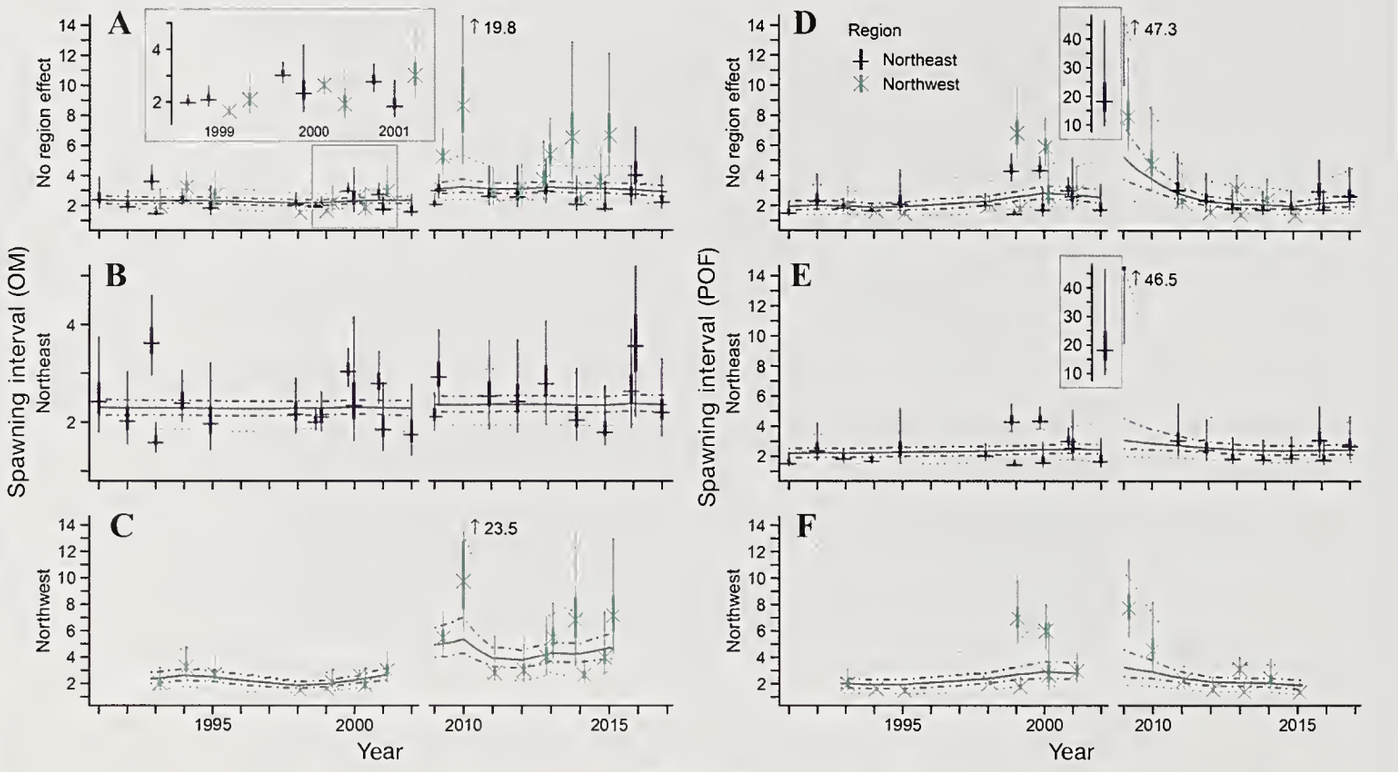

Figure 4

Estimated red snapper (*Lutjanus campechanus*) spawning interval from 1991 through 2002 and 2009 through 2017 in the northern Gulf of Mexico (GOM), calculated on the basis of evidence of oocyte maturation (OM, panels **A, B, C**) and postovulatory follicles (POFs, panels **D, E, F**). Spawning interval estimates for each study each year are indicated by black (northeastern GOM) or green (northwestern GOM) points with 50% (thick line) and 95% (thin line) credible intervals. Time series were estimated for combined regions (panels A, D) or separately in the northeast (panels B, E) and northwest (panels C, F). The horizontal solid line in each panel indicates the annual time series trend and the dashed lines show the 50% and 95% credible intervals. Extreme credible interval values are indicated by arrows. Note the difference in scale of the Y axis in graph B. The inset in graph A clarifies spawning interval estimates from 1999 through 2001 because of the large number of studies during those years. The insets in graphs D and E are study level spawning interval values that exceed the y-axis scale.

35.7 (29.1–43.1) eggs/g ovary-free body weight in 2017 (Fig. 5A). When regions were considered separately, RBF showed more modest changes in the northeastern region where estimated values changed from 70.7 (58.8–84.1) eggs/g ovary-free body weight in 1991 to 85.3 (75.0–97.4) eggs/g ovary-free body weight in 2000 and then decreased to 51.4 (41.1–62.9) eggs/g ovary-free body weight in 2017 (Fig. 5B). In contrast, RBF varied substantially in the northwestern region, shifting from 33.6 (21.3–50.0) eggs/g ovary-free body weight in 1994 to a high of 84.7 (68.2–103.3) eggs/g ovary-free body weight body weight in 2001 and then decreasing to 32.0 (25.8–39.2) eggs/g ovary-free body weight in 2015 (Fig. 5C). Because data from the northwestern GOM were available only between 1994 and 2015, annual estimates cover a smaller range.

Discussion

As a result of management-based recovery, red snapper abundance in the GOM has increased rapidly in recent years (Cass-Calay et al., 2015, SEDAR 52, 2018). Given this increasing abundance, and in particular the likelihood of the age structure of the stock becoming less truncated, Porch et al. (2015) and Kulaw et al. (2017) commented on the need to monitor red snapper reproductive traits over time. Regarding reproduction, two competing conditions may occur as a stock rebuilds. The first condition is an increase in abundance of older ages, which may lead to increased population-level egg production because red snapper reproductive metrics (e.g., batch fecundity, spawning frequency, and spawning season duration) all increase with size and age (Fitzhugh et al., 2012b; Lowerre-Barbieri et al., 2015; Porch et al., 2015). For many species, increasing age of mothers is also positively associated with egg and larval survival (Hixon et al., 2014) and there is evidence of a link between nutrition of reproductive females and egg and larval quality in red snapper (Papanikos et al., 2003, Bardon-Albaret and Saillant, 2017). Therefore, the age structure of recovering fish populations is an important management concern (Hixon et al., 2014, Barnett et al., 2017). A second condition, however, is

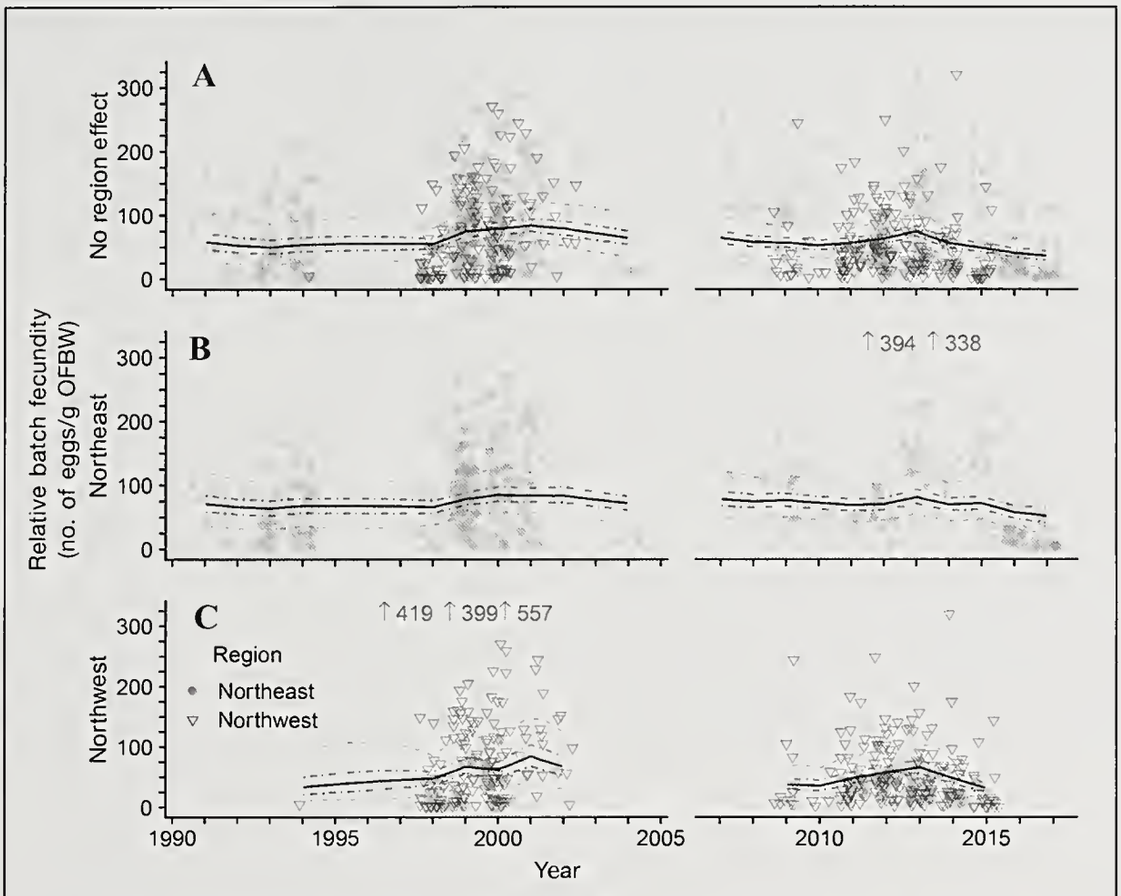

Figure 5

Estimated red snapper (*Lutjanus campechanus*) relative batch fecundity (number eggs/g ovary-free body weight, OFBW) from 1991 through 2004 and 2007 through 2017 in the northern Gulf of Mexico (GOM). Individual relative batch fecundity values are represented by circles (northeastern GOM) and triangles (northwestern GOM). The solid line indicates the annual trend with the dashed lines showing the 50% and 95% credible intervals. The trend was estimated for regions combined (graph **A**) and separately for the northeast (graph **B**) and northwest (graph **C**). Extreme values are indicated by arrows in the region-specific panels but are omitted from the combined-region plot for visual clarity.

that there is an overall reduction in surplus energy for growth and reproduction as the population increases (McBride et al., 2015, Porch et al., 2015). Decreases in fecundity with increasing fish density have been previously reported (Rose et al., 2001, Forrester et al., 2011, Hixon et al., 2012), and this decrease has been hypothesized to be a function of competition, food availability, or habitat availability. Thus density-dependence predicts a compensatory response wherein egg production may decline as population increases (Rose et al., 2001, Kulaw et al., 2017), possibly reflecting reproductive tradeoffs. Both conditions must be considered in order to track stock productivity over time (Trippel, 1995, Rose et al., 2001).

Our temporal meta-analysis models provide a unique approach to understanding potential changes in female red snapper reproductive parameters over a 27-year period. Although some reproductive parameters of red snapper, such as female spawning fraction with fish size, region, depth, and month (Porch et al., 2015) and variations in fecundity by habitat (Karnauskas et al., 2017) have been previously modeled, our study is the first effort to use modeling to quantify decade-level changes in red snapper reproduction. Both Porch et al. (2015) and Karnauskas et al. (2017) explicitly modeled an age-structured population. Our purpose was to more fully evaluate whether there is evidence for a compensatory response by examining key elements of egg production as represented by spawning interval, fecundity, and duration of spawning season (i.e., based on the GSI). Compensation can be very difficult to detect from empirical field data which often come from short-term studies (Rose et al., 2001). This challenge prompted our focus on meta-analysis. We examined trends over 27 years and based on many separate studies, and therefore age data were often not available. Therefore, we modeled spawning interval averaged across multiple age classes, and the size-age effect on fecundity was standardized to the degree possible by examination of RBF. Nor did we explicitly account

for time-of-year in spawning interval and RBF analyses, despite evidence that these parameters may vary throughout the reproductive season (Fitzhugh et al., 2012b, Lowerre-Barbieri et al., 2015). However, most studies commonly focused on reproductive sampling for these parameters during peak (summer) reproductive months, thus eliminating some temporal variation.

Our analyses indicate there was an overall decrease in egg production between 1991 and 2017, a decrease in RBF, and either no change or an increase in spawning interval. These differences were more pronounced in the northwestern GOM than in the northeastern GOM. Athough there was a downward trend in relative batch fecundity for the northeast, no substantial changes were estimated. There was no change in spawning interval in the northeast, whereas an increase was seen in the northwest when the OM method was used to calculate spawning interval. The lack of a meaningful change in spawning interval values with the POF method was likely due to large variations in the spawning interval values across months. Fish with POFs were more infrequently captured at the beginning and ending of the reproductive season than fish undergoing OM, leading to smaller sample sizes. Despite the duration of the spawning season remaining relatively constant from 1994 through 2017, a decrease in total egg production (lower RBF, greater spawning interval) suggests lower annual fecundity in the stock, particularly in the northwestern GOM. Our analyses suggest the potential of a compensatory reproductive effect may be more evident in the northwestern GOM. This compensatory effect may correspond with stock assessment projections of higher levels of spawning stock biomass and a greater likelihood of sustained recovery in the west (Cass-Calay et al., 2015, SEDAR 52, 2018), resulting in increased fish density and greater competition for resources as discussed above.

Differences in the population structure of red snapper stocks between the eastern and western GOM have been previously identified. The northwestern GOM shows evidence of greater numbers of older red snapper, particularly in the last 8–10 years (Saari et al., 2014, Cass-Calay et al., 2015, Porch et al., 2015, Karnauskas et al., 2017, SEDAR 52, 2018), as well as greater numbers of eggs and larvae (Lyczkowki-Shultz and Hanisko, 2007, Hanisko et al., 2017). There is also evidence of a metapopulation structure of northern GOM red snapper; the demographic differences between GOM regions are supported by genetic analysis (Gold and Saillant, 2007, Puritz et al., 2016). Previous findings of differences in maturity, growth, and demographics between the eastern and western GOM have suggested that density-dependent processes may be occurring (Fitzhugh et al., 2004, Jackson et al., 2007, Saari et al., 2014). Kulaw et al. (2017) recently reported more evidence of regional differences in comparing reproductive traits from Alabama and Louisiana red snapper sampled ~10 years apart, and again invoked compensation to help explain these differences. As with the present study, they saw a decreased trend in spawning frequency (increased spawning interval) and provided evidence for decreased GSI and increasing age at maturity in their northwestern GOM study area. Kulaw et al. (2017) reported that a more detectable trend of declining reproductive output was evident among younger females in the west than in the east of the Mississippi River. However, Kulaw et al. (2017) tempered their conclusions regarding the degree of density dependence by age because of their limited sample size, and pointed to potential habitat factors in partially explaining their results.

Red snapper are most commonly found associated with underwater structures, and the type of structure (i.e., habitat) may influence reproduction. Higher reproductive output was found at natural versus artificial habitats on the outer Louisiana shelf area of study (Glenn et al., 2017, Kulaw et al., 2017), although natural and artificial reefs were at different depths which may confound the reported results. Red snapper inhabiting deep (60–100 m) artificial reefs have a longer spawning season and a higher percentage of spawning-capable and actively spawning females than red snapper at shallow (<20 m) reefs (Brown-Peterson and Moncrief[2]); these differences are likely related to larger fish captured at deeper depths. In contrast, differences in reproductive parameters were not seen among habitats in artificial and natural reefs in the same depth zone off Texas (Downey et al., 2018). High densities of young red snapper are particularly common on artificial structures, such as oil platforms and small artificial reefs, although these structures represent only a fraction of the area in the northern GOM (Karnauskas et al., 2017). The majority of the data since 2012 used in the analyses in the present study have been from artificial structures. Therefore, we cannot reject the possibility that age and habitat may be confounding influences in our results, but we examined red snapper from a wider geographic area and longer time period than those of previous studies.

Although we were unable to model regional differences in spawning seasonality, it is clear from our analysis that the peak spawning time for red snapper in the northern GOM of June through August has remained relatively constant over the 27-year period examined. This peak spawning period is well supported in the literature (Render, 1995; Collins et al., 1996; Fitzhugh et al., 2004). Our analysis suggests May is also a peak spawning month since 1994, which is corroborated by back calculated spawning dates of juvenile red snapper in 1995 (Szedlmayer and Conti, 1999). In addition, spawning capable female red snapper have been recently reported from April, September, and early October (Lowerre-Barbieri et al., 2012; Fitzhugh et al., 2012a). Our model used mean monthly GSI ≥ 1.0

[2] Brown-Peterson, N. J., and T. D. Moncrief. 2017. Does depth influence Red Snapper reproductive biology metrics? *In* Abstract book, 2017 Joint Meetings of Ichthyologists and Herpetologists, Austin, Texas, p. 69–70. Available from website.

to define reproductively active females, which does not reflect the presence of a few individual females with high GSI values in each month. Therefore, the majority of the population was likely not reproductively active in April, September, and October, thus leading to a monthly mean GSI < 1.0. Furthermore, our spawning duration estimates cannot account for half months (i.e., for a decrease in GSI in the second half of a month), and may thus result in a slight underestimation of spawning season duration. However, we do estimate a 4.5-month duration of the spawning season since 1994, which likely corresponds to a May through mid-September spawning season. An additional challenge in modeling spawning seasonality is the fact that GSI reflects proportion data, which can result in skewed model results. Finally, temperature is an important regulator of spawning seasonality, particularly at the beginning of the reproductive season (Brown-Peterson et al., 2002). Incorporation of a temperature component into future models of spawning seasonality may increase the robustness of the seasonal estimates. An understanding of the duration of the spawning season, as well as how it may vary across time and with age is important for the most accurate determinations of age and size at sexual maturity, spawning frequency, and annual fecundity, which are all important metrics for optimal management of red snapper stocks.

The estimated decline in red snapper reproductive parameters from 1991 through 2017 may raise concern for the continued recovery of the red snapper population, particularly in the northwestern GOM. However our results are primarily based upon reproductive samples from young females (≤ age 6), similar to those from other studies (Porch et al., 2015; Glenn et al.; 2017, Karnauskas et al.; 2017; Kulaw et al., 2017). Kulaw et al. (2017) suggest that reductions in reproductive output of young females may be more than offset by increasing contributions from older females. Unfortunately, older age females (e.g. ≥ age 9) are uncommon among reproductive studies despite estimates that show that peak per-capita reproductive output occurs around age 14 (Porch, 2007; Porch et al., 2015; Kulaw et al., 2017). Owing to the economic importance of GOM red snapper, we expect sampling for reproductive metrics to continue and possibly increase over time. Although slow to accrue, reproductive data are being collected from older females. The increasing abundance of older red snapper, particularly in the northwestern GOM (Porch et al., 2015, Karanauskas et al., 2017, Table 2.24 in SEDAR 52, 2018), suggests a changing population structure that has likely been aided by management regulations to reduce fishing pressure. Ultimately we do want to account for age-based effects of reproductive compensation and recommend modeling the sensitivity of compensation in predictions of stock status as discussed by Rose et al. (2001). Density-dependent reproductive compensation, if it exists, has important management implications because reproductive productivity is the basis for stock assessment projections and reference points (Rose et al., 2001, Porch et al., 2015). Continued monitoring and analysis of reproductive attributes over the long term, such as those presented here, will provide insights into red snapper biology and stock condition.

Acknowledgments

We thank D. Kulaw, H. Glenn, C. Downey and G. Stuntz for sharing raw data. Staff from the National Marine Fisheries Service (NMFS) Southeast Fisheries Science Center, T. Moncrief, and M. Oshima assisted with collection and analyses of NMFS and Mississippi data. X. Zhang and A. Chester made helpful comments on the manuscript. Analyses were performed on the Texas Advanced Computing Center Lonestar 5 supercomputer. Funding from the National Fish and Wildlife Federation in collaboration with the Mississippi Department of Environmental Quality, Covington Civil and Environmental Engineering and the Mississippi Department of Marine Resources (NBP) and the Office of Graduate Studies at the University of Texas-Austin (CRP) supported the authors.

Literature cited

Alexander, R. J.
2015. Comparing reproductive capacity of nearshore and offshore Red Snapper, *Lutjanus campechanus*, on artificial reefs in the western Gulf of Mexico. M.S. thesis, 84 p. Univ. Texas Rio Grande Valley, Brownsville TX.

Bagenal, T. B., and E. Braum.
1971. Eggs and early life history. *In* Methods for assessment of fish production in fresh waters, IBP 2nd ed. (W. F. Ricker, ed.), p. 159–181. Blackwell Science, Oxford, U.K.

Bardon-Albaret, A., and E. Saillant.
2017. Egg quality traits and predictors of embryo and fry viability in red snapper *Lutjanus campechanus*. Aquac. Rep. 7:48–56.

Barnett, A. K., T. A. Branch, R. A. Ranasinghe, and T. E. Essington.
2017. Old-growth fishes become scarce under fishing. Curr. Biol. 27: 2843–2848.e2.

Brown-Peterson, N. J., M. S. Peterson, D. L. Nieland, M. D. Murphy, R. G. Taylor, and J. R. Warren.
2002. Reproductive biology of female spotted seatrout, *Cynoscion nebulosus*, in the Gulf of Mexico: differences among estuaries? Environ. Biol. Fish. 63:405–415.

Brown-Peterson, N. J., K. M. Burns, and R. M. Overstreet.
2009. Regional differences in Florida red snapper reproduction. Proc. Gulf Carib. Fish. Inst. 61:149–155.

Brown-Peterson, N. J., D. M. Wyanski, F. Saborido-Rey, B. J. Macewicz, and S. K. Lowerre-Barbieri.
2011. A standardized terminology for describing reproductive development in fishes. Mar. Coast. Fish. 3:52–70.

Carpenter, B., A. Gelman, M. D. Hoffman, D. Lee, B. Goodrich, M. Betancourt, M. Brubaker, J. Guo, P. Li, and A. Riddell.
2017. Stan: A probabilistic programming language. J. Stat. Software 76(1), 32 p.

Cass-Calay, S. L, C. E. Porch, D. R. Goethel, M. W. Smith, V. Matter, and K. J. McCarthy.
2015. Stock assessment of red snapper in the Gulf of Mexico 1872–2015—with provisional 2014 landings. SEDAR red snapper 2014 update assessment, North Charleston, SC, 242 p. Available from website.

Collins, L. A., A. G. Johnson, and C. P. Keim.
1996. Spawning and annual fecundity of the red snapper (*Lutjanus campechanus*) from the northeastern Gulf of Mexico. *In* Biology, fisheries and culture of tropical groupers and snappers, International Center for Living Aquatic Resources Management (ICLARM) Proceedings 48 (F. Arreguin-Sanchez, J. L. Munfo, M .C. Balgos, and D. Pauly, eds.), p. 174–188. ICLARM, Manila, Philippines.

Cowan, Jr., J. H., K. M. Boswell, K. A. Simonsen, C. R. Saari, and D. Kulaw.
2012. Working paper for red snapper data workshop (SEDAR 31). SEDAR31-DW-03. SEDAR, North Charleston, SC. 49 p. [Available from website.]

Downey, C. H., M. K. Streich, R. A. Brewton, M. J. Ajemian, J. J. Wetz, and G. W. Stunz.
2018. Habitat-specific reproductive potential of Red Snapper: A comparison of artificial and natural reefs in the western Gulf of Mexico. Trans. Am Fish. Soc. 147:1030–1041.

Fitzhugh, G. R., M. S. Duncan, L. A. Collins, W. T. Walling Jr., and D. W. Oliver.
2004. Characterization of red snapper (*Lutjanus campechanus*) reproduction: for the 2004 Gulf of Mexico SEDAR. SDEAR7-DW-35. Contribution Series 04-10, National Marine Fisheries Service, Panama City, FL, 29 p.

Fitzhugh, G. R., E. T. Lang, and H. Lyon.
2012a. Expanded annual stock assessment survey 2011: red snapper reproduction. SEDAR31-DW-07. SEDAR, North Charleston, SC. 33 p. [Available from website.]

Fitzhugh, G. R., K. W. Shertzer, G. T. Kellison, and D. M. Wyanski.
2012b. Review of size- and age-dependence in batch spawning: implications for stock assessment of fish species exhibiting indeterminate fecundity. Fish. Bull. 110:413–425.

Forrester, G., L. Harmon, J. Helyer, W. Holden, and R. Karis.
2011. Experimental evidence for density-dependent reproductive output in a coral reef fish. Pop. Ecol. 53:155–163.

Gelman, A., J. B. Carlin, H. S. Stern, D. B. Dunson, A. Vehtari, and D. B Rubin.
2013. Bayesian data analysis, 3rd ed., 639 p. CRC Press, Boca Raton, FL.

Glenn, H. D., J. H. Cowan and J. E. Powers.
2017. A comparison of Red Snapper reproductive potential in the northwestern Gulf of Mexico: natural versus artificial habitats. Mar. Coast. Fish. 9:139-148.

GMFMC.
2007. Amendment 27 to the reef fish fishery management plan and Amendment 14 to the shrimp fishery management plan. Gulf of Mexico Fishery Management Council, Tampa, FL, 480 p.

Gold, J. R. and E. Saillant.
2007. Population structure of red snapper in the northern Gulf of Mexico. *In* Red snapper ecology and fisheries in the U. S. Gulf of Mexico, Symposium 60 (W. F. Patterson III, J. H. Cowan Jr., G. R. Fitzhugh, and D. L. Nieland, eds.), p. 201–216. Am. Fish. Soc., Bethesda, MD.

Goodyear, C.P.
1988. Recent trends in the red snapper fishery of the Gulf of Mexico. Technical Report CRD 87/88-19. National Marine Fisheries Service, Southeast Fisheries Science Center, Miami, Florida. [Available from website.]

Hanisko, D. S., A. G. Pollack, D. M. Drass, P. J. Bond, C. Stepongzi, T. Wallace, A. Millet, C. Cowan, C. M. Jones, G. Zapfe and G. W. Ingram Jr.
2017. Red Snapper (*Lutjanus campechanus*) larval indices of relative abundance from SEAMAP Fall Plankton Surveys, 1986 to 2016. SEDAR52-WP-11. SEDAR, North Charleston, SC, 36 p. [Available from website.]

Hixon, M. A., T. W. Anderson, K. L Buch, D. W. Johnson, J. B. McLeod, and C. D. Stallings.
2012. Density dependence and population regulation in marine fish: a large-scale, long-term field manipulation. Ecol. Monogr. 82:467–489.

Hixon, M. A., D. W. Johnson, and S. M. Sogard.
2014. BOFFFFs: on the importance of conserving old-growth age structure in fishery populations. ICES J. Mar. Sci. 71:2171–2185.

Jackson, M. W., J. H, Cowan Jr., and D. L. Nieland.
2007. Demographic differences in northern Gulf of Mexico Red Snapper reproductive maturation: implications for the unit stock hypothesis. *In* Red snapper ecology and fisheries in the U. S. Gulf of Mexico, Symposium 60 (W. F. Patterson III, J. H. Cowan, Jr., G. R. Fitzhugh, and D. L. Nieland, eds.), p. 217–227. Am. Fish. Soc., Bethesda, MD.

Karnauskas, M., J. F. Walter III, M. D. Campbell, A. G. Pollack, J. M. Drymon and S. Powers.
2017. Red snapper distribution on natural habitats and artificial structures in the northern Gulf of Mexico. Mar. Coast. Fish. 9:50–67.

Kulaw, D. H., J. H. Cowan, and M. W. Jackson.
2017. Temporal and spatial comparisons of the reproductive biology of northern Gulf of Mexico (USA) red snapper (*Lutjanus campechanus*) collected a decade apart. PLoS ONE 12(3):e0172360.

Lang, E. T. and B. J. Falterman.
2017. A comparison of sampling methods and continuation of red snapper life history metrics. SEDAR52-WP-07. SEDAR, North Charleston, 10 p. [Available from website.]

Lowerre-Barbieri, S. L. Crabtree, T. S. Switzer, and R. H. McMichael Jr.
2012. Spatio-temporal dynamics in red snapper reproduction on the west Florida Shelf, 2008-2011. SEDAR31-DW-07. SEDAR, North Charleston, SC. 11 p. [Available from website.]

Lowerre-Barbieri, S. L, L. Crabtree, T. Switzer, S. W. Burnsed, and C. Guenther.
2015. Assessing reproductive resilience: an example with South Atlantic red snapper *Lutjanus campechanus*. Mar. Ecol. Prog. Ser. 526:125–141.

Lyczkowski-Shultz, J., and D. S. Hanisko.
2007. A time series of observation on red snapper larvae from SEAMAP surveys, 1982–2003: seasonal occurrence, distribution, abundance, and size. *In* Red snapper ecology and fisheries in the U.S. Gulf of Mexico, Symposium 60 (W. F. Patterson III, J. H. Cowan Jr., G. R. Fitzhugh, and D. L. Nieland, eds.), p. 3–23. Am. Fish. Soc., Bethesda, MD.

McBride, R. S., S. Somarakis, G. R. Fitzhugh, A. Albert, N. A. Yaragina, M. J. Wuenschel, A. Alonso-Fernandez, and G. Basilone.
2015. Energy acquisition and allocation to egg production in relation to fish reproductive strategies. Fish Fish. 16:23–57.

McElreath, R.
2016. Statistical rethinking: a Bayesian course with examples in R and Stan, 469 p. CRC Press/Taylor & Francis, Boca Raton, FL.

Papanikos, N., R. P. Phelps, K. Williams, A. Ferry, and D. Maus.
2003. Egg and larval quality of natural and induced spawns of red snapper, *Lutjanus campechanus*. Fish Phys. Biochem. 28:487–488.

Porch, C. E.
2007. An assessment of the red snapper fishery in the U.S. Gulf of Mexico using a spatially-explicit age-structured model. *In* Red snapper ecology and fisheries in the U. S. Gulf of Mexico, Symposium 60 (W. F. Patterson III, J. H. Cowan Jr., G. R. Fitzhugh, and D. L. Nieland, eds.), p.355–384. Am. Fish. Soc., Bethesda, MD.

Porch, C. E., G. R. Fitzhugh, E. T. Lang, H. M Lyon, and B. C. Linton.
2015. Estimating the dependence of spawning frequency on size and age in Gulf of Mexico red snapper. Mar. Coast. Fish. 7:233–2245.

Puritz, J. B., J. R. Gold and D. S. Portnoy.
2016. Fine-scale partitioning of genomic variation among recruits in an exploited fishery: causes and consequences. Sci. Rep. 6:36095.

R Core Team.
2017. R: a language and environment for statistical computing. R Foundation for Statistical Computing, Vienna, Austria. Available from website.

Render, J. H.
1995. The life history (age, growth, and reproduction) of red snapper (*Lutjanus campechanus*) and its affinity for oil and gas platforms. Ph.D. diss., 76 p. Louisiana State Univ., Baton Rouge, LA.

Rose, K. A., J. H. Cowan Jr., K. O. Winemiller, R. A. Myers, and R. Hilborn.
2001. Compensatory density dependence in fish populations: importance, controversy, understanding and prognosis. Fish Fish. 2:293–327.

Saari, C. R., J. H. Cowan Jr., and K. M. Boswell.
2014. Regional differences in the age and growth of red snapper (*Lutjanus campechanus*) in the U.S. Gulf of Mexico. Fish. Bull. 112:261–273.

SEDAR 7.
2005. Stock assessment of SEDAR 7: Gulf of Mexico red snapper. Southeast Data, Assessment, and Review, Charleston, SC, 480 p.

SEDAR 31.
2013. SEDAR 31: Gulf of Mexico red snapper. Southeast Data, Assessment, and Review, Charleston, SC, 294 p.

SEDAR 52.
2018. SEDAR 52: Stock assessment report Gulf of Mexico red snapper, North Charleston, SC, 435 p.

Stan Development Team.
2017. Stan modeling language users guide and reference manual, vers. 2.16.0. Available from website.

Szedlmayer, S. T., and J. Conti.
1999. Nursery habitats, growth rates, and seasonality of age-0 red snapper, *Lutjanus campechanus*, in the northeast Gulf of Mexico. Fish. Bull. 97:626–635.

Trippel, E. A.
1995. Age at maturity as a stress indicator in fisheries. Bioscience 45:759–771.

National Marine
Fisheries Service
NOAA

Fishery Bulletin
established in 1881

Spencer F. Baird
First U.S. Commissioner
of Fisheries and founder
of *Fishery Bulletin*

Using oxytetracycline validation for confirmation of changes in vertebral band-pair deposition rates with ontogeny in sandbar sharks (*Carcharhinus plumbeus*) in the western North Atlantic Ocean

Lisa J. Natanson (contact author)[1]
Bethany M. Deacy[2]

Email address for contact author: lisa.natanson@noaa.gov

[1] Northeast Fisheries Science Center
National Marine Fisheries Service, NOAA
28 Tarzwell Drive
Narragansett, Rhode Island 02882

[2] Riverside Technologies, Inc.
for National Marine Fisheries Service, NOAA
3500 Delwood Beach Road
Panama City, Florida 32408

Abstract—Age underestimation of many shark species, such as the sandbar shark (*Carcharhinus plumbeus*), has been proven with age validation methods including bomb radiocarbon dating, oxytetracycline (OTC) injection, and tag-recapture data. Validation studies indicate that band-pair deposition in vertebral centra may not be directly related to time, especially in older individuals of a species. In this study, vertebrae from tagged, OTC-injected, and recaptured sandbar sharks were examined to determine if band-pair deposition past the OTC mark matched time at liberty. In 6 of 8 OTC-injected sharks at liberty for >1 year, band-pair count past the OTC mark underestimated time at liberty by 24–58%. Additionally, growth rates derived from tag-recapture data were slower than those described by previously published vertebral band-pair growth curves but were similar to those predicted by previous bomb radiocarbon dating and OTC results from this study. Together, the results from these studies indicate that modeling tag-recapture data may be more accurate for age determination in elasmobranchs given that band-pair counts on vertebral centra do not coincide with age throughout life. Analyses indicate that sandbar sharks may be less productive than previously understood.

Manuscript submitted 13 August 2018.
Manuscript accepted 20 December 2018.
Fish. Bull. 117:50–58 (2019).
Online publication date: 8 February 2019.
doi: 10.7755/FB.117.1.6

The views and opinions expressed or implied in this article are those of the author (or authors) and do not necessarily reflect the position of the National Marine Fisheries Service, NOAA.

Research has shown that the rate of vertebral band-pair deposition in elasmobranchs is variable and not necessarily related to time (Harry, 2018; Natanson et al., 2018). At least 30% of studies attempting to validate the periodicity of vertebral band-pair deposition in elasmobranchs in relation to age have shown that ages were underestimated (Harry, 2018). Results from the use of oxytetracycline (OTC) injection, tag-recapture data, and bomb radiocarbon dating for validation indicate that band-pair deposition in sharks can approximate time in certain life stages (e.g., Campana et al., 2002; Natanson et al., 2002; Francis et al., 2007; Andrews et al., 2011; Wells et al., 2013; Hamady et al., 2014; Passerotti et al., 2014; Natanson and Skomal, 2015; Kinney et al., 2016; Harry, 2018). A change in band-pair deposition rate often occurs at the approach of maturity, indicating that band-pair deposition rate changes with shifts in the growth rate associated with energetic demands required by a maturing fish. In some species, such as the Pacific angel (*Squatina californica*) and basking (*Cetorhinus maximus*) sharks, there is no apparent link to time at any life stage (Natanson and Cailliet, 1990; Natanson et al., 2008). Furthermore, examination of vertebral band-pair counts in relationship to vertebral and somatic growth in 7 elasmobranch species has revealed a relationship between body girth and band-pair deposition. This finding indicates that, although there may be a coincidental link to time in band-pair deposition, band-pair deposition is more likely related to vertebral structure (Natanson et al., 2018). The results of all of these studies reemphasize the importance of direct validation of all sizes of a species (Beamish and McFarlane, 1983).

The sandbar shark (*Carcharhinus plumbeus*) is a common coastal carcharhinid that is widely distributed in the world's oceans (Ebert et al., 2013). In the western North Atlantic Ocean, the sandbar shark is distributed from southern Massachusetts to Florida, into the Gulf of Mexico, and to southern Brazil (Castro, 2011). This shark has been the primary

target species of the bottom longline fishery for coastal sharks since the 1980s (NMFS, 1993). In 2007, amendments to the Consolidated Atlantic Highly Migratory Species Fisheries Management Plan limited the take of the sandbar shark to a research fishery with the intent to collect life-history and catch data (NMFS, 2007). Since the implementation of this research fishery, collected vertebral samples have been used for age and growth analysis for the stock assessment of this species (SEDAR, 2011, 2017).

Discrepancies exist among the previously published age and growth studies on sandbar sharks, largely because of lack of validation of band-pair periodicity in the early vertebral studies (Casey et al., 1985; Casey and Natanson, 1992; Sminkey and Musick, 1995; Andrews et al., 2011; Hale and Baremore, 2013; Romine et al., 2013). Both growth curves generated in models from tag-recapture data and results from bomb radiocarbon analyses suggest slower growth and a longer lifespan than that estimated by using band-pair counts on vertebral centra (Casey and Natanson, 1992; Andrews et al., 2011). Additionally, results from the bomb radiocarbon technique indicate that band-pair counts approximated annual deposition only until 10–12 years of age (Andrews et al., 2011).

We report on a long-term field study undertaken by the National Marine Fisheries Service's Cooperative Shark Tagging Program to validate the band-pair periodicity of the sandbar shark in the western North Atlantic Ocean. Results from recaptured sandbar sharks that were tagged and injected with OTC between 1985 and 2017 are presented and compared with results from previous studies. We also updated the tag-recapture growth curve of sandbar sharks generated by Casey and Natanson (1992) to refine growth estimates.

Materials and methods

The Cooperative Shark Tagging Program tagged 39,405 and recaptured 1603 sandbar sharks between 1962 and 2017. Data recorded at tagging and recapture included size (fork length, total length, or weight), sex, location, and date; these data are referred to as *tag-recapture data* for the remainder of this paper. Sharks were tagged and recaptured by biologists, fisheries observers, and commercial and recreational fishermen in the United States. Sharks tagged for age validation studies were injected with a dose of OTC (25 mg per 1 kg of body weight), primarily by biologists on research vessels, and precisely measured before release. Only vertebrae from sharks with a reliably measured fork length (FL, from the tip of the snout to the fork in the tail, over the body) or total length (TL, from the tip of the snout to a point on the horizontal axis intersecting a perpendicular line extending downward from the tip of the upper caudal lobe to form a right angle, over the body; Kohler et al., 1996) at both tagging and recapture were used in this study. We determined the reliability of measurement data on the basis of prior knowledge of the individual measuring the shark or detailed questioning of those individuals as to the method used. Measurements were converted to over-the-body FL, when necessary, by using the following equation (Kohler et al., 1996; n=3734; coefficient of determination [r^2]=0.9933):

$$FL = 0.8175(TL) + 2.5676. \quad (1)$$

Processing of vertebrae

For each shark, multiple vertebrae were removed from the area just posterior to the branchial chamber wherever possible; vertebrae were obtained closer to the head when sampling occurred onboard commercial vessels. We acknowledge that vertebral centra from different parts of the vertebral column in carcharhinids have been shown to have varying band-pair counts associated with vertebral size (Natanson et al., 2018). Preliminary data show that, for sandbar sharks in the size range used in this study, band-pair count will be consistent along the vertebral column, allowing us to use vertebra from differing parts of the body (senior author, unpubl. data). All vertebrae processed for band-pair counts were stored frozen or in 70% ethyl alcohol in the dark until processing. Individual vertebrae were sectioned laterally through the focus by using gross sectioning (Natanson et al., 2006).

Validation with oxytetracycline marking

The accuracy of vertebral band-pair counts for use as annual indicators of growth was determined by using individuals that were recaptured after they were injected with OTC, tagged, and released. Between 1985 and 2017, 7556 tagged sandbar sharks were injected with OTC, and data from 279 sharks (3.7%) were returned by 2017. Vertebrae obtained from 12 of these recaptured sandbar sharks were examined. Two pictures of each section, in the identical position, were taken by using 1) reflected white light for band-pair counts and 2) reflected long-wave UV light (366 nm) with the exposure increased to 20 s to obtain images of the OTC mark. Images were taken with a Nikon DSR12[1] digital camera (Nikon Corp., Tokyo, Japan) attached to a Nikon SMZ1500 stereo microscope (Nikon Instruments, Inc., Melville, NY). Magnification varied with the size of the section, and a scale was included in each photo.

Band pairs (consisting of one opaque and one translucent band; Casey et al., 1985) were counted and marked independently by 2 experienced age readers using image editing software (Adobe Photoshop Elements 6, Adobe, Inc., San Jose, CA). Each band pair was marked on an individual layer in Adobe Photoshop by the readers following Natanson et al. (2018), and each layer was considered a count. Once the readers

[1] Mention of trade names or commercial companies is for identification purposes only and does not imply endorsement by the National Marine Fisheries Service, NOAA.

Table 1

Tag-recapture data and vertebral band-pair counts for 12 recaptured sandbar sharks (*Carcharhinus plumbeus*) injected with oxytetracycline (OTC) and tagged between 1983 and 2009 in the western North Atlantic Ocean. The relationship between years at liberty (YAL) and counts of vertebral band pairs (BP) is included (BP–YAL). An asterisk (*) indicates an estimated length. The last 4 sharks were either at liberty for less than 1 year or had no visible OTC mark and were not included in analysis. TFL=fork length at tagging; RFL=fork length at recapture; VR=vertebral radius; M=mature; and UNK=unknown sex.

Specimen ID code	Sex	TFL (cm)	RFL (cm)	Date tagged	Date recaptured	YAL	Growth (cm)	No. of BPs past OTC mark	Total no. of BPs	BP–YAL	Maturity	Underestimation between BP and YAL (%)
CM1025	F	119	159	5/16/2001	6/28/2017	16.12	40	7.0	14.0	−9.12	M	56.58
CM1029	F	136	156	11/14/2000	5/26/2010	9.53	20	4.0	14.0	−5.53	UNK	58.03
CM1024	M	129	154	5/2/2009	5/29/2017	8.10	25	4.0	13.0	−4.1	M	50.62
CM945	F	68	150	10/25/1996	8/8/2002	11.77	82	9.0	11.0	−2.77	UNK	23.53
CM1026	F	114	132	8/6/1986	7/29/1993	6.98	18	5.0	13.0	−1.98	UNK	28.37
CM867	M	115	134	5/19/1989	2/22/1993	3.76	19	2.5	10.0	−1.26	UNK	33.51
CM1031	M	56	156	9/21/1998	6/4/2014	15.70	100	15.5	16.0	−0.20	M	
CM1027	F	85	147	8/3/1996	7/27/2006	9.98	62	10.0	13.0	0.02	UNK	
CM751	M	56	59	7/31/1983	9/7/1983	0.10	3	<1				
CM932	F	150	153	11/14/2000	3/1/2001	0.29	3	<1				
CM1028	F	160	165*	4/22/2009	8/25/2010	1.34	5	No OTC				
CM1030	M	130*	153	5/4/2009	6/6/2011	2.01	23	No OTC				

agreed on a final count, a layer with the OTC mark was superimposed on the consensus layer. The transparency of the OTC layer was decreased until the marks on the consensus layer were visible.

Growth analysis with tag-recapture data

Data from only those sharks at liberty for >1 year and with a reliably measured body length at both tagging and recapture were used in growth curve analysis (n=149). Parameters for the von Bertalanffy growth function from the tag-recapture data were generated by using both the Gulland and Holt (1959) and GROTAG (Francis, 1988) models in R, vers. 3.5.1 (R Core Team, 2018).

The Francis (1988) method (GROTAG) uses maximum likelihood techniques to estimate growth parameters and variability from tagging data. A coefficient of variation of growth variability (v), the mean and standard deviation of measurement errors (s=standard deviation of measurement error), and outlier contamination (p) are estimated as well as growth rates at 2 user-selected lengths (α and β). The reference lengths, α and β, were chosen to lie within the range of tagged individuals. The form of the von Bertalanffy equation becomes

$$\Delta L = \left[\frac{\beta g_\alpha - \alpha g_\beta}{g_\alpha - g_\beta}\right]\left[1-\left(1+\frac{g_\alpha - g_\beta}{\alpha-\beta}\right)^{\Delta T}\right], \quad (2)$$

where L_1 = the length at tagging;
ΔL = the increment in length;
ΔT = the increment in time;
g_α = the mean annual growth rate at arbitrary length α; and
g_β = the mean annual growth rate at the arbitrary length β.

Mean annual growth rates for the GROTAG model were estimated at 60 and 160 cm FL to represent the size ranges of the sandbar shark. The simplest model, a linear fit with minimal parameters (α and s), was used initially, with additional parameters added to successively increase model complexity. Significant improvement in the model results was achieved by using log-likelihood ratio tests (Francis, 1988). The model searches for the set of parameters that maximize the log-likelihood ratio (λ). The introduction of additional parameters must increase λ by 1.92 to be significant (P<0.05) (Francis, 1988).

The value of the theoretical age at which a fish would have zero length (t_0) cannot be estimated from tagging data alone; rather, it requires an estimate of absolute size at age, such as size at birth. We calculated t_0 with the von Bertalanffy growth function (von Bertalanffy, 1939) by using the following equation:

$$t_0 = t + (1/k)[\ln\{(L_\infty - L_t)/L_\infty\}], \quad (3)$$

where L_t = known length at age (size at birth);
L_∞ = mean asymptotic fork length;
t = age; and
k = a growth constant (per year).

The t_0 values were calculated on the basis of an average size at birth of 47.7 cm FL (Casey et al., 1985) with t=0. Values for L_∞ and k were calculated in the tag-recapture models.

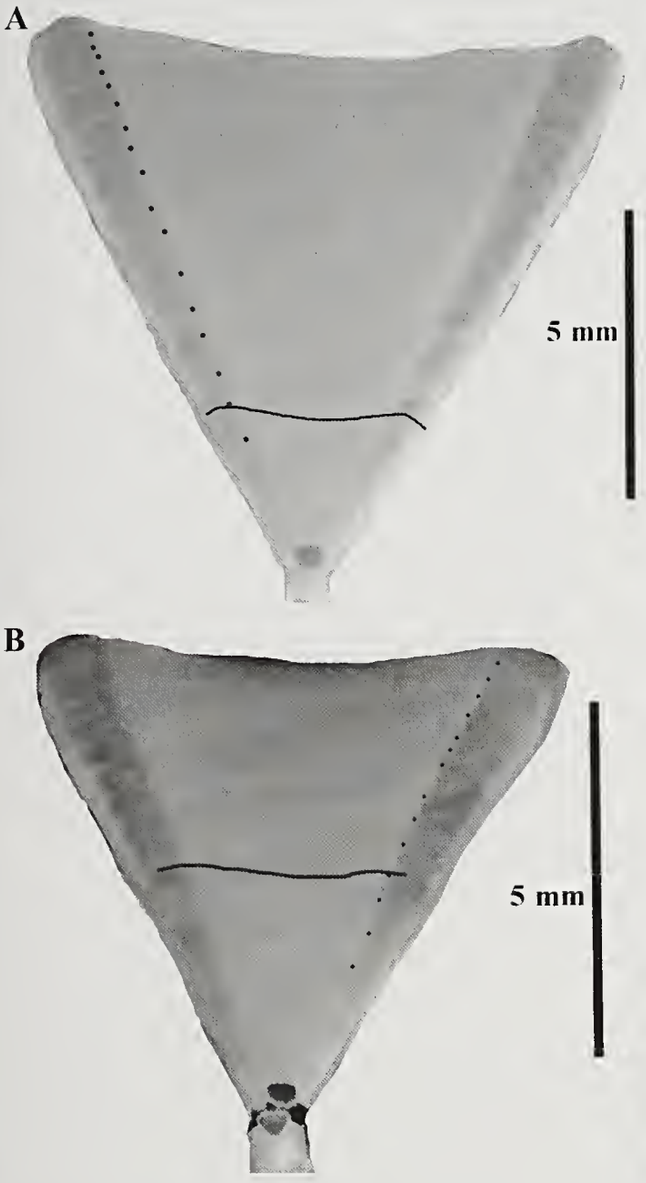

Figure 1

Images of sections of vertebral centra from 2 sandbar sharks (*Carcharhinus plumbeus*) injected with oxytetracycline (OTC) and tagged in the western North Atlantic Ocean in 1998 and 1996, respectively: (**A**) CM1031, which measured 156 cm in fork length (FL) at recapture in 2014, and (**B**) CM1027, which was 147 cm FL at recapture in 2006. The black line indicates the location of the OTC mark, and the black dots indicate the band pairs visible past the OTC mark.

To directly compare validated age estimates at recapture for OTC-injected sharks to the age estimates at size obtained from the tag-recapture models, age at tagging had to be assigned to each individual. Band-pair counts proximal to the OTC mark were used to assign age at tagging. Because counts of band pairs in sandbar sharks have been validated as annual up to 10–12 years (Branstetter, 1987; Andrews et al., 2011), if the band-pair count proximal to the OTC mark was less than 12, an age at tagging could be assigned. Age at recapture then was estimated by adding time at liberty after tagging to count of band pairs proximal to the OTC mark. For example, a shark (CM1029) had 10 band pairs before the OTC mark and was at liberty for 9.5 years, resulting in age estimates of 10.0 years at tagging and 19.5 years at recapture. Then, estimates of age at recapture, along with the sizes at recapture, were compared with growth curves from the GROTAG model from this study and vertebral and tag-recapture models from previous studies (Casey et al., 1985; Casey and Natanson, 1992). Numbers of band pairs past the OTC mark were plotted against time at liberty along with a 1:1 line to determine whether band-pair counts were annual after the OTC mark.

Results

Validation with oxytetracycline marking

Times at liberty for 12 recaptured sharks that were injected with OTC ranged from 0.1 to 16.1 years. Vertebrae from 10 of these specimens had a distinct OTC mark; 2 had no visible mark. Eight of these 10 recaptured sharks were at liberty for >1 year (3.8–16.1 years) and were used for validation analyses (Table 1). The remaining 2 specimens were at liberty for 0.1 and 0.3 years (38–107 d), indicating that OTC was incorporated into the vertebra shortly after injection but growth distal to the mark was minimal. The size of specimens from which vertebrae were used ranged from 56 to 136 cm FL at tagging (Table 1). One shark (CM1031) was tagged as a young of the year; therefore, it also was considered to have a known age at tagging (56 cm FL). Assigning a date of birth of 1 May to this sandbar shark (Baremore and Hale, 2012) meant it was ~4 months old at tagging, and adding those 4 months to this shark's 15.7 years at liberty resulted in an estimate of 16.1 years for its age at recapture. Data from another known young-of-the-year shark (CM751) indicate that OTC was incorporated within a month; therefore, the OTC mark in this animal was very close to the first clear band pair, possibly confirming Branstetter's (1987) estimate that the first band pair is deposited at 6 months of age (Fig. 1).

Band-pair count past the OTC mark underestimated time at liberty from 23.5% to 58.0% in 6 of the 8 recaptured sandbar sharks and validated annual deposition in the remaining 2 individuals at liberty for >1 year (Table 1, Fig. 2). Underestimation of age from the use of band-pair count past the OTC mark varied between 1.3 and 9.1 years. Although data are limited, age underestimation from the use of band-pair counts does not appear related to sex because band-pair counts underestimated ages for individuals of both sexes.

Sandbar sharks that were smaller at tagging (<100 cm FL) showed less deviation between band-pair count and time at liberty. Annual band-pair deposition past

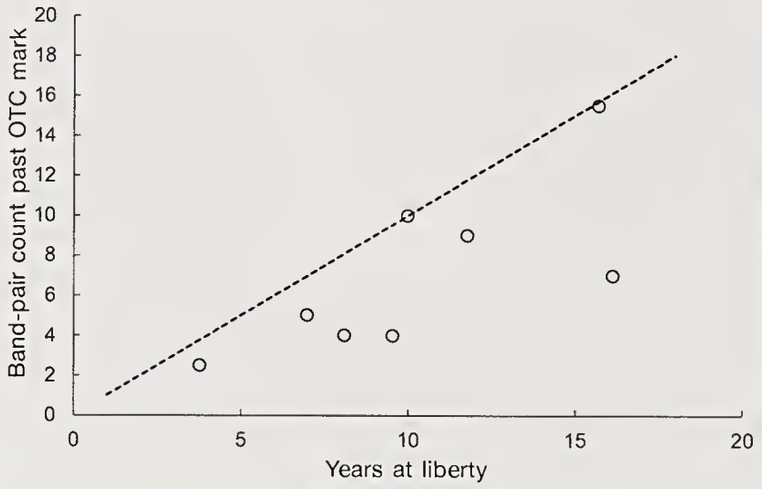

Figure 2

Relationship of time at liberty to count of vertebral band pairs past the mark from oxytetracycline (OTC) injection for the 8 recaptured sandbar sharks (*Carcharhinus plumbeus*) used in growth analysis for this study. These sharks were tagged from 1986 through 2009 in the western North Atlantic Ocean. The dashed line indicates the 1:1 relationship.

the OTC mark was seen in 2 of the 3 smallest sharks (CM1031 and CM1027), and the age of the third shark (CM945) was underestimated by 23.5% (Table 1). Conversely, the degree of underestimation was greater for sharks that were larger (≥129 cm FL) at tagging (CM1025, CM1029, and CM1024). On the basis of bomb radiocarbon validation (Andrews 2011), we would expect annual periodicity to be approximately 12 years; the amount of time at liberty past 12 years would determine the amount of age underestimation. Therefore, a lower amount of age underestimation is expected because of the limited time of growth beyond 12 years in 2 sharks (CM1031 and CM1027), which were small at tagging compared with the sharks at liberty for the same period of time but tagged at a larger size (CM1025 and CM 1029). For example, for 1 of these small sharks (CM1027), 13 total band pairs were counted and validated as annual, but for 2 of the large sharks (CM1025 and CM1029) counts of 14 band pairs underestimated times at liberty by 9.1 and 5.5 years, respectively (Table 1).

Growth analysis with tag-recapture data

Tag-recapture data for 149 sandbar sharks were used in the Gulland and Holt (1959) and GROTAG (Francis, 1988) models for growth analysis. Time at liberty ranged from 1.0 to 25.0 years, and size at tagging ranged from 48.0 to 172.8 cm FL (Suppl. Table) (online only). Tagging was conducted in all months except December, with most tags deployed from May through August (n=101). These sharks were recaptured in all months of the year, with the most sharks taken in June, July, and August (n=22 each) and the lowest numbers of sharks taken in September, November, and December (n=5, 4, 2, respectively). The results of the log-likelihood ratio tests using the GROTAG model (Francis, 1988) indicate that the more complex nonlinear model with all 6 of the parameters included was the best fit for these data (see estimates for Model 4 in Table 2). The mean annual growth rates were calculated at 60 cm FL (10.65 cm/year) and 160 cm FL (1.67 cm/year; Table 2). The fits failed for Models 1 and 5 (Table 2). We compared results for parameters of the von Bertalanffy growth function: estimates of L_∞ were higher and estimates of k were lower from the Gulland and Holt (1959) model than from the GROTAG model (Francis, 1988). In addition, although the growth curves from these 2 models look similar up to approximately age 20, the Gulland and Holt (1965) model produces a curve with slightly higher length-at-age estimates past this age (Table 3, Fig. 2). The ages validated with bomb radiocarbon dating for sharks in Andrews et al. (2011) and the known ages for OTC-injected sharks in this study follow the updated growth curves based on current tag-recapture data, rather than the growth curve based on previously published vertebral band-pair count data (Fig. 3).

Discussion

In view of current knowledge that using vertebral centra age estimates in larger sharks is not correct (Harry, 2018; Natanson et al., 2018), it is clear that growth models when used with extensive tag-recapture data can provide more accurate age estimates. As shown in this study, sharks with validated ages, such as those from OTC marking in this study and bomb radiocarbon dating (Andrews et al., 2011), are more closely aligned with tag-recapture-based growth curves than growth curves derived from vertebral band-pair counts. Sharks with validated ages started to deviate from the growth curves based on vertebral band-pair counts and followed the growth curves based on tag-recapture data by 12–16 years, indicating that, by this range of ages, variation among individual sharks in rate of band-pair deposition was possibly related to growth rate during the maturation process (Fig. 3).

Determination of age in elasmobranchs from band-pair counts on vertebral centra has relied on the caveat that each band pair represents a year. However, in 75% of the vertebrae from specimens in this study, it has been shown that the band pairs are not annual throughout life; band-pair counts underestimate age in these specimens. The 2 sharks that exhibited annual band-pair deposition were both tagged at smaller sizes; on the sample from the smallest individual, the OTC mark was seen just past the birth band, but, on the

Table 2

Log-likelihood ratio values and estimates of von Bertalanffy growth function parameters for 5 versions of the GROTAG model (Francis, 1988) fitted to tagging data for 149 sandbar sharks tagged between 1965 and 2013 in the western North Atlantic Ocean. The mean annual growth rates were calculated at 60 cm FL and 160 cm FL, and standard errors of the mean (SEs) are given. For each version of the model, a parameter was added. For a significant ($P<0.05$) improvement in fit, the introduction of one extra parameter must increase the log-likelihood function (λ) by at least 1.92 (Francis, 1988). An asterisk (*) indicates fixed parameters. There are no data for models 1 and 5 because of failed fits. AIC=Akaike information criterion; s=standard deviation of measurement error; m=mean measurement error; p=a contamination probability.

		Model				
Parameter	Symbol (unit)	1	2	3	4	5
Log likelihood	l		−550.3	−541.1	−539.1	
	AIC		1108.6	1092.2	1094.1	
Mean growth rates	G_{60} (cm/y)		14.17	11.00	10.65	
	SE				0.86	
	G_{160} (cm/y)		1.67	1.67	1.67	
	SE				0.48	
Growth variability	v	0*	0.098	0.166	0.149	0*
Measurement error	s (cm)		9.260	8.167	7.647	
	m (cm)	0*	0*	5.164	5.288	0*
Outliers	p	0*	0*	0*	0.022	

larger individual, the OTC mark was at the third band pair past the birth band (Fig. 1). The smaller of these 2 sharks (CM1031) was at liberty for 15.7 years, recaptured at a size of 156 cm FL, and classified as mature. The larger shark (CM1027), however, was recaptured at a size of 147 cm FL after 10 years at liberty and, on the basis of size, likely immature (estimated size at 50% maturity was 154.9 and 151.6 cm FL for females and males, respectively; Baremore and Hale, 2012). These 2 sharks had total band-pair counts of 16 and 13, which are just over the number of band pairs at which Andrews et al. (2011) detected a shift from annual to non-annual band-pair deposition (10–12 years).

Size at both tagging and recapture appears to influence the amount of age underestimation in our OTC specimens. The percentage of time underestimated by band-pair counts (23.5–58.0%) increased in relation to size at recapture and secondarily decreased with size at tagging, findings that are consistent with the conclusion that larger sharks (approaching maturity) have slower growth and deposit fewer band pairs than smaller sharks (young of the year and juveniles). For example, 2 sharks (CM1027 and CM1029) at liberty for approximately the same time but tagged at different sizes and, therefore, at different ages, had different outcomes regarding degree of age underestimation. In examined vertebral sections of the smaller of these 2 sharks (CM1027), 3 band pairs were visible before the OTC mark and deposition of band pairs before and after the OTC mark was annual. This individual's total age at recapture was 13.0 years, close to the age up to which band-pair deposition has been validated as annual for the sandbar shark (12 years; Andrews et al., 2011). In contrast, the other shark (CM1029) was tagged at a larger size and at an estimated age of 10.0 years, based on band-pair count before the OTC mark. The estimated total age for this shark was 19.5 years at recapture (10 band pairs + 9.5 years at liberty), past the validated ages for annual deposition (10–12 years). Band-pair deposition in this individual had slowed; therefore, its age was underestimated.

Casey et al. (1985) aged the sandbar shark using vertebral band-pair counts and tag-recapture data. Their data indicated slower growth rates from using tag-recapture data than from counting vertebral band pairs, leading them to suggest that ages based on vertebral band-pair counts underestimate true age. These findings were reinforced by the results of Casey and Natanson (1992) and Andrews et al. (2011), who used tag-recapture data and bomb radiocarbon dating, respectively. At the time of these earlier studies, the use of vertebral data was considered more robust than other methods, and age estimations based on vertebral band-pair counts were generally accepted over results from other methods of age determination. In particular, the older ages at maturity and longevity estimated by using models with tag-recapture data were not considered reliable partly as a result of the low L_∞ (often estimated by using this method because of a lack of large sharks reliably measured at tagging and recapture), which is highly linked to the k value (von Bertalanffy, 1938).

Table 3

The von Bertalanffy growth function parameters calculated by using tag-recapture data in models for sandbar sharks (*Carcharhinus plumbeus*) tagged and recaptured in the western North Atlantic Ocean: mean asymptotic fork length (L_∞), growth constant (k), and theoretical age at a length of zero (t_0).

Study	Model	L_∞	k	t_0	n
This study	Gulland and Holt (1959)	188.4	0.079	−3.678	149
This study	GROTAG (Francis, 1988)	178.6	0.094	−3.300	149
Casey and Natanson (1992)	Fabens (1965)	186.0	0.046	−6.450	33

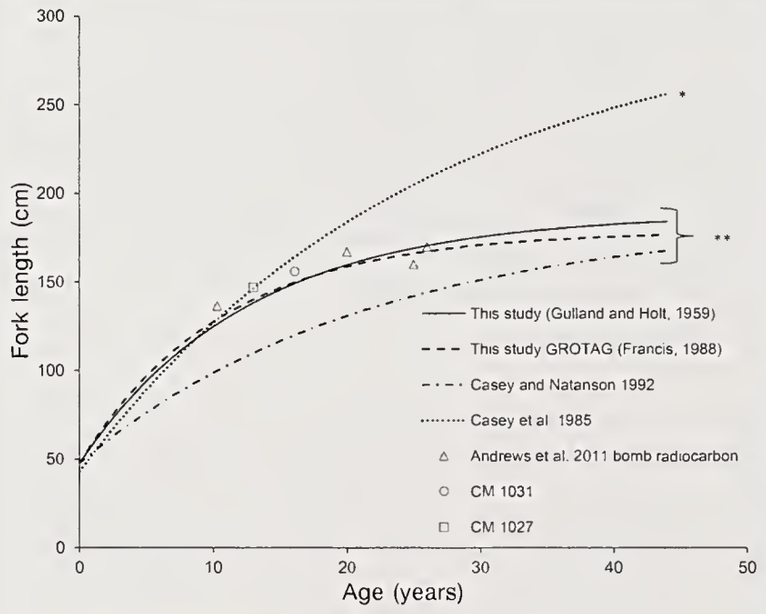

Figure 3

The von Bertalanffy growth curves generated in this study compared with previously published curves for the sandbar shark (*Carcharhinus plumbeus*). Estimated ages at recapture of oxytetracycline-injected sharks are included. The open triangles indicate ages validated with bomb radiocarbon dating for 4 specimens from Andrews et al. (2011). The open square and circle indicate the known ages used in this study for sandbar sharks tagged in 1996 (CM1027) and 1998 (CM 1031) in the western North Atlantic Ocean. The single asterisk (*) indicates a growth curve based on vertebral band-pair counts, and the double asterisks (**) indicate growth curves based on the use of tag-recapture data.

Modeling of tag-recapture data is provided as an alternate method of age determination. The growth curves derived from modeling tag-recapture data are verified by the close relationship of the estimated ages of OTC-marked individuals to the ages estimated for similarly sized fish by the tag-recapture growth curves. Both of the tag-recapture-derived models in this study output similar growth estimates to age 20 and predict higher k values than growth estimates derived by Casey and Natanson (1992), but tag-recapture models from both studies underestimate L_∞ (maximum observed size: 251 cm FL; NMFS[2]). We applied the size at 50% maturity calculated by Baremore and Hale (2012), 154.9 and 151.6 cm FL for females and males, respectively, to the parameters we calculated by using the GROTAG (Francis, 1988) and Gulland and Holt (1959) models: results indicate that female and male sandbar sharks reach 50% maturity at an age of approximately 18 and 17 years, respectively. These estimates of age at 50% maturity are higher than those predicted by counting vertebral band pairs (12 and 13 years for females and males, respectively; Casey et al., 1985) and lower than that predicted by using the previous tag-recapture data (nearly 30 years; Casey and Natanson, 1992).

Our findings corroborate those of other studies on sandbar sharks (Casey et al., 1985; Casey and Natanson, 1992; Andrews et al., 2011) as well as on a multitude of other shark and ray species (Harry, 2018) and support the use of modeling with tag-recapture data as an alternative method of age determination. These results reinforce the notion that band-pair deposition may misrepresent the age of individuals, possibly affecting management of the sandbar shark because underestimation of age leads to underestimation of reproductive potential and overestimation of yield.

Acknowledgments

We would like to thank G. Skomal, H. Pratt, and J. Casey for starting the OTC program. N. Kohler was instrumental in safe handling of sharks during OTC injections. We also thank J. Carlson and the observer program staff of the Panama City Lab, National Marine Fisheries Service, for processing and sending samples. Samples could not have been ob-

[2] NMFS (National Marine Fisheries Service). 2018. Unpubl. data. Panama City Laboratory, Southeast Fish. Sci. Cent., Natl. Mar. Fish. Serv., NOAA. 3500 Delwood Beach Rd., Panama City, FL 32408.

tained without the help of commercial and recreational fishermen and fisheries observers. We also thank S. Wintner and W. Driggers for providing critical reviews that improved this paper.

Literature cited

Andrews, A. H., L. J. Natanson, L. A. Kerr, G. H. Burgess, G. M. Cailliet.
2011. Bomb radiocarbon and tag-recapture dating of sandbar shark (*Carcharhinus plumbeus*). Fish. Bull. 109:454–465.

Baremore, I. E., and L. F. Hale.
2012. Reproduction of the sandbar shark in the western North Atlantic Ocean and Gulf of Mexico. Mar. Coast. Fish. 4:560–572.

Beamish, R. J., and G. A. McFarlane.
1983. The forgotten requirement for age validation in fisheries biology. Trans. Am. Fish. Soc. 112:735–743.

Branstetter, S.
1987. Age and growth validation of newborn sharks held in laboratory aquaria, with comments on the life history of the Atlantic sharpnose shark, *Rhizoprionodon terraenovae*. Copiea 1987:291–300.

Campana, S. E., L. J. Natanson, and S. Myklevoll.
2002. Bomb dating and age determination of large pelagic sharks. Can. J. Fish. Aquat. Sci. 59:450–455.

Casey, J. G., and L. J. Natanson.
1992. Revised estimates of age and growth of the sandbar shark (*Carcharhinus plumbeus*) from the western North Atlantic. Can. J. Fish. Aquat. Sci. 49:1474–1477.

Casey, J. G., H. L. Pratt Jr., and C. E. Stillwell.
1985. Age and growth of the sandbar shark (*Carcharhinus plumbeus*) from the western North Atlantic. Can. J. Fish. Aquat. Sci. 42:963–975.

Castro, J. I.
2011. The sharks of North America, 640 p. Oxford Univ. Press, Inc., New York, NY.

Ebert, D. A., S. Fowler, and L. Compagno.
2013. Sharks of the world: a fully illustrated guide, 528 p. Wild Nature Press, Plymouth, UK.

Fabens, A. J.
1965. Properties and fitting of the von Bertalanffy growth curve. Growth 29:265–289.

Francis, M. P., S. E. Campana, and C. M. Jones.
2007. Age under-estimation in New Zealand porbeagle sharks (*Lamna nasus*): is there an upper limit to ages that can be determined from shark vertebrae? Mar. Freshw. Res. 58:10–23.

Francis, R. I. C. C.
1988. Maximum likelihood estimation of growth and growth variability from tagging data. N. Z. J. Mar. Freshw. Res. 22:43–51.

Gulland, J. A., and S. J. Holt.
1959. Estimation of growth parameters for data at unequal time intervals. ICES J. Mar. Sci. 25:47–49.

Hale, L. F., and I. E. Baremore.
2013. Age and growth of the sandbar shark (*Carcharhinus plumbeus*) from the northern Gulf of Mexico and the western North Atlantic Ocean. Gulf Mex. Sci. 31:28–39.

Hamady, L. L., L. J. Natanson, G. B. Skomal, and S. R. Thorrold.
2014. Vertebral bomb radiocarbon suggests extreme longevity in white sharks. PLoS ONE 9(1):e84006.

Harry, A. V.
2018. Evidence for systemic age underestimation in shark and ray ageing studies. Fish Fish. 19:185–200.

Harry, A. V., A. J. Tobin, and C. A. Simpfendorfer.
2013. Age, growth and reproductive biology of the spot-tail shark, *Carcharhinus sorrah*, and the Australian blacktip shark, *C. tilstoni*, from the Great Barrier Reef World Heritage Area, north-eastern Australia. Mar. Freshw. Res. 64:277–293.

Kinney, M. J., R. J. D. Wells, and S. Kohin.
2016. Oxytetracycline age validation of an adult shortfin mako shark *Isurus oxyrinchus* after 6 years at liberty. J. Fish Biol. 89:1828–1833.

Kohler, N. E., J. G. Casey, and P. A. Turner.
1996. Length-weight relationships for 13 species of sharks from the western North Atlantic. Fish. Bull. 93:412–418.

Natanson, L. J., and G. M. Cailliet.
1990. Vertebral growth zone deposition in Pacific angel sharks. Copeia 1990:1133–1145.

Natanson, L. J., and G. B. Skomal.
2015. Age and growth of the white shark, *Carcharodon carcharias*, in the western North Atlantic Ocean. Mar. Freshw. Res. 66:387–398.

Natanson, L. J., J. J. Mello, and S. E. Campana.
2002. Validated age and growth of the porbeagle shark (*Lamna nasus*) in the western North Atlantic Ocean. Fish. Bull. 100:266–278.

Natanson, L. J., N. E. Kohler, D. Ardizzone, G. M. Cailliet, S. P. Wintner, and H. F. Mollet.
2006. Validated age and growth estimates for the shortfin mako, *Isurus oxyrinchus*, in the North Atlantic Ocean. Environ. Biol. Fish. 77:367–383.

Natanson, L. J., S. P. Wintner, F. Johansson, A. Piercy, P. Campbell, A. De Maddalena, S. J. B. Gulak, B. Human, F. C. Fulgosi, D. A. Ebert, et al.
2008. Ontogenetic vertebral growth patterns in the basking shark, *Cetorhinus maximus*. Mar. Ecol. Prog. Ser. 361:267–278.

Natanson, L. J., B. J. Gervelis, M. V. Winton, L. L. Hamady, S. J. B. Gulak, and J. K. Carlson.
2014. Validated growth estimates for *Carcharhinus obscurus* in the northwestern Atlantic Ocean, with pre- and post management growth comparisons. Environ. Biol. Fish. 97:881–896.

Natanson, L. J., G. B. Skomal, S. L. Hoffmann, M. E. Porter, K. J. Goldman, and D. Serra.
2018. Age and growth of sharks: do vertebral band pairs record age? Mar. Freshw. Res. 69:1440–1452.

NMFS (National Marine Fisheries Service).
1993. Fishery management plan for sharks of the Atlantic Ocean, 167 p. NOAA, Natl. Mar. Fish. Serv., Southeast Reg. Off., Silver Springs, MD.
2007. Final amendment 2 to the consolidated Atlantic highly migratory species fishery management plan, 726 p. NOAA, Natl. Mar. Fish. Serv., Off. Sustainable Fish., Highly Migratory Species Manage. Div., Silver Spring, MD.

Passerotti, M. S., A. H. Andrews, J. K. Carlson, S. P. Wintner, K. J. Goldman, and L. J. Natanson.
2014. Maximum age and missing time in the vertebrae of sand tiger shark (*Carcharias taurus*): validated lifespan from bomb radiocarbon dating in the western North Atlantic and southwestern Indian Oceans. Mar. Freshw. Res. 65:674–687.

R Core Team.
2018. R: a language and environment for statistical computing. R Foundation for Statistical Computing, Vienna, Austria. [Available from website, accessed July 2018.]
Romine, J. G., J. A. Musick, and R. A. Johnson.
2013. Compensatory growth of the sandbar shark in the western North Atlantic including the Gulf of Mexico. Mar. Coast. Fish. 5:189–199.
SEDAR (Southeast Data Assessment and Review).
2011. SEDAR 21 stock assessment report: HMS sandbar shark, 435 p. SEDAR, North Charleston, SC. [Available from website.]
2017. SEDAR 54 stock assessment report: HMS sandbar shark, 176 p. SEDAR, North Charleston, SC. [Available from website.]
Sminkey, T. R., and J. A. Musick.
1995. Age and growth of the sandbar shark, *Carcharhinus plumbeus*, before and after population depletion. Copeia 1995:871–883.
von Bertalanffy, L.
1938. A quantitative theory of organic growth (inquiries on growth laws II). Hum. Biol. 10:181–213.
Wells, R. J. D., S. E. Smith, S. Kohin, E. Freund, N. Spear, and D. A. Ramon.
2013. Age validation of juvenile shortfin mako (*Isurus oxyrinchus*) tagged and marked with oxytetracycline off southern California. Fish. Bull. 111:147–160.

National Marine Fisheries Service
NOAA

Fishery Bulletin
established in 1881

Spencer F. Baird
First U.S. Commissioner of Fisheries and founder of *Fishery Bulletin*

Growth of adult river herring that spawn in tributaries of the Potomac River in northern Virginia

C. J. Carroll Schlick
Kim de Mutsert

Email address for contact author: cjcschlick@gmail.com

Department of Environmental Science and Policy
George Mason University
Potomac Science Center
650 Mason Ferry Avenue, Room 1305
Woodbridge, Virginia 22191

Abstract—This study assessed the aging techniques and growth rates of river herring, the alewife (*Alosa pseudoharengus*) and blueback herring (*Alosa aestivalis*), in the tributaries of the Potomac River in northern Virginia. River herring are currently under moratoria in the Potomac River because of a lack of information about their populations. Ages determined from the use of otoliths and scales collected from river herring were compared to quantify aging bias and precision. For 2- and 3-year-old individuals, ages were commonly higher when derived from scales than when derived from otoliths. Length-at-age data were analyzed by using 9 growth models, and the best-fit-model was determined by using Akaike's information criterion (AIC). The outputs from the growth models were only slightly different, with differences of 10.6% and 10.5% in the AIC weights between best- and worst-fit models for alewife and blueback herring, respectively. Results from the use of a von Bertalanffy growth model indicate that alewife grew larger and faster than blueback herring (P<0.0001) and that females grew larger and faster than males for both species (P<0.0001). The findings of this study provide needed aging and growth information about 2 species within the Potomac River, where information about growth rates and population ages is limited.

Manuscript submitted 26 June 2018.
Manuscript accepted 7 February 2019.
Fish. Bull. 117:59–69 (2019).
Online publication date: 22 February 2019.
doi: 10.7755/FB.117.1-2.7

The views and opinions expressed or implied in this article are those of the author (or authors) and do not necessarily reflect the position of the National Marine Fisheries Service, NOAA.

The alewife (*Alosa pseudoharengus*) and blueback herring (*Alosa aestivalis*), collectively called *river herring*, were once important target species of commercial and recreational fisheries along the Atlantic coast of the United States and Canada. Returning to freshwater spawning grounds in early spring, river herring and other similar anadromous species were the targets of a thriving fishery after harsh winters for much of the northern Atlantic seaboard for centuries (Wharton, 1957; Fay et al.[1]; Jessop, 1994; Greene et al.[2]; ASMFC, 2012). Commercial landings of river herring declined by 98% in the United States from the 1950s (when detailed records were first kept) to the 1970s, and average landings in the Chesapeake Bay plummeted 99% or more from the 1970s to 2010 (NRDC[3]). Declines in populations of river herring throughout their geographical region have been attributed to overfishing and habitat degradation in spawning habitats; therefore, populations are termed *depleted* rather than *overfished* (Hightower et al., 1996; NMFS[4]; NRDC[3]). To promote the recovery of river herring, the Atlantic States Marine Fisheries Commission (ASMFC) established that commercial and recreational fisheries in any jurisdiction may not land river herring unless a sustainable fishery management plan has been approved starting in January 2012 (Greene et al.[2]; ASMFC, 2012).

In the stock assessment completed in 2017, the status of the alewife stock in the Potomac River was listed as stable, but the stock of blueback herring was listed as unknown (ASMFC, 2017). Data collection and

[1] Fay, C. W., R. J. Neves, and G. B. Pardue. 1983. Species profiles: life histories and environmental requirements of coastal fishes and invertebrates (mid-Atlantic)—alewife/blueback herring, 25 p. Div. Biol. Serv., U.S. Fish Wildl. Serv., FWS/OBS-82/11.9. U.S. Army Corps Eng., TR EL-82-4.

[2] Greene, K. E., J. L. Zimmerman, R. W. Laney, and J. C. Thomas-Blate. 2009. Atlantic coast diadromous fish habitat: a review of utilization, threats, recommendations for conservation, and research needs. Atl. States Mar. Fish. Comm. Habitat Manage. Ser. 9, 463 p. [Available from website.]

[3] NRDC (Natural Resource Defense Council). 2011. Petition to list alewife (*Alosa pseudoharengus*) and blueback herring (*Alosa aestivalis*) as threatened species and to designate critical habitat, 107 p. Nat. Resour. Defense Counc., Washington, D.C.

[4] NMFS (National Marine Fisheries Service). 2009. Species of concern: river herring (alewife and blueback herring) *Alosa pseudoharengus* and *A. aestivalis*, 8 p. Natl. Mar. Fish. Serv., Washington, D.C.

monitoring are considered top priorities for management of river herring, with an emphasis on total catch (including bycatch), validation of age determination, determination of population sizes, and determination of the effectiveness of restoration efforts (ASMFC, 2012, 2017). Data on the populations of river herring in the Potomac River have been limited to indices of juvenile abundance and to surveys of adults by using electrofishing or push nets (Schlick, 2016; ASMFC, 2017). The catch per unit of effort for adults captured in the Potomac River by the District of Columbia Department of Energy and Environment has increased since 2012 for both species; however, the geometric mean of catch of juvenile river herring does not have the same clear trend in seining data collected by the District of Columbia Department of Energy and Environment and Maryland Department of Natural Resources (ASMFC, 2017). The Potomac Environmental Research and Education Center of George Mason University has reported an increase in river herring catch since 1988 in Gunston Cove, a small embayment of the Potomac River (Schlick, 2016; Jones et al[5]).

Whether habitat degradation or overfishing are the major contributors to the decline of these populations, data on the characteristics of spawning populations of river herring are needed to help manage them. Growth rates can change over time because of overfishing or degradation of spawning habitat and through natural variation over time (Heino, 1998; Law, 2000; Heino and Godo, 2002; Wang and Höök, 2009). Additionally, these characteristics can differ within populations throughout their geographical range, even in close proximity (Sheppard et al.[6]; Tuckey and Olney, 2010). For example, alewife had statistically higher growth rates in the Nemasket River, Massachusetts, than in 3 other rivers in Massachusetts (Sheppard et al.[6]). Fish fecundity is directly related to size, with larger individuals in a population producing more eggs per spawning event (Lake and Schmidt[7]). Therefore, body size and growth rates are important in population analyses. Updating growth parameters of the species after severe declines in the population is important for current stock assessment strategies.

The von Bertalanffy growth function is the most commonly used model to describe the growth (in length or weight) of individuals within a fish population; however, for many species, the von Bertalanffy growth model is not the best fit (Quinn and Deriso, 1999; Katsanevakis and Maravelias, 2008; Haddon, 2011). Katsanevakis and Maravelias (2008) reported that the von Bertalanffy growth function was the best-fit model in 34.6% of 133 different data sets. A difference in the best-fit model between populations could be due to the parameters used in the model or the particular species not growing at an asymptotic rate, which is an assumption of the von Bertalanffy growth model (Katsanevakis and Maravelias, 2008). Today, multiple growth models can be constructed easily with the use of software programs; therefore, a useful way to determine the best-fit model is running multiple types of growth models (e.g., von Bertalanffy, Gompertz, and Richards) and then statistically comparing the growth parameters by using the Akaike's information criterion (AIC) (Burnham and Anderson, 2002; Katsanevakis and Maravelias, 2008).

Development of growth models is necessary for understanding population size and growth potential, information used to properly manage fisheries use, and can be achieved by using length-at-age data; however, length-at-age data for river herring have been used with little validation or standardization of aging techniques between scientists (ASMFC[8]). Aging of river herring has been accomplished through reading annuli on whole otoliths or on scales under a dissecting microscope; however, validation with known ages of individuals has not been documented for river herring (ASMFC[8]). Aging by reading scales is a nonlethal option but can result in less accurate age estimation because periods of minimal growth can result in false annuli on scales (Campana and Neilson, 1985; Beamish and McFarlane, 1987). Additionally, the methods developed by Cating (1953) for American shad (*A. sapidissima*) were the most cited methods for aging river herring by using scales until Duffy et al. (2011) reported that the transverse grooves on scales used in aging can vary over time and geographical range.

The goal of this study was to examine lengths, ages, and growth of adult river herring returning to tributaries of the Potomac River in 2007–2015 to spawn. The objectives to obtain this goal were to determine 1) the relationships between different measurements of length, 2) bias between using scales and using otoliths to estimate age, 3) the best-fit model by examining multiple growth models, and 4) growth parameters by using the best-fit model. Understanding length, age, and growth parameters is crucial for the determination of the reproductive capacity, potential restoration time

[5] Jones, R. C., K. de Mutsert, and A. Fowler. 2017. An ecological study of Gunston Cove 2016: final report, 181 p. Potomac Environ. Res. Educ. Cent., George Mason Univ., Fairfax, VA. [Available from website.]

[6] Sheppard, J. J., P. D. Brady, M. P. Armstrong, and G. A. Nelson. 2010. Characterizing contemporary and historic age structure of alewives (*Alosa pseudoharengus*) in Massachusetts spawning runs: final report, 110 p. [Available from Mass. Div. Mar. Fish., 30 Emerson Ave., Gloucester, MA 01983.]

[7] Lake, T. R., and R. E. Schmidt. 1998. The relationship between fecundity of an alewife (*Alosa pseudoharengus*) spawning population and egg productivity in Quassaic Creek, a Hudson River tributary (HRM 60) in Orange County, New York. *In* Final reports of the Tiber T. Polgar Fellowship Program, 1997 (J. R. Waldman and W. C. Nieder,eds.), p. II-1–24. Hudson River Foundation, NY. [Available from website.]

[8] ASMFC (Atlantic States Marine Fisheries Commission). 2014. 2013 river herring ageing workshop report, 88 p. Atl. States Mar. Fish. Comm., Washington, D.C. [Available from website.]

line, and overall health of river herring populations, whose current statuses are unknown.

Materials and methods

Study sites

Adult river herring were sampled at 5 locations: Pohick Creek, Accotink Creek, Dogue Creek, Quantico Creek, and Cameron Run, all third-order tributaries that run through northern Virginia and drain into the Potomac River south of Washington, D.C. (Fig. 1). This stretch of the Potomac River is tidally influenced freshwater, which continues into the lower portions of each creek (Jones et al., 2008). River herring have been documented to spawn in each creek below the Virginia fall line (Jones et al.[9]; Schlick, 2016; Jones et al.[5]).

Field methods

Adults migrating upstream through Accotink Creek and Pohick Creek (Fig. 1) were sampled by blocking each creek for 24 h by using a hoop net with a mesh of 1.3 cm and snow fencing with a mesh of 5.1 cm once a week from mid-March through May from 2007 through 2015. Cameron Run was sampled the same way from 2013 through 2015 (Fig. 1). In 2007 and 2008, adult river herring were collected from Quantico Creek and Dogue Creek by electrofishing (Fig. 1). All captured adult alewife (n=1707) and blueback herring (n=1159) were counted and measured, and their sex was determined. Adults that did not survive capture (598 alewife and 304 blueback herring) were frozen unless dissection occurred within 48 h of capture. Adults were measured for wet weight in grams and for standard length (SL), fork length (FL), and total length (TL) in millimeters. Scales were collected, cleaned by using a mild detergent, and dried flat (ASMFC[8]). Sagittal otoliths were collected and stored dry.

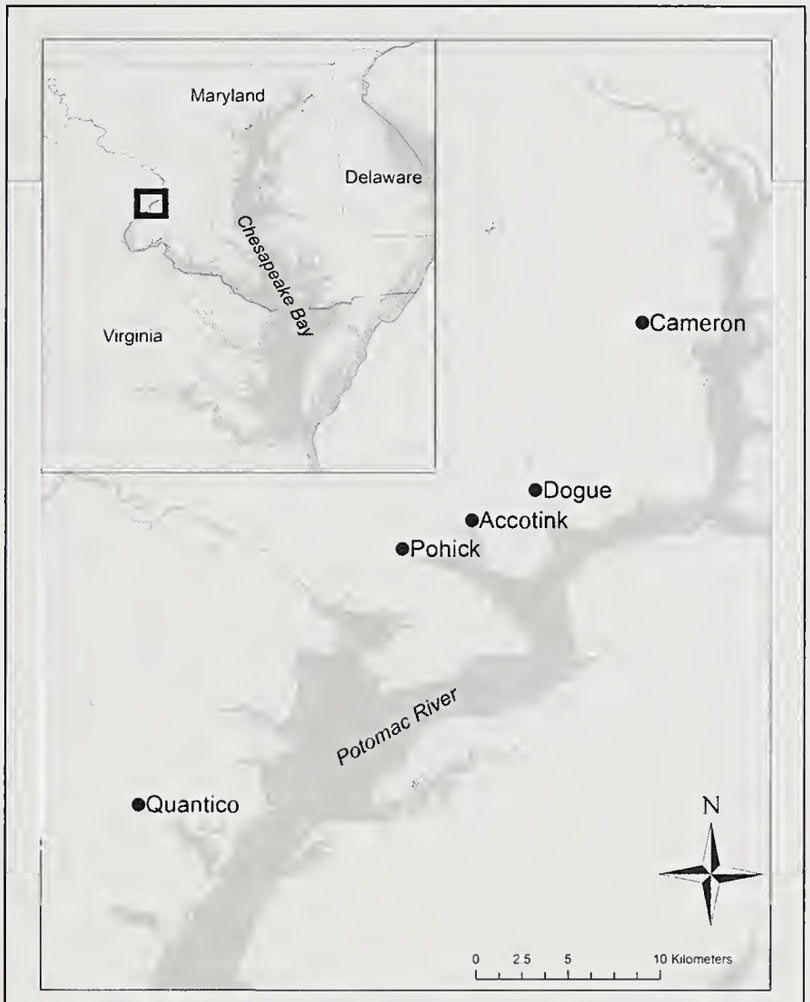

Figure 1

Map of locations where adult river herring, alewife (*Alosa pseudoharengus*) and blueback herring (*Alosa aestivalis*), were sampled from 2007 through 2015 within small tributaries that lead to the Potomac River in northern Virginia. There are 5 locations: Quantico Creek, Pohick Creek, Accotink Creek, Dogue Creek, and Cameron Run. Map data sources: U.S. Geological Survey, 1:250,000-scale Hydrologic Units of the United States; Esri, U.S. National Atlas Water Feature Lines.

Laboratory methods

Sagittal otoliths were cleaned of all fish debris by using water. Two separate readers viewed otoliths under a dissecting microscope on a black background by using reflected light following procedures outlined in the report of the ASFMC workshop on aging of river herring held in 2013 (ASMFC[8]). Samples were excluded from analysis when an age was not agreed upon. From each fish, 5–6 scales were cleaned with water and a mild detergent; then they were sandwiched between 2 slides, examined, photographed by using a camera mounted on a dissecting microscope with transmitted light, and read for annuli (ASMFC[8]). Because river herring were captured during spawning season, the edges of otoliths and scales were counted as a year (Cating, 1953).

Age validation

It was assumed that ages from analysis of otoliths were more likely to be accurate than ages from analysis of scales because scales contain more false annuli and are more susceptible to environmental degradation (Campana and Neilson, 1985; Beamish and McFarlane, 1987; Besler, 1999). Additionally, readers agreed on 858 of 861

[9] Jones, R. C., K. de Mutsert, and G. D. Foster. 2014. An ecological study of Hunting Creek 2013: final report, 113 p. George Mason Univ., Fairfax, VA. [Available from website.]

otolith readings but on only 792 of 828 scale readings. Otolith readings were compared with scale readings to verify ages of scales by using age bias and precision analyses in RStudio[10], vers. 1.0.153 (RStudio, Inc., Boston, MA) and the R package FSA, vers. 0.7.3 (Ogle, 2015). Plots of age bias were created by plotting ages agreed upon by otolith readers versus ages from scale readings to visually examine data for systematic bias in aging scales (Campana et al., 1995). Ages within the age-bias plot were analyzed by using a *t*-test to determine if ages from scales agree with ages from otoliths (Campana et al., 1995). To statistically test for symmetry, McNemar's test, Evans–Hoenig test, and Bowker's test were used to determine the differences around the main diagonal of the age-bias plot (Evans and Hoenig, 1998). Average coefficient of variation (ACV) was used to find the variability in ages determined by using ages from otoliths versus ages from scales (Campana, 2001).

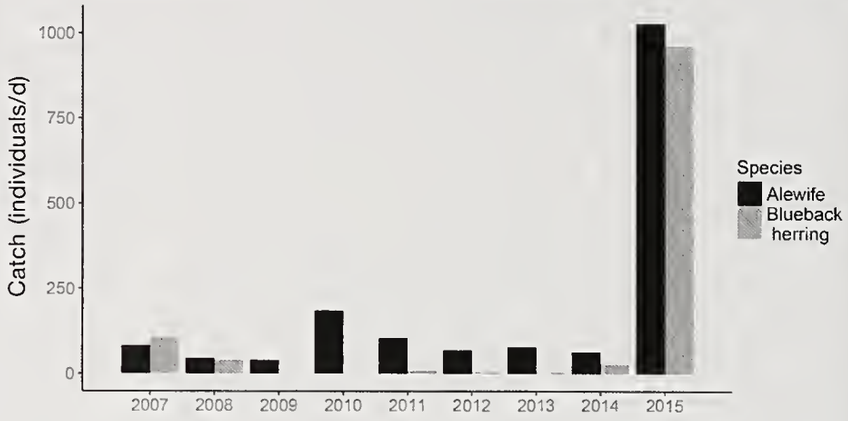

Figure 2

Number of alewife (*Alosa pseudoharengus*) and blueback herring (*Alosa aestivalis*) captured per day in tributaries of the Potomac River with hoop nets from 2007 through 2015 and by electrofishing in 2007 and 2008 by the Potomac Environmental Research and Education Center of George Mason University.

Statistical analyses

Relationships between SL and FL, SL and TL, and FL and TL were estimated on the basis of linear regression analyses. Length-at-age data were used to determine growth curves in 9 different growth models: von Bertalanffy (von Bertalanffy, 1938), Gompertz (Gompertz, 1825), Laird–Gompertz (Laird, 1964; Zweifel and Lasker, 1976), Richards (Richards, 1959), linear (Haddon, 2011), logistic (Ricker, 1975), Ratkowsky (Ratkowsky, 1986), Francis (Francis, 1988), and Cerrato (Cerrato, 1990). All analyses were conducted in Microsoft Excel (vers. 16.7; Microsoft Corp., Redmond, WA) by using Solver, an add-in tool available in Excel (Haddon, 2011). Growth models were run using SL as the measure for length to increase sample size in this study because some of the captured river herring had damaged caudal fins, making TL and FL unreliable or unattainable measures. However, past documentation of growth parameters for river herring were done with FL or TL. To directly compare this study's results with those of past studies, the von Bertalanffy growth function was run with FL and TL for each species; mean asymptotic lengths (L_∞) are reported in parentheses in the "Discussion" section when applicable for comparison with results of other studies.

The best-fit model was determined by using the AIC (Akaike, 1974; Hilborn and Mangel, 1997; Burnham and Anderson, 2002). The use of the AIC allows non-nested models to be compared and over-parameterization of a model to be taken into context (Hilborn and Mangel, 1997). The AIC was then transformed to AIC weights to determine which model was furthest from the true AIC value (Burnham and Anderson, 2002).

An analysis of residual sum of squares was conducted on the best-fit model to determine if there are sex-specific differences in growth parameters. Finally, a likelihood ratio was used to test which growth parameters are responsible for any differences between sexes. The likelihood ratio is a chi-square distribution with degrees of freedom (df) that compares the sums of squares of the models for each combination of growth parameters by estimating each parameter individually through the growth model while holding some parameters constant and calculating the sums of squares for each combination of parameters.

Results

Alewife (n=1707) were captured in tributaries of the Potomac River for 9 consecutive years from 2007 through 2015, and 598 of these fish were dissected for aging. Blueback herring (n=1159) were captured in 2007 and 2008 and from 2011 through 2015, and 304 of them were dissected for aging. In 2015, the catch of both species was an order of magnitude higher than the catch of any other year during this study (Fig. 2). Methods and locations of sampling were consistent from 2009 through 2015, except that Cameron Run was added from 2013 through 2015, resulting in the capture of 1 alewife, 6 alewife, and 16 alewife in each of those 3 years, respectively. Therefore, the increased catch of alewife in 2015 was not due to increased effort.

[10] Mention of trade names or commercial companies is for identification purposes only and does not imply endorsement by the National Marine Fisheries Service, NMFS.

Table 1

The equations used to convert between values of standard length (SL), fork length (FL), and total length (TL) in millimeters for alewife (*Alosa pseudoharengus*) and blueback herring (*Alosa aestivalis*) captured from tributaries of the Potomac River in northern Virginia during 2007–2015. Also provided are coefficients of multiple determination (R^2), or proportions of variance, to indicate the correlation between variables used to determine the equations.

Species	Conversion	Equation	n	R^2
Alewife	SL to FL	FL=1.0076(SL)+18.832	1056	0.920
Alewife	SL to TL	TL=1.0922(SL)+31.529	1002	0.873
Alewife	FL to TL	TL=0.9852(FL)+33.807	1001	0.968
Blueback	SL to FL	FL=1.0208(SL)+14.675	630	0.928
Blueback	SL to TL	TL=1.1446(SL)+18.644	630	0.930
Blueback	FL to TL	TL=1.104(FL)+6.02	630	0.972

Length–length relationship

Alewife had a mean SL of 210.8 mm (standard deviation [SD] 13.57), mean FL of 231.2 mm (SD 14.25), and mean TL of 261.9 mm (SD 15.85). Blueback herring had a mean SL of 202.1 mm (SD 11.80), mean FL of 221.0 mm (SD 12.51), and mean TL of 250.0 mm (SD 14.00). The relationships between SL, FL, and TL were highly significant for alewife and blueback herring (with all proportions of variance, or coefficients of multiple determination, >0.85; Table 1).

Aging

Alewife Otoliths were collected from 574 alewife over 9 consecutive years (2007–2015), and readers agreed on all ages except for 1 alewife. Ages ranged from 2 to 7 years with a median age of 3 years for both females (n=244) and males (n=329). Scales could be read for 532 of the 574 dissected alewife. Scale aging revealed reader bias, particularly in younger ages. Fish aged as 2 and 3 years old from scale readings commonly had younger ages that the 2 readers agreed upon from their otolith analyses, and fish assigned ages of 5, 6, and 7 years from scale analyses commonly had older age estimates from otolith readings; however, for fish at ages of 4, 6, and 7 years based on scale readings, estimates were not statistically different from ages based on otolith analyses (Table 2). Biases in ages between scale and otolith readings were statistically different in the McNemar's, Evans–Hoenig, and Bowker's tests: P=0.0032, P=0.0089, P=0.0001, respectively. Ages determined with the use of scales and otoliths agreed for 83.1% of the samples and were within 1 year of each other for an additional 15.0% of samples, with an ACV of 3.8%, indicating that the ages were precise according to standards established by Campana (2001).

Blueback herring Blueback herring were sampled from 2007 through 2015, but none were captured in 2009 and 2010. Otolith readers agreed on ages for 285 of

Table 2

The number of samples for each comparison of ages between otolith and scale readings for alewife (*Alosa pseudoharengus*) captured between 2007and 2015 in the Potomac River in northern Virginia, with t-test statistics (t) to indicate bias for each age. An asterisk (*) indicates when the ages determined by reading scales were significantly different from the age determined by reading otoliths.

	Scale age							
Otolith age	2	3	4	5	6	7	t	P
2	16	22	1	1	–	–	6.51	<0.0001*
3	–	222	20	2	2	–	4.60	<0.0001*
4	–	10	140	8	–	–	−0.47	0.6388
5	–	–	14	49	2	–	−3.21	0.0084*
6	–	–	2	2	11	1	−1.58	0.2824
7	–	–	–	2	1	4	−1.99	0.2824

Table 3

The number of samples for each comparison of ages between otolith and scale readings for blueback herring (*Alosa aestivalis*) captured in 2007 and 2008 and between 2011 and 2015 in the Potomac River in northern Virginia, with *t*-test statistics (*t*) to indicate bias for each age. An asterisk (*) indicates when the ages determined by reading scales were significantly different from the age determined by reading otoliths.

	Scale age						
Otolith age	2	3	4	5	6	*t*	*P*
2	41	13	–	–	–	4.10	0.0007*
3	–	143	12	–	–	3.63	0.0151*
4	–	1	32	–	–	−1.00	0.6496
5	–	3	2	8	–	−2.55	0.0762
6	–	–	1	–	3	−1.00	0.6496

287 samples. Ages ranged from 2 to 6 years, with a median age of 3 years for both females (n=123) and males (n=164). Scales could be read for 260 of 287 dissected blueback herring, with the ages of 2 and 3 years commonly overaged by readers and statistically biased on the basis of McNemar's, Evans–Hoenig, and Bowker's tests (all tests: P<0.0001; Table 3). Ages agreed between scale and otolith readings for 87.3% of the samples and were within 1 year of each other for an additional 10.8% of the samples. The ACV was 3.2%, indicating that the aging of samples were precise (Campana, 2001).

Growth models

The best-fit model for alewife was the linear growth model, and the worst-fit model was the Richards growth model (Table 4). The best-fit model for blueback herring was the logistic growth model, and the worst-fit model was the linear growth model (Table 4). However, the AIC weights were only 10.6% and 10.5% different between the best-fit and worst-fit models for alewife and blueback herring, respectively (Table 4). For this reason, the von Bertalanffy growth function, the most traditionally used growth model, was used to

Table 4

Rank of Akaike's information criterion weights (w) calculated for alewife (*Alosa pseudoharengus*) and blueback herring (*Alosa aestivalis*) based on sample size (n), number of parameters (k), sums of squares (SSQ), and Akaike's information criterion for model selection (AIC_i) from each growth model used in this study.

Species	Growth model	*n*	*k*	SSQ	AIC_i	*w* (%)	Rank
Alewife	Cerrato	559	3	96,589	1702.954	11.432	5
	Francis	559	3	96,589	1702.954	11.432	5
	Gompertz	559	3	96,582	1702.936	11.533	3
	Laird–Gompertz	559	3	96,582	1702.936	11.533	3
	Linear	559	2	97,165	1702.398	15.093	1
	Logistic	559	3	96,576	1702.921	11.621	2
	Ratkowsky	559	3	96,589	1702.954	11.432	5
	Richards	559	4	96,537	1704.823	4.490	9
	von Bertalanffy	559	3	96,589	1,702.954	11.432	5
Blueback herring	Cerrato	285	3	34,956	828.756	13.170	4
	Francis	285	3	34,956	828.754	4.914	8
	Gompertz	285	3	34,955	828.751	13.170	4
	Laird–Gompertz	285	3	34,955	828.751	13.193	2
	Linear	285	2	36,429	831.863	2.782	9
	Logistic	285	3	34,953	828.744	13.240	1
	Ratkowsky	285	3	34,956	828.754	13.170	4
	Richards	285	4	34,948	830.726	13.193	2
	von Bertalanffy	285	3	34,956	828.754	13.170	4

Table 5

Parameter estimates from von Bertalanffy growth function for males, females, and sexes combined of alewife (*Alosa pseudoharengus*) and blueback herring (*Alosa aestivalis*), with subsequent sums of squares (SSQ) from model fitting and sample size. The parameters are mean asymptotic length (L_∞), given in standard length in centimeters, growth rate coefficient (K), and the time (or age) at which the average length was zero (t_0).

Species	Model	Sex	L_∞ (cm)	K (per year)	t_0 (per year)	SSQ	n
Alewife	von Bertalanffy	Male	233.8	0.218	−5.97	30,131	329
		Female	250.9	0.237	−5.25	34,579	244
		Combined	257.2	0.179	−6.04	96,589	573
Blueback herring	von Bertalanffy	Male	213.7	0.387	−3.27	8,763	162
		Female	219.0	0.837	−0.75	11,522	123
		Combined	220.3	0.525	−1.69	34,956	285

examine the difference between sexes. All of the models converged, indicating that enough data was available for the models to successfully run.

The von Bertalanffy growth parameters differed between alewife and blueback herring ($P<0.0001$). Alewife grew faster and obtained larger sizes than blueback herring (Table 5). A likelihood ratio test confirmed the difference between species was not due to coincidence ($\chi^2=39$, df=3, $P<0.0001$); however, no single parameter was responsible for this difference.

For alewife, parameters between sexes were statistically different when the von Bertalanffy growth function was used ($P<0.0001$). The models for both species show females growing faster than males and attaining larger values of L_∞ (Table 5, Fig. 3A). The standardized residuals for the von Bertalanffy growth curve were randomly distributed, indicating that the model was a good fit (Fig. 3B). A likelihood ratio test confirmed that the difference between sexes was not due to coincidence ($\chi^2=229$, df=3, $P<0.0001$); however, differences were not significant between individual parameters.

For blueback herring, an analysis of residual sum of squares revealed that female blueback herring grew significantly larger and faster than males ($P<0.0001$; Table 5, Fig. 4A), and a likelihood ratio test confirmed the differences were significant ($\chi^2=138$, df=3, $P<0.0001$). Standardized residuals between the von Bertalanffy growth function and observed values were random (Fig. 4B). Differences between sexes were based on the interactions between the parameters of L_∞ and growth rate coefficient (K) ($\chi^2=8$, df=2, $P=0.02$) and interactions between L_∞ and the time (or age) at which the average length was zero (t_0) (von Bertalanffy:

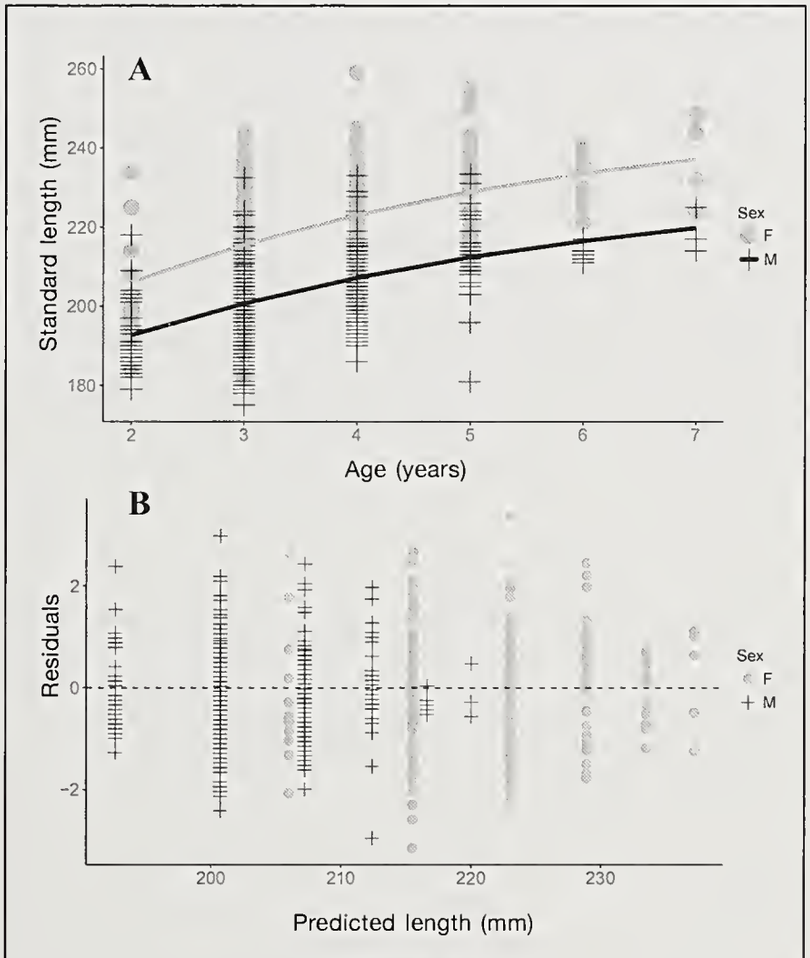

Figure 3

(**A**) Observed length at age for female (gray dots) and male (black plus signs) alewife (*Alosa pseudoharengus*) captured in the Potomac River between 2007 and 2015, with predicted length at age from von Bertalanffy growth models (solid lines). (**B**) Standardized residuals versus fitted values for the von Bertalanffy growth curves for female (gray dots) and male (black plus signs) alewife.

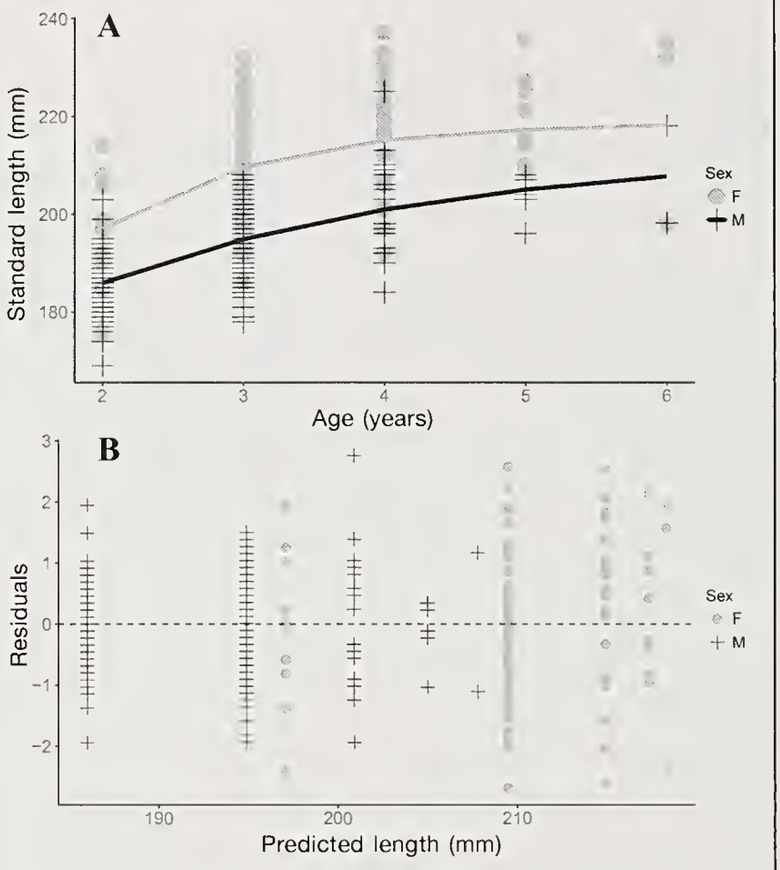

Figure 4

(**A**) Observed length at age for female (gray dots) and male (black plus signs) blueback herring (*Alosa aestivalis*) captured in the Potomac River in 2007 and 2008 and from 2011 through 2015, with predicted length at age from von Bertalanffy growth models (solid lines). (**B**) Standardized residuals versus fitted values for the von Bertalanffy growth curves for female (gray dots) and male (black plus signs) blueback herring.

χ^2=5, df=2, P=0.01). When a Bonferroni adjustment was used, the critical P-value became 0.007. With this new P-value, only testing the whole model for each sex was still statistically different, indicating that the differences between the sexes were not a coincidence but that none of the model parameters explain the differences by themselves.

Discussion

Females grew faster and larger than males for both species of river herring. Similar to the outcome of this study, previous studies have documented larger and faster-growing females for both species (Marcy, 1969; Loesch and Lund, 1977; Loesch, 1987). Additionally, alewife grew faster and larger than blueback herring, a finding that also has been documented by previous studies (Netzel and Stanek, 1966; Messieh, 1977; Jones et al., 1978; Fay et al.[1]; Klauda et al., 1991). In the Saint John River in New Brunswick, Canada, female alewife grew fastest and largest, followed by male alewife, then female blueback herring and male blueback herring. However, in the Albemarle Sound, North Carolina, female blueback herring grew faster and larger than male alewife. Fay et al.[1] provided average length-at-age data from multiples studies, information that indicates that growth rates of alewife and blueback herring were not consistent between studies (Fay et al.[1]). For example, in Georges Bank, alewife had a larger average length at age than blueback herring for every age, but in the Connecticut River larger average length varied between these species on the basis of age (Netzel and Stanek, 1966; Marcy, 1969; Fay et al.[1]). Why these differences in growth rates occurred between these studies is unclear. It could be due to differences in geography or time, given that both have been documented to affect growth of fish populations.

The estimates of L_∞ for alewife (273.9 mm FL) and for blueback herring (267.0-mm-FL) from this study are smaller than previously published estimates from other studies. The NOAA Northeast Fisheries Science Center conducted a bottom-trawl survey from 1973 through 1987 and used the survey data to estimate L_∞: 282.6 mm FL for alewife and 267.0 mm FL for blueback herring (ASMFC, 2012). For both sexes, the L_∞ also was smaller for individuals examined in this study than for individuals captured in the Saint John River in New Brunswick (male and female alewife: 292 and 310 mm FL; male and female blueback herring: 231 and 260 mm FL; Messieh 1977) and in New Hampshire rivers (male and female alewife: 305 and 322 mm TL; male and female blueback herring: 287 and 328 mm TL; ASMFC, 2012). The differences between estimates of L_∞ were most likely due to a lack of older individuals captured in the Potomac River, a situation that can lead to a poor estimation of the L_∞ (Hilborn and Walters, 1992).

Alewife and blueback herring historically have been aged up to 14 and 9 years, respectively (ASMFC, 2012), but the maximum ages for these species in this study were 7 and 6 years. A lack of representation of older fish in a data set can result from high adult mortality rates, gear selectivity, or underaging of fish (Francis, 1988). High adult mortalities in river herring have been linked to increased stress during spawning migrations, historical overfishing practices, and current bycatch of adult fish (Hightower et al., 1996; Greene et al.[2]; ASMFC, 2012). This pattern has been seen for other adult anadromous fishes as well (Dunton et al., 2015). The current moratoria for river herring have been in effect regionally only for 3 years; therefore, older river herring have been protected for a limited part of their life span.

The K value was lower for alewife and male blue-

back herring in this study than for those in previous studies (Messieh, 1977; ASMFC, 2012), differences that could be due to a lack of smaller individuals in the previous studies. For this study, alewife ranging in age from 2 to 7 years and blueback herring ranging in age from 2 to 6 years were used; however, in both previous studies, river herring ranged from 3 years to more than 9 years (Messieh, 1977; ASMFC, 2012). When age-2 individuals were removed from the analysis in this study, K increased from 0.179 to 0.243 mm/year for alewife (both sexes combined) and from 0.525 to 0.697 mm/year for blueback herring (both sexes combined). One hypothesis for why age-2 individuals were available in this study and not in previous studies is that the populations could have spawned at earlier ages in this study because of years of overfishing, which has been documented in Atlantic cod (*Gadus morhua*) (Trippel, 1995), several Pacific salmon species (Ricker, 1981), and numerous other fish species (Darimont et al., 2009). Fishermen target large individuals within a population. With years of fishing pressure, a population adapts to spawning as smaller, younger individuals because individual fish that can spawn at smaller sizes are more likely to successfully spawn than slower maturing individuals (Ricker, 1981; Thorpe, 1993). A change in maturity schedules is important to document for estimating potential recruitment of a population and should be examined further.

The lack of ages from 0 to 1 years and ages ≥7 years also could have contributed to the similarities between the different growth models tested within this study because the parameters in each model are correlated to each other (Hilborn and Walters, 1992; Campana, 2001; Allen and Gwinn, 2013). Missing younger and older fish of a population can make model estimation difficult because these 2 ends of a population can influence growth more than the part of a population at median ages (Campana, 2001). The younger and older ends of a population can also be the most difficult to obtain because of increased mortality for older individuals, anadromous species being collected during spawning runs only (as in this study), or age estimation being hardest for these categories (Campana, 2001; ASMFC, 2012; ASMFC[8]). Even in this study, when scales were used for aging, younger individuals were overaged and older individuals were underaged.

The ASMFC River Herring Ageing Workshop found that participating state agencies also overaged younger fish and underaged older fish when using scales (ASMFC[8]). Many agencies base the methods for using scales to age river herring on the methods developed by Cating (1953) for American shad. Marcy (1969) developed transverse groove counts specific to river herring captured in Connecticut based on Cating's (1953) method. However, this method does not take geographical location into account as a factor on fish growth and scale formation (Duffy et al., 2011). The use of transverse grooves, outlined by Cating (1953) and Marcy (1969), to determine location of freshwater zones and the first 3 years of age resulted in inconsistencies between ages in different geographical regions within the distribution of American shad (Duffy et al., 2011). Age validation with known-age river herring needs to be completed for each geographical region for the analysis of scales to be reliable as an aging technique for river herring (ASMFC[8]). The ASMFC River Herring Ageing Workshop has developed protocols to standardize aging techniques and has started a reference collection for aging structures from different rivers throughout the East Coast of the United States (ASMFC[8]).

Using data sets with biased ages can result in poor population modeling and conflicting strategies for population management (Beamish and McFarlane, 1987; Bertignac and de Pontual, 2007; Katsanevakis and Maravelias, 2008; Tyszko and Pritt, 2017; Porta et al., 2018). Age biases can influence stock assessment by overestimating or underestimating growth or mortality, affecting policy decisions about a population (Beamish and McFarlane, 1987; Katsanevakis and Maravelias, 2008). Alewife in this study were more likely to be underaged by the use of scales, increasing the estimates for growth and mortality rates (Beamish and McFarlane, 1987). Management strategies for species that are not growing as fast as models indicate can lead to overfishing practices. Conversely, blueback herring were more often overaged when scales were used in this study. Therefore, growth and mortality predictions could be lower than real levels, possibly limiting the ability of management agencies to track how reactive a population is to fishing changes (Tyszko and Pritt, 2017). The ages presented here for this study are considered precise between readers on the basis of the ACV, but there was no way to determine accuracy without the use of known-age individuals. Currently, no known-age samples for either species of river herring are available for use (ASMFC[8]).

This study reveals the importance of validating aging techniques for species of river herring, as well as of continuing to monitor the ages and individual growth rates of the populations of alewife and blueback herring. Many management agencies are calling for an increase in run counts and abundance estimates of these populations (ASMFC, 2012, 2017). Documenting abundances of river herring is only a small component in understanding a population that may have dramatically changed over decades because of overfishing and degraded habitats. The additional age and growth estimates completed in this study provide information needed in the ongoing efforts to restore the once great fisheries that targeted these species.

Acknowledgments

Comments of 2 anonymous reviewers have improved the manuscript. We would like to acknowledge R. Jones for conception of the monitoring program and previous co-principal investigator R. Kraus for collection of the samples before 2011. We would like to thank M. Ogburn, C. Ahn, and K. Lewis for their insight into this

project. Logistical support was provided by J. van der Ham and B. Bachman. This study was funded by Fairfax County through its Department of Public Works and Environmental Services and by Alexandria Renew Enterprises. Mention of trade names or commercial companies does not imply endorsement by the Potomac Environmental Research and Education Center, George Mason University.

Literature cited

Akaike, H.
1974. A new look at the statistical model identification. IEEE Trans. Auto. Control 19:716–723.

Allen, M. S., and D. Gwinn.
2013. Population models for assessment and management of inland striped bass fisheries. Am. Fish. Soc. Symp. 80:351–364.

ASMFC (Atlantic States Marine Fisheries Commission).
2012. River herring benchmark stock assessment. Stock Assess. Rep. 12-02. 2 vols. Atl. States Mar. Fish. Comm., Washington, D.C. [Available from website.]
2017. River herring stock assessment update. 2 vols. Atl. States Mar. Fish. Comm., Washington, D.C. [Available from website.]

Beamish, R. J., and G. A. McFarlane.
1987. Current trends in age determination methodology. *In* Age and growth of fish (R. C. Summerfelt and G. E. Hall, eds.), p. 15–42. Iowa State Univ. Press, Ames, IA.

Bertignac, M., and H. de Pontual.
2007. Consequences of bias in age estimation on assessment of the northern stock of European hake (*Merluccius merluccius*) and on management advice. ICES J. Mar. Sci. 64:981–988.

Besler, D. A.
1999. Utility of scales and whole otoliths for aging largemouth bass in North Carolina. Proc. Annu. Conf. SEAWFA 53:119–129.

Burnham, K. P., and D. R. Anderson.
2002. Model selection and multimodel inference: a practical information-theoretic approach, 488 p. Springer-Verlag, New York.

Campana, S. E.
2001. Accuracy, precision and quality control in age determination, including a review of the use and abuse of age validation methods. J. Fish Biol. 59:197–242.

Campana, S. E., and J. D. Neilson.
1985. Microstructure of fish otoliths. Can. J. Fish. Aquat. Sci. 42:1014–1032.

Campana, S. E., M. C. Annand, and J. I. McMillan.
1995. Graphical and statistical methods for determining the consistency of age determinations. Trans. Am. Fish. Soc. 124:131–138.

Cating, J. P.
1953. Determining age of Atlantic shad from their scales. Fish. Bull. 85:187–199.

Cerrato, R. M.
1990. Interpretable statistical tests for growth comparisons using parameters in the von Bertalanffy equation. Can. J. Fish. Aquat. Sci. 47:1416–1426.

Darimont, C. T., S. M. Carlson, M. T. Kinnison, P. C. Paquet, T. E. Reimchen, and C. C. Wilmers.
2009. Human predators outpace other agents of trait change in the wild. Proc. Natl. Acad. Sci. U.S.A. 106:952–954.

Duffy, W. J., R. S. McBride, S. X. Cadrin, and K. Oliveira.
2011. Is Cating's method of transverse groove counts to annuli applicable for all stocks of American shad? Trans. Am. Fish. Soc. 140:1023–1034.

Dunton, K. J., A. Jordaan, D. O. Conover, K. A. McKown, L. A. Bonacci, and M. G. Frisk.
2015. Marine distribution and habitat use of Atlantic sturgeon in New York lead to fisheries interactions and bycatch. Mar. Coast. Fish. 7:18–32.

Evans, G. T., and J. M. Hoenig.
1998. Testing and viewing symmetry in contingency tables, with application to readers of fish ages. Biometrics 54:620–629.

Francis, R. I. C. C.
1988. Are growth parameters estimated from tagging and age–length data comparable? Can. J. Fish. Aquat. Sci. 45:936–942.

Gompertz, B.
1825. XXIV. On the nature of the function expressive of the law of human mortality, and on a new mode of determining the value of life contingencies. Philos. Trans. R. Soc. Lond. 115:513–583.

Haddon, M.
2011. Modelling and quantitative methods in fisheries, 2nd ed., 465 p. CRC Press, Boca Raton, FL.

Heino, M.
1998. Management of evolving fish stocks. Can. J. Fish. Aquat. Sci. 55:1971–1982.

Heino, M., and O. R. Godo.
2002. Fisheries-induced selection pressures in the context of sustainable fisheries. Bull. Mar. Sci. 70:639–656.

Hightower, J. E., A. M. Wicker, and K. M. Endres.
1996. Historical trends in abundance of American shad and river herring in Albemarle Sound, North Carolina. North Am. J. Fish. Manage. 16:257–271.

Hilborn, R., and C. J. Walters (eds.).
1992. Quantitative fisheries stock assessment: choice, dynamics and uncertainty, 570 p. Chapman and Hall, London.

Hilborn, R., and M. Mangel.
1997. The ecological detective: confronting models with data, 336 p. Princeton Univ. Press, Princeton, NJ.

Jessop, B. M.
1994. Homing of alewives (*Alosa pseudoharengus*) and blueback herring (*A. aestivalis*) to and within the Saint John River, New Brunswick, as indicated by tagging data. Can. Tech. Rep. Fish. Aquat. Sci. 2015, 22 p.

Jones, P. W., F. D. Martin, and J. D. Hardy Jr.
1978. Development of fishes of the mid-Atlantic Bight: an atlas of egg, larval, and juvenile stages. Vol. 1: Acipenseridae through Ictaluridae, 366 p. Biol. Serv. Prog., U.S. Fish Wildl. Serv., Washington, D.C.

Jones, R. C., D. P. Kelso, and E. Schaeffer.
2008. Spatial and seasonal patterns in water quality in an embayment-mainstem reach of the tidal freshwater Potomac River, USA: a multiyear study. Environ. Monit. Assess. 147:351–375.

Katsanevakis, S., and C. D. Maravelias.
2008. Modelling fish growth: multi-model inference as a better alternative to *a priori* using von Bertalanffy equation. Fish Fish. 9:178–187.

Klauda, R. J., S. A. Fischer, L. W. Hall Jr., and J. A. Sullivan.
1991. Alewife and blueback herring; *Alosa pseudoharen-*

gus and *Alosa aestivalis*. *In* Habitat requirements for Chesapeake Bay living resources, rev. ed. (S. L. Funderburk, J. A. Mihursky, S. J. Jordan, and D. Riley, eds.), p. 10.11–10.29. Living Resour., Chesapeake Bay Prog., Annapolis, MD.

Laird, A. K.
1964. Dynamics of tumor growth. Br. J. Cancer 18:490–502.

Law, R.
2000. Fishing, selection, and phenotypic evolution. ICES J. Mar. Sci. 57:659–668.

Loesch, J. G.
1987. Overview of life history aspects of anadromous alewife and blueback herring in freshwater habitats. Am. Fish. Soc. Symp. 1:89–103.

Loesch, J. G., and W. A. Lund.
1977. A contribution to the life history of the blueback herring, *Alosa aestivalis*. Trans. Am. Fish. Soc. 106:583–589.

Marcy, B. C., Jr.
1969. Age determinations from scales of *Alosa pseudoharengus* (Wilson) and *Alosa aestivalis* (Mitchill) in Connecticut waters. Trans. Am. Fish. Soc. 98:622–630.

Messieh, S. N.
1977. Population structure and biology of alewives (*Alosa pseudoharengus*) and blueback herring (*A. aestivalis*) in the Saint John River, New Brunswick. Environ. Biol. Fish. 2:195–210.

Netzel, J., and E. Stanek.
1966. Some biological characteristics of blueback herring and alewife from Georges Bank, July and October, 1964. Intl. Comm. Northwest Atl. Fish. Res. Bull. 3:106–110.

Ogle, D. H.
2015. Age comparisons. *In* Introductory fisheries analyses with R, p. 75–86. CRC Press, Boca Raton, FL.

Porta, M. J., R. A. Snow, and D. E. Shoup.
2018. Comparison of saugeye age estimates and population characteristics using otoliths and dorsal spines. JSEAWFA 5:23–29.

Quinn, T. J., and R. B. Deriso.
1999. Quantitative fish dynamics, 560 p. Oxford Univ. Press, New York.

Ratkowsky, D. A.
1986. Statistical properties of alternative parameterizations of the von Bertalanffy growth curve. Can. J. Fish. Aquat. Sci. 43:742–747.

Richards, F. J.
1959. A flexible growth function for empirical use. J. Exp. Bot. 10:290–301.

Ricker, W. E.
1975. Computation and interpretation of biological statistics of fish populations. Bull. Fish. Res. Board Can. 191, 382 p.

Ricker, W. E.
1981. Changes in the average size and average age of Pacific salmon. Can. J. Fish. Aquat. Sci. 38:1636–1656.

Schlick, C. J. C.
2016. Life history traits and population dynamics of river herring, alewife *Alosa pseudoharengus* and blueback herring *Alosa aestivalis* in Potomac River tributaries. Ph.D. diss., 254 p. George Mason Univ., Fairfax, VA. [Available from website.]

Thorpe, J. E.
1993. Impacts of fishing on genetic structure of salmonid populations. *In* Genetic conservation of salmonid fishes (J. G. Cloud and G. H. Thorgaard, eds.), p. 67–80. Plenum Press, New York.

Trippel, E. A.
1995. Age at maturity as a stress indicator in fisheries: biological processes related to reproduction in northwest Atlantic groundfish populations that have undergone declines. BioScience 45:759–771.

Tuckey, T. D., and J. E. Olney.
2010. Maturity schedules of female American shad vary at small spatial scales in Chesapeake Bay. North Am. J. Fish. Manage. 30:1020–1031.

Tyszko, S. M., and J. J. Pritt.
2017. Comparing otoliths and scales as structures used to estimate ages of largemouth bass: consequences of biased age estimates. North Am. J. Fish. Manage. 37:1075–1082.

von Bertalanffy, L.
1938. A quantitative theory of organic growth (inquiries on growth laws. II). Hum. Biol. 10:181–213.

Wang, H.-Y., and T. O. Höök.
2009. Eco-genetic model to explore fishing-induced ecological and evolutionary effects on growth and maturation schedules. Evol. Appl. 2:438–455.

Wharton, J.
1957. The bounty of the Chesapeake, 78 p. Univ. Press Virg. Charlottesville, VA.

Zweifel, J. R., and R. Lasker.
1976. Prehatch and posthatch growth of fishes—a general model. Fish. Bull. 74:609–621.

National Marine Fisheries Service
NOAA

Fishery Bulletin
established in 1881

Spencer F. Baird
First U.S. Commissioner of Fisheries and founder of *Fishery Bulletin*

Presence of a resting population of female porbeagles (*Lamna nasus*), indicating a biennial reproductive cycle, in the western North Atlantic Ocean

Lisa J. Natanson (contact author)[1]
Bethany M. Deacy[2]
Warren Joyce[3]
James Sulikowski[4]

Email address for contact author: lisa.natanson@noaa.gov

[1] Northeast Fisheries Science Center
National Marine Fisheries Service, NOAA
28 Tarzwell Drive
Narragansett, Rhode Island 02882

[2] Riverside Technologies, Inc.
for National Marine Fisheries Service, NOAA
3500 Delwood Beach Road
Panama City, Florida 32408

[3] Population Ecology Division
Bedford Institute of Oceanography
P.O. Box 1006
Dartmouth, Nova Scotia, Canada, B2Y 4A2

[4] Department of Marine Sciences
University of New England
11 Hills Beach Road
Biddeford, Maine 04005

Abstract—The porbeagle (*Lamna nasus*) is a slow-growing, late-maturing, long-lived pelagic shark that inhabits cold temperate waters. Previous research based on specimens collected from the western North Atlantic Ocean has indicated that this lamnid shark has an annual reproductive cycle. However, the results of a recent evaluation of reproductive tracts from a geographically segregated group of porbeagles within the western North Atlantic Ocean indicate the presence of females in a resting stage of maturity. The observation of a resting stage has implications not only in the reproductive cycle, biennial versus annual, of this species but also in the lifetime productivity. This finding indicates that this shark follows the typical lamnid resting period between pregnancies, a period that would decrease the lifetime output of young sharks and their resilience to direct and indirect fishing pressure.

Manuscript submitted 9 October 2018.
Manuscript accepted 8 March 2019.
Fish. Bull. 117:70–77 (2019).
Online publication date: 25 March 2019.
doi: 10.7755/FB.117.1-2.8

The views and opinions expressed or implied in this article are those of the author (or authors) and do not necessarily reflect the position of the National Marine Fisheries Service, NOAA.

The porbeagle (*Lamna nasus*), a pelagic shark in the family Lamnidae, inhabits the cold temperate waters of the North and South Atlantic, South Pacific, and southern Indian Oceans as well as the subantarctic region of the Southern Ocean (Castro, 2011). In the western North Atlantic Ocean, the porbeagle ranges from the Grand Banks of Newfoundland, Canada, to the Gulf of Maine and rarely south to New Jersey (Castro, 2011). Seasonal abundance is related to north–south migrations and reproductive stage (Aasen[1]; Aasen, 1963; Campana et al., 2008; Campana et al., 2010a). Reproductive migrations are indicated by the occurrence of both mature males and mature females off the Grand Banks of Newfoundland in fall for mating (Jensen et al., 2002). Juveniles are found along the entire range, but a presumed nursery area is located in the Gulf of Maine (senior author, unpubl. data; J. Sulikowski, unpubl. data) and the location of a pupping ground has been reported to be in the Sargasso Sea (Campana et al., 2010b). Like most large elasmobranchs, the porbeagle is slow growing and long lived (over 25 years) and has a relatively late age at maturity (8 years for males and 13 years for females), traits that make this species vulnerable to overexploitation and population depletion by direct and indirect fisheries (Natanson et al., 2002).

In the western North Atlantic Ocean, commercial fisheries that target porbeagles have existed since the 1960s, but catches rapidly declined in the latter part of that decade (Aasen[1]; Aasen, 1963; Campana et al.[2]). In the 1990s, Canadian fisher-

[1] Aasen, O. 1961. Some observations on the biology of the porbeagle shark (*Lamna nasus* L.). ICES C.M. Document 1961/109, 7 p.

[2] Campana, S., L. Marks, W. Joyce, and S. Harley. 2001. Analytical assessment of the porbeagle shark (*Lamna nasus*) population in the Northwest Atlantic, with estimates of long-term sustainable yield. Dep. Fish. Oceans, Can. Sci. Advis. Secr. Res. Doc. 2001/067, 17 p. [Available from website.]

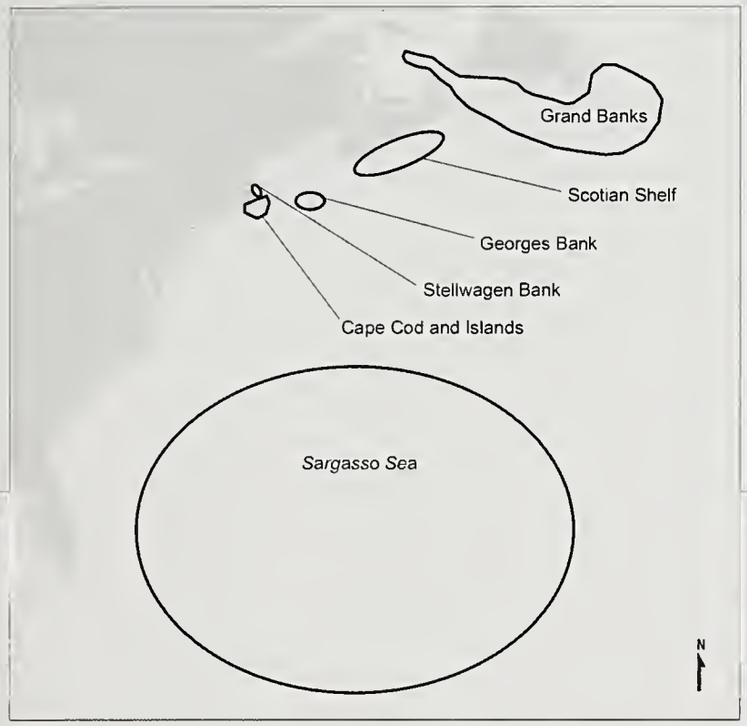

Figure 1

Map showing the areas used by female porbeagles (*Lamna nasus*) in different stages of maturity. The Grand Banks of Newfoundland and the Gulf of Saint Lawrence, Canada, form a reported mating area for porbeagles (Jensen et al., 2002). A portion of the Sargasso Sea has been identified as a pupping area (Campana et al., 2010b), and Stellwagen Bank is an area where females in a resting stage have been captured (this study). A portion of Georges Bank has been identified as a possible resting or mating area (Campana et al., 2010b; this study). Also shown are other locations where specimens were captured in this study.

men began a limited fishery on porbeagles. In an attempt to avoid overfishing, the government of Canada imposed catch quotas for the commercial porbeagle fishery from 1995 into the early 2000s through the Canadian Atlantic Pelagic Shark Integrated Fisheries Management Plan (Campana et al.[2]). In 2013, the fishery for porbeagles was closed in Atlantic Canada (Campana et al.[3]). Similarly, in 2008, the National Marine Fisheries Service implemented Amendment 2 to the Consolidated Atlantic Highly Migratory Species Fishery Management Plan (NMFS, 2007), which significantly reduced landings of porbeagles by U.S. commercial fisheries (Curtis et al., 2016).

Reproduction of lamnid sharks is distinct from that of the majority of other elasmobranchs (Gilmore et al., 2005). One unifying characteristic for this group is oophagy, as a means of embryonic nutrition, which requires a large ovary with relatively high oocyte production and high ovulation rates (Gilmore et al., 2005). In the strictly oophagous species, such as the shortfin mako (*Isurus oxyrinchus*) and the common thresher shark (*Alopias vulpinus*), multiple embryos per uterus, long gestation periods, and long resting periods (the period between parturition and the next pregnancy) with 1 or 2 years between pregnancies is typical (Mollet et al., 2000; Gilmore et al., 2005; Natanson and Gervelis, 2013).

Jensen et al. (2002) conducted a study on the reproduction of the porbeagle in the western North Atlantic Ocean, assessing sharks taken by the U.S. and Canadian commercial fishing industries and scientific research surveys in the late 1990s. The sampling for that study took place from the Grand Banks of Newfoundland to the Scotian Shelf and into the Gulf of Maine. Jensen et al. (2002) demonstrated that the majority of mature females caught in the Grand Banks portion of the study area (87 of 88 porbeagles examined) were gravid after November. On the basis of the observation that all mature female porbeagles are pregnant in fall in these areas, Jensen et al. (2002) suggested that, contrary to the reproduction of most other lamnids, the reproductive cycle for the porbeagle is annual. In this paper, we report the previously undocumented presence of females in a resting stage of maturity. This discovery indicates that porbeagles exhibit a biennial reproductive cycle rather than an annual cycle in the western North Atlantic Ocean, substantially decreasing their resilience to direct and indirect fishing pressures.

Materials and methods

Porbeagles were collected primarily from recreational fishermen at sportfishing tournaments held off Massachusetts and caught in the general vicinity of Stellwagen Bank or off Cape Cod (n=23; Fig. 1). A small number of porbeagles were captured on pelagic longlines onboard a U.S. commercial fishing vessel off the Grand Banks of Newfoundland (n=3). Sampling took place between 2004 and 2018. Additionally, data collected from porbeagle specimens captured between the Grand Banks of Newfoundland and Georges Bank prior to 2004, and used in Jensen et al. (2002), were reexamined.

Each shark was measured in fork length (FL), over the curve of the body from the tip of the nose to the fork of the tail, to the nearest millimeter and reported in centimeters. Whole weight was obtained when possible to the nearest pound and converted to kilograms.

A number of measurements and weights and information on conditions were taken from reproductive organs in female porbeagles to determine maturity stage. All specimens were measured fresh. Reproductive

[3] Campana, S. E., M. Fowler, D. Houlihan, W. Joyce, M. Showell, M. Simpson, C. Miri, and M. Eagles. 2015. Recovery Potential Assessment for Porbeagle (*Lamna nasus*) in Atlantic Canada. Dep. Fish. Oceans, Can. Sci. Advis. Secr. Res. Doc. 2015/041, 45 p. [Available from website.]

Table 1

Indices used to determine basic maturity in female porbeagles (*Lamna nasus*) based on data from Jensen et al. (2002) for female porbeagles caught between Georges Bank and the Grand Banks of Newfoundland, Canada, during 1979–1999. Adapted from Walker (2005b; table 4.1).

Organ	Index	Description	Maturity classification
Upper oviduct	UO-1	≤4.9 mm	Immature
	UO-2	>5 to ≤7 mm	Uncertain
	UO-3	>7 mm	Mature
Oviducal gland	OG-1	≤21 mm	Immature
	OG-2	>21 to ≤24 mm	Uncertain
	OG-3	>24 mm	Mature
Ovary length	OL-1	≤104 mm	Immature
	OL-2	>104 to ≤121 mm	Uncertain
	OL-3	>121 mm	Mature
Ovary width	OW-1	≤75.0 mm	Immature
	OW-2	>75.0 to ≤86.6 mm	Uncertain
	OW-3	>86.6 mm	Mature
Uterus length (total)	UL-1	≤343 mm	Immature
	UL-2	>343 to ≤475 mm	Uncertain
	UL-3	>475 mm	Mature
Uterus width	UW-1	≤26 mm	Immature
	UW-2	>26 to ≤43 mm	Uncertain
	UW-3	>43 mm	Mature
Membrane		Present	Immature
		Absent	Mature

tracts were measured on the right side of the specimen following Pratt (1979, 1993, 1996) and, specifically for the porbeagle, Jensen et al. (2002). Terminology follows Hamlett and Koob (1999) and Hamlett (1999), except where noted.

Reproductive organ measurements, taken to the nearest millimeter and at the widest part of the structure, included anterior oviduct width, oviducal gland width, ovary width and length, and uterus width and length. As per Jensen et al. (2002), 2 measurements were taken on the uterus: 1) from the anterior origin of the uterus to the vagina and 2) from the anterior origin of the uterus to the junction of the uteri (see fig. 1B in Jensen et al., 2002). Uterus width was taken midway along the anterior portion of the uterus (see fig. 1B in Jensen et al., 2002). For each ovary, oocytes were classified as mature if they contained yellow, vitellogenic material. The largest oocyte was measured in the field.

Males and females were classified as immature or mature, and mature females were further divided into 4 stages: ovulating, pregnant, postpartum, and resting. Using data from Jensen et al. (2002), we developed criteria for basic maturity classification (Table 1). Prior mating activity was assessed on the basis of the presence (immature) or absence (mature) of a vaginal membrane (hymen), and whether mating occurred recently was assessed on the basis of presence or absence of internal and external mating scars. The maturity stages of females were further determined by dissection: indications of past pregnancy included flaccid uteri (Pratt, 1979) and reduced ovaries with few mature or maturing oocytes. Individuals that appeared to have given birth in the current year were classified as postpartum, and those that had given birth but not recently were considered to be in a resting stage. A recently postpartum specimen was characterized by the presence of flocculent material consistent with portions of nutritive capsules along with milky uterine fluid (Gilmore et al., 2005); the uteri of a postpartum fish are very flaccid, and trophonemata are present (Natanson and Gervelis, 2013). Postpartum ovaries are generally large, hematose, and contain atretic oocytes.

Resting ovaries are often similar in appearance to the ovaries of almost mature juvenile sharks. It is, therefore, difficult to stage these fish by ovary condition alone, and other organ characteristics must be taken into account (Natanson and Gervelis, 2013). A late juvenile fish has a thin tubular uterus in contrast to the wider, slightly flaccid appearance of the resting uterus (previously expanded and then recovered) of adults. Additionally, a late-stage juvenile fish has a

Table 2

Collection data for female porbeagles (*Lamna nasus*) caught between 2004 and 2018 off Massachusetts, in the general vicinity of Stellwagen Bank or off Cape Cod, and off the Grand Banks of Newfoundland, Canada. All organ measurements are presented in millimeters unless otherwise noted. A dash indicates that there were no data for a field. A single asterisk (*) indicates that the fish was abnormally thin, its organs were small for its length, and it was not used in analysis. Two asterisks (**) indicate that the fish was classified as postpartum. T=tournament; CFV=commercial fishing vessel; RFV=recreational fishing vessel.

Maturity status	Date captured	Source	Fork length (cm)	Weight (kg)	Upper oviduct width	Oviducal gland width	Uterus width	Uterus length (upper)	Uterus length (total)	Ovary width	Ovary length	Maximum yolked egg diameter	Membrane	Ovary weight (g)
Juvenile	7/15/2017	T	202.0	120.2	4.8	6.5	8.3	190	260	42.3	71.7	none	Present	99
	7/15/2016	T	204.1	104.3	3.2	5.3	8.3	235	Unk	55.3	53.5	none	Present	73
	9/8/2016	CFV	215.7	–	8.6	23.1	46.3	270	520	130.0	180.0	4.0	Present	264
	7/16/2016	T	218.2	173.7	6.5	7.6	30.4	170	325	100.5	107.2	4.7	Present	158
	7/20/2013	T	219.4	141.5	–	–	–	–	–	–	–	–	–	–
	7/20/2013	T	221.4	142.0	6.5	19.5	19.8	–	430	85.0	135.0	none	Present	–
	7/13/2018*	T	234.7	151.0	4.2	5.2	10.0	210	320	73.3	87.2	none	Present	98
Adult	7/13/2018	T	215.3	152.9	9.0	23.2	35.5	235	435	120.0	150.0	none	Absent	204
	7/18/2008	T	217.5	150.6	12.3	24.5	41.4	Unk	460	109.0	158.0	3.0	Absent	–
	7/22/2006	T	221.0	146.5	8.3	25.0	53.8	240	440	130.0	160.0	3.1	Absent	340
	7/25/2009	T	223.0	163.7	9.5	28.9	49.7	210	440	128.0	180.0	3.0	Absent	463
	7/18/2015	T	224.4	160.6	9.0	20.9	35.9	190	440	115.0	160.0	none	Absent	–
	7/14/2017	T	227.0	152.4	8.3	18.8	26.4	240	470	160.0	158.0	none	Absent	335
	7/16/2005	T	231.0	171.5	7.0	20.9	59.5	310	550	165.0	210.0	3.5	Absent	545
	8/20/2011	T	233.0	181.4	9.6	24.3	64.4	350	500	120.0	180.0	3.5	Absent	319
	7/20/2013	T	234.2	177.4	6.0	22.2	58.8	–	471	140.0	160.0	none	Absent	–
	7/14/2017	T	237.7	181.0	8.4	28.7	53.8	270	512	150.0	150.0	none	Absent	321
	7/15/2005	T	238.0	171.5	11.3	24.4	75.8	290	470	150.0	210.0	3.2	Absent	448
	7/17/2004	T	239.0	181.4	7.6	27.7	62.9	250	320	132	195	3.3	Absent	445
	7/22/2011	T	241.0	224.5	14.5	22.4	115.0	290	530	145.0	180.0	none	Absent	668
	7/17/2015	T	241.0	196.0	8.3	18.6	74.2	250	485	143.0	225.0	none	Absent	700
	9/20/2016	CFV	244.2		11.7	19.0	70.4	330	569	150.0	160.0	<1	Absent	394
	7/20/2012	T	247.0	199.6	7.3	23.7	60.8	270	515	110.0	190.0	5.2	Absent	328
	9/7/2012**	T	247.6	272.5	7.4	32.3	140.0	355	–	165.0	252.0	4.0	–	–
	9/20/2015	RFV	248.0	219.1	9.6	32.5	100.3	390	575	130.0	200.0	4.0	–	650

vaginal membrane, an indication that it had not previously mated (mature virgin stage; Jensen et al., 2002), and a resting female has had prior mating experience and no vaginal membrane. A resting fish, as opposed to a recently postpartum fish, has recovered uteri, and its ovary no longer contains atretic oocytes; nor is its ovary hematose. The resting ovary has small, mostly non-yolked oocytes and is ready for vitellogenesis. In our study, maturity status of both sexes was assigned to each shark, at the time of dissection, on the basis of all previously described reproductive organ characteristics and was verified by comparison with measurements taken by Jensen et al. (2002) (Table 1; Suppl. Figs. 1–3) (online only).

Data from Jensen et al. (2002) were reevaluated to determine whether resting females had been classified as *adult* without distinguishing the specific condition or maturity stage (i.e., resting versus pregnant). To attempt to determine stage, reproductive organ measurements from adult females not classified as either pregnant or ovulating were compared with those obtained from known resting females. Additionally, notes taken at the time of dissection were used in evaluating the specific adult stage. Because it was known that these fish were adults, the distinction between stages had to be made between resting and ready-to-mate females; therefore, the condition of the ovary, including maximum oocyte size, was the primary consideration. Only those fish for which their maturity stage could be firmly classified were used (i.e., specimens for which ovary data were not available were not reevaluated).

Results

Complete reproductive necropsies were conducted on 26 female porbeagles (202.0–248.0 cm FL), of which 7 fish were immature (202.0–234.7 cm FL). Of the remaining 19 mature individuals, 1 porbeagle (247.6 cm FL) was postpartum and 18 individuals were in a resting stage (215.3–248.0 cm FL; Table 2). The resting females examined in this study had recovered uteri and ovaries

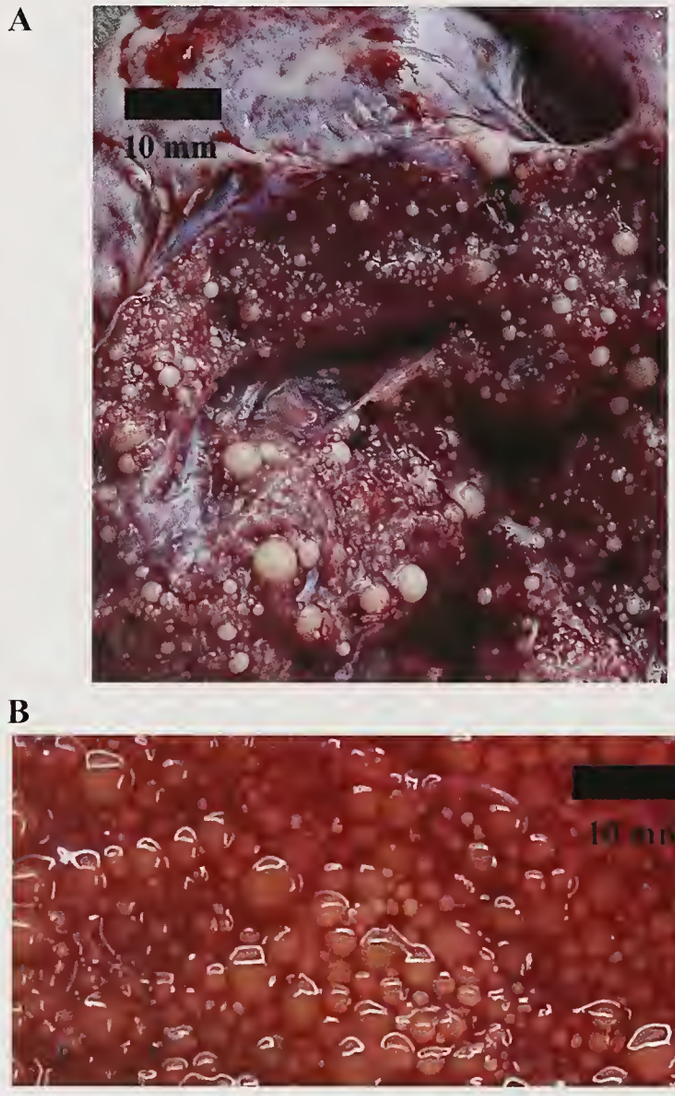

Figure 2

Photographs of the resting and ovulating stages of maturity in the porbeagle (*Lamna nasus*). (**A**) Ovary from a 248-cm-FL resting female caught in late September 2016 at the Grand Banks of Newfoundland, Canada. (**B**) Ripe ovary from a 249-cm-FL ovulating female caught in November 1999 at Saint Pierre Island, Canada. For reference, 10-mm scale bars are included.

that had few small follicles (Fig. 2A), compared with a ripe ovary with many large oocytes (Fig. 2B). Fourteen females that were in the resting stage and caught on Stellwagen Bank were examined between July and September (Fig. 1). In addition, 2 sharks in the resting stage were caught east and south of Cape Cod, Nantucket, and Martha's Vineyard in July, and 2 sharks in the resting stage were taken on the Grand Banks of Newfoundland in September (Fig. 1). Three mature and 2 immature male porbeagles also were caught in the Gulf of Maine–Stellwagen Bank area during sampling for this study but will not be discussed.

Data from Jensen et al. (2002) for 20 adult females were reexamined by using the staging criteria from our study (Table 1). For 3 of these females, enough data were not available. Of the remaining 17 reexamined porbeagles, 2 females were postpartum, 1 fish was ready to ovulate, 9 individuals were ovulating, and 5 females were resting (Table 3). The 5 porbeagles in a resting stage were caught in July on Cultivator Shoals, located on Georges Bank (n=1); in October on the Grand Banks of Newfoundland (n=1); and in April on the Scotian Shelf east of La Have Bank (n=3). This result indicates segregation of females in different maturity stages by time and location when compared with data from Jensen et al. (2002), who caught gravid and ovulating females primarily east of longitude 62°W, particularly in the area of the Grand Banks of New-

Table 3

Data from Jensen et al. (2002) reevaluated for this study for porbeagles (*Lamna nasus*) captured between 1989 and 1999 in the general vicinity of Georges Bank to off the Grand Banks of Newfoundland, Canada. All organ measurements are presented in millimeters unless otherwise noted. The vaginal membrane was absent in all of these specimens. A dash indicates that there were no data for a field.

Maturity status	Date captured	Fork length (cm)	Weight (kg)	Upper oviduct width	Oviducal gland width	Uterus width	Uterus length (upper)	Uterus length (total)	Ovary width	Ovary length	Maximum yolked egg diameter
Resting	7/19/1989	240.0	172.4	10.0	27.0	–	–	–	75.0	195.0	2.5
	4/2/1994	220.0	–	8.0	25.0	–	320.0	–	120.0	155.0	2.0
	4/6/1994	218.0	–	8.0	29.0	–	370.0	–	80.0	180.0	2.0
	4/7/1994	231.0	–	–	31.0	–	340.0	–	110.0	150.0	3.0
	10/23/1993	244.0	–	–	28.0	–	–	–	110.0	150.0	1.0
Ready to ovulate	11/26/1999	217.0	128.0	11.3	37.2	37.5	160.0	450.0	135.0	175.0	6.0
Ovulating	10/2/1999	234.0	155.0	9.0	30.0	42.0	184.0	435.0	139.0	153.0	4.0
	9/28/1999	228.5	–	5.0	28.0	39.0	235.0	535.0	126.0	177.0	6.0
	5/20/1999	230.5	118.5	6.0	21.0	48.0	235.0	514.0	122.0	169.0	3.0
	10/11/1999	221.0	–	9.0	35.0	36.0	205.0	470.0	180.0	193.0	6.0
	5/18/1999	240.0	144.0	6.0	24.0	54.0	228.0	514.0	111.0	148.0	–
	10/2/1999	248.0		8.0	35.0	30.0	160.0	515.0	142.0	181.0	4.0
	5/18/1999	229.5	135.0	9.0	23.0	39.0	292.0	605.0	112.0	136.0	4.0
	6/1/1999	228.0	118.5	8.0	21.0	51.0	236.0	615.0	134.0	169.0	5.0
	5/6/1999	241.0	–		26.5	65.0	465.0	820.0	135.0	230.0	4.0
Postpartum	5/5/1999	230.0	132.0	8.0	24.0	54.0	336.0	568.0	147.0	165.0	4.2
	5/6/1997	221.2	–	8.7	26.9	–	530.0	–	140.0	170.0	–
Unable to be	6/2/1999	216.0	–	–	21.0	–	–	–	130.0	152.0	–
determined	5/6/1999	233.0	145.0	7.0	21.5	38.5	296.0	580.0	114.0	130.0	–
	4/8/1999	214.0	–	7.5	21.5	26.0	182.0	343.0		104.0	–

foundland and the mouth of the Saint Lawrence River (Fig. 2; Jensen et al., 2002).

Discussion

An essential component for assessing and managing populations of sharks is determining each species' reproductive biology (e.g., when sexual maturity occurs, the timing of seasonal cycles, or gestation length) (Walker, 2005a, 2005b). However, variability in these important reproductive parameters has been shown to occur within species (e.g., Lombardi-Carlson et al., 2003; Sulikowski et al., 2007; Castro, 2009; Driggers and Hoffmayer, 2009), complicating the management process. Therefore, because of the importance of reproductive data as inputs in demographic and population models (Cortés, 2002), it is imperative to accurately describe the life history of a species throughout its range.

Castro (2009) describes the complexities of the typical biennial reproductive cycle of the sand tiger (*Carcharias taurus*), a lamnid species that inhabits subtropical and temperate waters worldwide. It has been suggested that this species has a biennial cycle with consecutive vitellogenesis and gestation and with discontinuous ovulation in specimens captured in waters of Australia and the southwest Atlantic Ocean (Lucifora et al., 2002; Bansemer, 2009). However, in North America, information on reproductive cycle is inconclusive, and an annual instead of biennial cycle has been reported (Castro, 2009). Indeed, only annual reproduction may be considered because of the inability of researchers to find the resting segment of the population of sand tigers that may be highly localized and unsampled to date (Castro, 2009). The existence of a previously unsampled resting portion of the population of porbeagles is indicated by the results of our study.

As in other lamnid species, at some point during gestation, the ovaries of a female porbeagle become exhausted; by the time of parturition, an ovary is depleted and hematose and contains atretic oocytes. A depleted ovary must then recover to a condition ready for vitellogenesis (Fig. 2A). Because it has been suggested that birth occurs between April and June and that mating occurs in the fall, an ovary of a porbeagle is unlikely to recover enough to ovulate and sustain a new brood by September (Fig 2; Jensen et al., 2002; Castro, 2009). In addition, sampling for our study took place by recreational fishermen between July and September in an area (primary area: Stellwagen Bank) geographically distinct from the primary sampling area of Jensen et al. (2002) in waters between Nova Scotia and the Grand Banks of Newfoundland (Fig. 1). Therefore, the observation of females in a resting phase ap-

pears to represent a portion of the population that had remained unsampled until now.

Jensen et al. (2002) sampled porbeagles caught in commercial fisheries in an area of high abundance of porbeagles. They found that mature females in this area were either pregnant or ovulating, leading them to the conclusions that 1) this area is a mating ground and 2) porbeagles have annual reproduction. Further, the seasonality of spermatophore production, observations of females with fresh mating scars, and observations of males and females captured on the same longline indicate that porbeagles mate in the fall, primarily between September and November on the Grand Banks of Newfoundland and the vicinity (Jensen et al., 2002). Jensen et al. (2002) also predicted a gestation period of 8–9 months and pupping from April through June. According to Jensen et al. (2002), mature females would be recently postpartum in July and recovering to the point of mating (oocytes with diameters of ~3–6 mm) by September. However, this timing appears unrealistic for the samples collected in our study, on the basis of the condition of the resting ovaries observed in the summer (Fig. 2A). In addition, this study observed only one recently postpartum individual (caught in September), and the remainder of the individuals were recovered to the point where vitellogenesis had commenced. Therefore, on the basis of other lamnid studies and the known timing of porbeagle mating, oogenesis would require a year before they would be in mating condition, further indication that this shark has a biennial rather than an annual reproductive cycle.

An additional mating ground on Georges Bank has been indicated by the presence of "high catch rates of mature females, which did not appear to be feeding" in June 2007, observed by Campana et al. (2010a), although no detailed necropsy data were presented. However, because no males were captured with this group of females and the data of Jensen et al. (2002) indicates a fall mating season, it is unlikely that a mating aggregation occurs on Georges Bank in summer. On the basis of the findings of our study, we suggest that this aggregation was more consistent with resting than mating, particularly in light of the fact that Georges Bank is in geographic proximity to Stellwagen Bank (Fig. 1). Further, females assumed to be mature on the basis of size and tagged on Georges Bank, primarily in July 2008, have been shown to migrate to the Sargasso Sea. This migration was assumed to be for pupping (Campana et al., 2010b). On the basis of time of year, it is unlikely that these sharks were pregnant and would have had to travel to the mating area before pupping in the Sargasso Sea. The tracks of tagging data presented by Campana et al. (2010b; fig. 1) indicate that the sharks in that study did not travel to known mating grounds and were only assumed to be pregnant (no direct reproductive assessments were made). In light of the evidence from our study, for a resting area in Stellwagen Bank, and data from the Campana et al. (2010b) tagging study that indicate that porbeagles did not travel east of longitude 62°W but resided in the areas of the Gulf of Maine, Stellwagen Bank, and Georges Bank, it is possible that the females tagged by Campana et al. (2010b) were in a resting stage and transited to the Sargasso Sea for unknown reasons, possibly related to feeding.

The discovery of a resting portion of the population of porbeagles in the western North Atlantic Ocean has important implications for fisheries management. The inclusion of a resting period in the reproductive cycle of the porbeagle means at least some portion of the female population is not reproducing annually. A decrease in productivity on the basis of non-annual reproduction needs to be considered because such a decrease would reduce the resilience of this species to direct and indirect fishing pressures. Continued research on the migrations and distribution of porbeagles by their adult maturity stage is necessary to provide effective management for this species.

Acknowledgments

We thank the various shark tournament officials and fishermen for allowing us access to their catch. We also thank the captain and crew of the F/V *Eagle Eye II* for allowing us to sail onboard and sample catch and C. McCandless for making maps.

Literature cited

Aasen, O.
1963. Length and growth of the porbeagle (*Lamna nasus*, Bonnaterre) in the North West Atlantic. Fisk.dir. Skr., Havund. 13:20–37.

Bansemer, C. S.
2009. Population biology, distribution, movement patterns and conservation requirements of the grey nurse shark (*Carcharias taurus* Rafinesque, 1810) along the east coast of Australia. Ph.D. diss., 159 p. Univ. Queensland, Brisbane, Australia.

Campana, S., W. Joyce, L. Marks, P. Hurley, L. J. Natanson, N. E. Kohler, C. F. Jensen, J. J. Mello, H. L. Pratt Jr., S. Myklevoll, et al.
2008. The rise and fall (again) of the porbeagle shark population in the Northwest Atlantic. *In* Sharks of the open ocean: biology, fisheries and conservation (M. D. Camhi, E. K. Pikitch, and E. A. Babcock, eds.), p. 445–461. Blackwell Publishing, Ltd., Oxford, UK.

Campana, S. E., A. J. F. Gibson, M. Fowler, A. Dorey, and W. Joyce.
2010a. Population dynamics of porbeagle in the Northwest Atlantic, with an assessment of status to 2009 and projections for recovery. Collect. Vol. Sci. Pap. ICCAT 65(6):2109–2182.

Campana, S. E., W. Joyce, and M. Fowler.
2010b. Subtropical pupping ground for a cold-water shark. Can. J. Fish. Aquat. Sci. 67:769–773.

Castro, J. I.
2009. Observations on the reproductive cycle of some viviparous North American sharks. Aqua Int. J. Ichthyol. 15:205–222.

2011. The sharks of North America, 640 p. Oxford Univ. Press, Inc., New York.

Cortés, E.
2002. Incorporating uncertainty into demographic modeling: application to shark populations and their conservation. Conserv. Biol. 16:1048–1062.

Curtis, T. H., S. Laporte., E. Cortes, G. DuBeck, and C. McCandless.
2016. Status review report: porbeagle shark (*Lamna nasus*), 56 p. Final report to National Marine Fisheries Service, Office of Protected Resources. [Available from website.]

Driggers, W. B., III, and E. R. Hoffmayer.
2009. Variability in the reproductive cycle of finetooth sharks, *Carcharhinus isodon*, in the northern Gulf of Mexico. Copeia 2009:390–393.

Gilmore, R. G., Jr., O. Putz, and J. W. Dodrill.
2005. Oophagy, intrauterine cannibalism and reproductive strategy in lamnoid sharks. *In* Reproductive biology and phylogeny of Chondrichthyes: sharks, batoids, and chimaeras, vol. 3 (W. C. Hamlett, ed.), p. 435–462. Sci. Publishers, Enfield, NH.

Hamlett, W. C.
1999. Male reproductive system. *In* Sharks, skates and rays: the biology of elasmobranch fishes (W. C. Hamlett, ed.), p. 444–470. Johns Hopkins Univ. Press, Baltimore, MD.

Hamlett, W. C., and T. J. Koob.
1999. Female reproductive system. *In* Sharks, skates and rays: the biology of elasmobranch fishes (W. C. Hamlett, ed.), p. 398–443. Johns Hopkins Univ. Press, Baltimore, MD.

Jensen, C. F., L. J. Natanson, H. L. Pratt Jr., N. E. Kohler, and S. E. Campana.
2002. The reproductive biology of the porbeagle shark (*Lamna nasus*) in the western North Atlantic Ocean. Fish. Bull. 100:727–738.

Lombardi-Carlson, L. A., E. Cortés, G. R. Parsons, and C. A. Manire.
2003. Latitudinal variation in life-history traits of bonnethead sharks, *Sphyrna tiburo*, (Carcharhiniformes: Sphyrnidae) from the eastern Gulf of Mexico. Mar. Freshw. Res. 54:875–883.

Lucifora, L. O., R. C. Menni, and A. H. Escalante.
2002. Reproductive ecology and abundance of the sand tiger shark, *Carcharias taurus*, for the southwestern Atlantic. ICES J. Mar. Sci. 59:553–561.

Mollet, H. F., G. Cliff, H. L. Pratt Jr., and J. D. Stevens.
2000. Reproductive biology of the female shortfin mako, *Isurus oxyrinchus* Rafinesque, 1810, with comments on the embryonic development of lamnoids. Fish. Bull. 98:299–318.

Natanson, L. J., and B. J. Gervelis.
2013. The reproductive biology of the common thresher shark in the western North Atlantic Ocean. Trans. Am. Fish. Soc. 142:1546–1562.

Natanson, L. J., J. J. Mello, and S. E. Campana.
2002. Validated age and growth of the porbeagle shark, *Lamna nasus*, in the western North Atlantic Ocean. Fish. Bull. 100:266–278.

NMFS (National Marine Fisheries Service).
2007. Final amendment 2 to the consolidated Atlantic highly migratory species fishery management plan, 726 p. NOAA, Natl. Mar. Fish. Serv., Off. Sustainable Fish., Highly Migratory Species Manage. Div., Silver Spring, MD.

Pratt, H. L., Jr.
1979. Reproduction in the blue shark, *Prionace glauca*. Fish. Bull. 77:445–470.
1993. The storage of spermatozoa in the oviducal glands of western North Atlantic sharks. Environ. Biol. Fish. 38:139–149.
1996. Reproduction in the male white shark. *In* Great white sharks, the biology of *Carcharodon carcharias* (A. P. Klimley and D. G. Ainley, eds.), p. 131–138. Academic Press, San Diego, CA.

Sulikowski, J. A., W. B. Driggers III, T. S. Ford, R. K. Boonstra, and J. K. Carlson.
2007. Reproductive cycle of the blacknose shark *Carcharhinus acronotus* in the Gulf of Mexico. J. Fish Biol. 70:428–440.

Walker, T. I.
2005a. Management measures. *In* Management techniques for elasmobranch fisheries (J. A. Musick and R. Bonfil, eds.), p. 285–321. FAO Fish. Tech. Pap. 474. FAO, Rome.
2005b. Reproduction in fisheries science. *In* Reproductive biology and phylogeny of Chondrichthyes: sharks, batoids, and chimaeras, vol. 3 (W. C. Hamlett, ed.), p. 81–126. Sci. Publishers, Enfield, NH.

National Marine
Fisheries Service
NOAA

Fishery Bulletin
established in 1881

Spencer F. Baird
First U.S. Commissioner
of Fisheries and founder
of *Fishery Bulletin*

Sexual maturation in a male whale shark (*Rhincodon typus*) based on observations made over 20 years of captivity

Rui Matsumoto (contact author)[1,2]
Yosuke Matsumoto[1]
Keiichi Ueda[1,2]
Miwa Suzuki[3]
Kiyoshi Asahina[3]
Keiichi Sato[1,2]

Email address for contact author: r-matsumoto@okichura.jp

[1] Okinawa Churaumi Aquarium
Ishikawa 424
Motobu, Okinawa 905-0206, Japan

[2] Okinawa Churashima Research Center
Ishikawa 424
Motobu, Okinawa 905-0206, Japan

[3] College of Bioresource Sciences
Nihon University
Kameino 1866
Fujisawa, Kanagawa 252-0880, Japan

Abstract—A male whale shark (*Rhincodon typus*) has been kept in captivity at the Okinawa Churaumi Aquarium, Japan, for 23 years, providing a rare opportunity to observe sexual maturation of a male. In 2012, when the individual was 8.5 m in total length (TL), the claspers began to elongate, and the distal ends of the claspers changed into cauliflower-shaped forms. These morphological changes in the claspers were completed in 11 months. Plasma concentrations of sex hormones (testosterone and progesterone) increased in association with clasper elongation. After elongation, additional movements, including the adduction and crossing of claspers, were displayed, and a whitish fluid, which may have been semen, was discharged through the clasper grooves, indicating that the male was functionally mature after clasper elongation. These observations indicate that this captive whale shark reached maturity when it was 8.5 m TL and over 25 years in age. This size at maturity is consistent with observations in the wild. However, maturity in this individual captive animal may have occurred later than has been previously reported in nature.

Manuscript submitted 7 September 2018.
Manuscript accepted 11 April 2019.
Fish. Bull. 117:78–86 (2019).
Online publication date: 26 April 2019.
doi: 10.7755/FB.117.1-2.9

The views and opinions expressed or implied in this article are those of the author (or authors) and do not necessarily reflect the position of the National Marine Fisheries Service, NOAA.

In the wild, tracking animals, especially migratory aquatic vertebrates, throughout their entire life histories is extremely difficult. Animals often move over vast oceans and have long life spans, sometimes longer than those of humans. Therefore, the life history traits of such animals generally are based on fragmented information, obtained from dead specimens acquired opportunistically.

The process of sexual maturation in the whale shark (*Rhincodon typus*), the world's largest fish, remains poorly understood because of the difficulties associated with following individuals over long periods of time, both in the wild and in captivity. The Okinawa Churaumi Aquarium, located in Okinawa, Japan, has successfully maintained a whale shark for over 20 years in captivity, providing a unique opportunity to better follow maturation history in this species (e.g., Uchida et al., 2000; Martin, 2007). This male whale shark, named *Jinta*, has been exhibited since 1995 at the Ocean Expo Aquarium (renamed the Okinawa Churaumi Aquarium in 2002), representing the longest period of captivity for this species in the world. From 1995 to 2018, the total length (TL) of the animal increased from 4.6 to 8.7 m.

From our study of this shark, we report the process of sexual maturation in the male whale shark, focusing on morphological changes and movements of the claspers, possible semen ejection, and changes in the circulating levels of sex hormones. For male elasmobranchs, the degree of clasper elongation and calcification and increase in sex hormone levels are generally used as indicators of sexual maturation (Gelsleichter and Evans, 2012); however, continuous changes in these indicators

during the maturation process have never before been documented in whale sharks. This study was based on data from only one individual, but it is still noteworthy because this individual is the only whale shark that has been successfully maintained in captivity for such a long period. Our data provide important insights into the maturation of male whale sharks.

Materials and methods

Ethics

This study was conducted as part of the health monitoring for captive animals at the Okinawa Churaumi Aquarium. Animal welfare during rearing was maintained in strict accordance with the ethical guidelines of the Japanese Association of Zoos and Aquariums (JAZA[1]), which does not stipulate the experimental procedures to be followed. Therefore, this study did not require separate, specific approval from this association. Maintenance, animal handling, and all procedures associated with this study also were conducted in accordance with the ethical guidelines of Okinawa Churashima Foundation (OCF[2]), which specifies procedures for the care and welfare of higher vertebrates (reptiles, birds, and mammals); these guidelines did not contradict the guidelines of the Japanese Association of Zoos and Aquariums.

Captivity conditions

The male whale shark is kept at the Okinawa Churaumi Aquarium in an exhibition tank (Kuroshio Tank) with a length, width, and depth of 27, 35, and 10 m. The water in the tank is replaced continuously with natural seawater pumped directly from the East China Sea. The temperature and chemistry of the water in the tank are the same as those in the external environment. The roof of the tank is transparent; therefore, light intensity in the tank reflects that of natural sunlight. The shark is fed 0.5–0.8% of its body weight in euphausiids and sergestids every day.

Growth

The TL of the male whale shark was estimated by measuring the length from the snout-tip to the origin of the first dorsal fin (pre-first dorsal fin length [PD1]), to avoid measurement errors caused by lateral tail beats when TL was measured directly. The following equation, from Matsumoto et al. (2017), was used to estimate TL in centimeters:

$$LogTL = 0.964 \times logPD1 + 0.443.$$

The PD1 has been measured underwater directly by 2 scuba divers with a measuring tape, every year since the first year of captivity.

The growth rate was calculated for each growth stage by using segmented regression models (SRMs; Muggeo, 2003; Segura et al., 2013). The growth of elasmobranchs is generally divided into 2 stages, immature (juvenile) and mature (adult) (Jensen et al., 2002), or into 3 stages: immature, maturing, and mature (Saïdi et al., 2009). Therefore, we applied 2 SRMs that estimated 1 or 2 break points (BKs) expected to be turning points of the growth stages, following the method described by Muggeo (2003).

Clasper morphology

The morphological features of the claspers are used to indicate sexual maturation in elasmobranchs. We calculated the ratio of clasper outer length (CLO) to pelvic inner margin length (P2I) (i.e., CLO:P2I), as described by Compagno (1984). The CLO:P2I is a relative value that represents the degree of elongation from the posterior end of the pelvic fin. The CLO and P2I were analyzed with photogrammetry by using ImageJ, vers. 1.45 (Schneider et al., 2012) to take measurements from photographs of the ventral side of the pelvic region of the shark. The photographs were taken underwater annually from October 2005 through August 2011, and then they were taken monthly until October 2013.

Sex steroid hormones

The plasma concentrations of testosterone and progesterone (T and P4, respectively) were analyzed by using blood samples. Veterinarians took blood underwater from the radial vein of the pectoral fin, using a syringe with an 18-gauge needle, monthly from May 2008 through December 2013 (Ueda et al., 2017). Blood samples were then transferred to a blood-collection vacuum tube treated with heparin (VP-H050K[3], Terumo Corp., Tokyo, Japan). After centrifugation (3000 rpm for 15 min), plasma was collected and immediately stored at −80°C for subsequent hormonal analysis. After thawing, the plasma was mixed with diethyl ether, and steroids were extracted by using a common procedure (Suzuki et al., 1998). The extract was diluted 2.5 fold with 0.05 M Tris-HCl (pH 7.75) buffer solutions, so that it could be used for measurements. The plasma concentrations of both steroid hormones were determined through time-resolved fluorescent antibody analysis.

We compared the average blood levels of the hormones among the 3 observable developmental periods of the clasper: short (clasper tips and posterior margin of pelvic fins are at the same horizontal position), elon-

[1] JAZA (Japanese Association of Zoos and Aquariums). 1984. Japan Arboretum Aquarium Association ethics summary [Available from website.]

[2] OCF (Okinawa Churashima Foundation). 2016. Guide for care and use of laboratory animals of Okinawa Churashima Foundation, 11 p. [Available from Okinawa Churashima Found., Ishikawa 888, Motobu, Okinawa 905-0206, Japan.]

[3] Mention of trade names or commercial companies is for identification purposes only and does not imply endorsement by the National Marine Fisheries Service, NOAA.

Table

Fitted parameters from 2 segmented regression models (SRMs) for estimating the growth of the captive male whale shark (*Rhincodon typus*) at the Okinawa Churaumi Aquarium in Okinawa, Japan. The SRMs used 1 or 2 break points (BKs) expected to be turning points between the 3 growth stages: immature, maturing, and mature. The average monthly changes in growth of body length, during the immature stage (α_1), during the mature stage in the model with 1 BK or the maturing stage in the model with 2 BKs (α_2), and during the mature stage in the model with 2 BKs (α_3), are given with standard errors of the means (SEs). The turning points from the immature to mature stage in the 1-BK model (BK_1), from the immature to maturing stage in the 2-BK model (BK_1), and from the maturing to mature stage in the 2-BK model (BK_2) are given with 95% confidence intervals (CI). r^2=coefficient of determination.

	Slopes						
	α_1 (SE)	α_2 (SE)	α_3 (SE)	BK_1 (95% CI)	BK_2 (95% CI)	Intercept (SE)	r^2
Model with 1 BK	2.243 (0.072)	0.467 (0.320)	–	170.5 (154.5–186.4)	–	449.9 (8.2)	0.994
Model with 2 BKs	2.281 (0.086)	1.375 (0.428)	0.050 (0.729)	149.7 (117.8–181.7)	195.6 (162.8–228.3)	447.8 (8.6)	0.993

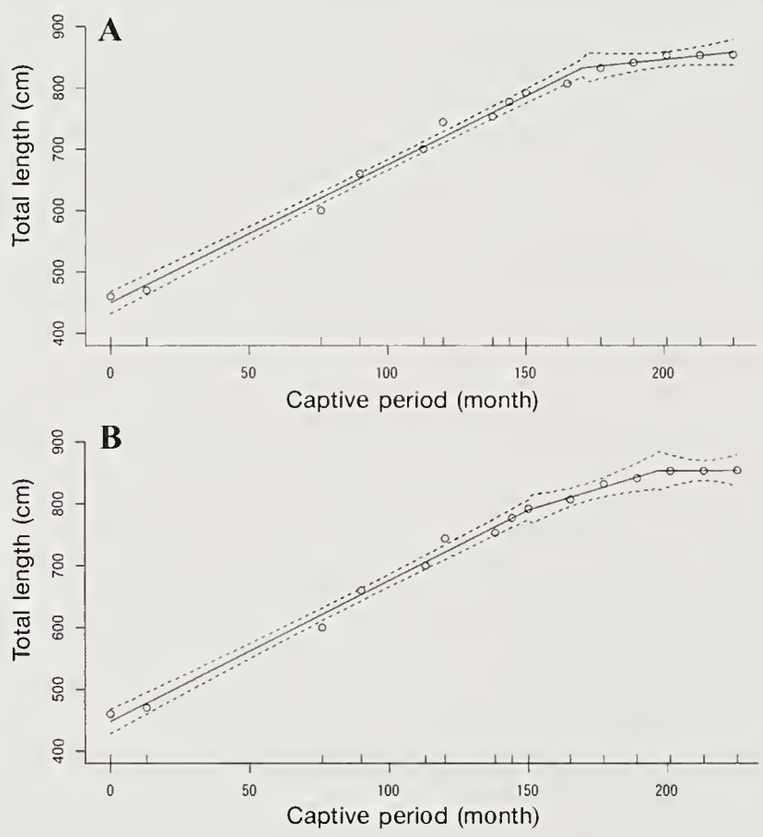

Figure 1

Change in monthly body length of a male whale shark (*Rhincodon typus*) in captivity at the Okinawa Churaumi Aquarium in Okinawa, Japan, given in centimeters in total length and represented by segmented regression models (SRMs) with (**A**) 1 and (**B**) 2 break points. The dotted lines indicate the 95% confidential intervals. The data used in the SRMs were collected from March 1995 through December 2013.

gating (claspers extending behind the posterior margin of pelvic fins), and completed (claspers no longer extending). Statistical analyses were conducted by using the nonparametric Kruskal–Wallis test followed by the nonparametric Steel–Dwass post-hoc test. The relationship between hormone levels and water temperature also was tested by using a regression analysis. Measurements are reported as means with standard errors (SEs), unless otherwise noted.

Results

Growth

According to the SRM that used 1 BK, the average growth rate for body length (slope) from March 1995 through May 2009 was 2.24 cm/month (SE 0.07) (Fig. 1A, Table). During this period, the TL increased from 460 to 832 cm. The average growth rate between May 2009 and December 2013 decreased to 0.47 cm/month (SE 0.32), with TL changing from 832 to 854 cm. Based on the estimates from the SRM that used 2 BKs (Fig. 1B), the average monthly growth from March 1995 through August 2007 was 2.28 cm (SE 0.07), with TL increasing from 460 to 789 cm (Table). From August 2007 through June 2011, the growth rate was 1.38 cm/month (SE 0.43) with TL changing from 789 to 852 cm. The growth rate from June 2011 through December 2013 was 0.05 cm/month (SE 0.73) with TL increasing from 852 to 854 cm. Both SRMs revealed that the individual grew in length rapidly until it reached approximately 800 cm TL. Considering annual growth in TL, the whale shark grew from 460 cm to >800 cm at a rate of 26.9 cm/

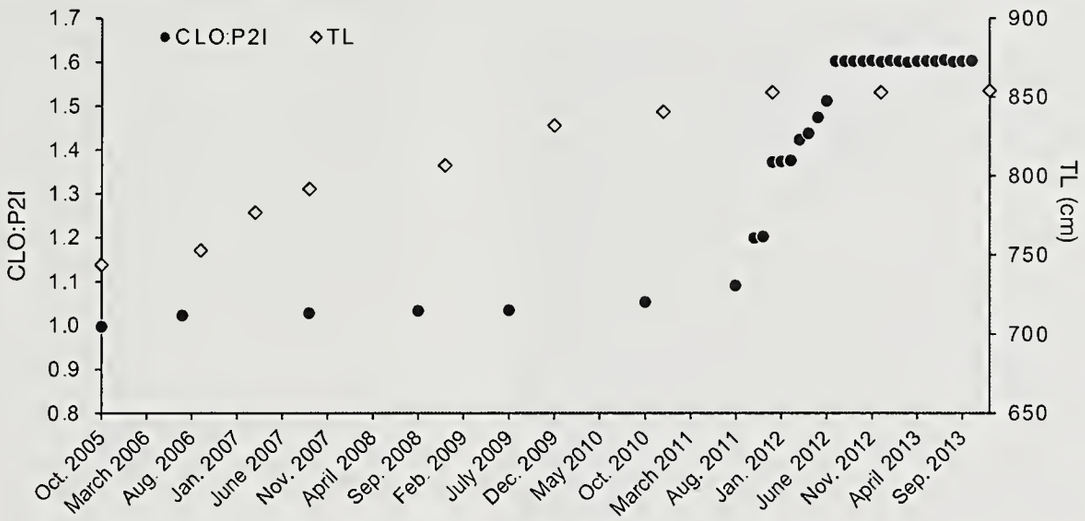

Figure 2

Relationship between the ratio of the clasper outer length to the pelvic inner length (CLO:P2I) and body length, given in centimeters in total length (TL), from October 2005 through October 2013 for a male whale shark (*Rhincodon typus*) in captivity at the Okinawa Churaumi Aquarium in Japan.

year (1-BK model) or 27.4 cm/year (2-BK model) from 1995 through 2008; after that time period, the growth rate decreased to 0.6–5.6 cm/year.

Clasper development and functionality

Clasper elongation was complete in 11 months (Fig. 2). Before August 2011, CLO:P2I was almost constant (1.00–1.09). After the claspers began to elongate posteriorly beyond the tip of the pelvic fin, CLO:P2I increased to 1.60 by July 2012; then this elongation ended, and the CLO:P2I remained constant.

The shape of the claspers changed as the claspers elongated (Fig. 3). Cauliflower-shaped tissues were formed at the distal ends of the claspers, and cartilage associated with the rhipidion (small cartilaginous elements located at the distal end of the clasper) was observed along clasper grooves.

The clasper became functional during a period of rapid elongation with skeletal development of the rhipidion. The whale shark began to display a new behavior in April 2012. The animal turned upside down, to an inverted position, while crossing both claspers simultaneously (Fig. 4, Suppl. Video) (online only). The tips of both claspers were spread along the groove

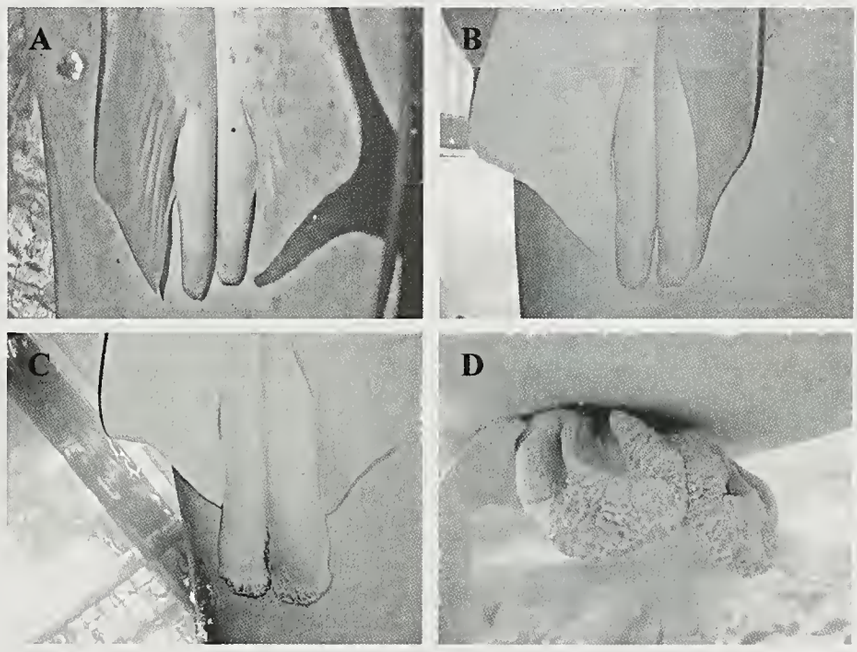

Figure 3

Images with ventral views showing morphological changes in the claspers of the male whale shark (*Rhincodon typus*) in captivity at the Okinawa Churaumi Aquarium, Japan, taken in (**A**) October 2005, (**B**) August 2011, and (**C**) July 2012, as well as (**D**) an image of a posterior view taken in February 2013 of the same whale shark.

Figure 4

Image with a ventral view of the rotational behavior of the clasper of the male whale shark (*Rhincodon typus*) in captivity at the Okinawa Churaumi Aquarium, Japan, taken in June 2012.

and inflected dorsally while they were crossed. The clasper that was placed on the top of the other varied among events, and both claspers had the top position interchangeably. In addition, starting in August 2012, a white milky fluid was released from the claspers when this behavior was displayed (Suppl. Video) (online only). However, it was not possible to confirm whether this fluid was semen because it dispersed and became diffused in the tank immediately after release.

Changes in hormonal levels

Changes in plasma concentrations of T and P4 were recorded among the 3 observable developmental periods of clasper development (Fig. 5). There were minimal changes in the concentrations of T and P4 during a short period (from May 2008 to July 2011), with mean T concentrations of 6.23 ng/mL (SE 0.52) and mean P4 concentrations of 0.50 ng/mL (SE 0.08) (Suppl. Table) (online only). However, T concentrations had large fluctuations during the elongating period (from August 2011 to July 2012), ranging between 31.95 and 8.42 ng/mL with a mean of 18.66 ng/mL (SE 3.06). In the elongating period, no change was notable in the levels of P4, with a mean of 0.79 ng/mL (SE 0.16) (Suppl. Table) (online only). In the completed period (from August 2012 to December 2013), T and P4 levels were higher, with means of 36.74 ng/mL (SE 9.46) and 1.21 ng/mL (SE 0.25), respectively, than those in the other 2 periods.

Among the 3 periods of clasper development, there was significant variation in levels of T (Kruskal–Wallis test: 29.40, $P<0.01$) and P4 (Kruskal–Wallis test: 7.30, $P=0.03$) (Fig. 6). Notably, T concentrations were significantly lower in the short period than in the elongating and completed periods (Steel–Dwass test: $P<0.01$ for both periods). However, there were no significant differences in T levels between the elongating and completed periods (Steel–Dwass test: $P=0.95$). Concentrations of P4 were also lower in the short period than in the completed period (Steel–Dwass test: $P=0.03$), although there were no significant differences in P4 levels between the short and elongating periods ($P=0.23$) or between the elongating and completed periods ($P=0.82$).

There were significant relationships between water temperature and concentrations of T (coefficient of determination [r^2]=0.42, $P<0.01$) and P4 ($r^2=0.26$, $P<0.01$) during the short period; whereas, these relationships were not significant during the elongating (T: $r^2=0.06$, $P=0.59$; P4: $r^2=0.14$, $P=0.40$) and completed (T: $r^2=0.14$, $P=0.17$; P4: $r^2=0.01$, $P=0.78$) periods (Fig. 7).

Discussion

Abrupt clasper elongation and increased levels of sex hormones observed in the male whale shark strongly indicate that the individual is sexually mature. Increases in hormone levels (T or P4) associated with male sexual maturation have been reported in various elasmobranchs (Rasmussen and Gruber, 1993), although the mode of action of these hormones remains unclear. Previous studies have hypothesized several functions of sex hormones (such as T), including the initiation of mating behavior (Rasmussen and Murru, 1992; Rasmussen and Gruber, 1993), spermiogenesis and spermiation (Tricas et al., 2000; Henningsen et al., 2008), and clasper elongation (Heupel et al., 1999; Sulikowski et al., 2005; Sulikowski et al., 2006; Awruch et al., 2008). Hormone levels were slightly correlated with changes in water temperature when the shark was immature; however, these correlations were not observed during and after the clasper elongation period, and hormone levels were also significantly greater after the shark started to mature sexually. Such patterns have not been previously reported in other elasmobranch species. Further studies are needed to clarify the relationships between hormone levels and water temperature during each growth stage.

Our data allow comparisons between wild and captive whale sharks. The individual studied here was considered mature at 8.5 m TL. This finding is consistent with the maturation size estimated for wild male whale sharks off the northwestern coast of Australia on the Ningaloo Reef, where 50% of 275 wild male whale sharks had attained maturity at 8.1 m TL and 95% of those sharks had done so by 9.1 m TL (Norman and Stevens, 2007). We were not able to determine the precise age of maturation in our shark because the shark's age was unknown when he was brought into the aquarium.

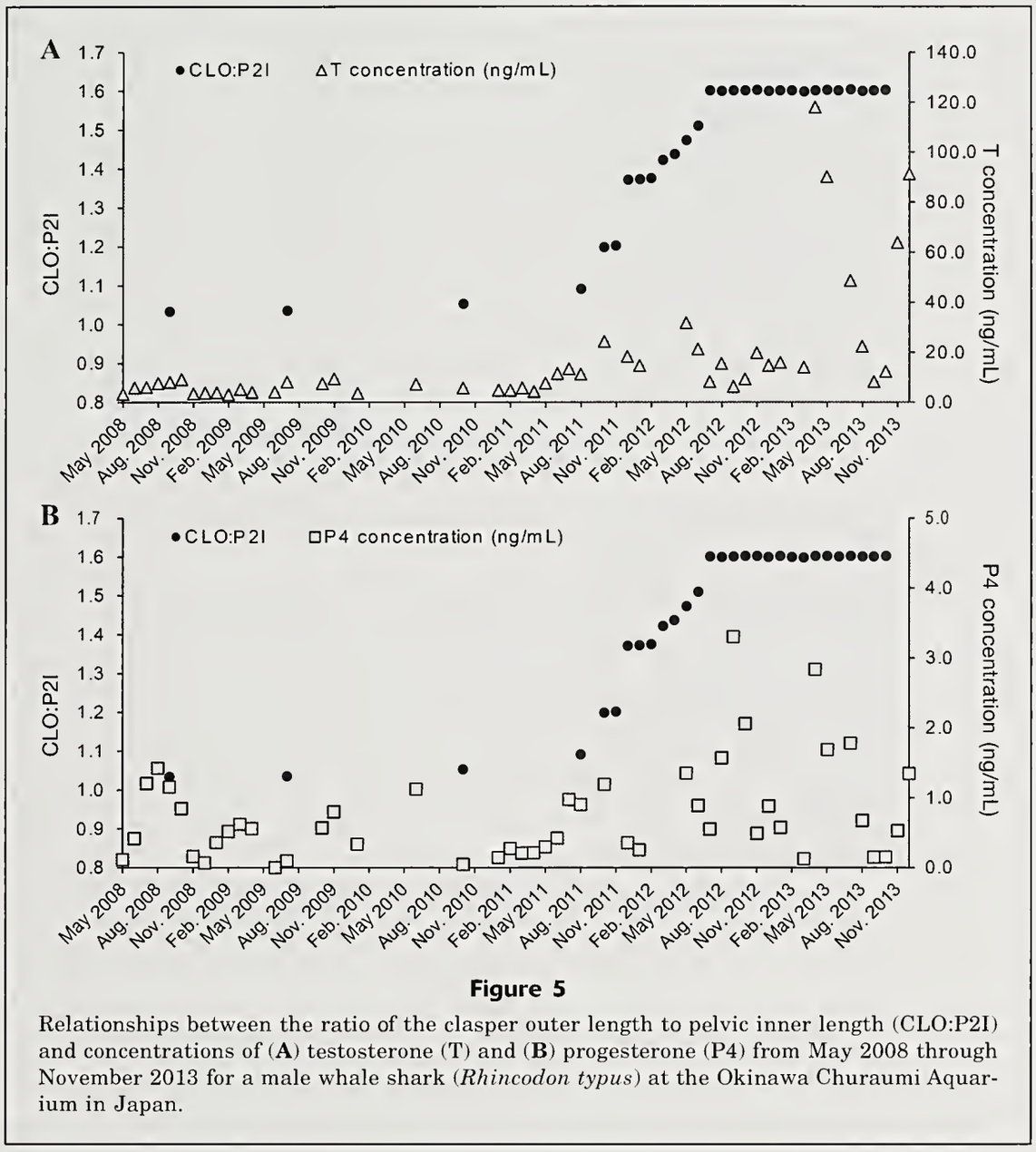

Figure 5

Relationships between the ratio of the clasper outer length to pelvic inner length (CLO:P2I) and concentrations of (**A**) testosterone (T) and (**B**) progesterone (P4) from May 2008 through November 2013 for a male whale shark (*Rhincodon typus*) at the Okinawa Churaumi Aquarium in Japan.

The age of live elasmobranchs can be estimated only by using growth models. Two studies have reported growth curves for the whale shark. Wintner (2000) estimated the ages of 15 dead whale sharks by counting the number of growth bands in vertebrae, assuming that a single pair of growth bands corresponds to 1 year, and generated a growth curve of this species. By using that growth curve, the age of our shark at capture (at a size of 460 cm TL) was estimated to be 10 or 14 years old. More recently, Hsu et al. (2014) provided new growth curves using a greater sample size (n=92) of species collected from the population in the northwestern Pacific Ocean. They estimated 2 growth curves on the basis of growth bands being deposited either once or twice a year, and they concluded that the band pairs were formed twice a year. The growth curve provided by Hsu et al. (2014) is likely applicable to estimate the age of our shark at capture because the shark was taken from the same region.

Based on the growth curve of Hsu et al. (2014), the age of our shark at the time of capture was estimated to be 7.6 years. Consequently, the estimated age at the time that clasper elongation ceased was 24.9 years. This result indicates that sexual maturation of our shark occurred later than the age at maturity estimated for wild individuals in the Indo-Pacific region (17 years old; Hsu et al., 2014). Meanwhile, Perry et al. (2018) estimated that males in the Maldives mature at 25 years, following the methods described by Hsu et al. (2014). This estimation is comparable to our result. The timing of sexual maturity of the whale shark may be associated more closely with size than with chronological age, a notion that is consistent with previous findings (Gelsleichter et al., 2002); however, further investigations are needed.

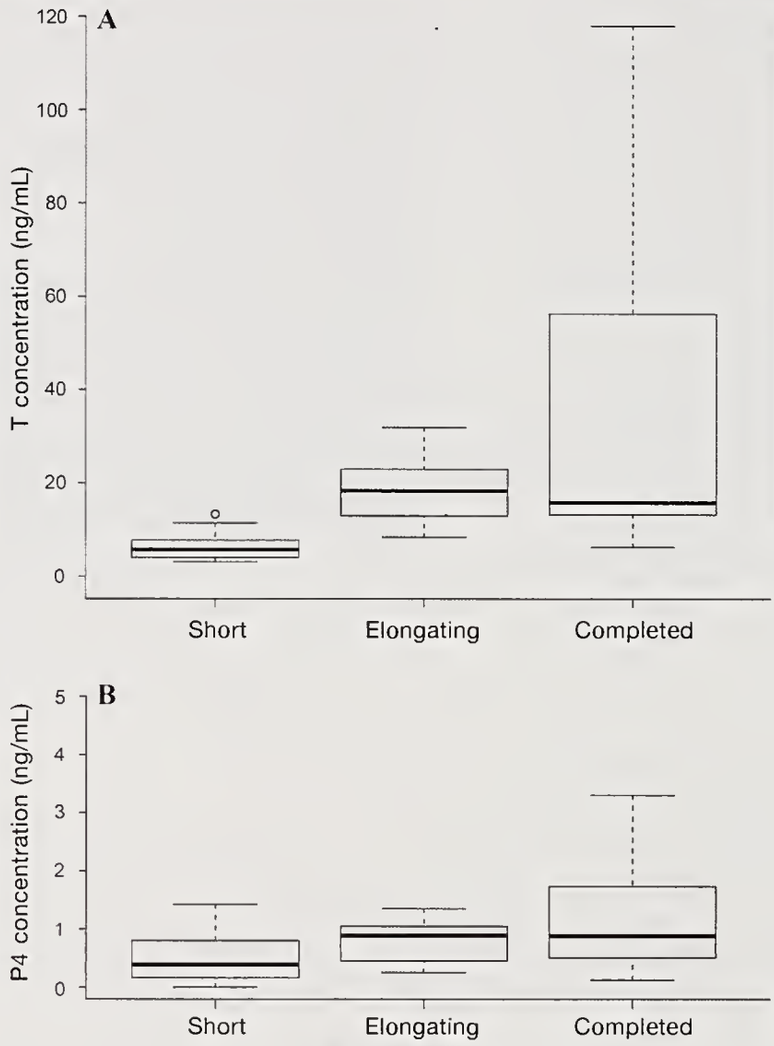

Figure 6

Comparisons of concentrations of the hormones (**A**) testosterone (T) and (**B**) progesterone (P4) from May 2008 to December 2013 in a male whale shark (*Rhincodon typus*) at the Okinawa Churaumi Aquarium, Japan, during the 3 developmental periods of the clasper: short, elongating, and completed. The box indicates the 25th and 75th percentiles, the whiskers indicate the minimum and maximum values, and the line within each box indicates the median value. A circle indicates an outlier.

The results of this study indicate that morphological and functional changes in the claspers during maturation occurred over a relatively short time, less than 1 year, in our shark. The animal began to display new clasper movements during the period of rapid clasper growth, behavior that has hitherto not been reported. These movements have been observed during the mating season in other elasmobranchs, including the tawny nurse shark (*Nebrius ferrugineus*), zebra shark (*Stegostoma fasciatum*), bull shark (*Carcharhinus leucas*), sandbar shark (*C. plumbeus*), and dasyatid rays (senior author, unpubl. data), and they sometimes occur in the absence of females (Ritter and Compagno, 2013). Moreover, a white milky fluid, which we suspect to be semen, was released from the tip of the claspers as the claspers crossed. Based on these observations, it is likely that the functional maturation of the claspers occurs in parallel with morphological changes.

In summary, observations of a captive male whale shark made over a period of 20 years have improved our understanding of the process of sexual maturation in this species. Maturation was associated with increased plasma concentrations of T and P4 and the rapid morphogenesis and functioning of claspers. Additional studies involving both captive and wild individu-

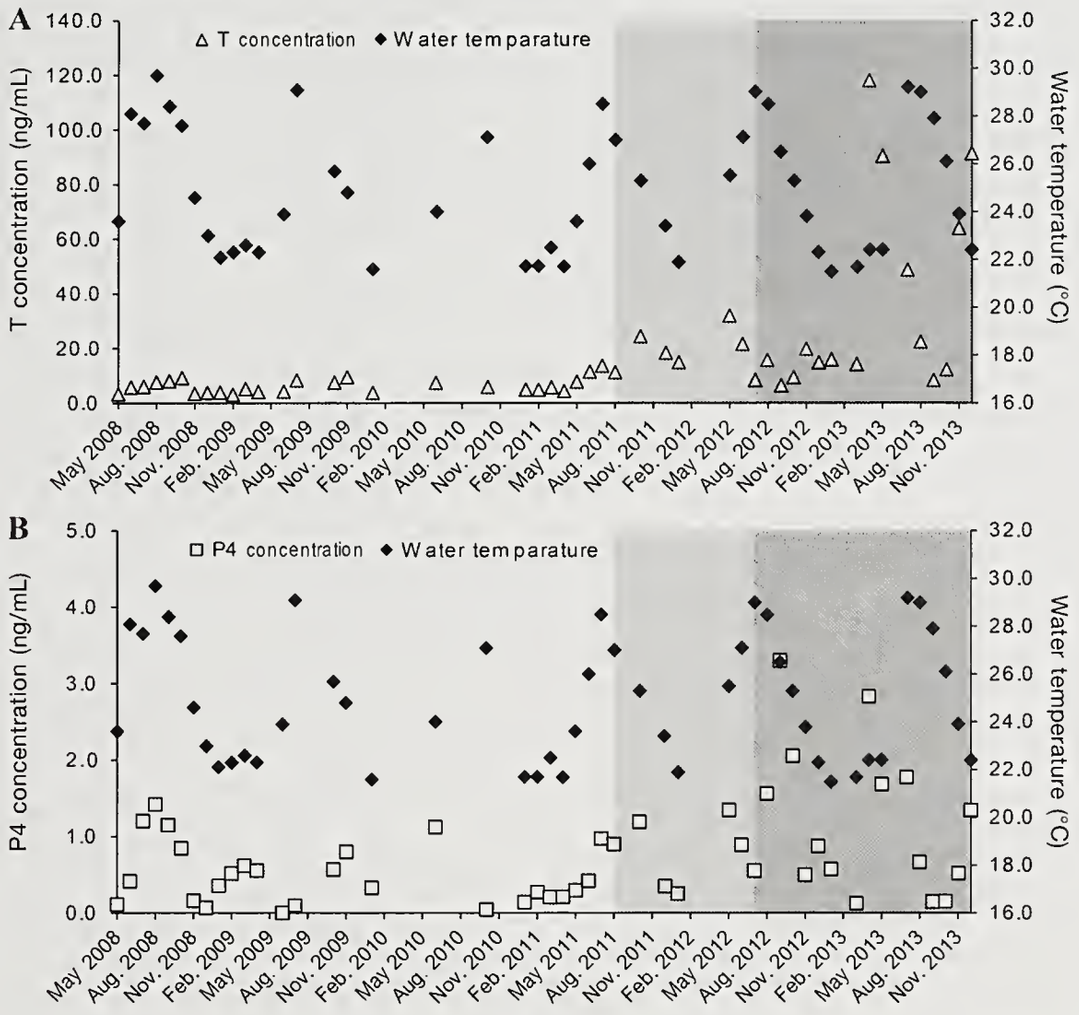

Figure 7

Relationship between water temperature and concentrations of (**A**) testosterone (T) and (**B**) progesterone (P4) from May 2008 through December 2013 in a male whale shark (*Rhincodon typus*) at the Okinawa Churaumi Aquarium in Japan. The period covers the 3 developmental periods of the clasper: short (T: r^2=0.42, P<0.01; P4: r^2=0.26, P<0.01), elongating (T: r^2=0.06, P=0.59; P4: r^2=0.14, P=0.40), and completed (T: r^2=0.14, P=0.17; P4: r^2=0.01, P=0.78). The background colors of white, light gray, and dark gray indicate the short, elongating, and completed periods, respectively.

als are needed to further advance the biology of the well-known but mysterious whale shark.

Acknowledgments

We express our gratitude to the Yomitan Fisheries Cooperative for collecting the whale shark used for these observations. We acknowledge H. Miyahara for providing us the opportunity to perform this research. We thank both A. Uno and K. Aoki from the Nihon University, for assistance with laboratory analyses, and R. Nozu, T. Tomita, and Y. Obayashi for their comments on this manuscript. We recognize S. Uchida, M. Toda, M. Nakazato, A. Yamashiro, K. Murakumo, and other colleagues for their valuable information and advice.

Literature cited

Awruch, C. A., N. W. Pankhurst, S. D. Frusher, and J. D. Stevens.
2008. Endocrine and morphological correlates of reproduction in the draughtboard shark *Cephaloscyllium laticeps* (Elasmobranchii: Scyliorhinidae). J. Exp. Zool. 309A:184–197.

Compagno, L. J. V.
1984. FAO species catalogue. Vol. 4. Sharks of the world: an annotated and illustrated catalogue of shark species known to date. Part 1—Hexanchiformes to Lamniformes. FAO Fish. Synop. 125, 249 p. FAO, Rome.

Gelsleichter, J., and A. N. Evans.
2012. Hormonal regulation of elasmobranch physiology. *In* Biology of sharks and their relatives, 2nd ed. (J.

C. Carrier, J. A. Musick, and M. R. Heithaus, eds.), p. 313–348. CRC Press, Boca Raton, FL.

Gelsleichter, J., L. E. L. Rasmussen, C. A. Manire, J. Tyminski, B. Chang, and L. Lombardi-Carlson.
2002. Serum steroid concentrations and development of reproductive organs during puberty in male bonnethead sharks, *Sphyrna tiburo*. Fish Physiol. Biochem. 26:389–401.

Henningsen, A. D., F. L. Murru, L. E. L. Rasmussen, B. R. Whitaker, and G. C. Violetta.
2008. Serum levels of reproductive steroid hormones in captive sand tiger sharks, *Carcharias taurus* (Rafinesque), and comments on their relation to sexual conflicts. Fish Physiol. Biochem. 34:437–446.

Heupel, M. R., J. M. Whittier, and M. B. Bennett.
1999. Plasma steroid hormone profiles and reproductive biology of the epaulette shark, *Hemiscyllium ocellatum*. J. Exp. Zool. 284:586–594.

Hsu, H. H., S. J. Joung, R. E. Hueter, and K. M. Liu.
2014. Age and growth of the whale shark (*Rhincodon typus*) in the north-western Pacific. Mar. Freshw. Res. 65:1145–1154.

Jensen, C. F., L. J. Natanson, H. L. Pratt Jr., N. E. Kohler, and S. E. Campana.
2002. The reproductive biology of the porbeagle shark (*Lamna nasus*) in the western North Atlantic Ocean. Fish. Bull. 100:727–738.

Martin, R. A.
2007. A review of behavioural ecology of whale sharks (*Rhincodon typus*). Fish. Res. 84:10–16.

Matsumoto, R., M. Toda, Y. Matsumoto, K. Ueda, M. Nakazato, K. Sato, and S. Uchida.
2017. Notes on husbandry of whale sharks, *Rhincodon typus*. *In* Elasmobranch husbandry manual II: recent advances in the care of sharks, rays and their relatives (M. Smith, D. Warmolts, D. Thoney, R. Hueter, M. Murray, and J. Ezcurra, eds.), p. 15–22. Ohio Biol. Surv., Columbus, OH.

Muggeo, V. M. R.
2003. Estimating regression models with unknown breakpoints. Stat. Med. 22:3055–3071.

Norman, B. M., and J. D. Stevens.
2007. Size and maturity status of the whale shark (*Rhincodon typus*) at Ningaloo Reef in Western Australia. Fish. Res. 84:81–86.

Perry, C. T., J. Figueiredo, J. J. Vaudo, J. Hancock, R. Rees, and M. Shivji.
2018. Comparing length-measurement methods and estimating growth parameters of free-swimming whale sharks (*Rhincodon typus*) near the South Ari Atoll, Maldives. Mar. Freshw. Res. 69:1487–1495.

Rasmussen, L. E. L., and F. L. Murru.
1992. Long-term studies of serum concentrations of reproductively related steroid hormones in individual captive carcharhinids. Aust. J. Mar. Freshw. Res. 43:273–281.

Rasmussen, L. E. L., and S. H. Gruber.
1993. Serum concentrations of reproductively-related circulating steroid hormones in the free-ranging lemon shark, *Negaprion brevirostris*. Environ. Biol. Fish. 38:167–174.

Ritter, E. K., and L. J. V. Compagno.
2013. Clasper flaring: maintenance behavior, or a normally hidden feature of male whitetip reef sharks, *Triaenodon obesus*? Open. Fish Sci. J. 6:10–12.

Saïdi, B., M. N. Bradaï, and A. Bouaïn.
2009. Reproductive biology and diet of *Mustelus punctulatus* (Risso, 1826) (Chondrichthyes: Triakidae) from the Gulf of Gabès, central Mediterranean Sea. Sci. Mar. 73:249–258.

Schneider, C. A., W. S. Rasband, and K. W. Eliceiri.
2012. NIH Image to ImageJ: 25 years of image analysis. Nat. Methods 9:671–675.

Segura, A. M., A. C. Milessi, R. Vögler, F. Galván–Magaña, and V. Muggeo.
2013. The determination of maturity stages in male elasmobranchs (Chondrichthyes) using a segmented regression of clasper length on total length. Can. J. Fish. Aquat. Sci. 70:830–833.

Sulikowski, J. A., P. C. W. Tsang, and W. H. Howell.
2005. Age and size at sexual maturity for the winter skate, *Leucoraja ocellata*, in the western Gulf of Maine based on morphological, histological and steroid hormone analyses. Environ. Biol. Fish. 72:429–441.

Sulikowski, J. A., J. Kneebone, S. Elzey, J. Jurek, W. H. Howell, and P. C. W. Tsang.
2006. Using the composite variables of reproductive morphology, histology and steroid hormones to determine age and size at sexual maturity for the thorny skate *Amblyraja radiata* in the western Gulf of Maine. J. Fish Biol. 69:1449–1465.

Suzuki, M., T. Tobayama, E. Katsumata, M. Yoshioka, and K. Aida.
1998. Serum cortisol levels in captive killer whale and bottlenose dolphin. Fish. Sci. 64:643–647.

Tricas, T. C., K. P. Maruska, and L. E. L. Rasmussen.
2000. Annual cycles of steroid hormone production, gonad development, and reproductive behavior in the Atlantic stingray. Gen. Comp. Endocrinol. 118:209–225.

Uchida, S., M. Toda, Y. Kamei, and H. Teruya.
2000. The husbandry of 16 whale sharks *Rhincodon typus*, from 1980 to 1998 at the Okinawa Expo Aquarium. *In* Abstracts of the American Elasmobranch Society 16th Annual Meeting; La Paz, Mexico, 14–20 June. [Available from website.]

Ueda, K., M. Yanagisawa, K. Murakumo, Y. Matsumoto, K. Sato, and S. Uchida.
2017. Physical examination, blood sampling, and sedation of large elasmobranchs. *In* Elasmobranch husbandry manual II: recent advances in the care of sharks, rays and their relatives (M. Smith, D. Warmolts, D. Thoney, R. Hueter, M. Murray, and J. Ezcurra, eds.), p. 255–262. Ohio Biol. Surv., Columbus, Ohio.

Wintner, S. P.
2000. Preliminary study of vertebral growth rings in the whale shark, *Rhincodon typus*, from the east coast of South Africa. Environ. Biol. Fish. 59:441–451.

National Marine Fisheries Service
NOAA

Fishery Bulletin
established in 1881

Spencer F. Baird
First U.S. Commissioner of Fisheries and founder of *Fishery Bulletin*

Comparison of video and diver observations of sharks from a fishery-independent trap-video survey off east-central Florida, including utility of an alternative method of video analysis

Roldan C. Muñoz (contact author)
Michael L. Burton

Email address for contact author: roldan.munoz@noaa.gov

Beaufort Laboratory
Southeast Fisheries Science Center
National Marine Fisheries Service, NOAA
101 Pivers Island Road
Beaufort, North Carolina 28516

Abstract—We assessed the utility of an alternative method of video analysis for generating data for sharks and compared observations of sharks from the use of baited remote underwater video stations (BRUVS) with observations made by scuba divers during surveys conducted simultaneously with BRUVS video recordings. Videos were made off east-central Florida as part of a fishery-independent trap-video survey of fish species in hard-bottom reef habitats. In videos from 25 of 72 sites, we observed sharks, including the nurse (*Ginglymostoma cirratum*), tiger (*Galeocerdo cuvier*), spinner (*Carcharhinus brevipinna*), sandbar (*C. plumbeus*), Atlantic sharpnose (*Rhizoprionodon terraenovae*), bull (*C. leucas*), and lemon (*Negaprion brevirostris*) sharks. In contrast, divers observed 3 species of sharks at 5 sites. We conclude that video observations are superior to diver observations for detecting sharks. Rapidly viewing an entire video (the alternative method), rather than viewing only a 20-min segment (the standard protocol), has the potential to increase the number of sites where sharks are observed and the number of shark species that are observed in video analysis (as it did, by 400% and 40%, respectively, in this study). This method holds promise for providing critical information without extraction of specimens and for aiding stock assessments and essential fish habitat delineation for these important predators.

Manuscript submitted 24 August 2018.
Manuscript accepted 12 April 2019.
Fish. Bull. 117:87–96 (2019).
Online publication date: 26 April 2019.
doi: 10.7755/FB.117.1-2.10

The views and opinions expressed or implied in this article are those of the author (or authors) and do not necessarily reflect the position of the National Marine Fisheries Service, NOAA.

Predation is recognized as a key ecological and evolutionary process, and sharks, a group that includes species capable of being the top predators in oceans, are important members of marine communities (Estes et al., 2011; Osgood and Baum, 2015; Barley et al., 2017). Sharks are capable of exerting top-down effects on prey from lower trophic levels over wide spatial and temporal scales (Osgood and Baum, 2015; Barley et al., 2017; Dulvy et al., 2017), and shark species are valuable targets of recreational and commercial fisheries. To help protect species that have relatively low reproductive rates, late maturity, and slow growth, the United States has implemented shark management measures that are some of the strongest worldwide (NMFS[1]). Despite conservation efforts, global bycatch of sharks and demand for shark fins and meat have resulted in ~25% of shark species listed as endangered, vulnerable, or near threatened by the International Union for Conservation of Nature (IUCN) in the IUCN Red List of Threatened Species (Heithaus et al., 2010; Dulvy et al., 2014; White et al., 2015; Ward-Paige, 2017), although recent analyses indicate preliminary recovery of certain stocks of sharks in U.S. waters of the Atlantic Ocean (Peterson et al., 2017). We lack even basic biological information for many sharks and their relatives, such that 46% of species on the IUCN Red List are classified as data deficient (Heithaus et al., 2010; Dulvy et al., 2014; White et al., 2015; Peterson et al., 2017).

Whereas fishery-independent surveys can provide valuable measures of relative abundance to inform stock assessments, one of the hindrances to accurate assessment of shark populations is the lack of fishery-independent surveys that are done on a stock-wide basis. The NOAA Northeast Fisheries Science Center conducts a biannual longline survey from the Gulf of Mexico to southern New England, and the NOAA Southeast Fisheries Science Center conducts an annual longline survey off the southeastern United States in the Atlantic Ocean and Gulf of Mexico. Although other fishery-in-

[1] NMFS (National Marine Fisheries Service). 2017. 2016 shark finning report to Congress, 117 p. [Available from website].

dependent surveys for sharks exist, most of them are spatially limited (Peterson et al., 2017).

The Southeast Reef Fish Survey (SERFS) is a fishery-independent monitoring and research program that targets reef fish species in continental shelf waters off the southeastern United States and is funded by the National Marine Fisheries Service. Annual sampling of this collaborative program, for which the Beaufort Laboratory of the Southeast Fisheries Science Center is a contributor, is done by using video cameras attached to chevron traps to survey a region from St. Lucie Inlet, Florida, to Cape Hatteras, North Carolina (Bacheler et al., 2014). This fishery-independent trap-video survey generates ~1500 video recordings, or samples, per year and targets species from hard substrates (limestone or hard-bottom reefs) on the continental shelf and continental shelf break of the southeastern United States. Because of time and personnel constraints, SERFS staff primarily evaluate videos for assessment of spatial distribution of reef fish species in the snapper-grouper complex and use a video-sampling method that involves viewing a subset of frames (number of frames [n]=41) from each video sample to calculate relative abundance (Bacheler et al., 2014; Schobernd et al., 2014). This video-sampling method may not be effective for species, such as sharks, that tend to be relatively rare or highly mobile (Schobernd et al., 2014; Bacheler and Shertzer, 2015).

Video is increasingly used as a fish survey and research tool in marine ecosystem research (see the review by Murphy and Jenkins, 2010), including for the study of elasmobranchs (Meekan and Cappo, 2004; Bond et al., 2012; White et al., 2013; Barley et al., 2017). The advantages of the use of remotely viewable underwater video (often recorded by cameras on baited stations) over traditional, direct underwater visual census (UVC) by scuba divers include the potential for longer survey times, removal of diver effects (attraction or avoidance) on target species (Kulbicki, 1998), and greater depth range and spatial replication. Particularly for relatively rare, large, and mobile species, such as elasmobranchs, UVC may produce biased estimates of population density (MacNeil et al., 2008; Ward-Paige et al., 2010; McCauley et al., 2012; Osgood and Baum, 2015).

The work described in this paper was conducted as part of a study (Bacheler et al., 2017) that compared observations of reef fish abundance from 3 techniques: diver census, video analysis, and sampling with traps (sampling of videos and traps was conducted with SERFS methods). The objective of the work reported here was to assess the utility of an alternative, rapid method of video analysis for generating data specifically for sharks. For this assessment, we used video recordings collected from sampling locations used by Bacheler et al. (2017). We determined species composition and relative abundance of sharks encountered in the Atlantic Ocean off east-central Florida by using UVC conducted by divers and analysis of videos from baited remote underwater video stations (BRUVS), and we compared our results with those of Bacheler et al. (2017). Given that diver and video methods are known to sample different members of fish communities (Colton and Swearer, 2010; Langlois et al., 2010; Watson et al., 2010; Barley et al., 2017), we also specifically compared the composition and relative abundance of shark species observed with these sampling approaches. The SERFS was designed to sample relatively sedentary reef fish species at a regional scale with a large number of sites across the continental shelf of the southeastern United States. We hypothesized that this work would reveal that the use of video can be a non-consumptive alternative or supplement to traditional sampling methods that require extraction (e.g., with longlines and gillnets) for providing estimates of relative abundance for a variety of sharks in the Atlantic Ocean.

Materials and methods

Study area

We conducted our study at a number of hard-bottom reef sites in temperate waters on the U.S. continental shelf off east-central Florida (Fig. 1). The continental shelf along the southeastern United States consists primarily of sand and mud substrates, but patches of hard, rocky reefs in temperate waters are scattered throughout the region and are important habitat for many reef fish species. Specific hard-bottom sites were chosen from sampling locations in the study area of the SERFS (Bacheler et al., 2014) by using 2 criteria: depths safe for diving (<32 m) and a history of traps catching reef fish. Hard-bottom habitats sampled in our work ranged from rocky ledges to patchily distributed rock outcrops and pavement, sometimes covered in a veneer of sand. All sampling occurred at depths between 18 and 30 m on 2–7 July 2014 aboard the M/V *Spree*, a 30.2-m aluminum-hulled vessel converted from use for oil field services to a live-aboard dive platform that was fitted with a pot hauler for this effort.

Chevron traps

We deployed a single chevron trap at each site sampled in this study. Chevron traps were shaped like an arrowhead and measured 1.7 m × 1.5 m × 0.6 m, with a volume of ~0.91 m^3 (Bacheler et al., 2014). The mouth of each trap, shaped like an upside-down teardrop, measured ~45 cm high and 18 cm wide, and the mesh size of each trap was 3.4 cm^2. We baited each trap with ~4 kg of menhaden (*Brevoortia* spp.). A soak time of 90 min was targeted for each trap, but actual soak time varied from 51 to 99 min, with a mean of 80.2 min (standard deviation [SD] 11.2). Each trap had a single 8-mm polypropylene line connecting it to 2 surface floats. Chevron traps were deployed with an average distance of 813 m separating them to provide some measure of independence between traps. The minimum

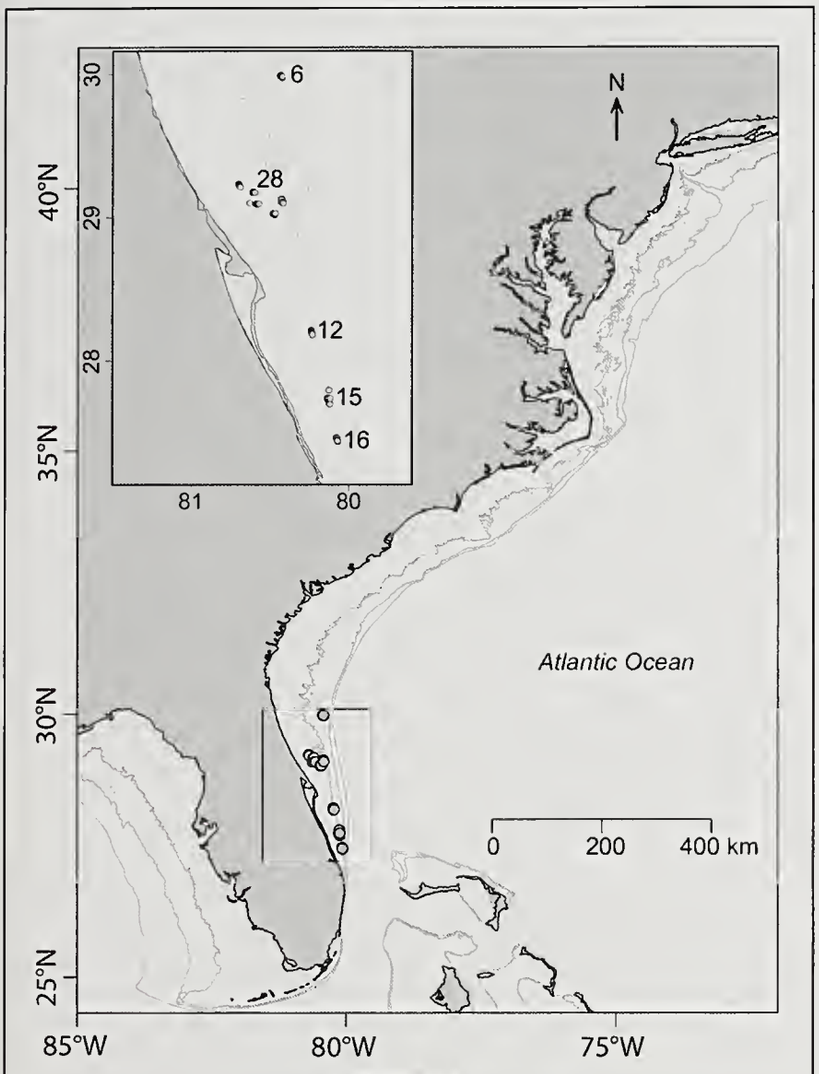

Figure 1

Map of the study area showing the locations of 77 sites off east-central Florida where baited remote underwater video stations were deployed and scuba divers conducted underwater visual census to survey shark species in July 2014. The inset map provides the number of sites in each cluster. Note that symbols indicating sampling locations often overlap in both maps. Gray lines in both maps indicate the 30-, 50-, and 100-m isobaths.

distance between 2 traps was 237 m, but these 2 sites were sampled more than 3 h apart.

Underwater video

We outfitted each chevron trap with 2 outward-looking video cameras, forming a 2-camera BRUVS. A high-definition Vixia HF S200[2] video camera (Canon U.S.A., Inc., Melville, NY) with a standard lens in an HF-S21 underwater housing (Gates Underwater Products, Inc., Poway, CA) was attached over the mouth of each trap, facing away from the trap. A second high-definition video camera (HD HERO4 Black, GoPro, Inc., San Mateo, CA) was attached over the nose of each trap (opposite the Canon camera), also looking outward. The Canon camera was used to record video for quantifying the number of fish at each site (i.e., for video analysis, a single, unique Canon video recording was reviewed for each site). The GoPro camera, which provided additional and sometimes better views of activity at a site if a fish passed closer to it, was used only when necessary to confirm identification of fish species.

Video recordings were ~90 min in length. The SERFS video-analysis protocol commences 10 min after a trap reaches the seafloor, with fish counted every 30 s during a 20-min period (or segment) for a total of 41 frames, each 1 s in duration. For this study, we reviewed videos in their entirety (rather than a subset of forty-one 1-s frames) at a speed that was approximately 2 times faster than the viewing speed used in the standard protocol, using a jog wheel (as part of our video editing hardware setup) for precise control of video speed. The jog wheel allowed us to rapidly review videos without exceeding a maximum rate that would have resulted in skipped video frames and potentially in missed fish detections. All sharks observed were identified (enabling collection of presence-absence data for each species and video recording) and counted, and, when possible, their sex was determined to be male if claspers were observed (sex data not shown). We compared the trap catch between sites with and without video observations of sharks by using a Mann–Whitney U test. We calculated frequency of occurrence for each species as the number of sites with observations of a given shark species divided by the total number of sampled sites.

We compared, using a chi-square test, the proportion of sites with sharks observed during the SERFS 20-min segment with the proportion of sites with sharks observed outside the 20-min segment (i.e., before, or the first 10 min after the trap reaches the seafloor, and after, or the part of the video from 30 min after the trap reaches the bottom to the end). Videos with observations of sharks were classified as either outside or within the 20-min segment. Videos classified as outside the 20-min segment had shark observations solely outside the segment. Videos classified as within the 20-min segment could include observations outside the segment in addition to observations within the segment, but the 2 classifications were mutually exclusive.

Underwater visual census

Within 10 min of the deployment of each BRUVS, 2 divers descended along the trap line until they could

[2] Mention of trade names or commercial companies is for identification purposes only and does not imply endorsement by the National Marine Fisheries Service, NOAA.

see the trap. Staying at least 15 m from the trap, divers counted fish and measured habitat features along 3 transects that were each 30 m long and 10 m wide (i.e., they surveyed 300 m^2 for each transect and 900 m^2 at each site). The chosen direction of the first transect was typically toward the part of a site that had the most hard-bottom substrate, beginning ~15 m from the trap, so that the trap and video sampling were disturbed as little as possible. The second transect was surveyed in the direction opposite of the first transect, and the third transect was perpendicular to the first 2 transects and often contained the least amount of hard-bottom habitat. The depths of habitats sampled by UVC were similar (with differences <2 m) in all cases to the depths at which traps were deployed and, therefore, the depths at which video recordings were made. Further details about the method and full results of UVC can be found in Bacheler et al. (2017).

For the work described in this manuscript, the primary interest in UVC data was whether divers encountered a shark at a particular site and, if they did, the recorded species identification for the sharks observed. We compared the identification of sharks by divers with that from video analysis at those sites where observations were positive for both survey methods. We used a chi-square test to compare the proportion of sites at which sharks were seen by divers with the proportion of sites for which sharks were seen in video analysis. All statistical analyses were conducted with SigmaPlot, vers. 11.0 (Systat Software, Inc., San Jose, CA).

Results

Species of sharks observed in videos

We reviewed 100.5 h of video and observed sharks in videos from 30 of 77 sites. In 5 cases, pairs of sites were located <500 m apart, and review of videos from these sites revealed that the same species of sharks were observed at both sites in each pair. Therefore, video recordings from one of the pair of sites (a total of 5 videos) were dropped from further analyses. As a result, 25 of 72 sites with shark observations, or 35% of videos, were used for analyses. The average length of video recordings was 78.5 min (SD 6.00). For most sites, a single species of shark was observed, as a solitary individual in video frames. However, for 2 sites, 2 nurse sharks (*Ginglymostoma cirratum*) were seen at the same time in a single video frame, and 2 Atlantic sharpnose sharks (*Rhizoprionodon terraenovae*) were seen in a single video frame from another site. In each of 18 videos, 1 species of shark was observed; 6 videos contained 2 species, and 1 video contained 4 species. In all of these analyzed videos, a minimum of 36 individual sharks were observed. At the 25 sites for which sharks were observed in videos, their associated chevron traps contained significantly more fish, with a mean of 71.9 individuals (SD 56.5), than those traps associated with the videos in which sharks were absent, with a mean of 48.4 individuals (SD 49.9) (n=47 sites; Mann–Whitney U test: U=397, P=0.03). No sharks were captured in traps, and the full results for trap catches can be found in Bacheler et al. (2017).

Seven species of sharks, including the nurse, tiger (*Galeocerdo cuvier*), spinner (*Carcharhinus brevipinna*), sandbar (*C. plumbeus*), Atlantic sharpnose, bull (*C. leucas*), and lemon (*Negaprion brevirostris*) sharks, were observed in videos (Fig. 2). Because of water turbidity and proximity of sharks to the camera, we were unable to identify to species carcharhinid sharks observed in videos from 2 sites. In most cases, the sharks that we observed were readily identifiable to species. However, one limitation of any method of analyzing video to sample fish is that taxa are not retained for positive identification.

Frequency of occurrence (Fig. 3) was greatest for the nurse shark, which was observed in videos from ~14% of sites (10 of 72 sites), followed by the tiger (8%, 6 sites), spinner (7%, 5 sites), sandbar (5%, 4 sites), and Atlantic sharpnose (4%, 3 sites) sharks. The bull shark, lemon shark, and sharks identified only to the family Carcharhinidae were observed in videos from 3% of sites (2 of 72 sites).

Comparison of methods

When the entire video was analyzed, sharks were observed at 4 times more sites than when only the SERFS 20-min segment was analyzed (28% versus 7% of the total number of sites, respectively; chi-square test: χ^2=9.5, df=1, P=0.002). Sharks frequently were observed in videos classified as outside of the 20-min segment. Of the 25 videos with sharks, 20 videos contained sharks exclusively outside of the 20-min segment, and 5 videos had sharks within the 20-min segment. Of these 5 videos, 3 videos included sharks that also were observed later in the video outside the 20-min segment. Of the 20 videos with sharks observed solely outside the 20-min segment, 2 videos had sharks before the 20-min segment (10%), and 18 videos contained sharks after the segment (90%).

Results from analyses of entire videos for sharks were superior to those based on UVC of transects by divers. A greater diversity of sharks were observed and sharks were recorded at a larger number of sites when the alternate video-analysis method was used than when divers used UVC. At 5 sites, sharks were detected both by using the SERFS 20-min video segment and by using UVC, although the individual sites where sharks were detected were mostly (except for 1 site) distinct between methods. By using UVC, 3 species of sharks were recorded at 5 sites (7% of sites, Table 1), and the use of video analysis resulted in observations of 7 species in videos from 25 sites (35% of sites; chi-square test: χ^2=15.2, df=1, P<0.001). Although a greater diversity of sharks overall was observed by using video analysis than by using UVC, site-specific comparisons of UVC and video data revealed differences in the presence and absence of sharks, as well as in the species of

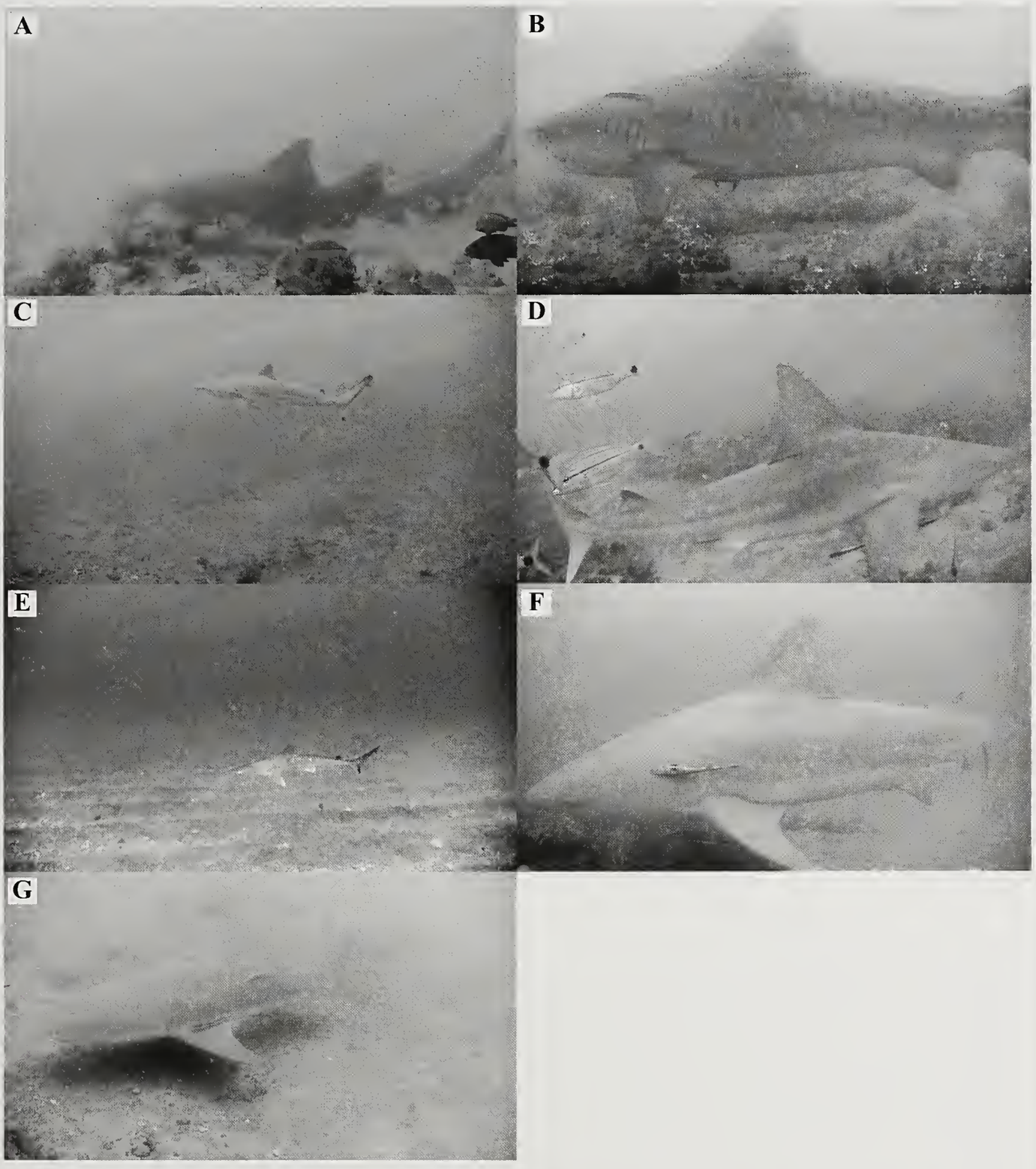

Figure 2

Still images from videos of the 7 species of sharks observed during analysis of video samples from baited remote underwater video stations deployed on the continental shelf off east-central Florida in July 2014: (**A**) nurse (*Ginglymostoma cirratum*), (**B**) tiger (*Galeocerdo cuvier*), (**C**) spinner (*Carcharhinus brevipinna*), (**D**) sandbar (*C. plumbeus*), (**E**) Atlantic sharpnose (*Rhizoprionodon terraenovae*), (**F**) bull (*C. leucas*), and (**G**) lemon (*Negaprion brevirostris*) sharks.

Table 1

Comparison of observations of shark species between 2 methods used: 1) underwater visual census conducted by scuba divers and 2) analysis of videos taken with baited remote underwater video stations. This comparison includes only observations from the 5 sites at which sharks were detected by divers. Diver surveys and station deployments occurred in July 2014 on the continental shelf off east-central Florida. A dash indicates that a shark was not observed in the video from this site.

Site number	Diver	Video
10	*Rhizoprionodon terraenovae*	–
34	*Ginglymostoma cirratum*	*G. cirratum*
44	*Carcharhinus plumbeus*	*G. cirratum*
55	*G. cirratum*	–
67	*G. cirratum*	G. *cirratum*, *Galeocerdo cuvier*

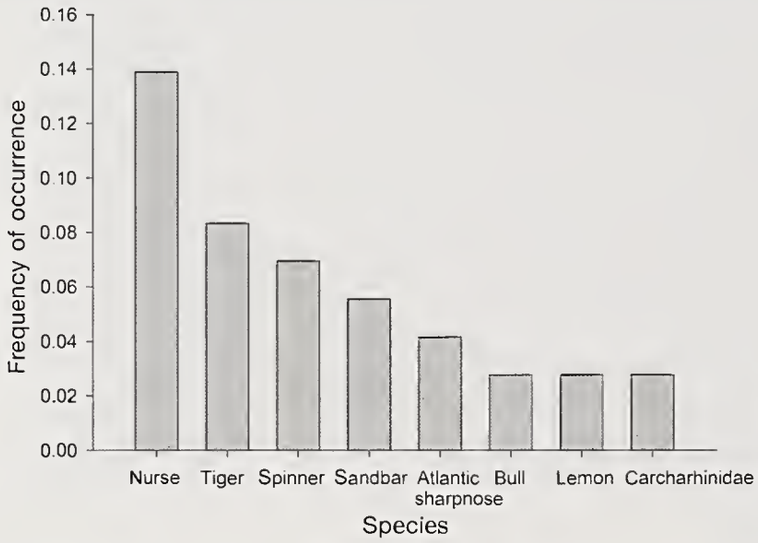

Figure 3

Frequency of occurrence of the 7 shark species observed through analysis of video recorded with baited remote underwater video stations in July 2014 off east-central Florida: nurse (*Ginglymostoma cirratum*), tiger (*Galeocerdo cuvier*), spinner (*Carcharhinus brevipinna*), sandbar (*C. plumbeus*), Atlantic sharpnose (*Rhizoprionodon terraenovae*), bull (*C. leucas*), and lemon (*Negaprion brevirostris*) sharks. Frequency of occurrence for each species was calculated as the number of sites with observations of a species divided by the total number of sampled sites. Two sharks could be identified only to the level of family (Carcharhinidae).

sharks observed through the use of these 2 sampling methods. In some cases, divers observed sharks that were not recorded in videos and vice versa, and in other cases the same species of sharks were observed both by divers and in videos (Table 1).

Comparing all 3 methods (entire video analyzed, only SERFS 20-min segment of video analyzed, UVC), a greater diversity and abundance of sharks were recorded when the entire video was analyzed. As a result, estimates of rank abundance for shark species differed by the method used (Table 2).

Discussion

By rapidly analyzing an entire video rather than only the 20-min subsample required by the SERFS protocol (an average of 58 min of additional video combined, before and after the subsample), we were able to observe sharks in videos from 400% more sites and increase the number of species recorded by 40%. Therefore, our estimates of relative abundance for these key fish community members changed from those determined by using the SERFS protocol. These findings confirm for species of sharks the results of Bacheler and Shertzer (2015), who suggested that fast-moving, solitary, infrequently encountered fish species had a higher probability of being missed in analysis of video subsamples and recommended increasing the number of video segments reviewed to target these types of species. Similarly, we observed sharks for more sites within the longer intervals (an average of 48 min of additional video) that followed the SERFS 20-min segments than within other parts of videos, and longer sampling intervals have been associated with increased arrival of targeted species in other studies that used underwater video (Watson, 2006; Watson et al., 2010).

Given the significant costs associated with large-scale marine research surveys, examination of a complete video to gain additional information on large-bodied, less-abundant species, such as sharks, represents a relatively simple way to add significant value to the already successful SERFS (e.g., Link et al., 2008; Mitchell et al., 2014; Bacheler et al., 2016). In addition, the regional coverage of the SERFS, together with habitat and environmental data (e.g., depth, temperature, salinity, pH, turbidity) that are collected annually at a large number of sites (~1500 sites per year), provides an important opportunity to collect relative abundance and habitat use information on relatively expansive spatial and temporal scales for a variety of shark species found in the Atlantic Ocean. For example, the distribution and biomass of sharks are influenced by physical factors, such as sea-surface temperature, oceanic primary productivity, and reef complexity, and by biological factors, such as competition, reproduction, lower-trophic-level biomass, and prey availability

Table 2

Rank relative abundance[1] of shark species from the use of 3 different sampling methods: analysis of entire video, analysis of a 20-min subsample of video (41 frames), and underwater visual census (UVC). Scuba divers conducted UVC surveys simultaneously with deployments of baited remote underwater video stations in July 2014 on the continental shelf off east-central Florida. Also provided are frequency of occurrence (FO) from analysis of entire videos and the mean number of individuals observed in video subsamples or by divers over an area of 300 m^2. A dash indicates that a species was not observed with this method.

	Sampling method					
	Entire video analyzed		Subsample of video analyzed		UVC	
Species	Rank relative abundance	FO	Rank relative abundance	Mean number of individuals	Rank relative abundance	Mean number of individuals
Ginglymostoma cirratum	1	14%	3	0.01	1	0.013
Galeocerdo cuvier	2	8%	–	–	–	–
Carcharhinus brevipinna	3	7%	1	0.30	–	–
C. plumbeus	4	5%	3	0.01	2	0.004
Rhizoprionodon terraenovae	5	4%	3	0.01	2	0.004
C. leucas	6	3%	2	0.03	–	–
Negaprion brevirostris	6	3%	–	–	–	–

[1] For each method, the smaller the number, the greater the relative abundance. See table S1 in Bacheler et al. (2017) for details about abundance determined with analysis of video subsamples and UVC for all fish species.

(Wirsing et al., 2007; Nadon et al., 2012; Heupel and Simpfendorfer, 2014). In this study, chevron traps associated with videos that recorded sharks contained significantly higher total numbers of individual fish than traps associated with videos in which sharks were absent, a result that may relate to prey availability at sites from which the former videos were collected.

Depending on the relative abundance of shark species encountered at the regional scale, these data could be used to generate species-specific abundance indices for shark stock assessments. Data gathered from video analysis can provide, without the need for extraction of sharks, estimates of relative abundance for a variety of coastal shark species on the continental shelf of the southeastern United States. A standardized, non-destructive method of video analysis can supplement traditional sampling methods (e.g., those that use longlines or gillnets). Brooks et al. (2011) compared estimates of shark relative abundance from the use of BRUVS and longline surveys, found significant positive correlations between methods for the more abundant species, and concluded that the use of videos from BRUVS represented a non-invasive, cost-effective alternative to the use of longlines for monitoring broad trends in the relative abundance of sharks. A shark-dedicated addition to the SERFS would complement the 3 large-scale regional longline surveys of sharks that currently operate in the southeastern United States: Cooperative Atlantic States Shark Pupping and Nursery Survey, Apex Predators Program Large Coastal Shark Survey, and Shark and Red Snapper Bottom Longline Survey. These surveys tend to have annual sample sizes or areas of coverage that are smaller than and mostly inshore of those of the SERFS.

In our study, 7 species of sharks were observed in videos from 25 of 72 sites (35% of sites). This proportion of sites with sharks is high relative to a regional survey of the entire Great Barrier Reef, off northeastern Australia, that detected sharks in videos collected during 25% of 2438 BRUVS deployments (Espinoza et al., 2014), likely a result of the limited sample size and spatial coverage of our study. The most common finding in both studies is that a single species of shark was observed at each site. In our study, the nurse shark was observed in greater abundance than other species, followed in descending order by the tiger, spinner, and sandbar sharks. An assessment of population status for the sandbar shark found the stock to be overfished but that overfishing was not occurring (SEDAR, 2017), and the results of recent studies indicate potential recovery since the early 1990s for the tiger, spinner, sandbar, bull, and lemon sharks (Carlson et al., 2012; Peterson et al., 2017). The only other species observed in our study that has been assessed by the National Marine Fisheries Service, the Atlantic sharpnose shark, was not found to be overfished (SEDAR, 2013).

The results of our study support the idea that analysis of videos from BRUVS is superior to the use of UVC by divers for detecting sharks, in agreement with reports from other studies (Meekan and Cappo, 2004; McCauley et al., 2012; Osgood and Baum, 2015; Barley et al., 2017). The use of BRUVS provides 1) a way

to control for species-specific differences in attraction to or avoidance of divers (Kulbicki, 1998; Watson and Harvey, 2007), 2) superior detection capacity (McCauley et al., 2012), 3) easy deployment at much greater depths and in environments where diver safety may be a concern (De Vos et al., 2015), and 4) longer soak times and sampling intervals because BRUVS are not subject to decompression limits (Watson et al., 2010). Additionally, the lower relative costs and fewer personnel required for deployment of BRUVS, compared with those of large-scale UVC or longline sampling, allow larger sample sizes (Willis et al., 2000; Brooks et al., 2011) and facilitate the deployment of BRUVS at large spatial scales (White et al., 2013; Espinoza et al., 2014; Santana-Garcon et al., 2014). Studies of temperate, subtropical, and coral reefs in Western Australia determined that analysis of videos from BRUVS results in greater species richness and a greater number of targeted, carnivorous large-bodied species, such as those in the families Lethrinidae and Serranidae, whereas UVC conducted by divers results in observations of more site-attached, cryptic small-bodied species, such as some members of the families Pomacentridae, Labridae, and Scaridae (Langlois et al., 2010; Watson et al., 2010). On the other hand, observations in videos from BRUVS may be affected by currents and fish traits, such as appetite and search behavior, as well as by inter- or intraspecific interactions (Stoner et al., 2008; Barley et al., 2017).

In this study, sharks were observed at more sites and with a greater species diversity through analysis of video from BRUVS than with UVC conducted by divers. By using UVC, 3 species of sharks were recorded at 5 sites, but 7 species were observed in videos from BRUVS at 25 sites. Site-specific comparisons of data from the use of BRUVS and UVC revealed differences in the presence and absence of sharks and in the species of sharks observed. These differences may reflect species-specific responses (attraction or avoidance) to the presence of divers versus traps (Kulbicki, 1998; Meekan and Cappo, 2004; Watson and Harvey, 2007). For example, in our study, the tiger shark was not observed by divers but was the second-most abundant shark observed in videos from BRUVS. Meekan and Cappo (2004) also reported that divers rarely encountered hammerhead sharks (Sphyrnidae) and the tiger shark but that those taxa were recorded often in videos from BRUVS. Finally, differences in results between the use of UVC and analysis of videos from BRUVS in our study may reflect the difference in the spatial footprint of habitat sampled with the 2 methods: the area sampled with video recordings was not necessarily a subset of the habitat sampled with UVC, and in some cases there was no overlap at all between the areas covered by the 2 methods (Bacheler et al., 2017).

Sharks fill a key ecosystem role because of their predatory activity. Although some species are capable of feeding at the apex predator level, this group also includes planktivores, scavengers, and mesocarnivores. Sharks have been implicated in control of the abundance and biomass of prey in lower trophic levels and in maintenance of biological diversity (Heupel et al., 2014; Osgood and Baum, 2015; Terborgh, 2015; Frisch et al., 2016; Barley et al., 2017). Given that the SERFS annually samples ~1500 sites across the continental shelf from North Carolina to Florida, our observations of 7 species of sharks in videos from BRUVS deployed at a relatively small number of geographically restricted sites indicate that a targeted analysis, for sharks, of videos collected as part of the SERFS could provide critical information, without requiring extraction, for some of the 42 species[3] of sharks federally managed in the southeastern United States. Such an effort has the potential to provide estimates of relative abundance for assessments of shark stocks, improve predictions of spatiotemporal distribution, and aid in the identification of essential fish habitat for these important predators.

Acknowledgments

We thank N. Geraldi, D. Grenda, J. Hackney, M. Judge, G. Kellison, D. Meyer, and B. Teer for field assistance and the captain and crew of the M/V *Spree*. We acknowledge N. Bacheler, J. Carlson, A. Chester, A. Hohn, G. Kellison, K. Siegfried, and 3 anonymous reviewers for their comments on previous versions of this manuscript. Funding was provided by the Marine Fisheries Initiative of the National Marine Fisheries Service (grant no. 13MFIH0006).

Literature cited

Bacheler, N. M., and K. W. Shertzer.
2015. Estimating relative abundance and species richness from video surveys of reef fishes. Fish. Bull. 113:15–26.

Bacheler, N. M., D. J. Berrane, W. A. Mitchell, C. M. Schobernd, Z. H. Schobernd, B. Z. Teer, and J. C. Ballenger.
2014. Environmental conditions and habitat characteristics influence trap and video detection probabilities for reef fish species. Mar. Ecol. Prog. Ser. 517:1–14.

Bacheler, N. M., Z. H. Schobernd, D. J. Berrane, C. M. Schobernd, W. A. Mitchell, B. Z. Teer, K. C. Gregalis, and D. M. Glasgow.
2016. Spatial distribution of reef fish species along the Southeast US Atlantic Coast inferred from underwater video survey data. PLoS ONE 11(9):e0162653.

Bacheler, N. M., N. R. Geraldi, M. L. Burton, R. C. Muñoz, and G. T. Kellison.
2017. Comparing relative abundance, lengths, and habitat of temperate reef fishes using simultaneous underwater visual census, video, and trap sampling. Mar. Ecol. Prog. Ser. 574:141–155.

Barley, S. C., M. G. Meekan, and J. J. Meeuwig.
2017. Species diversity, abundance, biomass, size and tro-

[3] Atlantic highly migratory species, Table 1 of Appendix A to part 635—oceanic sharks, 54 C.F.R. 635 (2018). [Available from website].

phic structure of fish on coral reefs in relation to shark abundance. Mar. Ecol. Prog. Ser. 565:163–179.

Bond, M. E., E. A. Babcock, E. K. Pikitch, D. L. Abercrombie, N. F. Lamb, and D. D. Chapman.
2012. Reef sharks exhibit site-fidelity and higher relative abundance in marine reserves on the Mesoamerican Barrier Reef. PLoS ONE 7(3):e32983.

Brooks, E. J., K. A. Sloman, D. W. Sims, and A. J. Danylchuk.
2011. Validating the use of baited remote underwater video surveys for assessing the diversity, distribution and abundance of sharks in the Bahamas. Endanger. Spec. Res. 13:231–243.

Carlson, J. K., L. F. Hale, A. Morgan, and G. Burgess.
2012. Relative abundance and size of coastal sharks derived from commercial shark longline catch and effort data. J. Fish Biol. 80:1749–1764.

Colton, M. A., and S. E. Swearer.
2010. A comparison of two survey methods: differences between underwater visual census and baited remote underwater video. Mar. Ecol. Prog. Ser. 400:19–36.

De Vos, L., R. G. A. Watson, A. Götz, and C. G. Attwood.
2015. Baited remote underwater video system (BRUVs) survey of chondrichthyan diversity in False Bay, South Africa. Afr. J. Mar. Sci. 37:209–218.

Dulvy, N. K., S. L. Fowler, J. A. Musick, R. D. Cavanagh, P. M. Kyne, L. R. Harrison, J. K. Carlson, L. N. K. Davidson, S. V. Fordham, M. P. Francis, et al.
2014. Extinction risk and conservation of the world's sharks and rays. Elife 3:e00590.

Dulvy, N. K., C. A. Simpfendorfer, L. N. K. Davidson, S. V. Fordham, A. Brautigam, G. Sant, and D. J. Welch.
2017. Challenges and priorities in shark and ray conservation. Curr. Biol. 27:R565–R572.

Espinoza, M., M. Cappo, M. R. Heupel, A. J. Tobin, and C. A. Simpfendorfer.
2014 Quantifying shark distribution patterns and species-habitat associations: implications of marine park zoning. PLoS ONE 9(9):e106885.

Espinoza, M., E. J. I. Ledee, C. A. Simpfendorfer, A. J. Tobin, and M. R. Heupel.
2015 Contrasting movements and connectivity of reef-associated sharks using acoustic telemetry: implications for management. Ecol. Appl. 25:2101–2118.

Estes, J. A., J. Terborgh, J. S. Brashares, M. E. Power, J. Berger, W. J. Bond, S. R. Carpenter, T. E. Essington, R. D. Holt, J. B. C. Jackson, et al.
2011. Trophic downgrading of planet Earth. Science 333: 301–306.

Frisch, A. J., M. Ireland, J. R. Rizzari, O. M. Lonnstedt, K. A. Magnenat, C. E. Mirbach, and J. P. A. Hobbs.
2016. Reassessing the trophic role of reef sharks as apex predators on coral reefs. Coral Reefs 35:459–472.

Heithaus, M. R., A. Frid, J. J. Vaudo, B. Worm, and A. J. Wirsing.
2010. Unraveling the ecological importance of elasmobranchs. *In* Sharks and their relatives II: biodiversity, adaptive physiology, and conservation (J. C. Carrier, J. A. Musick, and M. R. Heithaus, eds.), p. 611–638. CRC Press, Boca Raton, FL.

Heupel, M. R., and C. A. Simpfendorfer.
2014. Importance of environmental and biological drivers in the presence and space use of a reef-associated shark. Mar. Ecol. Prog. Ser. 496:47–57.

Heupel, M. R., D. M. Knip, C. A. Simpfendorfer, and N. K. Dulvy.
2014. Sizing up the ecological role of sharks as predators. Mar. Ecol. Prog. Ser. 495:291–298.

Kulbicki, M.
1998. How the acquired behaviour of commercial reef fishes may influence the results obtained from visual censuses. J. Exp. Mar. Biol. Ecol. 222:11–30.

Langlois, T. J., E. S. Harvey, B. Fitzpatrick, J. J. Meeuwig, G. Shedrawi, and D. L. Watson.
2010. Cost-efficient sampling of fish assemblages: comparison of baited video stations and diver video transects. Aquat. Biol. 9:155–168.

Link, J., J. Burnett, P. Kostovick, and J. Galbraith.
2008. Value-added sampling for fishery independent surveys: don't stop after you're done counting and measuring. Fish. Res. 93:229–233.

MacNeil, M. A., N. A. J. Graham, M. J. Conroy, C. J. Fonnesbeck, N. V. C. Polunin, S. P. Rushton, P. Chabanet, and T. R. McClanahan.
2008. Detection heterogeneity in underwater visual-census data. J. Fish Biol. 73:1748–1763.

McCauley, D. J., K. A. McLean, J. Bauer, H. S. Young, and F. Micheli.
2012 Evaluating the performance of methods for estimating the abundance of rapidly declining coastal shark populations. Ecol. Appl. 22:385–392.

Meekan, M. G., and M. Cappo.
2004. Non-destructive techniques for rapid assessment of shark abundance in northern Australia, 36 p. Aust. Inst. Mar. Sci., Townsville, Australia.

Mitchell, W. A., G. T. Kellison, N. M. Bacheler, J. C. Potts, C. M. Schobernd, and L. F. Hale.
2014. Depth-related distribution of postjuvenile red snapper in southeastern US Atlantic Ocean waters: ontogenic patterns and implications for management. Mar. Coast. Fish. 6:142–155.

Murphy, H. M., and G. P. Jenkins.
2010. Observational methods used in marine spatial monitoring of fishes and associated habitats: a review. Mar. Freshw. Res. 61:236–252.

Nadon, M. O., J. K. Baum, I. D. Williams, J. M. McPherson, B. J. Zgliczynski, B. L. Richards, R. E. Schroeder, and R. E. Brainard.
2012. Re-creating missing population baselines for Pacific reef sharks Conserv. Biol. 26:493–503.

Osgood, G. J., and J. K. Baum.
2015. Reef sharks: recent advances in ecological understanding to inform conservation. J. Fish Biol. 87:1489–1523.

Peterson, C. D., C. N. Belcher, D. M. Bethea, W. B. Driggers III, B. S. Frazier, and R. J. Latour.
2017. Preliminary recovery of coastal sharks in the southeast United States. Fish Fish. 18:845–859.

Santana-Garcon, J., M. Braccini, T. J. Langlois, S. J. Newman, R. B. McAuley, and E. S. Harvey.
2014. Calibration of pelagic stereo-BRUVs and scientific longline surveys for sampling sharks. Methods Ecol. Evol. 5:824–833.

Schobernd, Z. H., N. M. Bacheler, and P. B. Conn.
2014. Examining the utility of alternative video monitoring metrics for indexing reef fish abundance. Can. J. Fish. Aquat. Sci. 71:464–471.

SEDAR (Southeast Data Assessment and Review).
2017. SEDAR 54—Stock assessment report: HMS sandbar shark, 176 p. SEDAR, North Charleston, SC. [Available from website].
2013. SEDAR 34—Stock assessment report: HMS Atlantic sharpnose shark, 296 p. SEDAR, North Charleston, SC. [Available from website].

Stoner, A. W., B. J. Laurel, and T. P. Hurst.
2008. Using a baited camera to assess relative abundance of juvenile Pacific cod: field and laboratory trials. J. Exp. Mar. Biol. Ecol. 354:202–211.

Terborgh, J. W.
2015. Toward a trophic theory of species diversity. Proc. Natl. Acad. Sci. U.S.A. 112:11415–11422.

Tickler, D. M., T. B. Letessier, H. J. Koldewey, and J. J. Meeuwig.
2017. Drivers of abundance and spatial distribution of reef-associated sharks in an isolated atoll reef system. PLoS ONE 12(5):e0177374.

Ward-Paige, C. A.
2017. A global overview of shark sanctuary regulations and their impact on shark fisheries. Mar. Policy 82:87–97.

Ward-Paige, C., J. M. Flemming, and H. K. Lotze.
2010. Overestimating fish counts by non-instantaneous visual censuses: consequences for population and community descriptions. PLoS ONE 5(7):e11722.

Watson, D. L.
2006. Use of underwater stereo-video to measure fish assemblage structure, spatial distribution of fishes and change in assemblages with protection from fishing. Ph.D. diss., 188 p. Univ. Western Australia. Perth, Australia.

Watson, D. L., and E. S. Harvey.
2007. Behaviour of temperate and sub-tropical reef fishes towards a stationary SCUBA diver. Mar. Freshw. Behav. Physiol. 40:85–103.

Watson, D. L., E. S. Harvey, B. M. Fitzpatrick, T. J. Langlois, and G. Shedrawi.
2010. Assessing reef fish assemblage structure: how do different stereo-video techniques compare? Mar. Biol. 157:1237–1250.

White, E. R., M. C. Myers, J. M. Flemming, and J. K. Baum.
2015. Shifting elasmobranch community assemblage at Cocos Island—an isolated marine protected area. Conserv. Biol. 29:1186–1197.

White, J., C. A. Simpfendorfer, A. J. Tobin, and M. R. Heupel.
2013. Application of baited remote underwater video surveys to quantify spatial distribution of elasmobranchs at an ecosystem scale. J. Exp. Mar. Biol. Ecol. 448:281–288.

Willis, T. J., R. B. Millar, and R. C. Babcock.
2000. Detection of spatial variability in relative density of fishes: comparison of visual census, angling, and baited underwater video. Mar. Ecol. Prog. Ser. 198:249–260.

Wirsing, A. J., M. R. Heithaus, and L. M. Dill.
2007. Can measures of prey availability improve our ability to predict the abundance of large marine predators? Oecologia 153:563–568.

National Marine Fisheries Service
NOAA

Fishery Bulletin
established in 1881

Spencer F. Baird
First U.S. Commissioner of Fisheries and founder of *Fishery Bulletin*

Insights, from genetic analyses, into stock-specific distribution of juvenile steelhead (*Oncorhynchus mykiss*) from the Columbia River during early marine migration

Donald M. Van Doornik (contact author)[1]
David R. Kuligowski[1]
Cheryl A. Morgan[2]
Brian J. Burke[3]
Todd R. Seamons[4]

Email address for contact author: don.vandoornik@noaa.gov

[1] Conservation Biology Division
Northwest Fisheries Science Center
National Marine Fisheries Service, NOAA
7305 Beach Drive East
Port Orchard, Washington 98366

[2] Cooperative Institute for Marine Resources Studies
Hatfield Marine Science Center
Oregon State University
2030 South Marine Science Drive
Newport, Oregon 97365

[3] Fish Ecology Division
Northwest Fisheries Science Center
National Marine Fisheries Service, NOAA
2725 Montlake Boulevard East
Seattle, Washington 98112

[4] Washington Department of Fish and Wildlife
1111 Washington Street Southeast
Olympia, Washington 98501

Abstract—For anadromous Pacific salmon (*Oncorhynchus* sp.), ocean conditions during their initial entry into the marine environment can greatly affect their survival. Different life history types or stocks may experience different conditions during their marine entry because routes of early marine migration can differ among types or stocks. Steelhead (*O. mykiss*) from the Columbia River are believed to migrate offshore quickly once they enter the ocean, but little is known about whether life history or stock-specific differences in early marine migration exist. We assembled a baseline of steelhead genetic data that allowed us to estimate the genetic stock of origin for juvenile steelhead that had been caught off the coasts of Washington and Oregon in May, shortly after their out-migration from freshwater. We found differences in the average locations of the various genetic stock groups of the Columbia River, dissimilarities that were most likely due to differences in the timing of the marine entry of juveniles. We also observed considerable variation among years in the average location where we caught steelhead and in the number of steelhead caught, results indicating that freshwater or marine conditions can influence the behavior or survival of steelhead.

Manuscript submitted 25 July 2018.
Manuscript accepted 11 April 2019.
Fish. Bull. 117:97–106 (2019).
Online publication date: 26 April 2019.
doi: 10.7755/FB.117.1-2.11

The views and opinions expressed or implied in this article are those of the author (or authors) and do not necessarily reflect the position of the National Marine Fisheries Service, NOAA.

Anadromous Pacific salmon (*Oncorhynchus* sp.) utilize the marine environment for rapid growth to maturity. Results of studies have indicated that the initial months after entry into saltwater are important to the survival of steelhead and that this time period affects year-class strength (Pearcy, 1992; Hare and Francis, 1995). Therefore, understanding their marine distribution and migration, and how they respond to different marine conditions during those initial months, can provide knowledge of the variables that contribute to strong year classes.

The Columbia River is home to several species of salmonids, many of which have been listed as threatened or endangered under the U.S. Endangered Species Act, including steelhead (*Oncorhynchus mykiss*). Steelhead are the life history variant of *O. mykiss* that migrate from their place of birth in freshwater to the ocean, where they remain for several years before returning to their river of origin to spawn. For steelhead from the Columbia River Basin, populations in the Lower, Middle, and Upper Columbia, Upper Willamette, and Snake Rivers are listed as threatened (NWFSC, 2015). Despite the imperiled status of these populations, the greatest number of steelhead in the Pacific Northwest are produced in the Columbia River (Busby et al., 1996), contributing significantly to highly valued recreational and tribal fisheries throughout the region.

The Columbia River contains 2 phylogenetic groups (subspecies) of steelhead that are separated by the Cascade Mountain Range: coastal steelhead (*O. mykiss irideus*) and Columbia River redband steelhead (*O. mykiss gairdnerii*), the latter

Table 1

Genetic stock groups and run types of the 148 populations of steelhead (*Oncorhynchus mykiss*) used in genetic stock identification analyses in this study of the early marine migration of steelhead from the Columbia River. The 2 phylogenetic groups or subspecies of steelhead are coastal steelhead (*O. mykiss irideus*) and Columbia River redband steelhead (*O. mykiss gairdnerii*), commonly referred to as *inland steelhead*.

Genetic stock group	Phylogenetic group	No. of populations	Run type
Puget Sound/Strait of Juan de Fuca	Coastal	12	Winter
Washington coast	Coastal	7	Winter
Lower Columbia River summer run	Coastal	4	Summer
Lower Columbia River winter run	Coastal	17	Winter
Middle and Upper Columbia River/Lower Snake River	Inland	67	Summer
Middle and Upper Snake River	Inland	28	Summer
Oregon coast	Coastal	7	Summer, winter
Klamath Mountains Province	Coastal	3	Summer, winter
Northern California	Coastal	2	Summer, winter
Central Valley, California	Coastal	1	Winter

of which is commonly referred to as *inland steelhead* (Busby et al., 1996; Blankenship et al., 2011). Within these groups, there are 2 life history types that are identified by the time of year when they return to freshwater and by their maturity status when they arrive in freshwater. The inland group is composed almost exclusively of summer-run steelhead (Busby et al., 1996). These are stream-maturing steelhead that enter freshwater between May and October, when they are still sexually immature, and remain in freshwater for several months until they mature and spawn. Summer-run stocks are present also in populations of coastal steelhead, but this group is primarily composed of winter-run steelhead. Winter-run steelhead are ocean-maturing fish that enter freshwater between November and April almost fully mature, and they spawn shortly after entry into a river.

Steelhead of the Columbia River out-migrate from freshwater to saltwater through the Columbia River estuary in springtime, with peak out-migration occurring in mid-May (Weitkamp et al., 2012; Weitkamp et al., 2015). They travel through the estuary quickly (Dawley et al., 1986) and, after reaching the marine environment, move quickly into offshore waters before heading north to the Gulf of Alaska (Burgner et al., 1992; Brodeur et al., 2004; Quinn and Myers, 2004; Daly et al., 2014). This movement contrasts with that of other salmonids, such as Chinook (*Oncorhynchus tshawytscha*) and coho (*O. kisutch*) salmon, which remain closer to the coast as they migrate northward (Van Doornik et al., 2007; Teel et al., 2015). The rapid offshore migration of steelhead could be related to a need to quickly travel to areas where the fish larvae on which they prey are more abundant (Daly et al., 2014). However, it is not known if there are stock-specific differences in routes of early marine migration.

Variation among individuals in migration routes can affect survival (Furey et al., 2015), and, if differences in migration routes among stocks exist, factors, such as oceanographic conditions, hatchery practices, or management of water flow through the hydroelectric dams of the Columbia River, could affect the survival of different stocks in different ways. Therefore, our goals for this study were to determine if there are differences in the early marine migration of steelhead among genetic stock groups and if any such differences vary from year to year.

Materials and methods

Sample collection and genotyping

To estimate the genetic stock to which each juvenile steelhead belonged, we first had to create a baseline of genotypic data for steelhead populations whose members were likely to be found in our study area. No such baseline existed; therefore, we compiled genotypic data collected by several genetics laboratories based on the West Coast of the United States. Data for populations of Puget Sound, the Strait of Juan de Fuca, and the Washington coast were provided by the Washington Department of Fish and Wildlife (T. Seamons, unpubl. data). Data for steelhead of the Columbia River were obtained from the Columbia River Inter-Tribal Fish Commission and Idaho Department of Fish and Game (data available from website, accessed January 2016; Hess et al.[1]; Matala et al., 2014). The NOAA Northwest

[1] Hess, J. E., N. R. Campbell, A. P. Matala, and S. R. Narum. 2013. 2012 annual report: genetic assessment of Columbia River stocks, 147 p. Div. Fish Wildl., Bonneville Power Admin., U.S. Dep. Energy, Portland, OR [Available from website, accessed July 2018.]

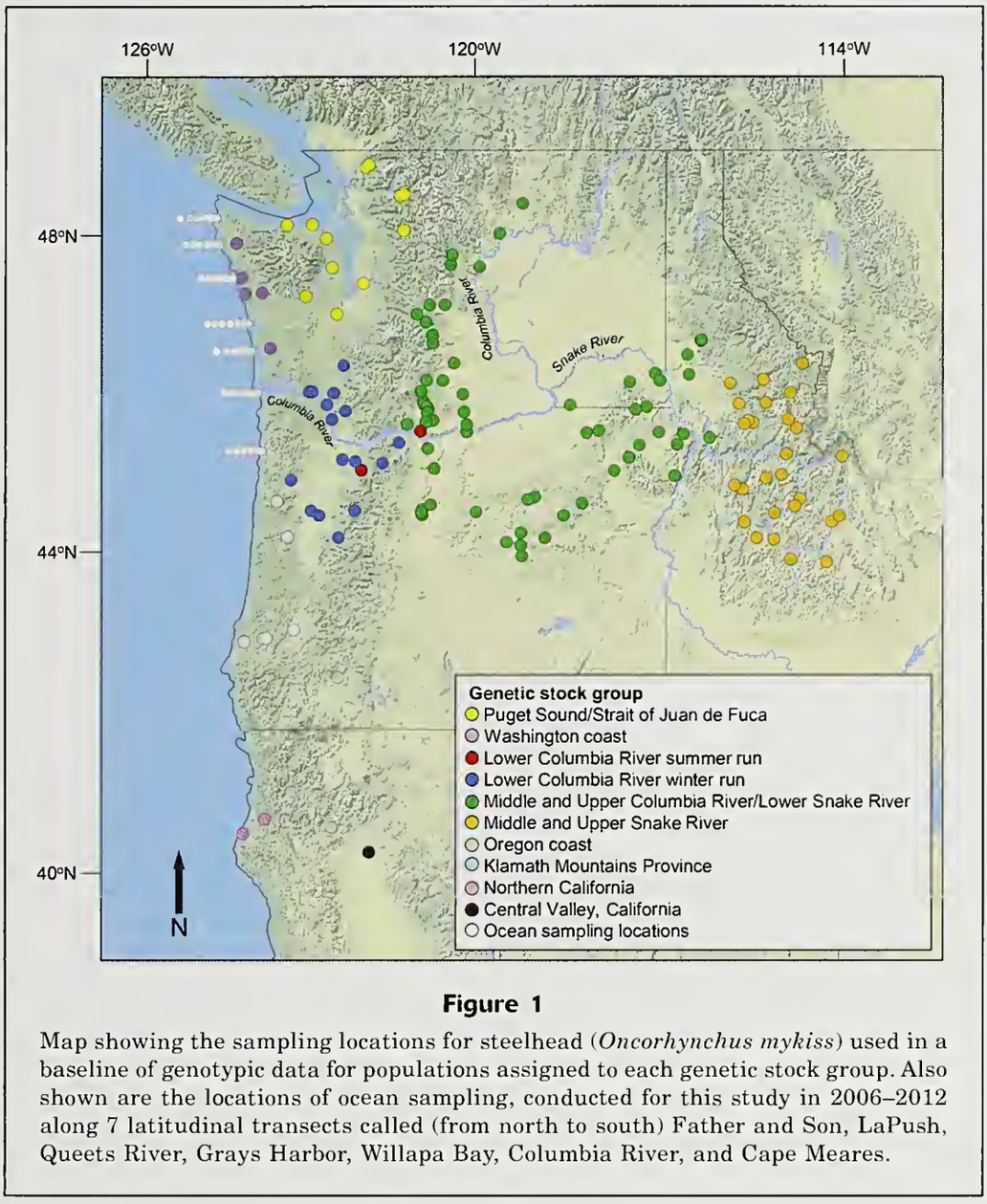

Figure 1

Map showing the sampling locations for steelhead (*Oncorhynchus mykiss*) used in a baseline of genotypic data for populations assigned to each genetic stock group. Also shown are the locations of ocean sampling, conducted for this study in 2006–2012 along 7 latitudinal transects called (from north to south) Father and Son, LaPush, Queets River, Grays Harbor, Willapa Bay, Columbia River, and Cape Meares.

Fisheries Science Center collected genotypes for samples collected from coastal rivers of Oregon and California (data available from website, accessed December 2017). The compiled baseline consisted of genotypes of 9934 steelhead from 148 populations (Table 1, Fig. 1).

Ocean-caught samples were obtained as part of a much larger project studying the early marine ecology of salmon from the Columbia River (Brodeur et al., 2000; Brodeur et al., 2005). The steelhead samples used in this study were collected from trawl hauls made in May in each year of the period 2006–2012. Sampling was conducted off the coasts of Washington and Oregon along 7 transects, from 48°13.7′N to 45°29.0′N (Fig. 1), by towing a Nordic 264-rope trawl (Nor'Eastern Trawl Systems, Inc.[2], Bainbridge Island, WA) at a speed of approximately 1.6 m/s for 30 min (Brodeur et al., 2005). The same vessel, gear, trawling depth, and speed were implemented each year. At the time of capture, fish were identified to species, measured (in fork length), and then frozen on board the sampling vessel. In the laboratory, fish were thawed, re-measured, and examined for marks indicating hatchery origin, such as adipose fin clips or coded-wire tags, and a portion of their caudal fin tissue was preserved in 100% ethanol.

Procedures for genotyping samples differed slightly among the laboratories contributing data to this project, but all were similar to the method described by Hess et al.[1]. In general, fish were genotyped for 131 or 180 single nucleotide polymorphism (SNP) loci (Hess et al.[1]) by amplifying loci of interest through the use of polymerase chain reactions (PCR). The resulting PCR products were then visualized by using genotyping platforms from either Fluidigm Corp. (South San Francisco, CA) or Illumina, Inc. (San Diego, CA).

[2] Mention of trade names or commercial companies is for identification purposes only and does not imply endorsement by the National Marine Fisheries Service, NOAA.

Genetic stock identification

Estimates of the stock of origin for each fish were made by using genetic stock identification (GSI). To perform GSI, we used the algorithms employed by the software ONCOR (Kalinowski et al., 2007). The ONCOR program uses the partial-Bayesian algorithms of Rannala and Mountain (1997) with an expectation maximization algorithm to assign individuals to their most likely population of origin by using a baseline of genetic information collected from samples of known origin. A critical assumption of this method is that all possible source populations are in the baseline. This assumption is unlikely to be met in most studies of this type, including ours. However, assignment likelihoods are correlated with the hierarchical genetic structure typical of salmonids such that, if the source population is not in the baseline but a genetically similar population is, the unknown individual will likely be assigned to the correct hierarchical genetic group for the actual source population. The groups to which we assigned our samples were determined by examining the accuracy of different configurations with leave-one-out cross-validation analyses.

Once the genetic stock groups were established, we employed a 2-tiered approach to determine the genetic stock origin of each ocean-caught steelhead. First, we used the program ONCOR to assign individuals to 1 of 7 genetic stock groups from a baseline of 131 SNP loci from 148 populations sampled in an area from the Central Valley of California to Puget Sound, Washington. This first tier of GSI assignments provided us with the resolution adequate for determining whether samples originated from the Columbia River Basin or from another region. The accuracy of this baseline was estimated by using the leave-one-out method as implemented in ONCOR. This leave-one-out method removes an individual fish from the baseline and treats it like an individual with an unknown origin, while assigning it to a group by using the remaining individuals in the baseline. This procedure is repeated for all individuals in the baseline, and a running total of how many of the assignments were correct is used to estimate the accuracy of the baseline.

Second, samples that were assigned to the Columbia River genetic stock group during the first analysis were then analyzed with ONCOR by using a baseline of 180 SNP loci from 116 populations of the Columbia River (Hess et al.[1]), to determine to which of the 4 genetic stock groups of the Columbia River each of those fish belonged. The accuracy of this baseline was also tested by using the leave-one-out method.

Some of the assignments of fish sampled from the Columbia River were made by using the technique known as *parentage-based tagging*, with the software SNPPIT, vers. 1.0 (Anderson[3]). Parentage-based tagging is accomplished by genotyping as many hatchery adult broodstock within a region as possible and then implementing parentage assignments to identify the offspring of those adults when they are sampled in a mixture of unknown individuals (Steele et al., 2013). Although we were not necessarily interested in knowing the hatchery of origin of our samples, this method can increase the accuracy of the GSI assignments because offspring are assigned directly to their parents rather than to a geographic region on the basis of their genotype frequencies. At the time of our analyses, parentage-based tagging data were available only for adults that spawned in 2009–2012 at hatcheries in the Snake River (data available from website, accessed January 2016).

Stock distributions and catch

Using the genetic stock assignments for each fish, we examined stock-specific distributions in our study area. To obtain a measure of steelhead relative abundance, we calculated values of stock-specific catch per unit of effort (CPUE) simply as the number of fish caught divided by the number of kilometers trawled. We then compared CPUE among years. In addition, we calculated the average CPUE for each stock for each year and then averaged those values across years to estimate an overall stock-specific CPUE, giving equal weight to all years.

Steelhead that originate from the Columbia River represent several distinct genetic stock groups and origins (hatchery and wild), but they all enter the ocean at close to the same location, the mouth of the Columbia River. To examine differences in early marine migration among these groups, latitude and longitude values were averaged for all fish originating from the same genetic stock group. Latitude and longitude values had been recorded for each trawl haul during sampling. These annual averages of latitude and longitude for each genetic stock group then were averaged over all years, to equally weight each year, and standard deviations were calculated. Differences in latitude also were converted to distance in kilometers (by using a conversion calculator available from the NOAA National Hurricane Center at website, accessed November 2018).

Results

Genetic stock groups

The genetic stock groups we chose for genetic assignments were those that provided the highest degree of geographic resolution, while still retaining high accuracy and close alignment with the distinct population segments identified in assessments completed as

[3] Anderson, E. C. 2010. Computational algorithms and user-friendly software for parentage-based tagging of Pacific salmonids. Final report submitted to the Pacific Salmon Commission's Chinook Technical Committee (US Section), 43 p. [Available from website, accessed July 2018.]

Table 2

Percentage of individuals correctly assigned to their stock of origin, determined by using leave-one-out simulations, for 7 genetic stock groups of steelhead (*Oncorhynchus mykiss*), ranging from the Central Valley of California to Puget Sound, Washington. The genetic stock groups in the left column represent the groups from which fish originated, and the genetic stock groups in the column heads identify the genetic stock group to which fish were assigned by using genetic stock identification.

Genetic stock group	Puget Sound Strait of Juan de Fuca	Washington coast	Columbia River	Oregon coast	Northern California	Klamath Mountains Province	Central Valley, California
Puget Sound/Strait of Juan de Fuca	90.3%	6.6%	2.3%	0.8%	0.0%	0.0%	0.0%
Washington coast	8.1%	84.1%	6.4%	1.3%	0.0%	0.0%	0.0%
Columbia River	0.3%	0.3%	99.2%	0.1%	0.0%	0.0%	0.0%
Oregon coast	2.3%	4.7%	6.3%	86.7%	0.0%	0.0%	0.0%
Northern California	0.0%	0.0%	0.0%	0.0%	100.0%	0.0%	0.0%
Klamath Mountains Province	0.0%	0.0%	0.0%	0.0%	0.0%	100.0%	0.0%
Central Valley, California	0.0%	0.0%	0.0%	0.0%	0.0%	0.0%	100.0%

Table 3

Percentage of individuals correctly assigned to their stock of origin, determined by using leave-one-out simulations, for 4 Columbia River genetic stock groups of steelhead (*Oncorhynchus mykiss*). The genetic stock groups in the left column represent the groups from which fish originated, and the genetic stock groups in the column heads identify which genetic stock groups fish were assigned to by using genetic stock identification.

Genetic stock group	Lower Columbia River summer run	Lower Columbia River winter run	Middle and Upper Columbia River/Lower Snake River	Middle and Upper Snake River
Lower Columbia River summer run	89.2%	10.8%	0.0%	0.0%
Lower Columbia River winter run	5.4%	93.4%	1.0%	0.2%
Middle and Upper Columbia River/Lower Snake River	0.1%	0.1%	91.4%	8.4%
Middle and Upper Snake River	0.0%	0.0%	7.6%	92.4%

required under the Endangered Species Act (Busby et al., 1996; NWFSC, 2015). The first-tier baseline, with 131 loci from 148 coast-wide populations, had high self-assignments within each reporting group (Table 2). The overall within-group self-assignment average was 94.1%. The least accurate group for this configuration was the Washington coast group, with an average of 84.1%. The majority of the incorrect assignments for this group were made to the Columbia River group.

The second-tier baseline, with 180 loci from 109 populations of the Columbia River, had an overall within-group self-assignment accuracy of 91.9% (Table 3). The least accurate group for this baseline was the Lower Columbia River summer-run group, with an average of 89.2% and the majority of incorrect assignments made to the Lower Columbia River winter-run group.

Of our ocean-caught samples, 34 fish had been tagged previously with coded-wire tags, which provided identification of their hatchery of origin. These fish originated from 4 of our genetic stock groups and provided a further means to assess the accuracy of our baselines and genetic stock groups. Our GSI estimates agreed 100% with the stock origins indicated by the tags for those samples.

Genetic stock identification

During the surveys conducted in May, 490 steelhead were caught, with high variation in the number of fish caught among years (Table 4). The majority (68.8%) of the fish caught were marked, indicating that they had a hatchery origin. This proportion is an underestimate of the true proportion of fish with a hatchery origin in our sample, given that the marking rate of steelhead from hatcheries in the Columbia River was 83.2% during our sampling period (Regional Mark Processing Center, Regional Mark Information Database, available from website, accessed July 2017). Steelhead captured in the trawl hauls originated from 8 of the 10 genetic reporting groups, but the vast majority of them were from the Columbia River (78.3%). Only one steelhead was identified as having originated from any of the 3

Table 4

The number of juvenile steelhead (*Oncorhynchus mykiss*) caught each year from each genetic stock group, the number that were marked with a tag or fin clip, and the overall catch per unit of effort (CPUE) for each year in the period 2006–2012 and summarized over all sampling stations in a study area from Puget Sound, Washington, to the Central Valley of California.

Year	Total number	Puget Sound/ Strait of Juan de Fuca	Washington coast	Lower Columbia River summer run	Lower Columbia River winter run	Mid and Upper Columbia River Lower Snake River	Mid and Upper Snake River	Oregon coast	Central Valley, California	Marked	Overall CPUE
2006	234	2	16	33	44	82	54	3	0	193	2.095
2007	45	5	11	2	19	5	0	2	1	17	0.273
2008	72	4	23	4	9	12	16	4	0	40	0.446
2009	41	4	8	3	8	8	10	0	0	29	0.274
2010	46	1	10	6	18	7	3	1	0	27	0.397
2011	38	2	9	3	11	8	4	1	0	23	0.173
2012	14	0	0	1	1	5	7	0	0	8	0.151

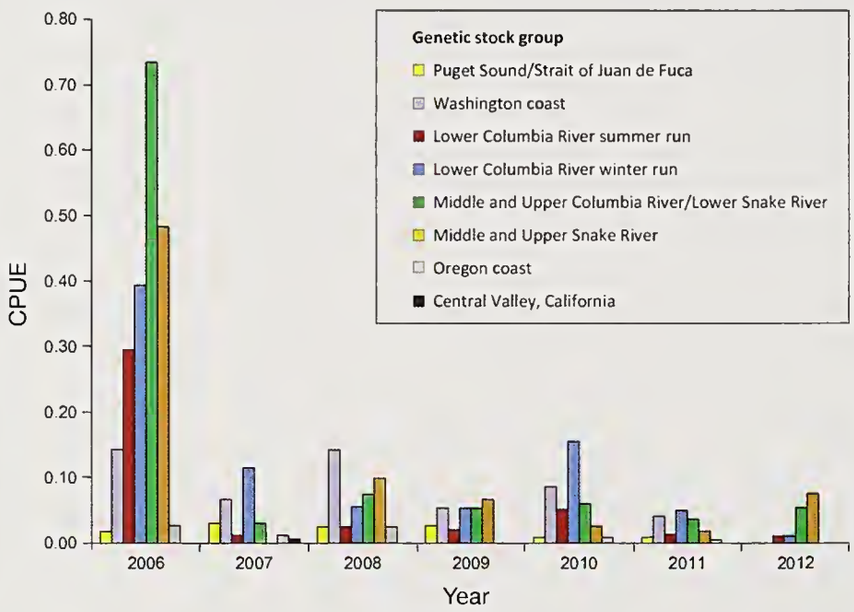

Figure 2

Catch per unit of effort (CPUE) of steelhead (*Oncorhynchus mykiss*) from trawl hauls conducted in 2006–2012 off the coasts of Washington and Oregon, by genetic stock group and year. Values of CPUE were calculated as the number of fish caught divided by the number of kilometers trawled.

southernmost genetic stock groups (in the Central Valley of California). That individual was not included in subsequent analyses.

Stock distributions and catch

There was considerable variation in CPUE among years (Fig. 2). The CPUE values in 2006 were considerably greater than those in any other year, especially for the genetic stock groups that included populations in the Snake River. The genetic stock group with the greatest CPUE value varied over the study period, but it was usually a group of the Columbia River, except in 2008, when the group from the Washington coast had the greatest CPUE value (Table 4).

There was also considerable variation in CPUE among transects of the trawl hauls each year (Fig. 3). In 2006, the distribution of the steelhead caught was different than in all the other years because most of the steelhead were caught in the 3 southernmost transects, especially in those off Cape Meares, Oregon. Steelhead were caught on that transect in only one other year: 2012. The transect in Willapa Bay, Washington, was where most of the steelhead were caught in 2010, especially Lower Columbia River winter-run fish, whereas the greatest concentration of fish occurred on the northernmost transect, Father and Son, in 2011. The catch in other years was spread more evenly among transects.

On average, steelhead from each genetic stock group were found north of the mouth of the Columbia River (Fig. 4). Lower Columbia River steelhead were found farther north than other stock groups of the Columbia River. In particular, the Lower Columbia River winter-run steelhead were found farther north than all other stock groups, although there was considerable overlap in the standard deviations of latitudes among all groups. The greatest difference in latitude (90 km) was

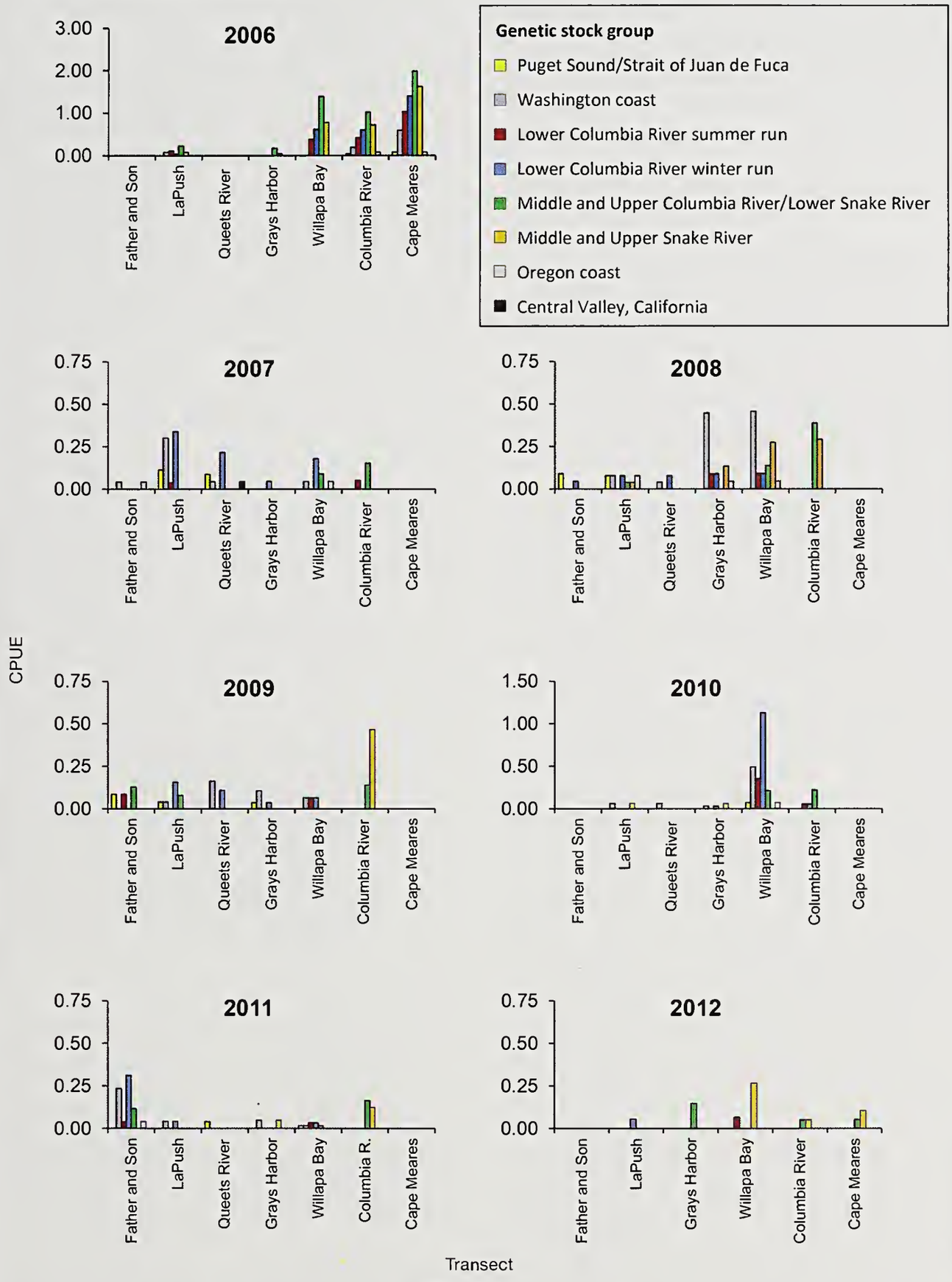

Figure 3

Catch per unit of effort (CPUE) of steelhead (*Oncorhynchus mykiss*) from trawl hauls conducted in 2006–2012 off the coasts of Washington and Oregon, by transect. Transects are arranged north to south on the x-axis. Note that the y-axis scale is different for 2006 and 2010. For transect locations, see Figures 1 and 4.

between the Lower Columbia River winter-run and the Middle and Upper Snake River groups. The Lower Columbia River winter-run group also was found farther north (44 km) than the Lower Columbia River summer-run group. The average longitude values indicate that we tended to catch steelhead at our westernmost (farthest from shore) sampling stations.

Discussion

Using GSI, we examined the distribution of steelhead juveniles off the coast of Oregon and Washington during their early marine migration and found differences in relative abundance and distribution among genetic stocks and years. From this work, we provide the first published evidence of stock-specific distributions of juvenile steelhead from the Columbia River. Steelhead from the Lower Columbia River winter- and summer-run groups were found, on average, farther north than fish from other genetic stock groups of the Columbia River. The simplest explanation for this observation is a difference in the timing of marine entry among these groups. Lower Columbia River steelhead have been observed to migrate through the estuary earlier than other genetic stock groups of steelhead from the Columbia River (Weitkamp et al., 2015). Therefore, at the time of our sampling, they had been in the ocean for a longer period, giving them more time to travel north. We also observed that between the Lower Columbia River steelhead genetic stock groups, the winter-run fish were found farther north than the summer-run fish. Additional analysis of data from Weitkamp et al. (2015) revealed that, on average, Lower Columbia River winter-run steelhead passed through the estuary 3.1 d earlier than summer-run steelhead, a finding that could explain why we found them farther north, but this difference in timing was not significant (t=1.52, P=0.203).

Although our research focused on stocks of steelhead from the Columbia River, there were a few interesting results regarding other stocks. Of note is the presence of fish from the Oregon coast in our catches, indicating that not all steelhead from that area migrate directly to offshore waters before heading north, as has been generally accepted (Myers, 2018). Some of these fish may have migrated up to 300 km north before they entered our study area. However, given the low CPUE values for this stock, the majority of them may already have been offshore outside of our study area and the few that were caught likely were migrating closer to the coast. Also, in our study area, we caught steelhead that were assigned to the genetic stock group from Puget Sound and the Strait of Juan de Fuca, indicating that they did not migrate north immediately (we caught them at locations that were south of the entrance to the Strait of Juan de Fuca, through which they pass). However, the Chambers Creek hatchery steelhead stock, a stock that originated in Puget Sound, has been raised and released extensively by hatcheries in Washington, including those located on rivers of the Washington coast and the Lower Columbia River (Busby et al., 1996). Therefore, it is possible that the fish we caught were progeny of stock from Chambers Creek released into rivers not within the Puget Sound Basin.

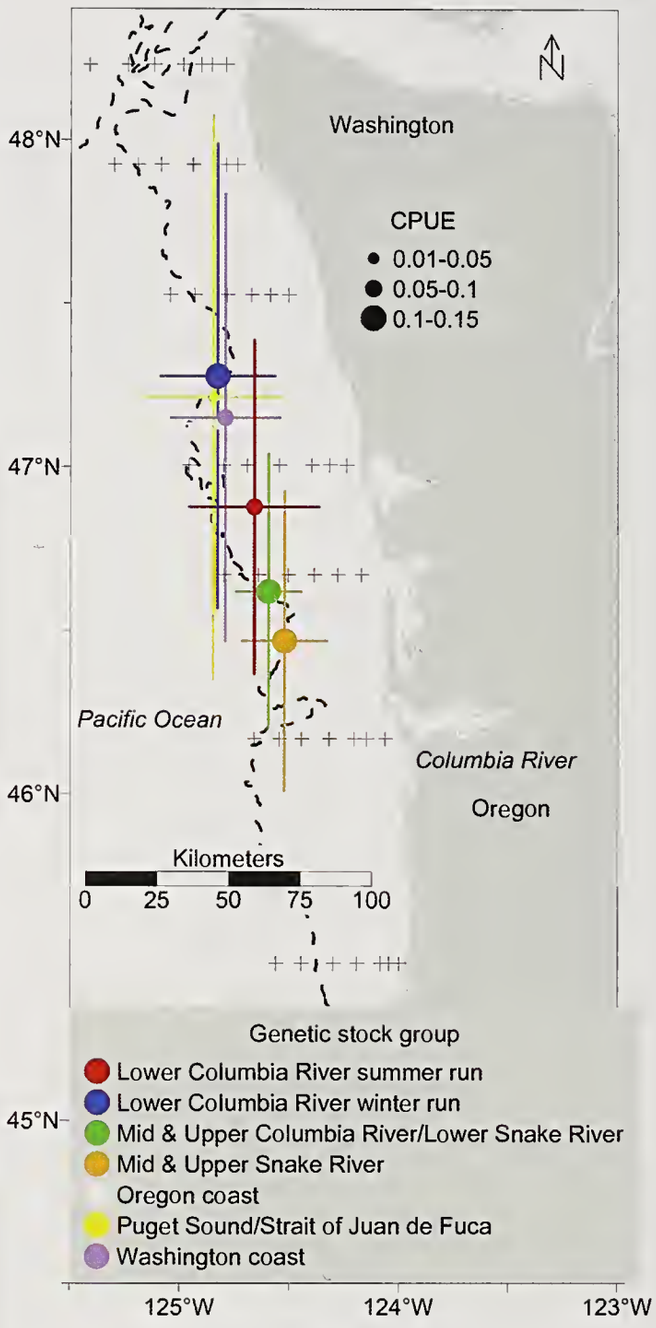

Figure 4

Average latitude and longitude over all years, with standard deviations, of the locations where juvenile steelhead (*Oncorhynchus mykiss*) from each genetic stock group were caught in 2006–2012 off the coasts of Washington and Oregon. The diameters of the circles indicate the average catch per unit of effort (CPUE) for each genetic stock group. Plus signs indicate locations of ocean sampling, and the black dotted line traces the 180-m depth contour.

We observed a considerable difference in both CPUE and location of juvenile steelhead between 2006 and the other years of our study period. It is possible that some of the variability in our sampling success was a result of sampling essentially in the right place at the right time, a time and place that varies from year to year. For example, in 2007, we caught no steelhead from the Middle and Upper Snake River and very few steelhead from the Middle and Upper Columbia River or Lower Snake River. The numbers of releases of hatchery-reared steelhead from those areas in 2007 were similar to those in other years (Fish Passage Center, hatchery releases of steelhead during 2006–2016, available from website, accessed February 2017); therefore, the timing of our sampling may have resulted in our failure to catch fish from those stocks. We know that juvenile steelhead do not stay in our study area for long. McMichael et al. (2013) found evidence that juvenile steelhead from the Columbia River migrate away from the mouth of the Columbia River at a faster rate than Chinook salmon and that they exit the plume area soon after entering the ocean, mostly within 3 d. In another study, few juvenile steelhead were caught in trawl hauls conducted 1 month later in June along the same transects used in our study (Daly et al., 2014). It's likely that annual variability in the timing of marine entry and quick migration away from coastal waters, evidenced by the fact that we caught most of our samples at the sampling stations farthest from shore, combined to cause variability in our sampling success.

A thorough evaluation of both freshwater and marine environmental drivers of migration behavior could help describe the interannual and inter-stock differences we found. Flow can influence river migration rate and, therefore, timing of ocean arrival. Temperature and food conditions can alter growth rates, resulting in disparity in size of fish among years or stocks and influencing migration behavior. Importantly, differences in survival can influence the spatial and temporal distributions of the surviving individuals, which are then represented in our catches. However, initial comparisons with some basic measures of environmental variables (river volume, river plume location and volume, and marine temperature and salinity) did not highlight obvious drivers of interannual and inter-stock abundance and distribution (data from these comparisons are not shown).

The baseline of genetic data that we assembled allowed us to identify stock-specific distributions of juvenile steelhead upon their entry into the ocean. The ability to identify the stock of origin of both tagged and untagged steelhead will be invaluable for future research into the possibility that forces that affect the survival of steelhead during early marine migration influence different genetic stock groups differently.

Acknowledgments

We thank the captain and crew of the F/V *Frosti* for providing a safe and professional sampling platform and the many people who assisted with sample collection efforts. Thanks also to B. Beckman, D. Teel, and L. Weitkamp for providing helpful reviews of previous versions of this manuscript.

Literature cited

Blankenship, S. M., M. R. Campbell, J. E. Hess, M. A. Hess, T. W. Kassler, C. C. Kozfkay, A. P. Matala, S. R. Narum, M. M. Paquin, M. P. Small, et al.
2011. Major lineages and metapopulations in Columbia River *Oncorhynchus mykiss* are structured by dynamic landscape features and environments. Trans. Am. Fish. Soc. 140:665–684.

Brodeur, R. D., W. T. Peterson, G. W. Boehlert, E. Casillas, M. H. Schiewe, M. B. Eldridge, S. T. Lindley, J. H. Helle, and W. R. Heard.
2000. A coordinated research plan for estuarine and ocean research on Pacific salmon. Fisheries 25(6):7–16.

Brodeur, R. D., J. P. Fisher, D. J. Teel, R. L. Emmett, E. Casillas, and T. W. Miller.
2004. Juvenile salmonid distribution, growth, condition, origin, and environmental and species associations in the Northern California Current. Fish. Bull. 102:25–46.

Brodeur, R. D., J. P. Fisher, R. L. Emmett, C. A. Morgan, and E. Casillas.
2005. Species composition and community structure of pelagic nekton off Oregon and Washington under variable oceanographic conditions. Mar. Ecol. Prog. Ser. 298:41–57.

Burgner, R. L., J. T. Light, L. Margolis, T. Okazaki, and S. Ito.
1992. Distribution and origins of steelhead trout (*Oncorhynchus mykiss*) in offshore waters of the North Pacific Ocean. Int. N. Pac. Fish. Comm., Bull 51, 95 p. [Available from website.]

Busby, P. J., T. C. Wainwright, G. J. Bryant, L. J. Lierheimer, R. S. Waples, F. W. Waknitz, and I. V. Lagomarsino.
1996. Status review of West Coast steelhead from Washington, Idaho, Oregon, and California. NOAA Tech. Memo. NMFS-NWFSC-27, 181 p.

Daly, E. A., J. A. Scheurer, R. D. Brodeur, L. A. Weitkamp, B. R. Beckman, and J. A. Miller.
2014. Juvenile steelhead distribution, migration, feeding, and growth in the Columbia River estuary, plume, and coastal waters. Mar. Coast. Fish. 6:62–80.

Dawley, E. M., R. D. Ledgerwood, T. H. Blahm, C. W. Sims, J. T. Durkin, R. A. Kirn, A. E. Rankis, G. E. Monan, and F. J. Ossiander.
1986. Migrational characteristics, biological observations, and relative survival of juvenile salmonids entering the Columbia River estuary, 1966–1983, 256 p. Bonneville Power Admin., Portland, OR, and Northwest Alaska Fish. Sci. Cent., Natl. Mar. Fish. Serv., Seattle, WA. [Available from website.]

Furey, N. B., S. P. Vincent, S. G. Hinch, and D. W. Welch.
2015. Variability in migration routes influences early marine survival of juvenile salmon smolts. PLoS ONE 10(10):e0139269.

Hare, S. R., and R. C. Francis.
1995. Climate change and salmon production in the northeast Pacific Ocean. *In* Climate change and northern fish populations (R. J. Beamish, ed.), p. 357–372. Can. Spec. Publ. Fish. Aquat. Sci. 121.

Kalinowski, S. T., K. R. Manlove, and M. L. Taper.
2007. ONCOR: a computer program for genetic stock identification. Montana State Univ., Bozeman, MT. [Available from website, accessed January 2009.]

Matala, A. P., M. W. Ackerman, M. R. Campbell, and S. R. Narum.
2014. Relative contributions of neutral and non-neutral genetic differentiation to inform conservation of steelhead trout across highly variable landscapes. Evol. App. 7:682–701.

McMichael, G. A., A. C. Hanson, R. A. Harnish, and D. M. Trott.
2013. Juvenile salmonid migratory behavior at the mouth of the Columbia River and within the plume. Anim. Biotel. 1:1–14.

Myers, K. W.
2018. Ocean ecology of steelhead. *In* The ocean ecology of Pacific salmon and trout (R. J. Beamish, ed.), p. 779–904. Am. Fish. Soc., Bethesda, MD.

NWFSC (Northwest Fisheries Science Center).
2015. Status review update for Pacific salmon and steelhead listed under the Endangered Species Act: Pacific Northwest, 351 p. [Available from website, accessed July 2018.]

Pearcy, W. G.
1992. Ocean ecology of North Pacific salmonids, 179 p. Univ. Wash. Press, Seattle, WA.

Quinn, T. P., and K. W. Myers.
2004. Anadromy and the marine migrations of Pacific salmon and trout: Rounsefell revisited. Rev. Fish Biol. Fish. 14:421–442.

Rannala, B., and J. L. Mountain.
1997. Detecting immigration by using multilocus genotypes. Proc. Natl. Acad. Sci. U.S.A. 94:9197–9201.

Steele, C. A., E. C. Anderson, M. W. Ackerman, M. A. Hess, N. R. Campbell, S. R. Narum, and M. R. Campbell.
2013. A validation of parentage-based tagging using hatchery steelhead in the Snake River basin. Can. J. Fish. Aquat. Sci. 70:1046–1054.

Teel, D. J., B. J. Burke, D. R. Kuligowski, C. A. Morgan, and D. M. Van Doornik.
2015. Genetic identification of Chinook salmon: stock-specific distributions of juveniles along the Washington and Oregon coasts. Mar. Coast. Fish. 7:274–300.

Van Doornik, D. M., D. J. Teel, D. R. Kuligowski, C. A. Morgan, and E. Casillas.
2007. Genetic analyses provide insight into the early ocean stock distribution and survival of juvenile coho salmon off the coasts of Washington and Oregon. North Am. J. Fish. Manage. 27:220–237.

Weitkamp, L. A., P. J. Bentley, and M. N. C. Litz.
2012. Seasonal and interannual variation in juvenile salmonids and associated fish assemblage in open waters of the lower Columbia River estuary. Fish. Bull. 110:426–450.

Weitkamp, L. A., D. J. Teel, M. Liermann, S. A. Hinton, D. M. Van Doornik, and P. J. Bentley.
2015. Stock-specific size and timing at ocean entry of Columbia River juvenile Chinook salmon and steelhead: implications for early ocean growth. Mar. Coast. Fish. 7:370–392.

National Marine Fisheries Service
NOAA

Fishery Bulletin
established in 1881

Spencer F. Baird
First U.S. Commissioner of Fisheries and founder of *Fishery Bulletin*

Age determination and growth of the blue shark (*Prionace glauca*) in the western North Pacific Ocean

Yuki Fujinami (contact author)[1]
Yasuko Semba[1]
Sho Tanaka[2]

Email address for contact author: y.fuji925@gmail.com

[1] National Research Institute of Far Seas Fisheries
Japan Fisheries Research and Education Agency
5-7-1, Orido, Shimizu
Shizuoka 424-8633, Japan

[2] School of Marine Science and Technology
Tokai University
3-20-1, Orido, Shimizu,
Shizuoka 424-8610, Japan

Abstract—Accurate estimation of growth parameters is vital for stock assessments and management of exploited species. To determine if changes in sex-specific growth parameters of the blue shark (*Prionace glauca*) have occurred in the North Pacific Ocean following population declines in the 1980s and 1990s, we analyzed data obtained from the vertebrae of 659 male and 620 female sharks that had precaudal lengths (PCLs) of 33.4–258.3 cm and were captured over a wide geographic area between 2010 and 2016. Maximum counts of growth bands were 18 for males and 17 for females. Significant (P<0.001) between-sex differences were detected in growth parameters. We estimated parameters of the von Bertalanffy growth function: for males, the theoretical asymptotic length (L_∞) was 284.9 cm PCL, the growth coefficient (k) was 0.117/year, and the theoretical age at zero length (t_0) was −1.35 years, and, for females, L_∞ was 257.2 cm PCL, k was 0.146/year, and t_0 was −0.97 years. Sexual discrepancies in growth rates are likely a function of differences in energy allocation relating to reproduction between sexes. Given that no remarkable change in growth parameters was observed over 3 decades, life history parameters of this population do not appear to have been affected by shifts in stock abundance or environmental fluctuation.

Manuscript submitted 2 June 2018.
Manuscript accepted 18 April 2019.
Fish. Bull. 117:107–120 (2019).
Online publication date: 30 April 2019.
doi: 10.7755/FB.117.1-2.12

The views and opinions expressed or implied in this article are those of the author (or authors) and do not necessarily reflect the position of the National Marine Fisheries Service, NOAA.

The blue shark (*Prionace glauca*) is a large pelagic species found worldwide from temperate waters to the tropics, from 60°N to 50°S (Nakano and Stevens, 2008). This species is one of the most prolific and resilient of all sharks (Smith et al., 1998; Cortés et al., 2010) and the most abundant pelagic shark globally (Nakano and Stevens, 2008). Blue sharks are also a valuable fisheries resource that is commonly caught in pelagic longline fisheries both as a target species and as bycatch (Nakano and Stevens, 2008). Their meat, liver (oil), cartilage, and fins are used in many countries (Clarke et al., 2006; Camhi et al., 2008). Consequently, stock assessments of this species have been conducted by several regional fisheries management organizations to implement appropriate regional conservation and management strategies.

Accurate age and growth information is essential for sustainable management of exploited species. Such basic life history parameters are necessary to estimate population growth rates, age at recruitment, mortality rates, and longevity (Campana, 2001; Goldman et al., 2012; Yokoi et al., 2017). Because sexual dimorphism is common in shark species—with females being typically larger than males (Sims, 2005)—life history parameters should be based on sex-specific growth equations for proper stock assessment and management (Punt and Walker, 1998; Chang and Liu, 2009). Estimates of parameters, such as "spawning biomass" (the term *spawning biomass* is used in stock assessment reports to represent the biomass of reproductive organisms), maximum sustainable yield, and fishing intensity, can be strongly biased when an assessment does not take sexual dimorphism into consideration (Wang et al., 2005).

Several studies have reported age and growth information for blue sharks of the North Pacific Ocean (Cailliet and Bedford, 1983; Tanaka et al., 1990; Nakano, 1994; Blanco-Parra et al., 2008). However, variation in growth parameters reported in these studies could be caused by differences in sample size and size range (e.g., Cailliet and Bedford, 1983; Henderson et al., 2001; Blanco-Parra et al., 2008) and in aging technique and precision (Tanaka et

al., 1990). Additionally, growth parameters of sharks can vary as a consequence of population density (e.g., Sminkey and Musick, 1995; Carlson and Baremore, 2003; Cassoff et al., 2007). Therefore, estimation of growth parameters requires that the effects of these sampling and technical biases be taken into consideration.

It has been considered that the growth parameters described by Nakano (1994), for blue sharks of the North Pacific Ocean, are representative of the life history of this species and for this population (ISC, 2017), given that a relatively large number of samples were collected over a wide area throughout the North Pacific Ocean in 1982 and 1983. However, stock biomass of blue sharks in the North Pacific Ocean decreased in the 1980s, reached their lowest level in the early 1990s, and increased from the mid-1990s to 2005 (Hiraoka et al., 2016; Ohshimo et al., 2016; ISC, 2017). Therefore, it is possible that life history parameters, such as growth rate and age at maturity, of this population had changed over these 3 decades because stock biomass fluctuated widely. Accordingly, our objectives were to determine 1) present-day sex-specific growth parameters of blue sharks in the western North Pacific Ocean, on the basis of analysis of vertebrae of a wide size range collected from a large geographic area throughout the year, and 2) if any change in growth rate had occurred over the last 3 decades.

Materials and methods

Sample collection

Blue sharks were captured between 2010 and 2016 by Japanese research vessels (longline, driftnet, and trawl) and by commercial longliners operating in the western North Pacific Ocean (Fig. 1A). Sex was determined by presence or absence of the male copulatory organs (claspers). Precaudal length (PCL), the distance from the tip of the snout to the precaudal pit, and dorsal length (DL), the distance from the origin of the first dorsal fin to the origin of the second dorsal fin, in a natural position were measured to the nearest centimeter for specimens collected by

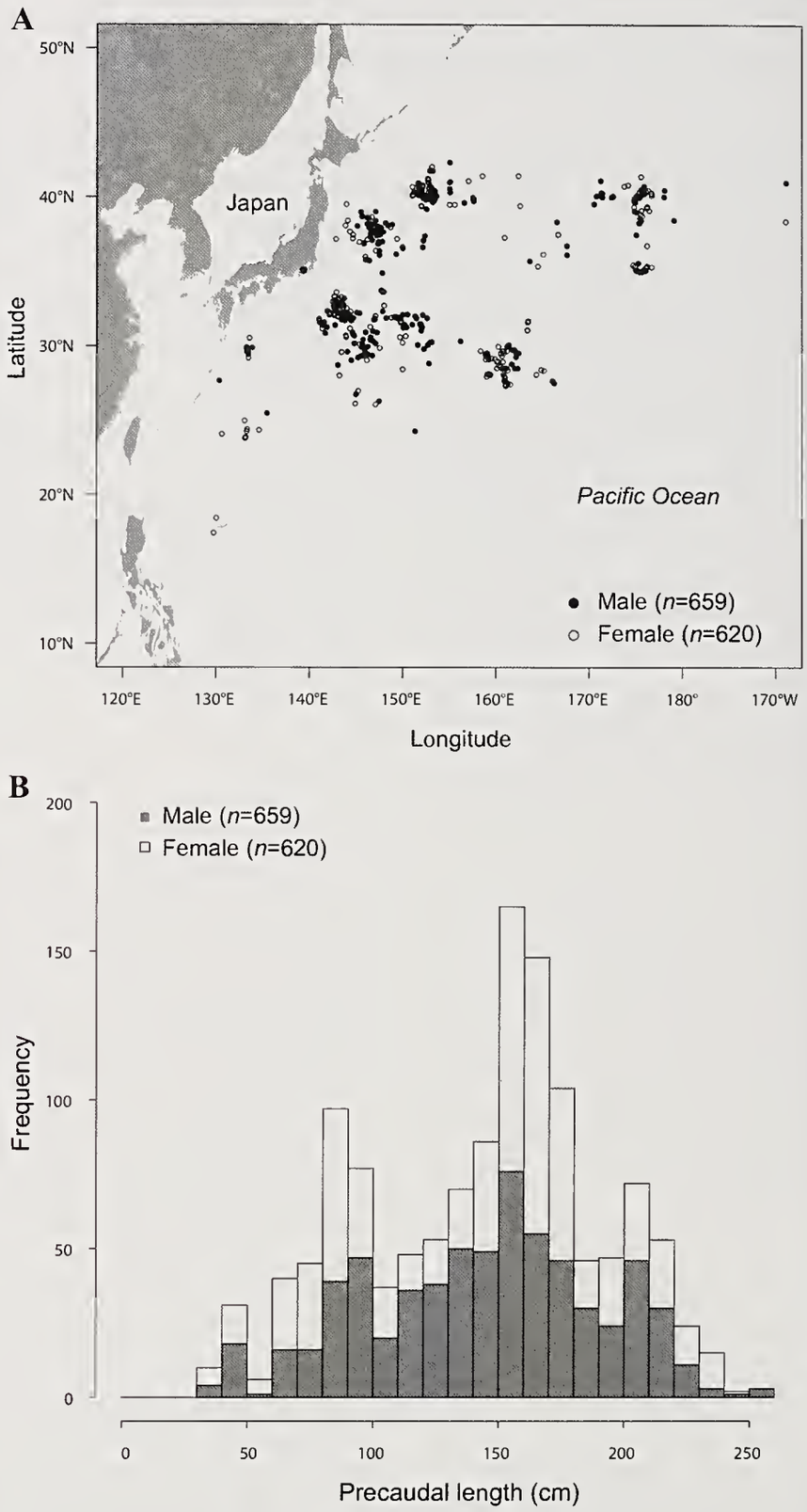

Figure 1

(**A**) Map of sampling locations and (**B**) length-frequency distribution for blue sharks (*Prionace glauca*) captured between 2010 and 2016 in the western North Pacific Ocean. The letter *n* refers to the number of samples used for growth analysis.

using a research vessel. Only DL was measured for sharks caught by commercial vessels because the head and viscera were removed prior to measurement; DL was converted to PCL following Fujinami et al. (2017).

Age determination

Cervical vertebrae were excised from the region above the branchial chamber and stored frozen until processing. Vertebral centra were boiled for approximately 20 min to remove most connective tissue, then stored in 70% ethanol before being washed in running water, soaked in sodium hydroxide solution (5000 mol/m^3 NaOH), and scrubbed with a polishing buff (20-cm microfiber cloth; Sankei Co.[1], Tokyo, Japan) to remove residual connective tissue from their surfaces. After cleaning, centra were washed in running water, cut longitudinally into 2 sections by using a diamond saw (MC-110; Maruto Instrument Co., Tokyo, Japan) with the focus slightly to one side to avoid cutting the focus (Fig. 2A); each half-cut section was then air-dried for 24 h. The centrum radius (CR), from the focus to the edge of the centrum perpendicular to the direction of the cutting plane, was measured to the nearest 0.01 mm by using a digital microscope (VH-8000; Keyence Corp., Osaka, Japan). The CR to PCL relationship was estimated by using linear regression and was compared by sex by using analysis of covariance (ANCOVA).

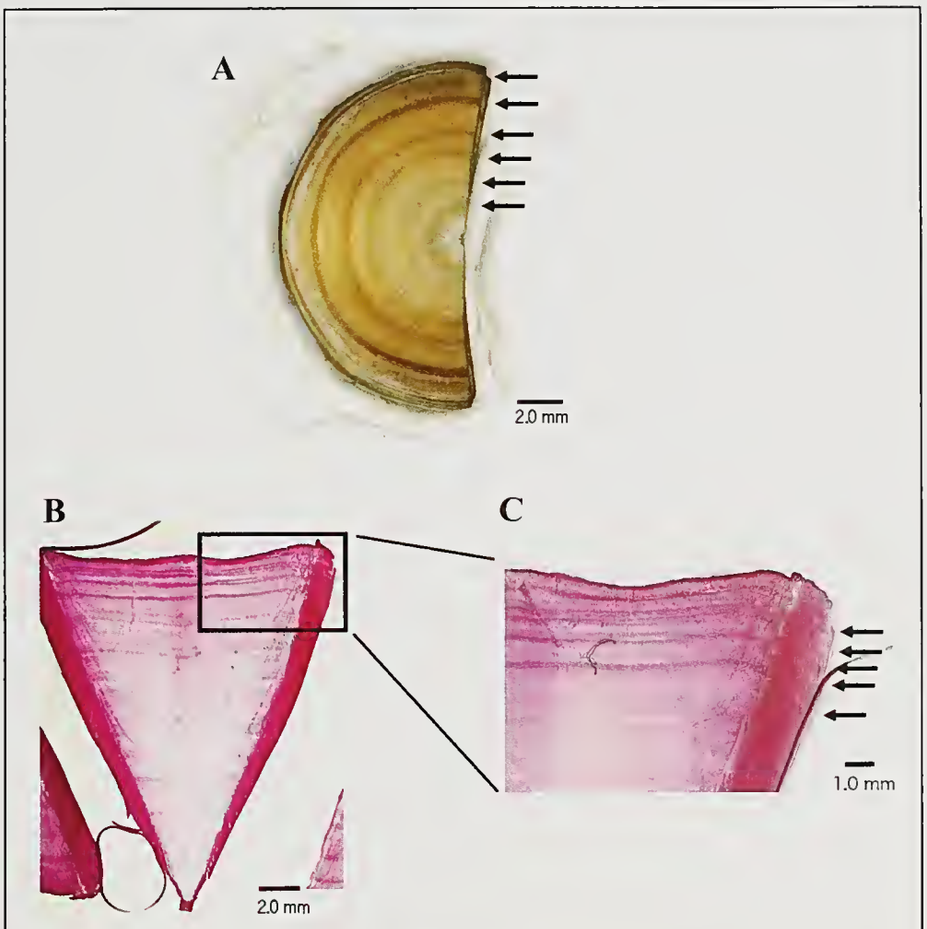

Figure 2

Images of vertebrae from blue sharks (*Prionace glauca*) captured between 2010 and 2016 in the western North Pacific Ocean. Vertebra were treated to enhance growth bands by using (**A**) a burn method and (**B** and **C**) thin-sectioning after staining with alizarin red. Black arrows indicate observed growth bands for 2 sharks of different lengths, one less than and another greater than 200 cm in precaudal length (PCL): (**A**) 181.0 cm PCL and (**B**) 252.0 cm PCL. Panel C provides an enlarged image of the vertebra in panel B.

For blue sharks, Fujinami et al. (2018a) recommended use of a burn method (for younger individuals) simultaneously with other methods, such as thin sectioning, bomb radiocarbon dating, or tag-recapture dating (for older individuals). Accordingly, we used a burn method, which is highly efficient and is accurate for aging of small- and medium-sized blue sharks (<200 cm PCL) (Fujinami et al., 2018a), and a thin-sectioning method, which is useful for aging older sharks (e.g., Matta et al., 2017).

Growth bands on vertebrae of specimens less than 200 cm PCL were enhanced by burning the centrum in accordance with Fujinami et al. (2018a). Vertebral centra were heated to 250°C in a drying oven (DO-300A; AS ONE Corp., Osaka, Japan) for 6–12 min (Fig. 2A). For larger specimens (>200 cm PCL), centra were sectioned (1.0 mm) by using a sliding microtome (Retoratome REM-710; Yamato Kohki Industrial Co., Asaka, Japan) without embedding, after they were cleaned and cut in half as described previously. Sections were stained with alizarin red for 2 min in accordance with Berry et al. (1977) and rinsed in running tap water for approximately 10 min (Fig. 2B). Finally, stained sections were dehydrated through a graded ethanol series (70%, 80%, 90%, and 100%) and mounted on microscope slides.

Burned centra were observed by using the shadowing method (Francis and Maolagáin, 2000; Semba et al., 2009) with a digital microscope and fiber-optic light. Sections were observed by using an SZX7 stereo microscope (Olympus Corp., Tokyo, Japan) with reflected light. We defined a growth-band pair as one convex band (dark, narrow) and one concave band (light, broad) on the centrum surface when the burn method was used, and we defined a band pair as one

[1] Mention of trade names or commercial companies is for identification purposes only and does not imply endorsement by the National Marine Fisheries Service, NOAA.

translucent band and one opaque band on the corpus calcareum when the thin-sectioning method was used. We counted the number of convex structures for the burn method and translucent bands for the sectioning method. A single reader (reader 1: senior author) twice counted bands at 2 different times without prior knowledge of specimen length. A third count was made if the first and second counts did not coincide. If the third count was the same as either the first or second count, the duplicated measure was used in analysis; if the third count did not agree, a sample was excluded from analysis. A random subsample of 200 individuals was read by a separate reader (reader 2: S. Tanaka) to ensure consensus in interpretation of growth bands. To evaluate inter- (both readers) and intrareader (reader 1) aging precision, an index of average percentage error (IAPE) (Beamish and Fournier, 1981) and mean coefficient of variation (CV) (Chang, 1982) were calculated. An age-bias plot also was constructed to test inter- and intrareader counts (Campana et al., 1995).

For age estimation, we assumed a tentative birth date of 1 June on the basis of the birth season estimated by Fujinami et al. (2017). The first band (birth band) was considered to be formed after parturition on the basis of the observation of vertebral centra of near-term embryos and neonates (see the "Results" section). In addition, we assumed subsequent growth bands formed annually, on 1 December (see the "Results" section); therefore, the age of each specimen was calculated as follows:

$$Age = (\alpha - 1) + \frac{(\beta - 6)}{12} (\alpha \geq 1, 1 \leq \beta \leq 12), \quad (1)$$

where α = the number of convex structures (translucent bands) deposited after the birth band; and
β = the month when the individual was caught.

Age verification

To verify periodicity of growth-band formation, the most peripheral structure on each centrum was classified as either convex (translucent) or concave (opaque). We analyzed monthly changes in frequency of each band on the centrum edge throughout the year. The periodicity of growth-band pairs was verified by using a statistical model developed by Okamura and Semba (2009). Three models were constructed according to different periodicities of growth-band formation: an annual cycle, a biannual cycle, or no seasonal cycle. Okamura and Semba (2009) suggested that the model with the lowest Akaike's information criterion (Burnham and Anderson, 2002) is preferred because it is estimated to be closest to the unknown reality that generated the data. Vertebral centra with only one band (birth band) were excluded from analysis.

Growth analysis

The von Bertalanffy growth function (von Bertalanffy, 1938) was fitted to observed length-at-age data by using the maximum likelihood approach with the optim function in R (vers. 3.3.0; R Core Team, 2016), as follows:

$$L_t = L_\infty (1 - e^{-k(t - t_0)}), \quad (2)$$

where L_t = the predicted length at age t (in years);
L_∞ = the theoretical asymptotic length (in centimeters);
k = the growth coefficient (per year); and
t_0 = the theoretical age at zero length.

We used Kimura's likelihood ratio to test for a significant difference in the growth parameters of males and females (Kimura, 1980). We tested the null hypothesis (H_0, all parameters are different between sexes) versus the alternative hypothesis (H_1–H_3, the sex-specific growth model, in which one of the parameters is shared for each sex, and H_4, all parameters are shared between sexes). The 95% confidence intervals (95% CIs) of parameter estimates were derived from 2000 resampled data sets by using the bootstrap method.

Theoretical longevity (t_{max}) was estimated following methods of Taylor (1958) and Fabens (1965):

$$t_{max} = t_0 - \frac{\ln(0.05)}{k} \text{ (Taylor, 1958) and} \quad (3)$$

$$t_{max} = 5\frac{(\ln_2)}{k} \text{ (Fabens, 1965).} \quad (4)$$

Age at maturity and maternity

According to criteria described by Fujinami et al. (2017), sexual maturation in males was classified into 3 stages on the basis of calcification of the claspers and testis development (for details, see Suppl. Table 1) (online only): 1) immature juvenile, 2) maturing juvenile, and 3) mature adult. For females, sexual maturity was assessed on the basis of uterine width, ovarian development, and the presence of embryos or fertilized eggs, with 5 stages recognized (for details, see Suppl. Table 1) (online only): 1) immature juvenile, 2) maturing juvenile, 3) mature adult, 4) mature pregnant, and 5) mature postpartum. The maturation stage of each specimen was converted into binary data (immature=0, mature=1) at age intervals of 1 year for statistical analysis. A logistic regression model was fitted to the binomial maturity data, to determine ages at 50% maturity for both sexes, as follows:

$$Y = 1 / [1 + exp\{-(\alpha + \beta\chi)\}], \quad (5)$$

where Y = the proportion of mature individuals of each age;
χ = age; and
α and β = coefficients.

A generalized linear model with a binomial error structure and logit-link function was used to estimate the α and β coefficients by using R. Female maternity ogive also was determined by using maternal condition according to criteria described by Fujinami et al. (2017) (for details, see Suppl. Table 1) (online only). Data for maternal condition (pregnant or postpartum) or non-maternal condition (immature or non-pregnant mature)

Table 1

Monthly numbers of vertebrae used for age determination of blue sharks (*Prionace glauca*) captured in 2010–2016 in the western North Pacific Ocean.

	Month												
Sex	Jan.	Feb.	March	April	May	June	July	Aug.	Sep.	Oct.	Nov.	Dec.	Total
Male	51	31	25	66	107	74	39	15	29	65	85	72	659
Female	25	44	42	65	61	61	29	0	22	69	97	105	620
Total	76	75	67	131	168	135	68	15	51	134	182	177	1279

were converted to binomial data (non-maternal condition=0, maternal condition=1). The logistic function was fitted to these data in the same way as it was fitted to the maturity data for estimating age at 50% maturity.

Results

Age determination and verification

Cervical vertebrae were collected from 1347 blue sharks (688 males, 645 females, and 14 sex undetermined). Of these sharks, for growth analysis, we used data for 1279 individuals (659 males and 620 females; Table 1), which had PCLs of 33.4–258.3 cm for males and 33.4–243.3 cm for females (Fig. 1B). The sex-specific relationship between CR and PCL trended in a linear fashion, with no significant difference between sexes (ANCOVA: F=3.70, P=0.06). The sex-combined equation for the relationship of CR and PCL was PCL=15.96CR+20.85 (coefficient of determination [r^2]=0.920, n=1279).

Counts of growth bands were 1–18 for males and 1–17 for females. There was a high level of both inter- and intrareader agreement in band counts (Fig. 3, A and B). However, errors associated with age estimates of older sharks were larger than those associated with ages for younger sharks, although sample sizes were small. In repeat counts by reader 1, the counts for 710 samples (55.5%) agreed completely and the counts for 467 samples (36.5%) differed by one band. For inter-reader comparison of counts of 200 vertebrae, the counts for 86 samples (43.0%) agreed completely

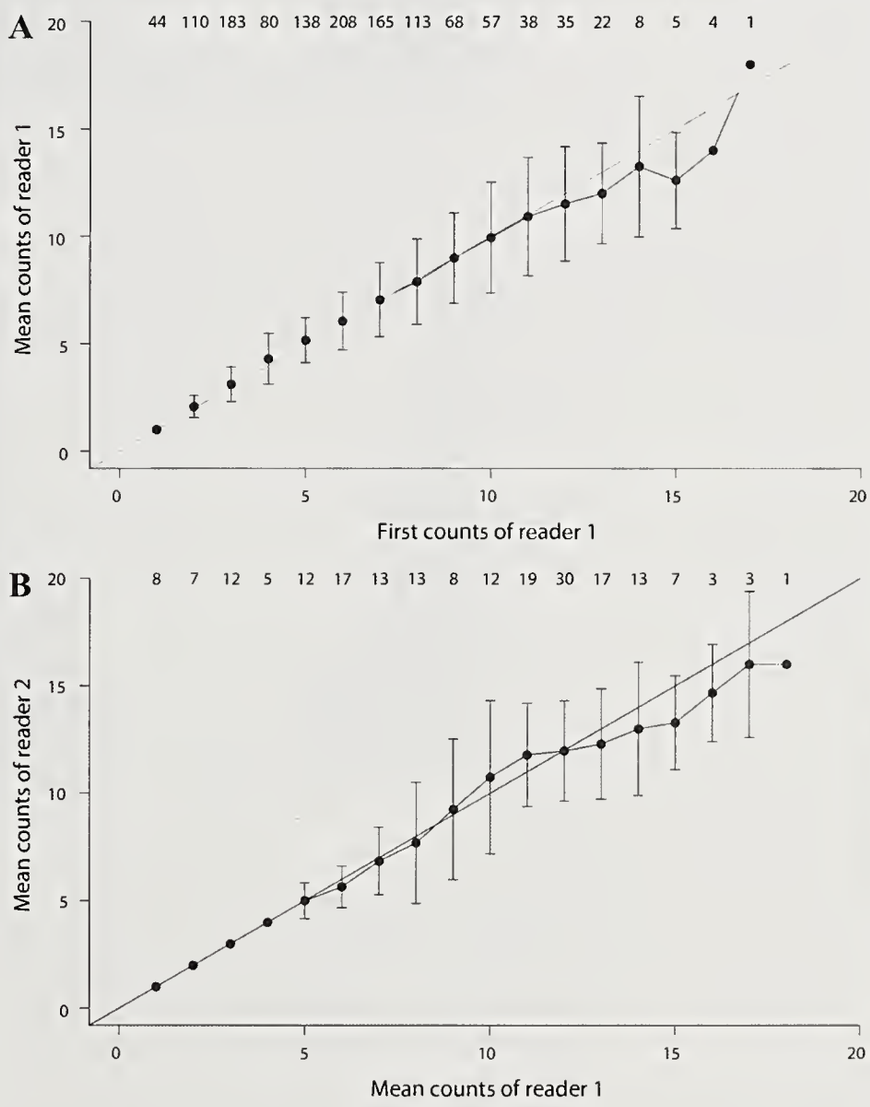
A
44 110 183 80 138 208 165 113 68 57 38 35 22 8 5 4 1
Mean counts of reader 1
First counts of reader 1
B
8 7 12 5 12 17 13 13 8 12 19 30 17 13 7 3 3 1
Mean counts of reader 2
Mean counts of reader 1

Figure 3

Age-bias plots of pairwise comparison of vertebral counts (**A**) by reader 1 (intrareader: first counts versus mean counts) and (**B**) by separate readers (inter-reader: reader 1 versus reader 2) for blue sharks (*Prionace glauca*) captured between 2010 and 2016 in the western North Pacific Ocean. Error bars represent 95% confidence intervals. The diagonal line indicates 1:1 equivalence. Numbers at the top of the graph denote the sample sizes for each count.

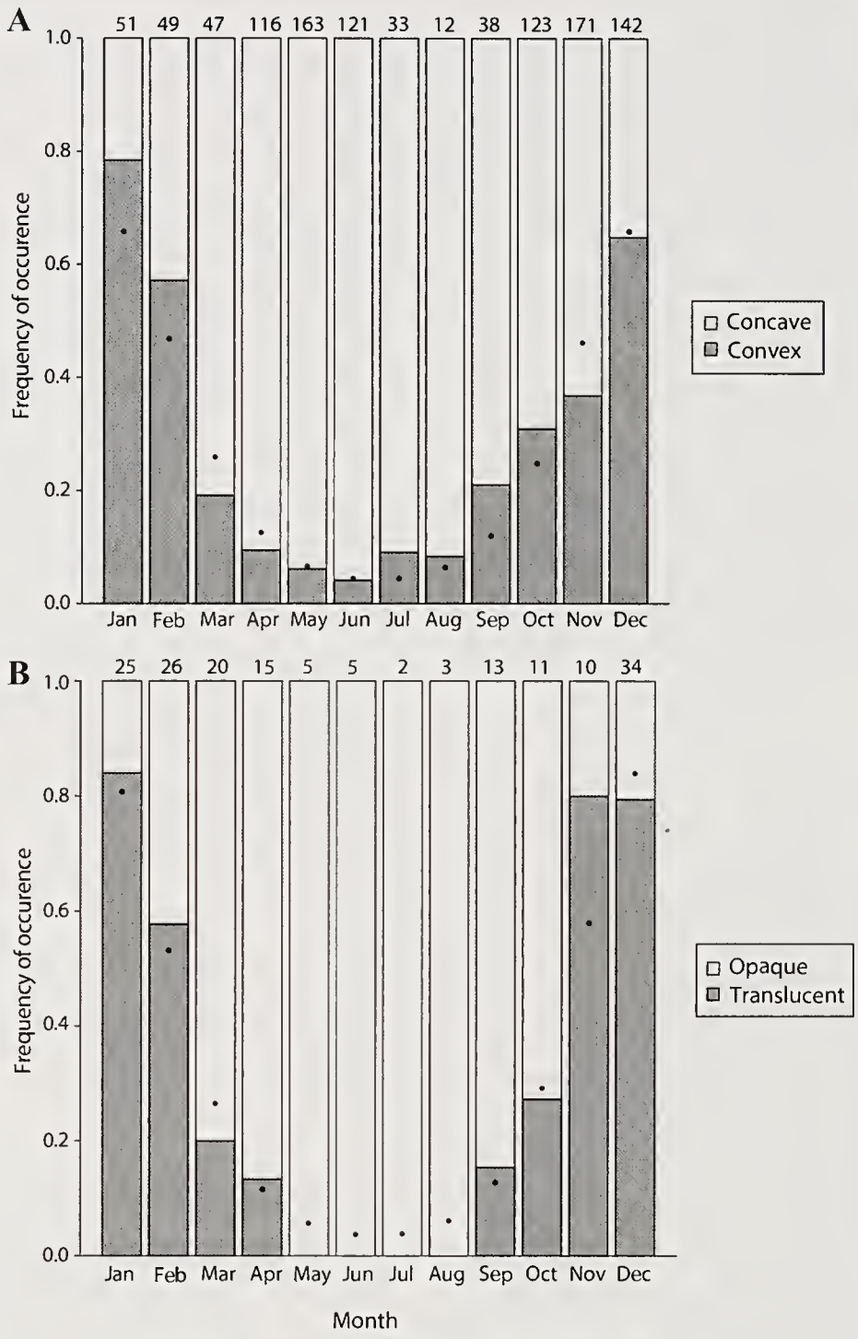

Figure 4

Monthly changes in frequency of occurrence for (**A**) convex and concave structures observed on vertebral centra of blue sharks (*Prionace glauca*) less than 200 cm precaudal length (PCL) and (**B**) translucent and opaque band pairs observed on centrum edges for blue sharks larger than 200 cm PCL. Sharks were captured in the western North Pacific Ocean during 2010–2016. The black dots denote the probability of an annual cycle for growth-band formation, predicted by using the model of Okamura and Semba (2009). The numbers above bars represent monthly sample size.

and the counts for 61 samples (30.5%) differed by only one band. For intra- (reader 1) and inter-reader (reader 1–2) evaluations of precision, the IAPE values were 3.7% and 5.3% and the CV values were 4.2% and 5.9%. No pre-birth band was apparent on near-term embryos captured in May, but one growth (narrow) band was apparent on neonates captured in late June and July.

Monthly characterization of the centrum edge differed throughout the year both for specimens less than 200 cm PCL (n=1066) and for specimens greater than 200 cm PCL (n=169) (Fig. 4). The proportion of con-

Table 2

Comparison of goodness of fit for statistical models developed for 3 different periodicities of growth-band formation in blue sharks (*Prionace glauca*) of 2 size classes defined by precaudal length (PCL). The model with the lowest Akaike's information criterion (AIC) is preferred because it is estimated to be closest to the unknown reality that generated the data. The ΔAIC statistic is the relative difference between the best model (which has an ΔAIC of zero) and each of the other models in the set.

Size class	Periodicity of band formation	AIC	ΔAIC
Individuals <200 cm PCL	Annual cycle	1009.8	0.0
	Biannual cycle	1232.5	222.7
	No cycle	1283.7	273.9
Individuals >200 cm PCL	Annual cycle	169.0	0.0
	Biannual cycle	240.1	71.1
	No cycle	236.1	67.1

Table 3

Results from likelihood ratio tests (Kimura, 1980) for the von Bertalanffy growth model used to examine differences in growth parameters between male and female blue sharks (*Prionace glauca*) in the western North Pacific Ocean. The parameters of the von Bertalanffy growth model are the theoretical asymptotic length (L_∞), measured in centimeters in precaudal length; the annual growth coefficient (k); and the theoretical age, measured in years, at zero length (t_0). H_0=null hypothesis (all growth parameters differ by sex).

		Male			Female				
Test	Hypothesis	L_∞	k	t_0	L_∞	k	t_0	χ^2	P-value
H_0 vs. H_1	L_∞ (male) = L_∞ (female)	267.4	0.134	−1.16	267.4	0.133	−1.10	16.36	<0.001
H_0 vs. H_2	k (male) = k (female)	268.6	0.133	−1.14	266.5	0.133	−1.12	14.94	<0.001
H_0 vs. H_3	t_0 (male) = t_0 (female)	273.4	0.130	−1.14	263.0	0.136	−1.14	12.37	<0.001
H_0 vs. H_4	All parameters same between sexes	267.1	0.134	−1.13	267.1	0.134	−1.13	21.66	<0.001

vex structures (Fig. 4A) and translucent bands (Fig. 4B) tended to increase from the boreal autumn to winter, peaking in January, and to be lowest in summer. In contrast, concave structures (Fig. 4A) and opaque bands (Fig. 4B) were prevalent in summer and least common in winter. The results of the statistical analysis of Okamura and Semba (2009) indicate that the annual cycle of band formation was most plausible because the model with that periodicity had the smallest Akaike's information criterion (Table 2).

Growth parameters

There was a significant difference between the sexes in estimates for parameters of the von Bertalanffy growth function (Table 3). Females had a higher growth coefficient (k=0.146/year) than males (k=0.117/year), but their theoretical asymptotic length (L_∞=257.2 cm PCL) was shorter than that for males (L_∞=284.9 cm PCL) (Table 4, Fig. 5). Growth rates of both sexes were similar until an age of approximately 7 years, after which the female growth rate gradually decreased relative to that for males of the same age.

The maximum observed age was 17.3 years for males and 15.8 years for females. Theoretical longevity estimates, calculated by using methods of Taylor (1958) and Fabens (1965), were 24.3 and 29.6 years for males and 19.5 and 23.7 years for females. These values were greater than the maximum observed age for either sex.

Age at maturity and maternity

Maturity data were available for 414 males (33.4–252.0 cm PCL) and 365 females (33.4–238.0 cm PCL). The youngest mature individuals were 4.0 years old, and, for both sexes, the maximum age recorded for an immature individual was 7.0 years. The age at which 50% of males were mature was 5.9 years (95% CI: 5.3–6.4 years), and that of females was 5.3 years (95% CI: 4.7–5.7 years) (Fig. 6, A and B). Maternity condition data were available for 354 females (33.4–238.0 cm PCL); the age at which 50% of females were in maternal con-

Table 4

Estimates, with 95% confidence intervals (95% CIs), of the parameters for the von Bertalanffy growth model used to examine differences in growth parameters between sexes for blue sharks (*Prionace glauca*) in the western North Pacific Ocean. The parameters are the theoretical asymptotic length (L_∞), measured in centimeters in precaudal length; the annual growth coefficient (k); and the theoretical age, measured in years, at zero length (t_0).

Sex	Parameter	L_∞	k	t_0
Male	Estimate	284.9	0.117	−1.35
	Lower 95% CI	258.0	0.109	−1.44
	Upper 95% CI	294.6	0.145	−0.90
Female	Estimate	257.2	0.146	−0.97
	Lower 95% CI	246.6	0.131	−1.17
	Upper 95% CI	267.6	0.163	−0.79

dition was 6.7 years (95% CI: 6.3–7.2 years) (Fig. 6C), an age that is 1.4 years older than the estimate of age at 50% maturity for females.

Discussion

In this study, we simultaneously used a burn method (Fujinami et al., 2018a) for specimens less than 200 cm PCL and a thin-sectioning method (e.g., Matta et al., 2017) for individuals greater than 200 cm PCL. Ages of blue sharks of the North Pacific Ocean have been determined previously by using silver nitrate impregnation and thin-sectioning methods (Table 5). The convex and concave structures that we observed by using the burn method correspond with the translucent and opaque bands apparent in silver nitrate impregnation (Fujinami et al., 2018a) and sectioning with alizarin red for older specimens, respectively, indicating that our approach with simultaneous use of a burn method and sectioning provides comparable age estimates for the size range compared. The precision of ages estimated by using a burn method and silver nitrate impregnation was high for small- and medium-sized individuals (<200 cm PCL), particularly when the burn method was used, and the precision for both methods was lower for older specimens (Fujinami et al., 2018a). Use of the burn method tended to result in counts of fewer bands than the use of the thin-sectioning method when band counts exceeded 11, for a subsample (n=97) of individuals exceeding 190 cm PCL (Suppl. Table 2) (online only). Shark vertebral growth and band-pair deposition are both tightly linked to somatic growth; therefore, vertebral growth decreases in older specimens (i.e., the vertebral edge narrows in older sharks) (Natanson et al., 2018). Such limited growth for older specimens is detectable in thin sections; however, it is much more difficult to determine in intact vertebrae (Matta et al., 2017). Consequently, we believe that the simultaneous use of burn and thin-sectioning methods provides a more accurate estimate of age than the use of only a single method.

We observed banding patterns in blue sharks similar to those reported previously. Nakano (1994) suggested that the birth band of blue sharks of the North Pacific Ocean forms just after summer and that subsequent growth bands form annually in the boreal winter (on the basis of silver nitrate impregnation). Slow growth-zone formation from late autumn to winter and fast growth-zone formation during spring and summer also were reported by Wells et al. (2017) on the basis of research that involved analysis of vertebrae from blue sharks injected with oxytetracycline and tagged and recaptured in the eastern North Pacific Ocean. Our results, from the use of both burn and thin-sectioning methods, are similar to those of previous studies in the North Pacific Ocean: narrow bands (slow growth) are formed in the winter, and broad bands (fast growth) are formed in the summer. Therefore, we assert that growth-band deposition after the birth band in blue sharks of the North Pacific Ocean occurs annually, regardless of the aging technique and geographic area of sampling used to estimate ages. Consequently, the increment between the first and second bands represents about 6 months of growth (tentative birth period in June, subsequent band formation in December)—a result similar to that reported by Nakano (1994). Similar patterns also have been reported in other species, such as the blacktip shark (*Carcharhinus limbatus*) (Branstetter, 1987) and the shortfin mako (*Isurus oxyrinchus*) (Semba et al., 2009). Several triggers, such as environment experienced (e.g., water temperature), prey availability, physiological differences, and movement patterns, might be related to postnatal band formation (e.g., Natanson and Cailliet, 1990; Wells et al., 2017).

The asymptotic length of blue sharks in the eastern North Pacific Ocean (Cailliet and Bedford, 1983; Blanco-Parra et al., 2008) is much smaller than that of blue sharks in the western North Pacific Ocean (Tanaka et al., 1990; Nakano, 1994; and herein, see Table 5). To provide quantitative estimation for growth parameters, access to specimens from neonate to larger and older individuals is necessary because estimates of growth parameters generally are affected by small sample sizes of small or large specimens (Campana, 2001; Goldman et al., 2012). Growth parameters we report for this study differ from those reported for sharks in the eastern North Pacific Ocean (Cailliet and Bedford, 1983; Blanco-Parra et al., 2008), possibly because few larger and older specimens (most individuals were less than 200 cm PCL) were represented in samples in those studies. The size range of specimens reported from the central South Pacific Ocean by Joung et al. (2017) is similar to the range we report, as are estimates of growth parameters, especially asymptotic length (Table 5). However, our estimated female as-

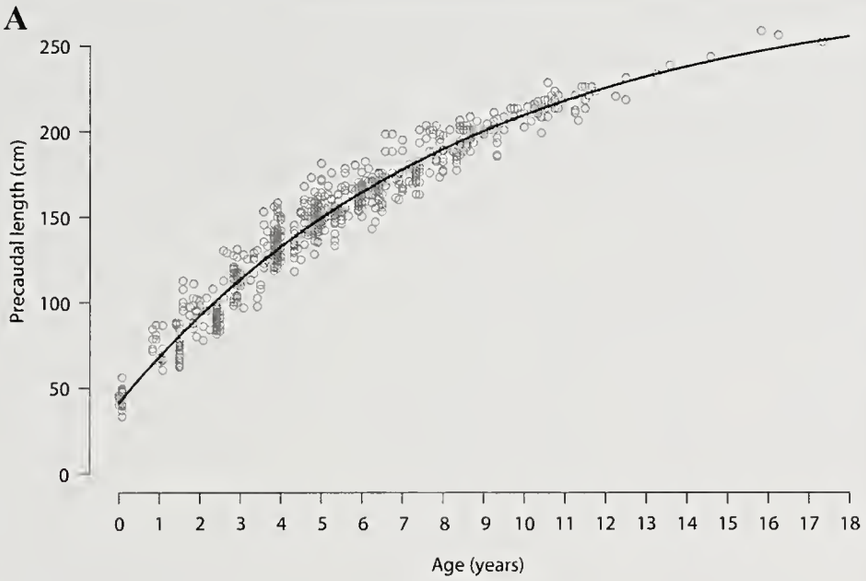

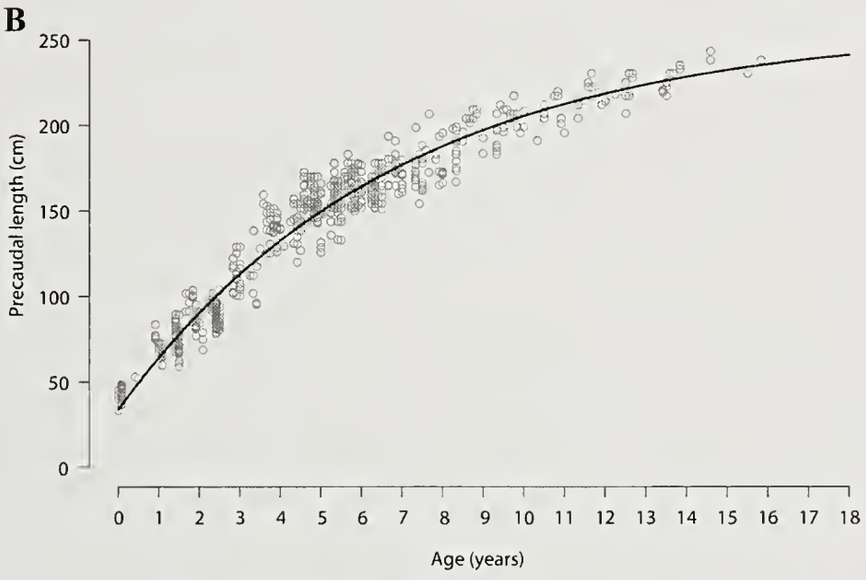

Figure 5

Plot of von Bertalanffy growth curves fitted to observed length-at-age data for (**A**) male and (**B**) female blue sharks (*Prionace glauca*) captured between 2010 and 2016 in the western North Pacific Ocean.

ymptotic length is less than that reported for the North Atlantic Ocean (Skomal and Natanson, 2003; Table 5), possibly because a greater size range of individuals was examined in that study. Although we cannot discount the possibility of underestimation, we can assert that, at least for blue sharks in the North Pacific Ocean, our estimation of growth parameters used more specimens of a greater size range than that of any previous study.

Another possible reason for variation in growth parameters among studies could be differences in aging technique and precision (Tanaka et al, 1990). Whereas most previous studies on blue sharks of the North Pacific Ocean have used silver nitrate impregnation to age specimens (Table 5), we simultaneously used 2 complementary techniques (burn and thin-sectioning methods) to effectively age sharks of different lengths (Fujinami et al., 2018a). As discussed previously, growth bands apparent from the use of a burn method and silver nitrate impregnation are comparable; therefore, we consider any effect of technique to be slight. Furthermore, because we used the thin-sectioning method on older sharks, we minimized underestimation of age. The aging precision (IAPE and CV) that we achieved by combining techniques is comparable to that from the use of a single technique like thin sectioning (Lessa et al., 2004), silver nitrate impregnation (Blanco-Parra et al., 2008), or X-ray imaging (Joung et al., 2017; Joung et al., 2018). Consequently, our aging

Table 5

Estimates of growth parameters of the von Bertalanffy growth function for blue sharks (*Prionace glauca*) from previous studies. Total lengths (TLs) and fork lengths (FLs) from studies were converted to precaudal length (PCL) by using conversion factors of Fujinami et al. (2017). The parameters are the theoretical asymptotic length (L_∞), measured in centimeters; the annual growth coefficient (k); and the theoretical age, measured in years, at zero length (t_0). n=sample size used in the age determination.

Region	Sex	n	Size range (cm PCL)	L_∞	k	t_0	Max. age	Aging method	Study citation
N Pacific	Male	43	–	284.8	0.10	−1.38	11	Stained thin section	Tanaka et al. (1990)
	Female	152	–	233.4	0.16	−1.01	8		
N Pacific	Male	148	–	289.7	0.13	−0.76	10	Silver nitrate staining	Nakano (1994)
	Female	123	–	243.3	0.14	−0.85	10		
NE Pacific	Male	38	18.1–192.9	226.6	0.18	−1.11	9	Silver nitrate staining	Cailliet and Bedford (1983)
	Female	88		184.9	0.25	−0.80	9		
NE Pacific	Male	122	59.4–206.9	230.1	0.10	−2.44	16	Silver nitrate staining	Blanco-Parra et al. (2008)
	Female	62	66.5–192.8	181.5	0.15	−2.15	12		
NW Pacific	Male	659	33.4–258.3	284.9	0.12	−1.35	17	Burn method and stained thin section	This study
	Female	620	33.4–243.3	257.2	0.15	−0.97	16		
Central S Pacific	Male	173	87.5–242.0	290.0	0.13	−1.48	15	X-ray image	Joung et al. (2018)
	Female	86	82.1–227.9	254.0	0.16	−1.29	11		
N Atlantic	Combined	411	44.9–286.8	263.6	0.17	−1.43	16	Thin section	Skomal and Natanson (2003)
	Male	287		259.5	0.18	−1.35	16		
	Female	119		285.7	0.13	−1.77	15		
NE Atlantic	Combined	159	46.2–174.1	289.9	0.12	−1.33	6	Unstained whole	Henderson et al. (2001)
S Atlantic	Combined	742	74.3–249.8	270.9	0.13	−1.31	15	X-ray image	Joung et al. (2017)
SW Atlantic	Combined	236	131.8–238.1	270.9	0.16	−1.01	12	Thin section	Lessa et al. (2004)

precision was greater than reference IAPE and CV values (Campana, 2001) that are considered acceptable.

Our findings indicate that male blue sharks grow larger than females and that the difference in growth rate occurs after females reproduce (after the age of approximately 7 years). This fact is widely supported by previous studies for blue sharks of the Pacific Ocean (Table 5). However, although the occurrence of sexual differences in growth is well known in elasmobranchs, females typically grow larger than males (e.g., Cortés, 2000). Skomal and Natanson (2003) provided the only previous report of female blue sharks growing larger than males, but they considered the extremely large female (286.8 cm in calculated PCL, Table 5) in their study to be very rare given natural mortality. Skomal and Natanson (2003) also reported that differences in female growth began at ~7 years of age. Therefore, sexual differences in growth rates of blue sharks are likely attributable to differential energy allocation between sexes, as has been reported for several other shark species (e.g., Semba et al., 2009; Joung et al., 2018). In general, the onset of maturity results in reduced energy allocation toward growth and in increased allocation toward reproduction (Jensen, 1985) because mating, gestation, and parturition in female sharks consumes considerable energy (Francis and Duffy, 2005). Blue sharks are one of the most productive (high fecundity and annual reproductive cycle) viviparous sharks (Fujinami et al., 2017), unlike others in the family Carcharhinidae, indicating that females may expend more energy than males on reproduction (e.g., mating, gestation, pupping, and migration related to reproduction) and more energy on reproduction than on somatic growth following sexual maturation.

Whereas the male asymptotic length from our study is similar to that from Nakano (1994), the asymptotic length for females from our study is slightly greater (257.2 cm PCL, Table 5), possibly because we examined a greater number of large-sized females. Nevertheless, our growth parameters do not differ remarkably from those of Nakano (1994), indicating that shark growth rates have not changed demonstrably with shifts in stock abundance from the 1980s to the 2010s.

The most recent stock assessment of blue sharks in the North Pacific Ocean reported a prompt recovery of spawning biomass (ISC, 2017). Estimated female spawning biomass exceeded 300,000 metric tons (t) in the early 1980s, decreased to approximately 200,000 t in the 1990s, and began recovery from the late 1990s to reach 300,000 t in the 2010s. This upward population trend has been attributed to a decrease in fishing pressure following prohibition of high seas drift nets in 1992 and subsequent decrease in the numbers of longline vessels (Hiraoka et al., 2016). Although the difference in spawning biomass of blue sharks from the North Pacific Ocean between the early 1980s (Nakano, 1994) and the 2010s (our study) is not great, the biomass in the intervening years fluctuated considerably.

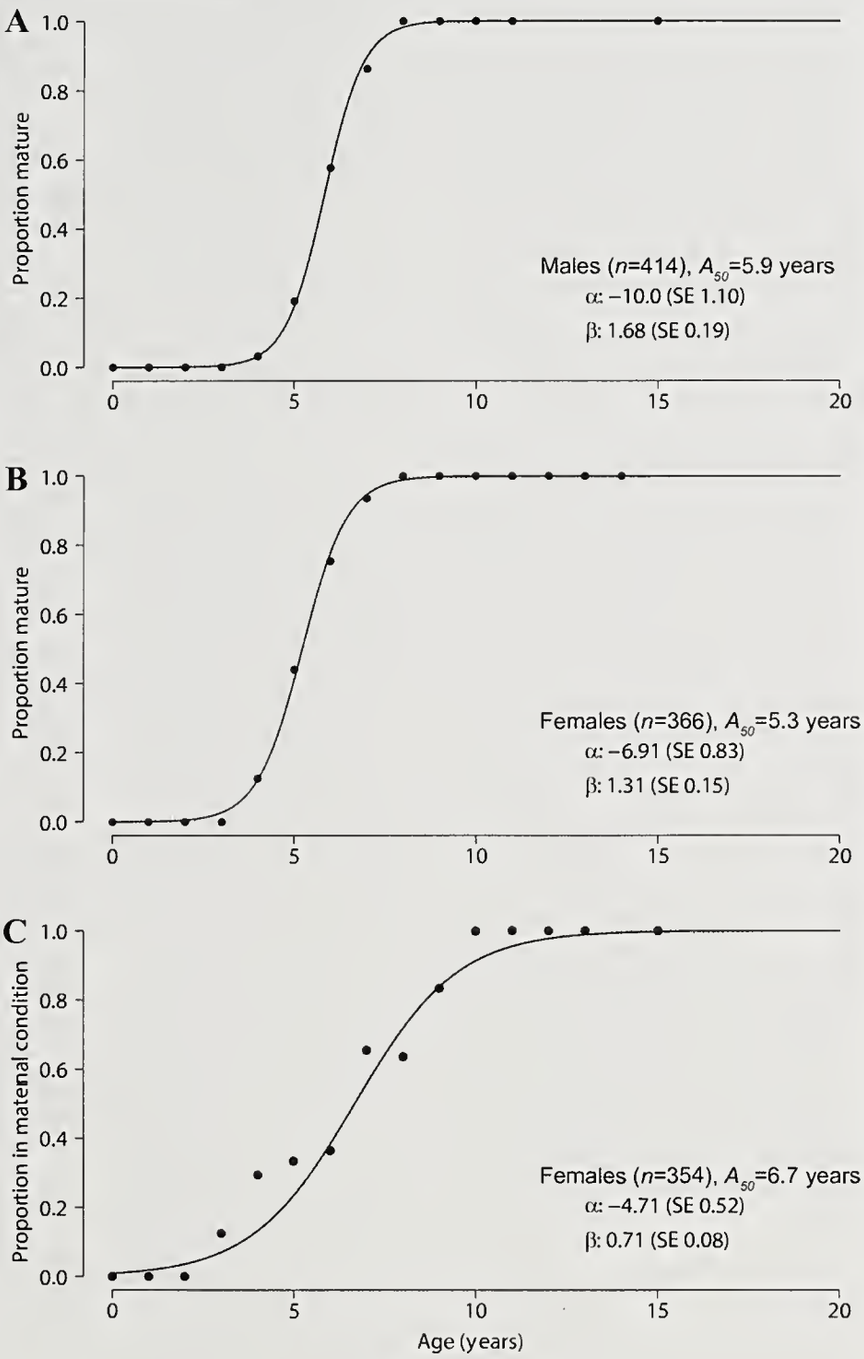

Figure 6

Maturity ogives for (**A**) male and (**B**) female blue sharks (*Prionace glauca*) and (**C**) maternity ogive for female blue sharks captured in the western North Pacific Ocean during 2010–2016. The dotted lines indicate 95% confidence intervals. Also provided are the age at 50% maturity (A_{50}) as well as the coefficients α and β with standard errors (SEs).

One possible reason for the variation is that growth and sexual maturation may have changed concomitant with declines in shark abundance during the 1980s, but, along with a rebounding of this population during the mid-1990s and 2005, these parameters might have recovered to and reached values comparable to pre-decline levels of the 1980s. Alternatively, the rapid stock fluctuation of the 1980s and 1990s might have had no effect on growth and maturation of blue sharks of the North Pacific Ocean. Reproductive parameters (e.g., size at maturity and gestation period) of sharks in the western North Pacific Ocean during 2010–2016 (Fujinami et al., 2017) differ little from those reported by Nakano (1994) for the period from 1978 to 1987.

Because a compensatory response can take a long time (e.g., Carlson and Baremore, 2003), the second of these explanations is more plausible.

Blue sharks have a considerable geographic range, from coastal to pelagic waters and from temperate regions to the tropics (Nakano and Stevens, 2008) in sea temperatures of 5.6–28.0°C (Nakano and Seki, 2003). This species is also an opportunistic feeder, with a diet that reflects abundance of local prey, such as fish and squid (e.g., Preti et al., 2012; Fujinami et al., 2018b). As such, blue sharks are likely tolerant of fluctuations in food resources, buffering the species from anthropogenic stress and changes in environmental conditions, such as water temperature (Levitus et al., 2005; Levitus et al., 2012) and prey abundance (Chavez et al., 2003). In addition to its high adaptability, this species' relatively fast growth and high productivity probably explain why it has been able to maintain high biomass levels, outnumbering other shark species in pelagic waters.

We establish that growth parameters of blue sharks of the North Pacific Ocean have not changed remarkably from levels observed from the 1980s to the present day, despite changes in stock abundance or environmental conditions. Because male blue sharks grew larger than females, and after the age of about 7 years had growth rates different from females, we believe a sex-specific approach for assessing stocks of blue sharks in the North Pacific Ocean is necessary. Given the number of samples in our study, their size range, and the accuracy of our aging technique, we believe the growth parameters that we report are appropriate for future stock assessments and management of blue sharks in the North Pacific Ocean. Bomb radiocarbon dating and tag-recapture techniques would further clarify growth rates of these sharks, given that current methods and structure-based aging techniques might underestimate age, especially for larger and older individuals (Harry, 2018; Natanson et al., 2018).

Acknowledgments

We appreciate the prolonged help of M. Sakai, H. Kidokoro, S. Suyama, J. Abo, K. Ishida, T. Oyama, M. Onodera, and S. Onodera, Japan Fisheries Research and Education Agency, and of M. Nemoto, Tokyo University of Marine Science and Technology, for assistance with sampling. Helpful comments on this manuscript were provided by S. Ohshimo and Y. Hiraoka, Japan Fisheries Research and Education Agency. This study was supported by the Japan Fisheries Agency.

Literature cited

Beamish, R. J., and D. A. Fournier.
1981. A method for comparing the precision of a set of age determinations. Can. J. Fish. Aquat. Sci. 38:982–983.

Berry, F. H., D. W. Lee, and A. R. Bertolino.
1977. Age estimates in Atlantic bluefin tuna: an objective examination and an intuitive analysis of rhythmic markings on vertebrae and in otoliths. Collect. Vol. Sci. Pap. ICCAT 6:305–317.

Blanco-Parra, M. P., F. Galván-Magaña, and F. Márquez-Farías.
2008. Age and growth of the blue shark, *Prionace glauca* Linnaeus, 1758, in the Northwest coast off Mexico. Rev. Biol. Mar. Oceanogr. 43:513–520.

Branstetter, S.
1987. Age and growth estimates for blacktip, *Carcharhinus limbatus*, and spinner, *C. brevipinna*, sharks from the northwestern Gulf of Mexico. Copeia 1987:964–974.

Burnham, K. P., and D. R. Anderson.
2002. Model selection and multimodal inference: a practical information-theoretic approach, 2nd ed., 488 p. Springer, New York.

Cailliet, G. M., and D. W. Bedford.
1983. The biology of three pelagic sharks from California waters, and their emerging fisheries: a review. CalCOFI Rep. 24:57–69.

Camhi, M. D., E. Lauck, E. K. Pikitch, and E. A. Babcock.
2008. A global overview of commercial fisheries for open ocean sharks. *In* Sharks of the open ocean: biology, fisheries and conservation (M. D. Camhi, E. K. Pikitch, and E. A. Babcock, eds.) p.166–192. Blackwell Publishing, Ltd., Oxford, UK.

Campana, S. E.
2001. Accuracy, precision and quality control in age determination, including a review of the use and abuse of age validation methods. J. Fish Biol. 59:197–242.

Campana, S. E., M. C. Annand, and J. I. McMillan.
1995. Graphical and statistical methods for determining the consistency of age determination. Trans. Am. Fish. Soc. 124:131–138.

Carlson, J. K., and I. E. Baremore.
2003. Changes in biological parameters of Atlantic sharpnose shark *Rhizoprionodon terraenovae* in the Gulf of Mexico: evidence for density-dependent growth and maturity? Mar. Freshw. Res. 54:227–234.

Cassoff, R. M., S. E. Campana, and S. Myklevoll.
2007. Changes in baseline growth and maturation parameters of Northwest Atlantic porbeagle, *Lamna nasus*, following heavy exploitation. Can. J. Fish. Aquat. Sci. 64:19–29.

Chang, J. H., and K. M. Liu.
2009. Stock assessment of the shortfin mako shark (*Isurus oxyrinchus*) in the Northwest Pacific Ocean using per recruit and virtual population analyses. Fish. Res. 98:92–101.

Chang, W. Y. B.
1982. A statistical method for evaluating the reproducibility of age determination. Can. J. Fish. Aquat. Sci. 39:1208–1210.

Chavez, F. P., J. Ryan, S. E. Lluch-Cota, and M. Ñiquen.
2003. From anchovies to sardines and back: multidecadal change in the Pacific Ocean. Science 299:217–221.

Clarke, S. C., M. K. McAllister, E. J. Milner-Gulland, G. P. Kirkwood, C. G. J. Michielsens, D. J. Agnew, E. K. Pikitch, H. Nakano, and M. S. Shivji.
2006. Global estimates of shark catches using trade records from commercial markets. Ecol. Lett. 9:1115–1126.

Cortés, E.
2000. Life history patterns and correlations in sharks. Rev. Fish. Sci. 8:299–344.
Cortés, E., F. Arocha, L. Beerkircher, F. Carvalho, A. Domingo, M. Heupel, H. Holtzhausen, M. N. Santos, M. Ribera, and C. Simpfendorfer.
2010. Ecological risk assessment of pelagic sharks caught in Atlantic pelagic longline fisheries. Aquat. Living Resour. 23:25–34.
Fabens, A. J.
1965. Properties and fitting of the von Bertalanffy growth curve. Growth 29:265–289.
Francis, M. P., and C. Duffy.
2005. Length at maturity in three pelagic sharks (*Lamna nasus*, *Isurus oxyrinchus*, and *Prionace glauca*) from New Zealand. Fish. Bull. 103:489–500.
Francis, M. P., and C. Ó. Maolagáin.
2000. Age, growth and maturity of a New Zealand endemic shark (*Mustelus lenticulatus*) estimated from vertebral bands. Mar. Freshw. Res. 51:35–42.
Fujinami, Y., Y. Semba, H. Okamoto, S. Ohshimo, and S. Tanaka.
2017. Reproductive biology of the blue shark (*Prionace glauca*) in the western North Pacific Ocean. Mar. Freshw. Res. 68:2018–2027.
Fujinami, Y., Y. Semba, S. Ohshimo, and S. Tanaka.
2018a. Development of an alternative ageing technique for blue shark (*Prionace glauca*) using the vertebra. J. Appl. Ichthyol. 34:590–600.
Fujinami, Y., S. Nakatsuka, and S. Ohshimo.
2018b. Feeding habits of the blue shark (*Prionace glauca*) in the northwestern Pacific based on stomach contents and stable isotope ratios. Pac. Sci. 72:21–39.
Goldman, K. J., G. M. Cailliet, A. H. Andrews, and L. J. Natanson.
2012. Assessing the age and growth of chondrichthyan fishes. *In* Biology of sharks and their relatives, 2nd ed. (J. C. Carrier, J. A. Musick, and M. R. Heithaus, eds.), p. 423–451. Blackwell Publishing, Ltd., Oxford, UK.
Harry, A. V.
2018. Evidence for systemic age underestimation in shark and ray ageing studies. Fish Fish. 19:185–200.
Henderson, A. C., K. Flannery, and J. Dunne.
2001. Observations on the biology and ecology of the blue shark in the North-east Atlantic. J. Fish Biol. 58:1347–1358.
Hiraoka, Y., M. Kanaiwa, S. Ohshimo, N. Takahashi, M. Kai, and K. Yokawa.
2016. Relative abundance trend of the blue shark *Prionace glauca* based on Japanese distant-water and offshore longliner activity in the North Pacific. Fish. Sci. 82:687–699.
ISC (International Scientific Committee for Tuna and Tuna-like Species in the North Pacific Ocean).
2017. Stock assessment and future projections of blue shark in the North Pacific Ocean through 2015, 73 p. Annex 13 to the Report of the seventeenth meeting of the International Scientific Committee for Tuna and Tuna-like Species in the North Pacific Ocean plenary session; Vancouver, Canada, 12–17 July 2017. [Available at website.]
Jensen, A. L.
1985. Relations among net reproductive rate and life history parameters for lake whitefish (*Coregonus clupeaformis*). Can. J. Fish. Aquat. Sci. 42:164–168.
Joung, S.-J., G.-T. Lyu, K.-Y. Su, H.-H. Hsu, and K.-M. Liu.
2017. Distribution pattern, age, and growth of blue sharks in the South Atlantic Ocean. Mar. Coast. Fish. 9:38–49.
Joung, S.-J., G.-T. Lyu, H.-H. Hsu, K.-M. Liu, and S.-B. Wang.
2018. Age and growth estimates of the blue shark *Prionace glauca* in the central South Pacific Ocean. Mar. Freshw. Res. 69:1346–1354.
Kimura, D. K.
1980. Likelihood methods for the von Bertalanffy growth curve. Fish. Bull. 77:765–776.
Lessa, R., F. M. Santana, and F. H. Hazin.
2004. Age and growth of the blue shark *Prionace glauca* (Linnaeus, 1758) off northeastern Brazil. Fish. Res. 66:19–30.
Levitus, S., J. Antonov, and T. Boyer.
2005. Warming of the world ocean, 1955–2003. Geophys. Res. Lett. 32(2):L02604.
Levitus, S., J. I. Antonov, T. P. Boyer, O. K. Baranova, H. E. Garcia, R. A. Locarnini, A. V. Mishonov, J. R. Reagan, D. Seidov, E. S. Yarosh, et al.
2012. World ocean heat content and thermosteric sea level change (0–2000 m), 1955–2010. Geophys. Res. Lett. 39(10):L10603.
Matta, M. E., C. A. Tribuzio, D. A. Ebert, K. J. Goldman, and C. M. Gburski.
2017. Age and growth of elasmobranchs and applications to fisheries management and conservation in the northeast Pacific Ocean. Adv. Mar. Biol. 77:179–220.
Nakano, H.
1994. Age, reproduction and migration of blue shark in the North Pacific Ocean. Bull. Nat. Res. Inst. Far Seas Fish. 31:141–256.
Nakano, H., and M. P. Seki.
2003. Synopsis of biological data on the blue shark, *Prionace glauca* Linnaeus. Bull. Fish. Res. Agen. 6:18–55.
Nakano, H., and J. D. Stevens.
2008. The biology and ecology of the blue shark, *Prionace glauca*. *In* Sharks of the open ocean: biology, fisheries and conservation (M. D. Camhi, E. K. Pikitch, and E. A. Babcock, eds.), p. 140–151. Blackwell Publishing, Ltd., Oxford, UK.
Natanson, L. J., and G. M. Cailliet.
1990. Vertebral growth zone deposition in Pacific angel sharks. Copeia 1990:1133–1145.
Natanson, L. J., G. B. Skomal, S. L. Hoffmann, M. E. Porter, K. J. Goldman, and D. Serra.
2018. Age and growth of sharks: do vertebral band pairs record age? Mar. Freshw. Res. 69:1440–1452.
Ohshimo, S., Y. Fujinami, K. Shiozaki, M. Kai, Y. Semba, N. Katsumata, D. Ochi, H. Matsunaga, H. Minami, M. Kiyota, et al.
2016. Distribution, body length, and abundance of blue shark and shortfin mako offshore of northeastern Japan, as determined from observed pelagic longline data, 2000–2014. Fish. Oceangr. 25:259–276.
Okamura, H., and Y. Semba.
2009. A novel statistical method for validating the periodicity of vertebral growth band formation in elasmobranch fishes. Can. J. Fish. Aquat. Sci. 66:771–780.
Preti, A., C. U. Soykan, H. Dewar, R. J. D. Wells, N. Spear, and S. Kohin.
2012. Comparative feeding ecology of shortfin mako, blue

and thresher sharks in the California Current. Environ. Biol. Fish. 95:127–146.

Punt, A. E., and T. I. Walker.
1998. Stock assessment and risk analysis for the school shark (*Galeorhinus galeus*) off southern Australia. Mar. Freshw. Res. 49:719–731.

R Core Team.
2016. R: a language and environment for statistical computing. R Foundation for Statistical Computing, Vienna, Austria. [Available from website, accessed May 2016.]

Semba, Y., H. Nakano, and I. Aoki.
2009. Age and growth analysis of the shortfin mako, *Isurus oxyrinchus*, in the western and central North Pacific Ocean. Environ. Biol. Fish. 84:377–391.

Sims, D. W.
2005. Differences in habitat selection and reproductive strategies of male and female sharks. *In* Sexual segregation in vertebrates (K. E. Ruckstuhl and P. Neuhaus, eds.), p. 127–147. Cambridge Univ. Press, Cambridge, UK.

Skomal, G. B., and L. J. Natanson.
2003. Age and growth of the blue shark (*Prionace glauca*) in the North Atlantic Ocean. Fish. Bull. 101:627–639.

Sminkey, T. R., and J. A. Musick.
1995. Age and growth of the sandbar shark, *Carcharhinus plumbeus*, before and after population depletion. Copeia 1995:871–883.

Smith, S. E., D. W. Au, and C. Show.
1998. Intrinsic rebound potentials of 26 species of Pacific sharks. Mar. Freshw. Res. 49:663–678.

Tanaka, S., G. M. Cailliet, and K. G. Yudin.
1990. Differences in growth of the blue shark, *Prionace glauca*: technique or population? *In* Elasmobranchs as living resources: advances in the biology, ecology, systematics, and status of the fisheries (H. L. Pratt, S. H. Gruber, and T. Taniuchi, eds.), p. 177–187. NOAA Tech. Rep. NMFS 90.

Taylor, C. C.
1958. Cod growth and temperature. ICES J. Mar. Sci. 23:366–370.

von Bertalanffy, L.
1938. A quantitative theory of organic growth. Hum. Biol. 10:181–213.

Wang, S.-P., C.-L. Sun, A. E. Punt, and S.-Z. Yeh.
2005. Evaluation of a sex-specific age-structured assessment method for the swordfish, *Xiphias gladius*, in the North Pacific Ocean. Fish. Res. 73:79–97.

Wells, R. J. D., N. Spear, and S. Kohin.
2017. Age validation of the blue shark (*Prionace glauca*) in the eastern Pacific Ocean. Mar. Freshw. Res. 68:1130–1136.

Yokoi, H., H. Ijima, S. Ohshimo, and K. Yokawa.
2017. Impact of biology knowledge on the conservation and management of large pelagic sharks. Sci. Rep. 7:10619.

Fishery Bulletin

Guidelines for authors

Contributions published in *Fishery Bulletin* describe original research in marine fishery science, fishery engineering and economics, and marine environmental and ecological sciences (including modeling). Preference will be given to manuscripts that examine processes and underlying patterns. Descriptive reports, surveys, and observational papers may occasionally be published but should appeal to an audience outside the locale in which the study was conducted.

Although all contributions are subject to peer review, responsibility for the contents of papers rests upon the authors and not on the editor or publisher. *Submission of an article implies that the article is original and is not being considered for publication elsewhere.*

All submissions are subject to a double-blind review to remove the identity of author and reviewer during the review process.

Plagiarism and double publication are considered serious breaches of publication ethics. To verify the originality of the research in papers and to identify possible previous publication, manuscripts may be screened with plagiarism-detection software.

Manuscripts must be written in English; authors whose native language is not English are strongly advised to have their manuscripts checked by English-speaking colleagues before submission.

Once a paper has been accepted for publication, online publication takes approximately 2 weeks.

There is no cost for publication in *Fishery Bulletin*.

Types of manuscripts accepted by the journal

Articles generally range from 20 to 30 double-spaced typed pages (12-point font) and describe an original contribution to fisheries science, engineering, or economics. Tables and figures are not included in this page count, but the number of figures should not exceed 1 figure for every 4 pages of text. Articles contain the following divisions: abstract, introduction, methods, results, and discussion.

Short contributions are generally less than 15 double-spaced typed pages (12-point font) and, like articles, describe an original contribution to fisheries science. They follow the same format as that for articles: abstract, introduction, methods, results, and discussion, but the results and discussion sections may be combined. They are distinguished from full articles in that they report a noteworthy new observation or discovery—such as the first report of a new species, a unique finding, condition, or event that expands our knowledge of fisheries science, engineering, or economics—and do not require a lengthy discussion.

Companion articles should be submitted together and are published together as a scientific contribution. Both articles should address a closely related topic and may be articles that result from a workshop or conference.

Preparation of manuscript

Title page should include authors' full names, mailing addresses, and the senior author's email address.

Abstract should be limited to 200 words (one-half typed page), state the main scope of the research, and emphasize the authors' conclusions and relevant findings. Do not review the methods of the study or list the contents of the paper. Because abstracts are circulated by abstracting agencies, it is important that they represent the research clearly and concisely.

General text must be typed in 12-point Times New Roman font throughout. A brief introduction should convey the broad significance of the paper; the remainder of the paper should be divided into the following sections: Materials and methods, Results, Discussion, and Acknowledgments. Headings within each section must be short, reflect a logical sequence, and follow the rules of subdivision (i.e., there can be no subdivision without at least 2 subheadings). The entire text should be intelligible to interdisciplinary readers; therefore, all acronyms, abbreviations, and technical terms should be written out in full and defined the first time they are mentioned. Abbreviations should be used sparingly because they are not carried over to indexing databases and slow readability for those readers outside a discipline. They should never be used for the main subject (species, method) of a paper.

For general style, follow the U.S. Government Publishing Office *Style Manual* (2016, available at website) and *Scientific Style and Format: the CSE Manual for Authors, Editors, and Publishers* (2014, 8th ed.) published by the Council of Science Editors. For scientific nomenclature, use the current edition of the American Fisheries Society's *Common and Scientific Names of Fishes from the United States, Canada, and Mexico* and its companion volumes (*Crustaceans, Mollusks, Cnidaria and Ctenophora*, and *World Fishes Important to North Americans*). For species not found in the above mentioned AFS publications and for more recent changes in nomenclature, use the Integrated Taxonomic Information System (ITIS, available at website), or, secondarily, the California Academy of Sciences *Catalog of Fishes* (available at website) for species names not included in ITIS. Common (vernacular) names of species should be lowercase. Citations must be given for the identification of specimens. For example, "Fish species were identified according to Collette and Klein-MacPhee

(2002); sponges were identified according to Stone et al. (2011)."

Dates should be written as follows: 11 November 2018. Measurements should be expressed in metric units, for example, "58 metric tons (t);" if other units of measurement are used, please make this fact explicit to the reader. Use numerals, not words, to express whole and decimal numbers in the general text, tables, and figure captions (except at the beginning of a sentence). For example, "We considered 3 hypotheses. We collected 7 samples in this location." Use American spelling. Refrain from using the shorthand slash (/), an ambiguous symbol, in the general text.

Cite all software, special equipment, and chemical solutions used in the study within parentheses in the general text, for example, "SAS, vers. 6.03 (SAS Institute, Inc., Cary, NC)."

Word usage and grammar that may be useful are the following:

- *Aging*
  For our journal, the word *aging* is used to mean both age determination and the aging process (senescence). Authors should make clear which meaning is intended where ambiguity may arise.

- *Fish and fishes*
  The plural of the word fish (a collective noun that implies individuals without regard to species) is *fish*.
  Example: The *fish* were collected by trawl net.
  Example: The numbers of *fish* collected that season were less than the numbers from previous years.

  The plural for *fish species* is *fishes* (a contrived plural used by taxonomists to mean several or more *fish species*) or one can use *fish species* (which is preferred in this journal for clarity across disciplines).
  Example: The *fishes* of Puget Sound [biodiversity is implied] or
  Example: The *fish species* of Puget Sound [preferred plural for clarity across disciplines].

- *Crab and crabs, squid and squids, etc.*
  The plural of the word *crab* (i.e., many individuals without regard to species) is *crab*.
  Example: The crab were sorted by weight.
  Example: Many red king *crab* were dying [Many individuals of one species of crab.]

  The plural of *crab species* is *crabs* (a word used by taxonomists) or *crab species* (the latter is preferred in this journal for clarity).
  Example: These *crabs* were selected for treatment. [Different crab species are implied.]
  Example: These *crab species* were selected for treatment. [Preferred word choice for clarity of meaning.]
  Example: Snow *crabs* are found throughout the North Pacific Ocean and Bering Sea. [There are 2 species of snow crab and therefore the word *crabs* can be used here.]
  Example: *Two species* of snow *crab* are found throughout the North Pacific Ocean and Bering Sea. [Preferred usage for clarity.]
  Example: Three crabs were selected for treatment. [3 species of crab are implied.]
  Example: Three crab species were selected for treatment. [Preferred word choice for clarity.]

- *Fisherman and fisher*
  We use *fisherman* and *fishermen* in this journal not *fisher* and *fishers*. One can always use crew member, vessel operator, and angler (the latter for recreational fishing.

- *The definite article with common names of species*
  When the singular common name of a species represents the entire class or group to which it belongs, use the definite article.
  Example: Only one species of the genus *Salmo* is found in the Atlantic Ocean—*the* Atlantic salmon (*Salmo salar*).
  Example: The sonic emissions of *the* bottlenose dolphin are complex.

  For plural common names, this rule does not apply.
  Example: Chinook salmon are found throughout the Pacific Ocean.
  Example: Bottlenose dolphins are found in temperate and tropical waters.

- *Sex*
  For the meaning of male and female, use the word *sex*, not *gender*. Do not write "fish were sexed." Write, "sex was determined."

- *Participles*
  As adjectives, participles must modify a specific noun or pronoun.
  Example: Using mark-recapture methods, these scientists determined the size of the population. [Correct. The participle *using* modifies the word *scientists*.]
  Example: These scientists, based on the collected data, concluded that the mortality rate of these fish had increased. [Incorrect. The scientists were not based on the collected data.]
  Example: These scientists concluded, on the basis of collected data, that the mortality rate of these fish had increased. [Correct. The offending participle has been eliminated and an adverbial phrase modifies the verb *concluded*.]

Equations and mathematical symbols should be set from a standard mathematical program (MathType or Equation Editor). Equations formatted in LaTex are not acceptable. For mathematical symbols in the general text (α, χ^2, π, $\pm$, etc.), use the symbols provided by

the MS Word program and italicize all variables, except those variables represented by Greek letters and the superscript and subscript parts of variables and expressions. Do not use photo mode when creating these symbols in the general text, and do not cut and paste equations, letters, or symbols from a different software program.

Number equations (if there are more than one) for future reference by scientists; place the number within parentheses at the end of the first line of the equation.

Literature cited section comprises published works and those accepted for publication (in press) in peer-reviewed journals. Follow the name and year system for citation format in this section (i.e., citations should be listed alphabetically by the authors' last names, and then by year if there is more than one citation by the same author. A list of abbreviations for citing journal titles can be found at this website.

Authors are responsible for the accuracy and completeness of all citations. Literature citation format: Authors (last name, followed by initials for first name and, if given, middle name of first author; then list names of additional authors with initials before last names). Year. Title of article. Abbreviated title of the journal in which it was published. Always include either the range of page numbers (for a journal article) or a total number of pages (for a book or other type of publication). List a sequence of citations in the general text chronologically, for example, "(Smith, 1932: Green. 1947; Smith and Jones, 1985)." Avoid the use of multiple citations when a single citation sufficiently supports a statement; cite the work that first reported the information that supports a statement, not all of the subsequent works.

Acknowledgments should be no more than 6 lines of text. Only those who have contributed in an outstanding way should be acknowledged by name. For recognition of other persons or groups, use a general term, such as *crew, observers,* or *research coordinators*, and do not include names with these terms.

Digital object identifier (doi) code ensures that a publication has a permanent location online. A doi link (which may include a doi code) should be included at the end of citations of published literature. Authors are responsible for submitting accurate doi links. Faulty links will be deleted at the page-proof stage.

Footnotes are used for all documents that have not been formally peer reviewed and for observations and personal communications, but these types of references should be cited sparingly in manuscripts submitted to the journal.

All reference documents, administrative reports, internal reports, progress reports, project reports, contract reports, personal observations, personal communications, unpublished data, manuscripts in review, and council meeting notes are footnoted in 9-point font and placed at the bottom of the page on which they are first cited. Footnote format is the same as that for formal literature citations. A link to the online source (e.g., [Available from http://www... , accessed July 2017.]), or the mailing address of the agency or department holding the document, should be provided so that readers may obtain a copy of the document.

Tables are often overused in scientific papers; it is seldom necessary to present all the data associated with a study. Tables should not be excessive in size and must be cited in numerical order in the text. Headings should be short but ample enough to allow the table to be intelligible on its own.

All abbreviations and unusual symbols must be explained in the table legend. Other incidental comments may be footnoted with numeral footnote markers. Use asterisks only to indicate significance in statistical data. Do not put a table legend on a page separate from the table; place the legend above the table. *Do not submit tables in photo mode.*

- Note probability with a capital, italic *P*.
- Provide a zero before all decimal points for values less than one (e.g., 0.07).
- Round all values to 2 decimal points.
- Use a comma in numbers of 5 digits or more (e.g., 13,000 but 3000).

Figures must be cited in numerical order in the text. Graphics should aid in the comprehension of the text, but they should be limited to presenting patterns rather than raw data. The number of figures should not exceed 1 figure for every 4 pages of text. Place panel labels **A, B, C,** etc., within the upper-left area of graphs and photos. Avoid placing labels vertically.

Figure legends should explain all symbols and abbreviations seen in the figure and should be double spaced on a separate page at the end of the manuscript.

Line art and halftone figures should be saved at resolutions >600 dots per inch (dpi) and >300 dpi, respectively. Color is allowed in figures to show morphological differences among species (for species identification), to show stain reactions, to show gradations (such as those of temperature and salinity within maps), and to distinguish between numerous lines and symbols in graphs. Figures approved for color should be saved in CMYK format.

All figures must be submitted as PDF, TIFF, or EPS files.

- Capitalize only the first letter of the first word and proper nouns in all labels within figures.
- Do not use overly large font sizes in maps and for axis labels in graphs.

- Do not use bold fonts or bold lines in figures.
- Do not place outline rules around graphs.
- Place a north arrow and label degrees latitude and longitude (e.g., 170°E) in all maps.
- Use symbols, shadings, or patterns (not clip art) in maps and graphs.

Supplementary materials that are considered essential, but are too large or impractical for inclusion in a paper (e.g., metadata, figures, tables, videos, and websites), may be provided at the end of an article. These materials are subject to the editorial standards of the journal. A URL to the supplementary material and a brief explanation for including such material should be sent at the time of initial submission of the paper to the journal.

- **Metadata, figures, and tables** should be submitted in standard digital format (MS Word or PDF file) and should be cited in the general text, for example, as "...was determined (Suppl. Table 3, Suppl. Fig. 1)."
- **Websites** should be cited with a URL in the general text.
- **Videos** must not be larger than 30 MB to allow a swift technical response for viewing the video. Authors should consider whether a short video uniquely captures what text alone cannot capture for the understanding of a process or behavior under examination in the article. Supply an online link to the location of the video.

Copyright law does not apply to *Fishery Bulletin,* which falls within the public domain. However, if an author reproduces any part of an article from *Fishery Bulletin*, reference to source is considered correct form (e.g., Source: Fish. Bull. 97:105).

Failure to follow these guidelines and failure to correspond with editors in a timely manner will delay publication of a manuscript.

Submission of manuscript

Submit a manuscript online at the ScholarOne Manuscripts website for *Fishery Bulletin.* Commerce Department authors should submit papers under a completed NOAA Form 25-700. For further details on electronic submission, please contact the associate editor, Cara Mayo, at

cara.mayo@noaa.gov.

When requested, the text and tables should be submitted in MS Word format. Each figure should be sent as a separate PDF, TIFF, or EPS file. Send a copy of a figure in the original software if conversion to any of these formats yields a degraded version of the figure.

Questions? If you have questions regarding these guidelines, please contact the managing editor, Kathryn Dennis, at

kathryn.dennis@noaa.gov.

Questions regarding manuscripts under review should be addressed to Associate Editor Cara Mayo.

Please note that Sharyn Matriotti has retried after serving for 29 years as the managing editor of *Fishery Bulletin.*

Fishery Bulletin

Subscription form

Superintendent of Documents **Publications** Order Form

*5178

☐ YES, please send me the following publications:

____ Subscriptions to *Fishery Bulletin*
for $32.00 per year ($44.80 foreign)

The total cost of my order is $ _____ . Prices include regular domestic postage and handling and are subject to change.

_____
(Company or Personal Name) (Please type or print)

_____
(Additional address/attention line)

_____
(Street address)

_____
(City, State, ZIP Code)

_____
(Daytime phone including area code)

_____
(Purchase Order No.)

Charge your order. IT'S EASY!

Please Choose Method of Payment:

☐ Check payable to the Superintendent of Documents
☐ GPO Deposit Account ☐☐☐☐☐☐☐–☐
☐ VISA or MasterCard Account
☐☐☐☐☐☐☐☐☐☐☐☐☐☐☐☐
☐☐☐☐ (Credit card expiration date)

To fax your orders (202) 512-2104

_____
(Authorizing Signature)

Mail to: Superintendent of Documents
P.O. Box 979050, St. Louis, Missouri 63197
Tel. no. (U.S. callers): 866-512-1800
Tel. no. (International callers): 1-202-512-1800

Thank you for your order!

Also available online at
http://bookstore.gpo.gov/actions/GetPublication.do?stocknumber=703-023-00000-2
email: ContactCenter@gpo.gov

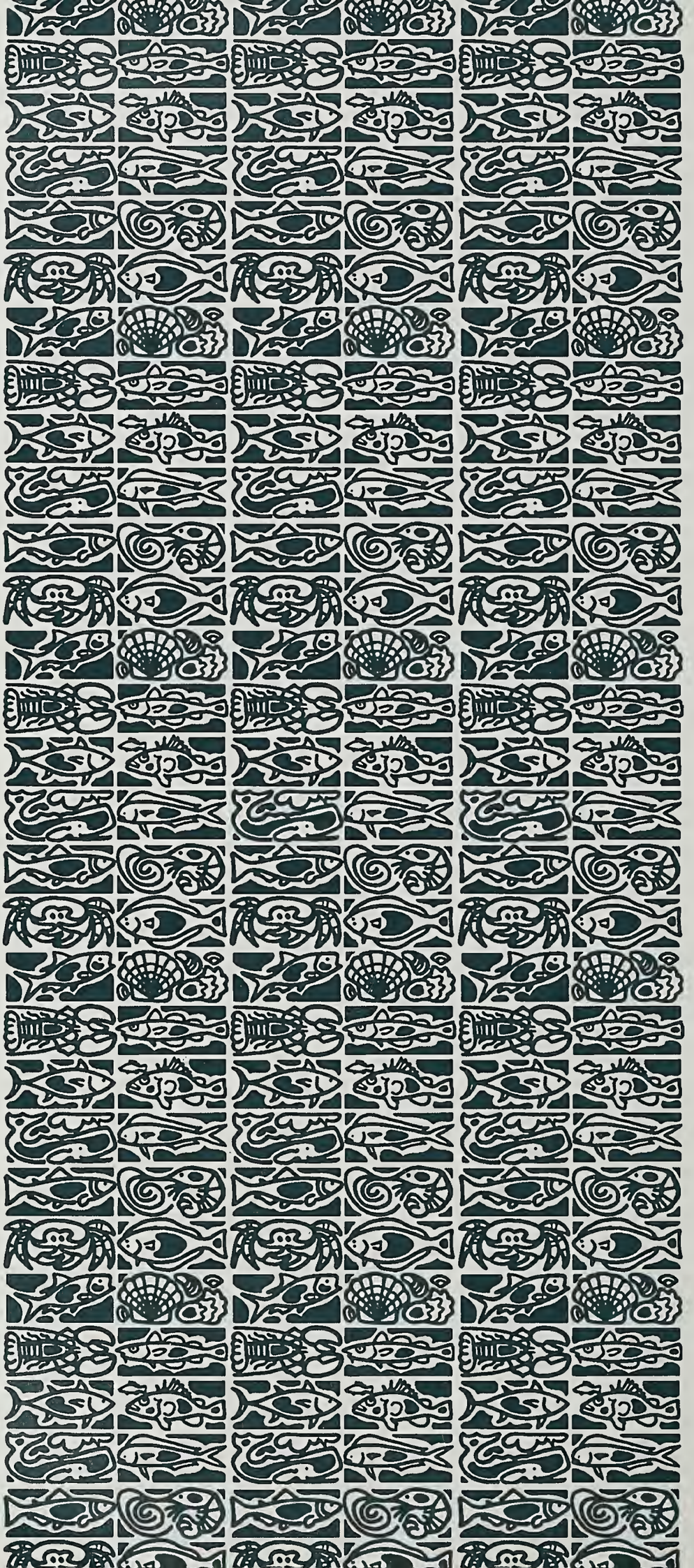

SMITHSONIAN LIBRARIES
3 9088 02019 4627